CELL CYCLE CONTROL AND FATE DETERMINATION DURING MALE GAMETOGENESIS IN *ARABIDOPSIS THALIANA*

CHEN ZHONG

(B. Medical Sci. Peking University)

A THESIS SUBMITTED

FOR THE DEGREE OF DOCTOR OF PHILOSOPHY

DEPARTMENT OF BIOLOGICAL SCIENCES

NATIONAL UNIVERSITY OF SINGAPORE

2009

ACKNOWLEDGEMENTS

I would like to express my wholehearted gratitude to my supervisor, Professor Frederic BERGER, for offering me the opportunity to pursue the Ph.D. degree in his laboratory and introducing me to the wonderful and exciting world of plant science. I deeply appreciate Fred for his excellent supervision, consistent encouragement, and great support throughout the course of my research work, and also for his invaluable amendments to my thesis.

My sincere thanks go to my graduate supervisory committee members: Dr. Toshiro ITO, Dr. Yuehui HE and Dr. Huck Hui NG for their invaluable suggestions and great encouragement during the course of my work.

I thank all my current lab members in Chromatin and Reproduction Group: Lijing, Pauline, Sarah, Heike, Jeanie, Ramesh, Thiet, and Peiqi for sharing experiences and creating a helpful working environment. My thanks to former members of the lab: Jonathan, Mathieu, Tadashi and Sebastien. Thanks also go to my attachment students Shihui, Meilun and Kim.

I appreciate all facilities of Temasek Life Sciences Laboratory, especially thank to Graham and Ouyang Xuezhi from Microscopy and Imaging Facility. I thank the funding from Temasek Life Sciences Laboratory and Singapore Millennium Foundation.

My deepest appreciation goes to my wife Shijie, my parents and parents-in-law, for their love, encouragement and support for all these years. Finally, my affection goes to my newborn daughter Yinuo, you bring me so much fun and awareness of responsibility.

September 2009

TABLE OF CONTENTS

LIST OF FIGURES

LIST OF TABLES

LIST OF ABBREVIATIONS

Units and measurements

bp	base pairs
g	gram(s)
h	hour(s)
kb	kilo base -pairs
L	litre(s)
M	Molar
min	minute(s)
ml	mililitre(s)
mM	Milimolar
nm	nanometer(s)
ng	nanogram(s)
rpm	revolution per minute
s	second(s)
°C	Degree Celsius
µg	microgram(s)
µl	microlitre(s)
µM	Micromolar

Frequently mentioned genes and proteins

ASF1	ANTISILENCING FACTOR 1
CAF1	Chromatin Assembly Factor 1
CDKA	Cyclin Dependent Kinase A
FAS1	FASCIATA1
FAS2	FASCIATA2
FIS	Fertilization Independent Seed
HIRA	HISTONE REGULATORY A
HTR10	HISTONE THREE RELATED 10
MSI1	MULTICOPY SUPPRESSOR OF IRA1
Pc-G	Polycomb group
pRb	Retinoblastoma protein
PRC2	Polycomb group (Pc-G) repressive complexes 2
RBR	Retinoblastoma-related protein

SUMMARY

Development is a process by which muticellular organisms arise from a single cell. During this process, the cell number increases by cell division and the cells become different from each other by cell differentiation. How cell division and cell differentiation are tightly coordinated during development still remains largely elusive.

During my PhD, I used Arabidopsis as a tool to investigate the relationship between cell proliferation and cell differentiation during pollen development. The Arabidopsis pollen grains undergo two stereotypical cell divisions. The pollen precursors produced by meiosis are called microspores. They enlarge and divide asymmetrically to produce a larger vegetative cell and a smaller generative cell. The generative cell undergoes a second symmetrical mitosis to form two identical sperm cells. The two cell types are distinguished from each other by cellular architecture, chromatin organization and specifically expressed proteins. Hence, pollen development, with only two mitoses and two cell lineages, is an ideal model system to dissect the effects on the cell cycle from effects on cell fate.

In the first half of my PhD, I investigated the role of the S phase chaperones – Chromatin Assembly Factor 1 (CAF1) during pollen development. My work showed that MSI1 is required in a functional CAF1 complex. Loss of activity of the CAF1 pathway delays the cell cycle during pollen development. Prevention of the second pollen mitosis generates a fraction of CAF1-deficient pollen grains comprising a vegetative cell and a single sperm

cell, which both express corresponding cell fate markers correctly. The single sperm is functional and fertilizes indiscriminately either female gamete. My results thus suggest that pollen cell fate is independent from cell cycle regulation.

In the second half of my PhD, I studied the impact of hyperproliferation caused by the homologue of the tumor suppressor Retinoblastoma (RBR). I found that hyperproliferation caused by the loss of RBR affects mostly vegetative cells. These defects are rescued by preventing cell proliferation arising from down-regulation of the cycle dependent kinase A (CDKA), leading to the hypothesis that *rbr* primarily targets cell cycle regulation with a secondary impact on cell fate.

In parallel, based on the finding that *cdka* rescues *rbr* phenotypes, I started a suppressor screen with *rbr*, looking for novel RBR interacting pathways. I screened through about 3000 lines and eventually found 4 lines which that had a significant increase in *rbr* transmission rate and produced pollen with a hypo-proliferation phenotype. These suppressor lines will be mapped to get the molecular identity.

CHAPTER I

INTRODUCTION

1.1. HOW DO COMPLEX MULTICELLULAR ORGANISMS DEVELOP?

Development is a process by which multicellular organisms arise from a single cell. During this process, the cell number increases by cell division, and following fate determination, cells differentiate from each other into morphologically and functionally distinct cell types. Depending on the cell type, each cell lineage undergoes a typical number of cell divisions prior to differentiation. The degree of cell division is also modulated by physiological parameters. During development, the organism gains multicellularity gradually through complicated patterns of cell division and cell differentiation. How cell division and cell differentiation are tightly coordinated during development still remains largely unsolved.

1.1.1. Cell cycle overview

One cell divides into two cells by going through the mitotic cell cycle (Fig. 1-1). During the synthetic (S) phase, the DNA is replicated and during the mitotic (M) phase, DNA condenses, the sister chromatids segregate to the daughter cells, which are then separated by cytokinesis. The S phase and M phase are preceded by the gap phases G1 and G2 respectively, during which growth and differentiation take place. Each phase of the cell cycle is precisely controlled temporally to ensure that the replication and segregation of the chromosomes occur in a proper order with high fidelity. Progression through the cell cycle is regulated at two major checkpoints, the G1/S transition and the G2/M transition. Control mechanisms operate at these checkpoints to ensure chromosome integrity and the completion of each stage of the cell cycle before the initiation of the following stage.

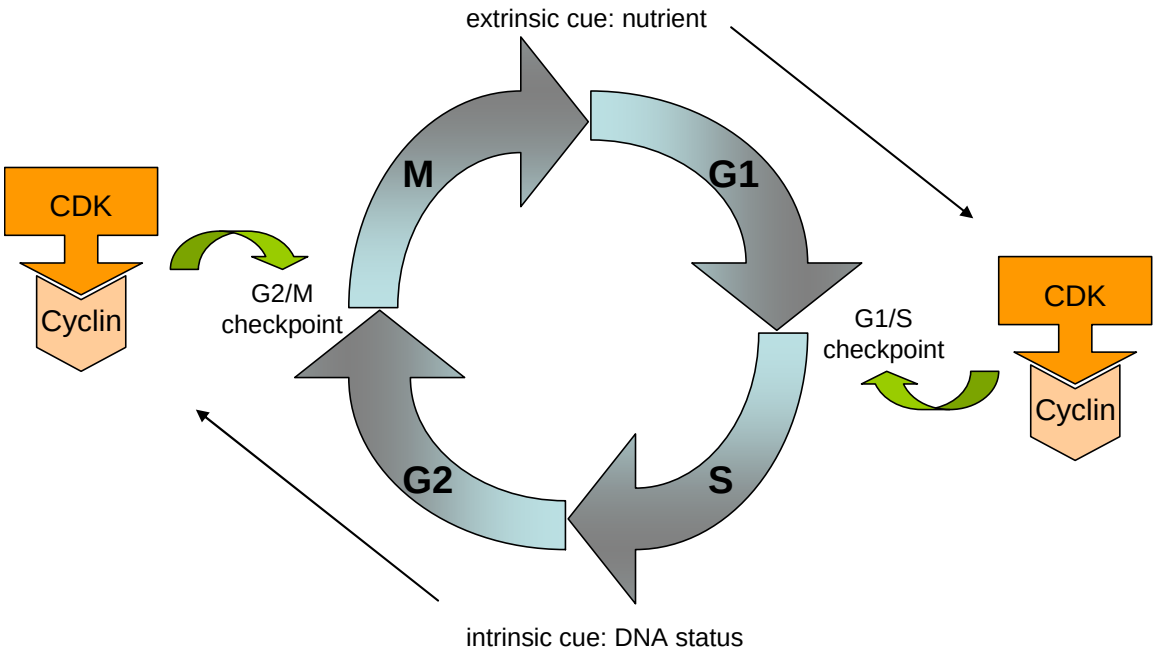

Fig. 1-1. CDK and Cyclin in eukaryotic cell cycle control. CDK/Cyclin complex triggers the progression through the cell cycle at two major checkpoints, the G1/S transition and the G2 /M transition. CDK acts as the processor of multiple signaling pathways conferring intrinsic and extrinsic cues to the cell cycle machinery.

1.1.1.1. Animal CDKs and cyclins

Progression through the cell cycle checkpoints is regulated by a class of highly conserved heterodimeric protein kinases containing a regulatory Cyclin and a catalytic Cyclin Dependent Kinase (CDK) (Fig. 1-1). CDKs sense the internal and external signals to ensure the appropriate pace of the cell cycle (Morgan, 1997). CDKs are activated and phosphorylate their substrates only when associated with a cyclin. The oscillating expression and degradation of cyclins generate the basis of the cell-cycle-dependent activity of CDKs. At different cell cycle stages, specific CDK/cyclin complexes assemble and phosphorylate a specific set of proteins essential for checkpoint function and initiation of the next phase (Morgan, 1997).

In addition, the activity of CDK/cyclin complexes is regulated by phosphorylation or dephosphorylation and the interaction with regulatory proteins. Cyclin-Dependent Kinase Inhibitors (CKIs) are able to block CDK/cyclin kinase function (Sherr and Roberts, 1999) whereas Cyclin-Dependent Kinase Activating Kinases (CAKs) fully activate CDKs by phosphorylation. These regulatory mechanisms help to fine-tune the intrinsic activity of CDK/cyclin complexes and respond to intrinsic developmental and external signals regulating the cell cycle.

1.1.1.2. Plant CDKs and cyclins

In Arabidopsis the CDK with a bona fide PSTAIRE sequence in its cyclin binding domain is CDKA, which plays a pivotal role at both the G1/S and G2/M transitions. As plants have no orthologs of the mammalian G1/S specific CDK4 and CDK6 genes,

CDKA is seemingly the only CDK active at the G1/S and G2/M transitions. Plants possess unique class B-type CDKs that have not been described in any other organism (Joubes et al., 2000). Arabidopsis harbors two CDKB1 (CDKB1;1 and CDKB1;2) with the PPTALRE sequence in the cyclin-binding domain and CDKB2 (CDKB2;1 and CDKB2;2) with the PPTTLRE sequence in the cyclin-binding domain (Vandepoele et al., 2002). CDKBs are specialized in the regulation of mitosis. The plant D type cyclins are uniquely responsive to both exogenous cytokinins (Riou-Khamlichi et al., 1999) and sucrose (Riou-Khamlichi et al., 2000) and play important roles at the G1/S transition.

1.1.1.3. Features of plant cell cycle

In higher plants, most fundamental control mechanisms identified in fungi and animals that govern cell divisions are conserved. Plants use CDKs, cyclins, KRPs (CDK inhibitors), the retinoblastoma protein, E2F/DP transcription factors, and WEE kinases to control the progression through cell cycle phases (Stals and Inze, 2001). Genome-wide analysis of core cell cycle genes in Arabidopsis showed plant specific components of cell cycle genes such as the B-type CDKs and specific KRPs. and a larger number of cyclins (Vandepoele et al., 2002). In addition more than half of the genes in Arabidopsis belong to gene families with three or more members (Blanc et al., 2000). This can be explained by extensive gene duplication of the Arabidopsis genome (Vision et al., 2000). The 22 core cell cycle genes are part of a segmental duplication in the Arabidopsis genome (Vandepoele et al., 2002). Finally, why plants retained such a high complexity might be explained because the sessile plant cannot escape adverse conditions, so plants evolved

the high number of cell cycle genes to ensure fine-tuning of development in response to the changing environment.

Although there are a few plant-specific regulators of the cell cycle, it has become obvious that most pathways regulating the cell cycle are conserved between plants and animals. Still, as plant cells do not move, in contrast to animal cells, it is possible that some aspects of coordination of cell differentiation with cell division are specific to plants.

1.1.2. Cell differentiation overview

Sexually reproducing organisms develop from a single zygote into embryos through definition of cell types assembled in tissues and organs. Embryogenesis is dominated by cell division parallel to the gradual specification of the various domains where cell types differentiate. Cell differentiation refers to the irreversible process by which the function of a cell specializes. Differentiation dramatically changes the cell size, shape, metabolism and responsiveness to intrinsic (endocrine and paracrine) and extrinsic (environmental) signals. Differentiation involves highly-controlled modifications in patterns of gene expression. Hence, within an organism cells acquire dramatically different physical characteristics derived from the same genome. The number of different cell types increases as the organism develops, and new cell types arise from particular pre-existing cell types through a hierarchical series of decisions. Following each decision in the developmental hierarchy, cells become irreversibly committed to a certain fate in most of the cases. However, certain decisions are reversible as in plant root, ablation of Quiescent

Center cells leads to the re-specification of stele cells to Quiescent Center cells (van den Berg et al., 1997).

Cell differentiation can be illustrated by Drosophila neuroblasts (Fig. 1-2), which generate the majority of cells in the central nervous system. Neuroblasts undergo asymmetrical cell division, generating two daughters of distinct size and fate. The larger daughter maintains the neuroblast identity and is able to undergo an additional asymmetrical division, whereas the smaller daughter becomes a ganglion mother cell committed to differentiation and terminally divides into two neurons or two glial cells. By repeated self-renewing asymmetric divisions, neuroblasts generate a large number of differentiated progeny during their lifetime (Chia et al., 2008). The undifferentiated neuroblast retains active proliferation whereas cell division becomes restricted in differentiated neurons and glial lineages.

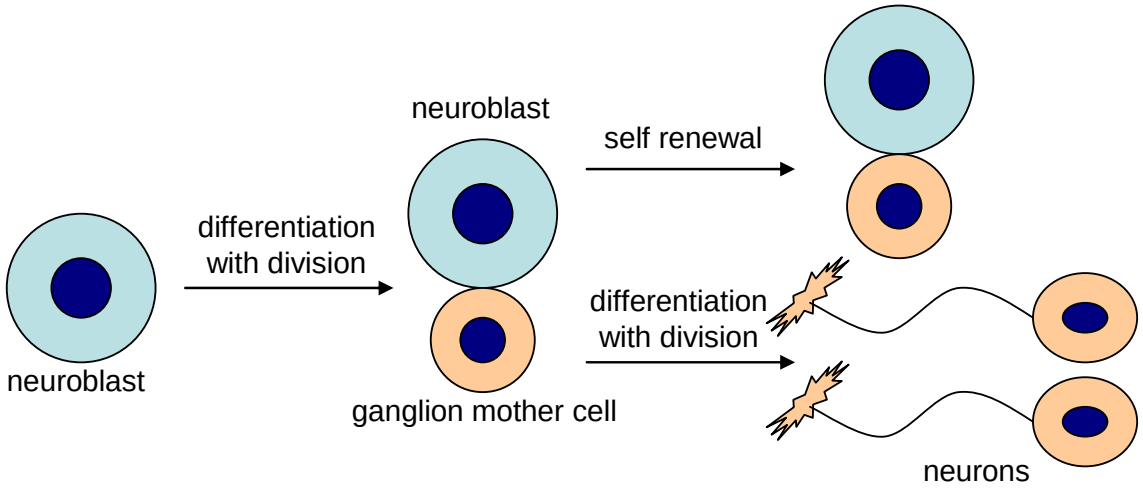

Fig. 1-2. Drosophila neuroblast differentiation. Drosophila neuroblasts divide asymmetrically into a neuroblast and ganglion mother cell. Differentiation takes place at the first division. Then the ganglion mother cell divides symmetrically with differentiation into two neurons.

1.1.3. Coordination of cell cycle and cell differentiation

In a developmental context, the cell cycle and cell differentiation are tightly coordinated both spatially and temporally. Adequate crosstalk between cell cycle regulatory mechanisms and cell differentiation is required for proper development. At the cellular level, cell cycle progression has to be coordinated with pattern formation. After a certain fate has been adopted, the cell cycle pattern has to be adapted for cell morphogenesis and physiology. At the tissue level, cell division and cell growth have to be precisely regulated to realize the body plan.

One of the important coordinators between cell cycle and cell differentiation is the Rb/E2F pathway (Harbour and Dean, 2000a) (Korenjak and Brehm, 2005). The Rb gene was identified two decades ago as the first tumor suppressor gene, and is responsible for the pediatric eye tumor retinoblastoma (Friend et al., 1986). During the cell cycle, the retinoblastoma tumor suppressor protein (pRb) plays a key role in regulating the G1/S transition by binding to and repressing E2F transcription factors (E2Fs). Upon phosphorylation by CDKs at late G1 stage, pRb loses its binding affinity for E2Fs (Weinberg, 1995). E2Fs were originally identified by their ability to interact and activate the human adenovirus E2 promoter (Helin et al., 1992). E2Fs act together with Distantly-related Proteins (DPs), which were identified soon afterwards (Helin et al., 1993). E2Fs and DPs regulate the expression of a variety of genes required for cell cycle progression and cell differentiation, such as the S-phase expressed gene *Proliferating Cell Nuclear Antigen* (*PCNA*) and the growth factor *TGF-β* (Dimova and Dyson, 2005). In addition to its key cell cycle regulatory function, pRb also recruits chromatin remodeling factors that

exert a broad range of cellular functions distinct from cell cycle control (Brehm and Kouzarides, 1999), including cell fate regulation (Macaluso et al., 2006), senescence (Funayama and Ishikawa, 2007), and apoptosis (Harbour and Dean, 2000b).

Its dual function in cell cycle and cell differentiation potentially enables Rb to coordinate cell cycle and cell differentiation, and several experiments have been conducted to test this hypothesis. However the elaborate relationship between cell cycle and differentiation in multicellular organisms largely complicates the interpretation of the experimental data, and conflicting results were obtained using different experimental strategies. For instance, a knock-out of Rb function in mice showed pleiotropic phenotypes. Loss of Rb caused abnormal proliferation before the formation of the nervous system and peripheral blood cells, indicating that its role is primarily devoted to cell proliferation restriction. However $Rb^{-/-}$ mice died on embryonic Day 13.5 due to apoptosis in the nervous system, defective hematopoiesis and loss of differentiation markers (Jacks et al., 1992), which favors the idea that Rb directly controls differentiation. Similarly ambiguous results were obtained in Arabidopsis when Rb expression was silenced by an inducible system in leaves (Desvoyes et al., 2006). The apparently contradictory results originate largely because that the phenotypes were analyzed in multicellular complex lineages after long periods during which cell division and developmental decision take place. As cell-cycle progression potentially determines further differentiation, and developmental signals further control cell-cycle progression, it is hard to pinpoint when and where the initial defect appears and what is the nature of the defect (derepression of cell proliferation or loss of cell differentiation or a combined impact). Therefore, analyzing Rb developmental

function requires a relatively simple experimental system in order to untangle the interdependence of cell cycle and cell differentiation.

During my PhD study, I used the Arabidopsis male gametic lineage, which consists in two cell divisions and a single cell fate commitment step as a tool to investigate the relationship between cell cycle and cell differentiation linked to Rb function.

1.2. ARABIDOPSIS DEVELOPMENT

1.2.1. The life cycle of Arabidopsis

Plant life cycles alternate a diploid sporophytic phase with a haploid gametophytic phase (Fig. 1-3). By contrast with many algae and mosses, the flowering plant Arabidopsis life cycle is dominated by the sporophytic phase. Sporophytes build up the main plant body with roots, shoots, leaves and flowers, but do not undergo sexual reproduction. Instead, meiotic divisions in specialized floral tissues lead to the formation of haploid microspores and megaspores. These spores initiate the second, haploid generation, called the gametophyte. In flowering plants the major function of the gametophytes is the production of haploid gametes. The fusion of the gametes gives rise to the zygote, which initiates a new diploid sporophyte generation, thereby completing the life cycle.

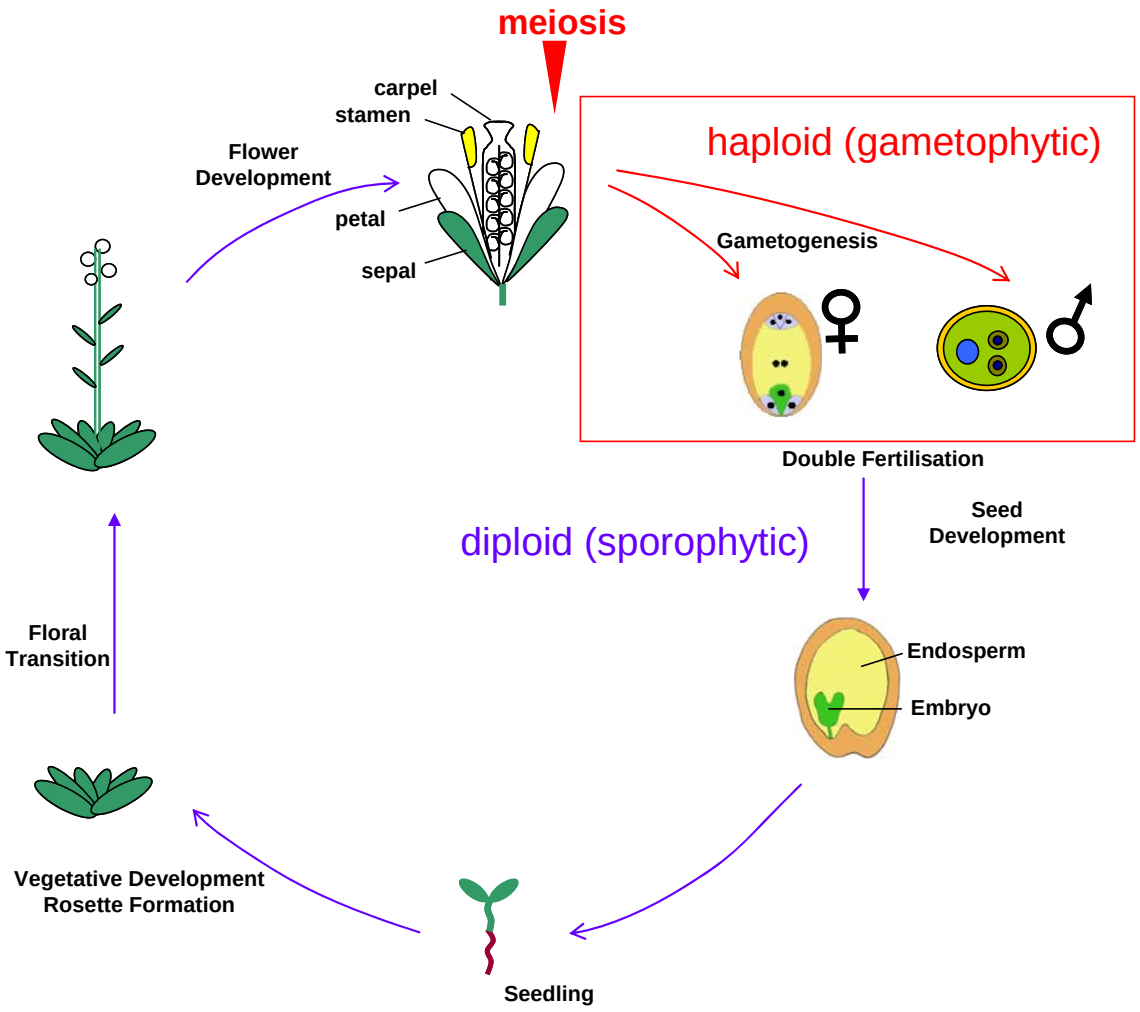

Fig. 1-3. The life cycle of *Arabidopsis thaliana*. *Arabidopsis* life cycle alternates between a diploid sporophytic phase and a haploid gametophytic phase. The sporophytic phase dominates the life cycle until meiosis initiates the gametophytic phase. Then double fertilization terminates the gametophytic phase and a new generation begins.

1.2.2. Flower: the display of sexual reproductive organ

Flowers contain both male and female reproductive organs. The flower consists of four concentric whorls or specific organs (Fig. 1-3). The first and second whorls are represented by sepals and petals respectively. Sepals and petals protect the reproductive organs in the third and fourth whorls and attract pollinators in many species. Stamens occupy the third whorl and produce the male gametophytes, which mature as pollen grains. Carpels enclosing female ovules constitute the fourth whorl at the center of the flower. Each ovule contains a female gametophyte.

1.2.3. Male gametophyte development

The Arabidopsis male gametophyte produces the pollen grain, a three-celled organism derived from stereotypical cell divisions. Male gametogenesis (Fig. 1-4) starts from stamen cells derived from the L2 layer (the layer next to the outer-most layer of the shoot apical meristem). The L2 cells divide into a primary parietal cell (PPC) and the sporogeneous cell (SC). The SC differentiates into the pollen mother cell (PMC), which undergoes meiosis to form a tetrad of haploid microspores. The microspore enlarges and then undergoes an asymmetric mitosis producing two unequal-sized daughters, the vegetative and the generative cells. The two cells of the bicellular pollen grain have strikingly different fates. The larger vegetative cell exits the cell cycle and does not divide again. It eventually evaginates a tip-growing structure – the pollen tube – that penetrates the ovary. The smaller generative cell is engulfed inside the cytoplasm of the vegetative cell and forms a specialized “cell within a cell” structure. The generative cell

constitutes the plant male germline, and undergoes the second pollen mitosis, producing the two male gametes, also called sperm cells (McCormick, 2004).

1.2.4. Female gametophyte development

The female gametophyte (Fig. 1-4), also termed the embryo sac, develops within the ovule in the carpel. In Arabidopsis the diploid megaspore mother cell undergoes meiosis and produces four haploid megaspores. Subsequently, three megaspores, generally towards the micropylar side where the pollen tube enters, undergo cell death. The remaining functional megaspore undergoes three rounds of mitosis without cytokinesis, resulting in an eight-nucleate coenocyte. During cellularization, two nuclei migrate toward the center of the developing female gametophyte and fuse together to form the homodiploid central cell. These events create the embryo sac, a seven-celled structure consisting of three antipodal cells, two synergid cells, one central cell, and one egg cell (Yadegari and Drews, 2004).

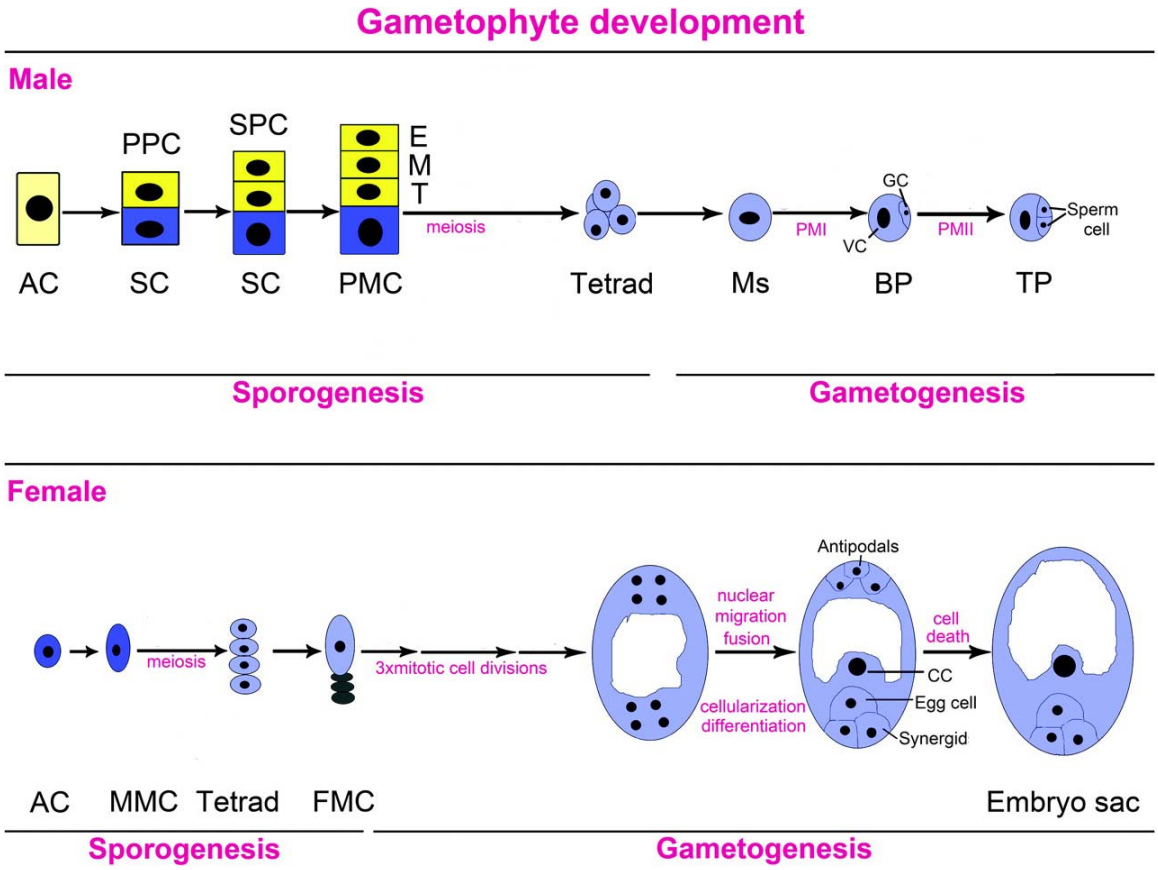

Fig. 1-4. Sequential Development of Gametophytes in *Arabidopsis*. AC, archesporial cell; BP, bicellular pollen; CC, central cell; E, endothecium; FMC, functional megaspore; GC, generative cell; M, middle layer; MMC, megaspore mother cell; Ms, microspore; PMC, pollen mother cell; PM I, pollen mitosis I; PM II, pollen mitosis II; PPC, primary parietal cell; SC, sporogenous cell; SPC, secondary parietal cell; T, tapetum; TP, tricellular pollen; VC, vegetative cell. (Adapted from Liu et al., 2008)

1.2.5. Double fertilization

After pollen maturation, the pollen grains are shed on the stigma, a specialized receptive tissue on the top of carpel. In contact with the stigma cells, the pollen grain hydrates and germinates a pollen tube which penetrates the maternal sporophytic tissue and grows towards the ovule. Pollen tube growth is guided by chemoattractants derived from target ovules. The two synergid cells on the side of the egg cell emit a diffusible cysteine-rich peptide, to attract the pollen tube at the last step of pollen tube guidance (Higashiyama et al., 2001) (Okuda et al., 2009). After penetrating the ovule, the pollen tube releases the two sperm cells. Then one of the sperm cells fertilizes the haploid egg cell to form the embryo while the second sperm cell fertilizes the diploid central cell initiating endosperm development. The process is called double fertilization, a unique feature in plant sexual reproduction (Faure et al., 2002) (Berger et al., 2008).

1.2.6. Seed development

Successful double fertilization initiates seed and fruit development. The seed is made up of three genetically distinct components: the diploid embryo develops into the next generation plant; the triploid endosperm surrounds the embryo and nurtures its growth and the seed coat is the outer-most tissue which is produced by the mother sporophyte.

1.2.6.1. Embryogenesis

During seed development the embryo-growth into the mature seedling comprises specific developmental stages of morphogenesis (Fig. 1-5). Embryogenesis commences with a 3-fold elongation of the zygote, followed by an asymmetric cell division, yielding a smaller

apical cell and a larger basal cell. Through successive divisions, two vertical and a horizontal, the apical cell gives rise to a sphere composed of eight cells, the octant stage embryo. Cells of the octant embryo undergo a tangential division yielding an outer layer of eight epidermal precursor cells and a layer of eight inner cells. The embryo then reaches the dermatogen stage. The divisions in the outer layer are predominantly anticlinal, whereas cell divisions of inner cells already reveal axis formation and regional differentiation. At this stage, the external shape of the embryo remains globular. The embryo assumes a triangular shape due to localized proliferation at two opposite positions in the apical region. The early heart stage embryo contains approximately 200 cells and at that stage, the primordia of cotyledons, hypocotyl and primary root are discernible. In torpedo and bent-cotyledon stage embryos, provascular tissues become recognizable within cotyledon primordia. The patterning of the tissues in the bent-cotyledon stage embryo basically equals that of the seedling (Berleth and Chatfield, 2002).

1.2.6.2. Endosperm development

Unlike the embryo, the endosperm doesn't contribute to the next generation beyond seed germination. Alongside the embryo growth, the endosperm also develops according to a distinct well-defined program (Fig. 1-5). The endosperm develops in two phases: syncytial and cellular. First, mitotic divisions of the fertilized central cell in the absence of cytokinesis form a syncytial endosperm containing several hundreds of nuclei. The endosperm nuclei are organized in three mitotic domains that proliferate at distinct rates: the micropylar endosperm (MCE) surrounds the embryo, the peripheral endosperm

(PEN) lines the inside of the seed integuments; and the chalazal endosperm (CZE) has dense cytoplasm and occupies the posterior pole where the maternal vascular tissue adjoins the seed integument (Sorensen et al., 2002).

The endosperm syncytial phase ends with cellularization, a specialized cytokinesis, after the eighth endosperm mitotic cycle (Sorensen et al., 2002). The remobilization of reserves upon germination is the last function of the endosperm before its death.

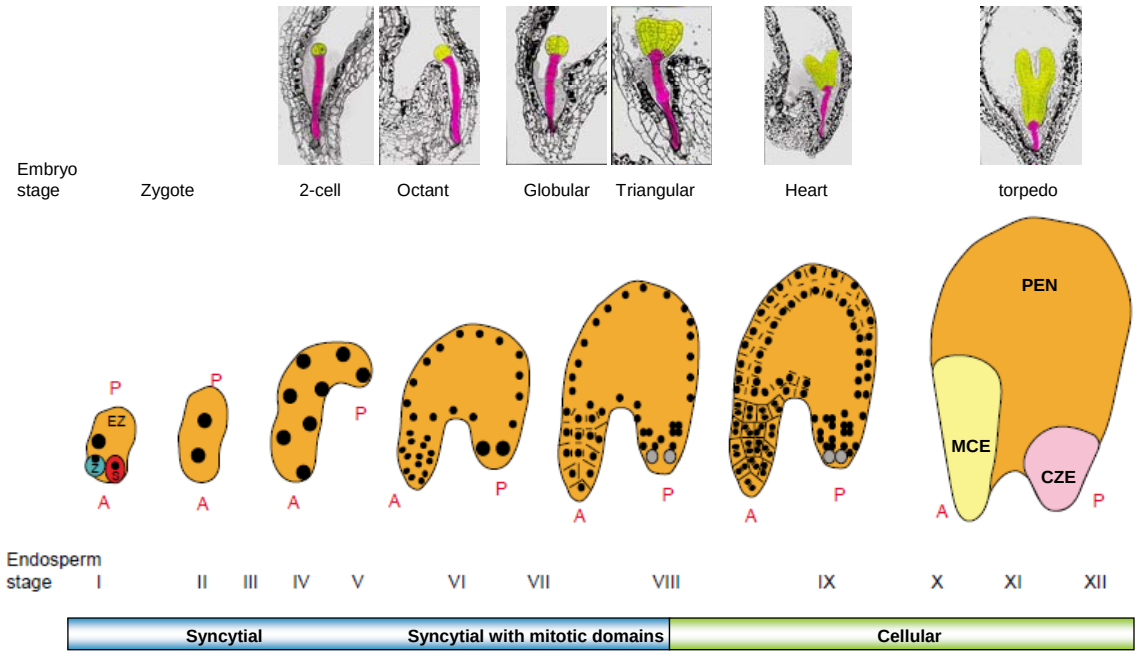

Fig. 1-5. Major steps of endosperm development with corresponding stage of embryogenesis in *Arabidopsis*. Double fertilization produces two zygotic products: a true zygote (Z) and an endosperm zygote (EZ). The true zygote undergoes embryogenesis shown on the top panel. Endosperm development is separated into two major phases at the eighth mitotic cycle, first the syncytial and then the cellular phase. From the anterior pole (A) to the posterior pole (P), three mitotic domains are defined: micropylar endosperm (MCE), peripheral endosperm (PEN) and chalazal endosperm (CZE). (Adapted from Berger, 2003)

1.3. POLLEN DEVELOPMENT

1.3.1. Asymmetric pollen mitosis and differential cell fate

The microspore enlarges while small vesicles develop inside the cytoplasm. The vesicles eventually fuse to form a large vacuole, which pushes the microspore nucleus to a peripheral position against the cell wall. The off-centered position of the dividing nucleus creates an asymmetry. There are no known morphological or molecular cues directing this asymmetry in the microspore.

After cytokinesis, one daughter cell is much smaller than the other. The two cells of the bicellular pollen grain have strikingly different fates. The larger vegetative cell acquires a dispersed chromatin and exits the cell cycle in G1. The vegetative cell inherits the bulk of cytoplasm of the microspore and accumulates an abundance of stored metabolites required for the rapid growth of the pollen tube. By contrast, the smaller generative cell has a nucleus with condensed chromatin and very limited number of organelles and stored metabolites. The generative cell, which can be considered as the plant male germline, undergoes a symmetric division to form two sperm cells.

1.3.1.1. The importance of the asymmetry in PMI

The asymmetrical division PMI is essential for the generative cell differentiation. In tobacco, the treatment of microspores with low concentrations of colchicine caused a symmetrical PMI, producing two equal-sized daughters expressing the vegetative cell fate marker LAT52-GUS. These results suggested that the vegetative cell fate is the

default fate during pollen development and that the activation of vegetative cell-specific genes can be uncoupled from nuclear division and cytokinesis (Eady et al., 1995).

1.3.1.2. Mutants affecting asymmetric mitosis

The asymmetric cytokinesis characteristic of PMI largely relies on the asymmetry generated by the cytoskeleton. The *gemini pollen 1(gem1)* mutant produces microspores that divide less asymmetrically than wild type (Park et al., 1998) (Park and Twell, 2001). GEM1 belongs to the family of microtubule-associated proteins MAP215 and is essential for the correct functioning of the phragmoplast (Twell et al., 2002). *gem2* shows similar phenotypes to *gem1*, but the gene identity is unknown (Park et al., 2004).

TIO is a plant homologue of the Ser/Thr protein kinase FUSED and plays roles in centrifugal plate expansion. Mutant *tio* microspores fail to complete cytokinesis, resulting in binucleate pollen grains (Oh et al., 2005). Two functionally redundant microtubule motor kinesins, PAKRP1/Kinesin-12A and PAKRP1L/Kinesin-12B, localize to the middle region of the phragmoplast to organize microtubules. The *kinesin-12A kinesin-12B* double mutant fails to form a cell plate due to disorganized microtubules (Lee et al., 2007). HINKEL (HIK) and TETRASPORE (TES) are the Arabidopsis orthologues of NACK1 and NACK2 kinesin-related proteins, which are essential for somatic cell cytokinesis in tobacco. The *hik-1 tes-1* double mutant shows cell plate expansion defects during cytokinesis at PMI (Oh et al., 2008). Hence PMI uses general machinery for cytokinesis.

In *gem1*, *gem2*, *tio*, *kinesin-12A*/*12B* and *hit-1*/*tes-1* mutants, a common feature is that the symmetrical division and cytokinetic defect disrupt pollen patterning and formation of the germline. The *sidecar pollen* (*scp*) microspore also fails to divide asymmetrically at PMI. Instead, the symmetric division produces two equal-sized cells. Interestingly however, one daughter cell still undergoes the asymmetric division, setting aside the germline. Eventually *scp* mature pollen contain an additional vegetative cell (Chen and McCormick, 1996). The gene responsible for the *scp* phenotype and the molecular mechanism underlying this unique division pattern are still unknown.

1.3.2. Models of cell-fate determination

Four models have been proposed to explain the distinct cell fates after PMI (Fig. 1-6). The first and second models assume a gametophytic factor that activates the vegetative cell fate once its concentration reaches a certain threshold at PMI. In the passive-repression model, the gametophytic factor is excluded from the generative cell pole, preventing expression of vegetative cell-specific genes in the generative cell (Fig. 1-6A). In the second active-repression model, a putative additional repressor of the gametophytic factor is concentrated at the generative cell pole to block activation of vegetative cell specific genes in the generative cell (Eady et al., 1995) (Fig. 1-6B). Recently a third model was proposed with the identification of a germline-restrictive silencing factor (GRSF) from Lily. GRSF recognizes silencer sequences in promoters of genes specific to the germline and represses these genes in cells that are not destined to become generative or sperm cells. GRSF is present in uninucleate microspores but becomes absent in the generative cell after PMI, parallel to the activation of the male germline–specific

transcriptional program (Fig. 1-6C). The release from GRSF-imposed repression might be a determining event in plant germline specification (Haerizadeh et al., 2006). A fourth scenario could involve a germline factor activating the generative cell fate and localized exclusively in the generative cell (Fig. 1-6D). One example is the MYB transcription factor DUO1, which is only expressed in the generative lineage and is responsible for activation of several genes essential for germline differentiation (Brownfield et al., 2009).

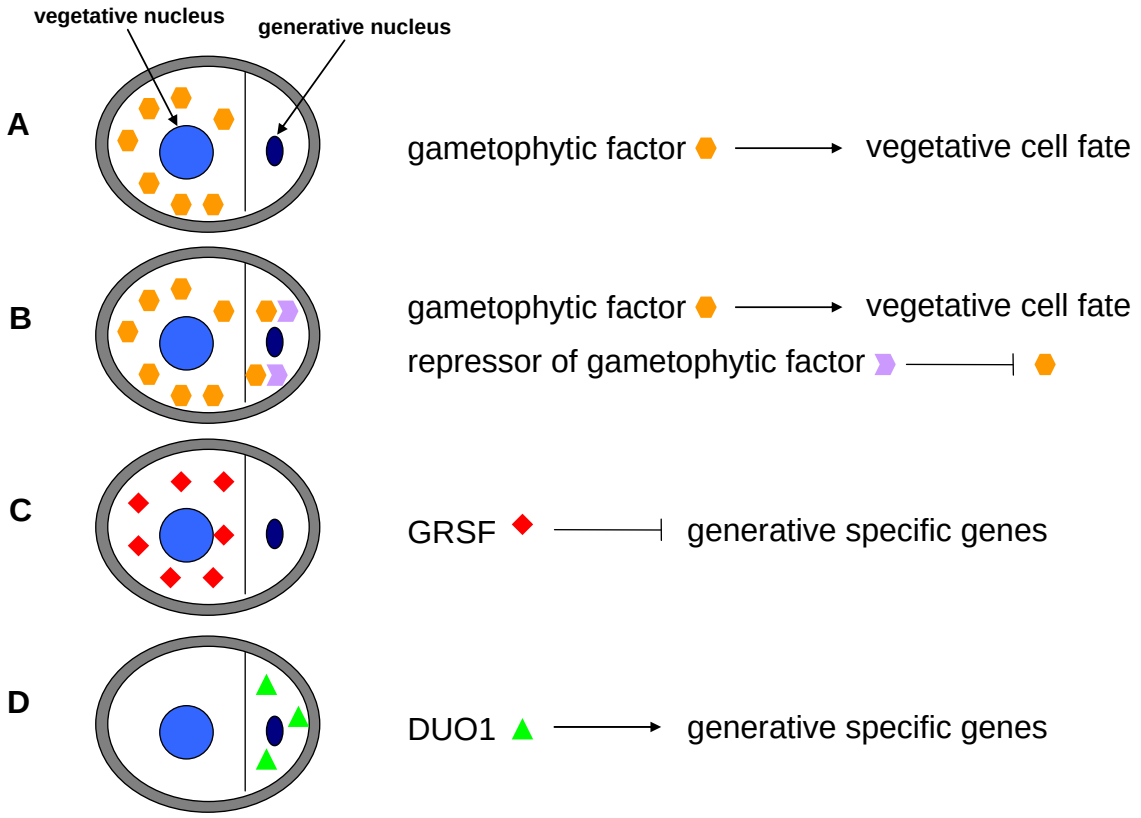

Fig. 1-6. Models of cell-fate determination at PMI. (A) A gametophytic factor activating the vegetative cell fate is excluded from the generative cell pole. (B) The gametophytic factor is distributed universally, and an additional repressor of the gametophytic factor is concentrated at the generative cell pole. (C) GRSF represses generative cell-specific genes is absent in the generative cell. (D) DUO1 activates the generative cell-specific genes and is localized exclusively in the generative cell.

1.3.3. Symmetric pollen mitosis and sperm cell formation

The generative cell further divides symmetrically, giving rise to the sperm cells. The timing of PMII is regulated differently among species. Arabidopsis, Rice and Maize shed tricellular pollen, as PMII takes place within the pollen grain prior to anthesis. In contrast, other species (Lily and Tobacco) shed bicellular pollen, and PMII occurs during pollen tube growth.

After PMII a new S phase is initiated during pollen maturation and is completed at the end of pollen tube growth in Arabidopsis. Several screens were performed looking for mutants defective in pollen development, but so far no mutant was shown to have multiple sperms due to cell cycle deregulation of PMII.

1.3.3.1. The two sperms, same or different?

Despite the symmetry of PMII leading to morphologically identical sperm cells, the dimorphism of sperm cells has been raised based on several observations. A cytoplasmic extension between one of the two sperm cells and the vegetative cell nucleus was observed by transmission electron microscopy in Plumbago. The sperm cell connected to the vegetative nucleus contains mitochondria, but no or fewer plastids and preferentially fertilizes the central cell (Russell, 1985). In maize lines carrying B chromosomes, the B centromere undergoes nondisjunction at PMII, so that one sperm cell acquires two B centromeres and the other acquires none (Rusche et al., 1997). Although early studies reported that B chromosomes are transmitted preferentially to the egg cell (Roman, 1948), this was not confirmed by more recent work (Faure et al., 2003). In Arabidopsis,

no dimorphism was reported amongst sperm cells, but a functional specialization of each sperm cell relative to the capacity to fertilize the egg cell or the central cell has remained unsolved.

1.3.3.2. Mutants affecting the generative cell division

Mutants affecting PMII have led to identification of components of the core cell cycle machinery. The Arabidopsis genome possesses only a single A-type cyclin-dependent kinase (CDKA) unlike animal genomes that encode two types of CDK acting at different cell phase transitions (Vandepoele et al., 2002). The generative cell of *cdka* mutant pollen does not usually divide to form two sperm cells. (Iwakawa et al., 2006) (Nowack et al., 2006). A similar phenotype is present in the *fbl17* mutant. FBL17 participates in the SKP1-CUL1-F-box protein E3 ubiquitin protein ligase complex, which degrades the CDK inhibitors KRP6 and KRP7 in a proteasome-dependent manner (Kim et al., 2008) (Gusti et al., 2009). The single generative-like cell is capable of fertilization indicating that generative cell differentiation may be uncoupled from cell division.

A single generative-like cell phenotype is also observed in the *duo1* mutant. Unlike *cdka* and *fbl17*, *duo1* pollen is sterile. *duo1* single generative-like cells complete S-phase but fail to enter mitosis (Durbarry et al., 2005). DUO1 encodes a R2R3 MYB protein expressed specifically in the generative lineage (Rotman et al., 2005) (Table 1-1). Recently, DUO1 has been shown to be required both in generative lineage differentiation and generative cell division. In *duo1*, the expression of male germline-specific genes (Table 1-1) such as *HISTONE THREE RELATED 10* and *GEX1* is prevented. The mutant *duo1* generative cells also lack expression of the G2/M regulator AtCycB1;1. Thus,

DUO1 is a key regulator in the production of functional sperm cells by linking germline specification and cell cycle progression (Brownfield et al., 2009).

Past studies have shown that the generative cell fate regulated by DUO1 is controlling cell type specific proliferation, which is essential in order to deliver sperm cells with fully replicated DNA. However the relationship between the timing of PMI and cell fate commitment remains unclear. It certainly requires asymmetrical location of factors although cell size could also be determinant.

Table 1-1. Cell lineage markers in pollen.

Gene ID	Gene	Reporter	Protein annotation	Expression and localization in pollen	Reference
At5g59040	MSP1	GUS	Unknown	MS	(Honys, 2006 #115)
At5g59040	LAT52	GFP	Transcription factor	VC; Nucleus	(Twell, 1992)
At3g60460	DUO1	RFP	R2R3 MYB transcription factor	GC-SC; Nucleus	(Durbarry, 2005); (Rotman, 2005)
At1g19890	HTR10	RFP	H3.3 histone variant	GC-SC; Nucleus	(Okada, 2005); (Ingouff, 2007)
At4g11150	E1/TUF	GFP	Vacuolar H^+-ATPase subunit E isoform 1	GC-SC; membrane	(Strompen, 2005 #407)
At5g55490	GEX1	GFP	Transmembrane domain protein	SC; membrane	(Engel, 2005)

1.4. AIM OF THE STUDY

In order to investigate the relationship between cell cycle and cell differentiation I used several genetic approaches to deregulate the cell cycle in Arabidopsis pollen, and observed the impact on cell differentiation during development.

I choose to focus my study on RBR and MSI1, which are likely amongst the pivotal controls linking cell division and cell fate. RBR and MSI1 participate in multiple protein complexes with a broad range of cellular functions and it is thus possible to dissect which complex is involved by targeting each specific complex component.

1.4.1. S phase chaperones – Chromatin Assembly Factor 1

During S phase, DNA replication is paralleled with the assembly of histones into nucleosomes. The Chromatin assembly factor 1 (CAF1) (Hennig et al., 2005) has a conserved chaperone activity for chromatin assembly at the DNA replication fork. CAF1 targets histone H3-H4 dimers to the newly synthesized DNA, thus allowing nucleosome assembly (Polo and Almouzni, 2006).

In mammals, CAF1 consists of the three proteins p150, p60 and p48. Loss of CAF1 activity affects cell viability and leads to activation of a DNA-damage signaling pathway that slows down the S phase and arrests the cell cycle (Haushalter and Kadonaga, 2003). In yeast, the CAF1 subunits Cac1, Cac2 and Cac3 are dispensable for cell viability (Ridgway and Almouzni, 2001), but loss of CAF1 causes increased sensitivity to DNA-

damaging stress (Linger and Tyler, 2005). In Arabidopsis, CAF1 contains FASCIATA1 (FAS1), FASCIATA2 (FAS2) and the pRbAp48 homolog MULTICOPY SUPPRESSOR OF IRA1 (MSI1) (Kaya et al., 2001). Reduction of FAS1 and FAS2 activities up-regulates the expression of genes in the DNA damage response pathway (Schonrock et al., 2006). In the absence of CAF1, cells endoreduplicate to higher levels, suggesting that loss of FAS1 or FAS2 affects the G2/M transition (Endo et al., 2006) (Exner et al., 2006) (Kirik et al., 2006) (Ramirez-Parra and Gutierrez, 2007). In addition to the deregulation of the cell cycle, the loss of CAF1 function causes a reduction in heterochromatin (Kirik et al., 2006), releases transcriptional gene silencing from endogenous transposons (Ono et al., 2006) and alters the pattern of histone acetylation and methylation at promoters of genes encoding components and regulators of the cell cycle (Ramirez-Parra and Gutierrez, 2007).

The CAF1 member MSI1 is also a component of Polycomb group (Pc-G) repressive complexes 2 (PRC2). PRC2 complexes methylate the lysine residue 27 of Histone 3 (H3K27) and maintain a repressive chromatin state. Loss of epigenetic marks causes cells to proliferate and de-differentiate. Members of the PRC2 that are active during Arabidopsis seed development are encoded by FERTILISATION INDEPENDENT SEED (FIS) genes: MSI1, MEDEA, FIE and FIS2 (Guitton and Berger, 2005a). *msi1* ovules initiate seed development in the absence of fertilization (Kohler et al., 2003). In addition to this gametophytic effect, a sporophytic effect causes defects in cell division in early stages of embryogenesis of the *msi1* homozygous mutant (Guitton and Berger, 2005b). MSI1-cosuppression plants revealed that MSI1 is required to maintain the correct

temporal and organ-specific expression of homeotic genes, and MSI1 was proposed to have an essential role for cell differentiation rather than proliferation (Hennig et al., 2003). In agreement with the role of MSI1 in cell differentiation, in Drosophila Schneider line 2 cells, p55 is only required for repression of developmentally regulated E2F targets and not for repression of cell-cycle-regulated E2F targets (Taylor-Harding et al., 2004).

In addition to the participation of CAF1 and PcG complexes, MSI1 binds to RBR in plants (Ach et al., 1997). Recently this binding was validated in Arabidopsis (Jullien et al., 2008). Thus, MSI1 appears to be an integrator of cell cycle, chromatin assembly and chromatin modification (Fig. 1-7).

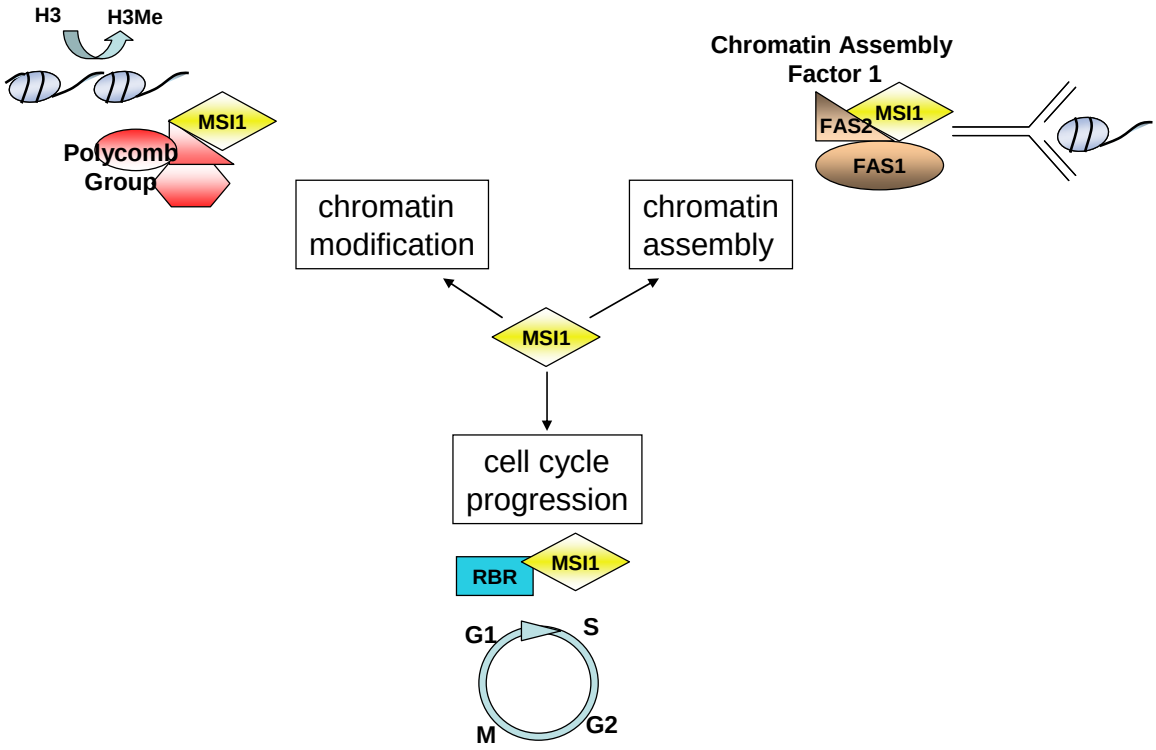

Fig. 1-7. MSI1 is an integrator of cell cycle, chromatin assembly and chromatin modification.

1.4.2. G1/S cell cycle repressor – RBR

Despite the complexity of cell cycle genes in Arabidopsis genome, Arabidopsis has a single Retinoblastoma-Related gene (RBR) (Vandepoele et al., 2002) (Fig. 1-8). Although the sequence homology is low, the RBR protein contains the two conserved A and B pocket domains and potential sites for phosphorylation. Arabidopsis contains six E2F related proteins and two distantly related DP (DP1 and DP2) members (Vandepoele et al., 2002) (Fig. 1-8).RBR represses the G1/S transition by binding to E2F. After phosphorylation by CDKA, RBR loses its affinity to E2F. Released E2F activates its target to initiate DNA replication. Structurally the E2Fs are divided into two subgroups: the first group contains E2FA, E2FB and E2FC. These three E2Fs have all the conserved domains including the DNA-binding, dimerization, transactivation and RB-binding domains. The second group contains DP-E2F-like proteins (DEL1, DEL2 and DEL3). DELs are structurally related to mammalian E2F7 and E2F8 that lack all the E2F-specific domains except the DNA-binding domain. In contrast to E2Fs, Arabidopsis DEL DNA-binding function does not require hetero-dimer formation with the two known dimerization partner proteins, DPA and DPB. The three E2Fs interact with RBR by physically associating within their C-terminal region, but there is no known binding site for RBR1 in DELs.

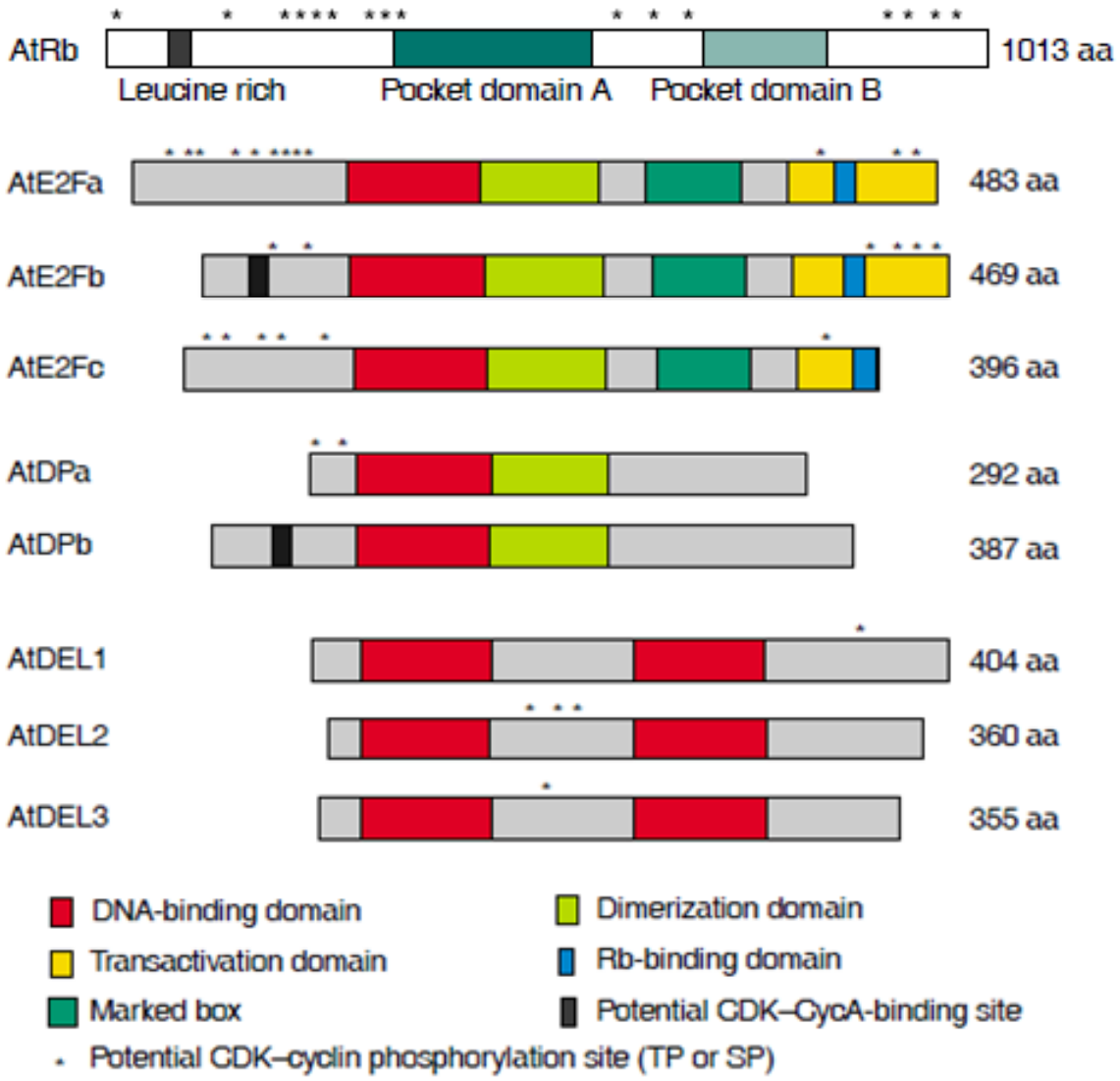

Fig. 1-8. Structural organization of pRb and E2F family proteins in Arabidopsis. Arabidopsis contains a single pRb homologue. Based on the conservation of different domains, the eight Arabidopsis E2F family proteins are classified into E2F, DP and DEL groups. (Adapted from Shen, 2002)

In plants, the study of RBR function started only in recent years after RBR was identified. Biochemical studies showed that the G1/S transition is similarly controlled as in animals. The E2Fs and DPs are inactive upon binding with RBR. Upon perceiving the growth stimulus, CDKD–cyclin D phosphorylates CDKA on Threonine 160/167, enabling CycD3;1 to bind. CyCD3;1 activates CDKA that in turn phosphorylates RBR. The phosphorylation of RBR releases the E2F complex, which induces the expression of S-phase-specific genes (Francis, 2007). Genetic studies found that RBR functions mainly in cell proliferation, cell differentiation and is linked with epigenetics (Fig. 1-9). Inactivation of *RBR* in Arabidopsis completely impairs female gametogenesis, which precludes a direct assessment of the role of RBR in post-embryonic development (Ebel et al., 2004) (Ingouff et al., 2006). Loss of RBR during female gametogenesis causes cell over-proliferation but does not seem to have a major impact on cell fate (Ingouff et al., 2006) (Jullien et al., 2008) (Johnston et al., 2008) (Ingouff et al., 2009). To understand the function of RBR in development, different inducible systems disrupting RBR expression or over-expressing RBR were developed. Virus-induced gene silencing of NbRBR in Tobacco led to deregulation of cell proliferation, differentiation, and endoreduplication (Park et al., 2005). RNA interference and inducible over-expression of Arabidopsis RBR showed impaired stem cell maintenance in roots (Wildwater et al., 2005). Inducible expression of a geminivirus RBR-binding protein in Arabidopsis leaves suggested that RBR inhibits cell division and endoreduplication in a cell type-dependent manner (Desvoyes et al., 2006). The leaf epidermal pavement cells and the mesophyll cells in the inner layers show distinct responses to RBR inactivation.

RBR represses MET1 expression (Jullien et al., 2008) and recruits members of chromatin modifying complexes; thereby the loss of RBR likely causes epigenetic modifications inherited through cell divisions as shown for deregulation of the activity of the DNA methylation (Chan et al., 2005) (Mathieu et al., 2007). Epigenetic modifications could impact cell fate with secondary effects on proliferation. Alternatively deregulation of cell proliferation could directly impact differentiation and cell fate. Thus it is difficult to analyze the direct impact of RBR on differentiation in experimental strategies perturbing RBR function during a large number of cell divisions before differentiation takes place.

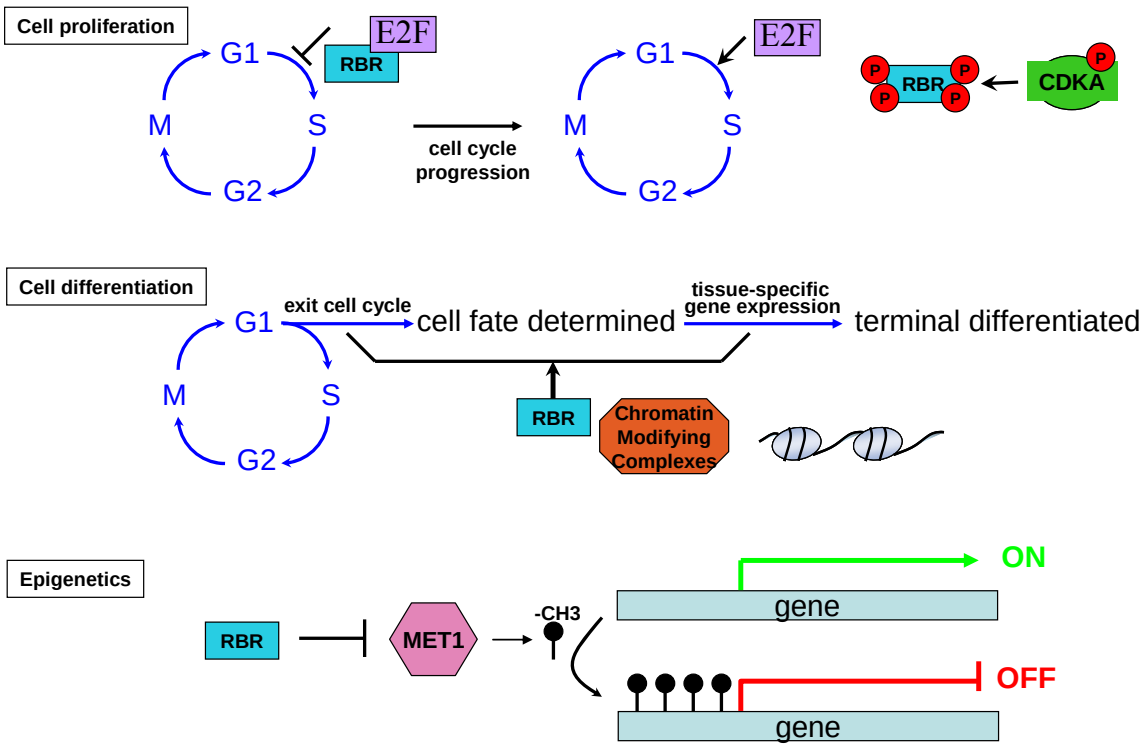

Fig. 1-9. RBR coordinates cell proliferation and cell differentiation, and is involved in epigenetic machinery.

1.4.3. Strategy of the study

I took the advantage of the simple cell cycle mode of pollen development to investigate the effect of *rbr* and *msi1* mutants on cell fate and division. In addition to its relatively simple developmental mode, pollen development offers the possibility to study the direct effect of the absence of essential functions. In plants heterozygous for a loss of function mutation, half of the haploid mutant microspores produced by meiosis inherit the mutation and experience a sudden deprivation of the function associated to the mutated gene. This unique feature allowed me to monitor the direct impact of the loss of RBR or MSI1 on cell proliferation and cell fate in developing pollen using a series of markers of cell fate (Table 1-1).

My study allowed me to observe the impact of cell cycle arrest on cell fate in response to the loss of MSI1 (Chapter 3.1) and the complex effect of hyperproliferation on cell fate linked with deregulation of RBR (Chapter 3.2). In addition I undertook a suppressor screen to identify additional controls involved in RBR function (Appendix I).

CHAPTER II

MATERIALS AND METHODS

2.1. MATERIALS

2.1.1. Plant material

The wild-type ecotypes Columbia (Col-0), Landsberg *erecta* (Ler), Enkheim (En) and C24 were provided by the Nottingham Arabidopsis Stock Centre. The *A. thaliana rbr* mutant alleles (Columbia accession) used in this study were *rbr-2* (SALK_002946; SALK collection), and *rbr-3* (GABI_170G02; GABI-Kat collection). The mutant allele *msi1-1* (Col background) was previously characterized and kindly provided by Lars Hennig (Kohler et al., 2003). The mutant allele *msi1-2* (C24 background) was previously described in the laboratory in Frederic Berger's group (Guitton et al., 2004). The mutant allele *msi1-3* (Ler background) was obtained and provided by Venkatesan Sundaresan. The mutant allele *msi1-4* (Col background) was obtained and kindly provided by Gary Drews and Jayson Punwani (University of Utah). Seeds of *qrt1*/*qrt1* (Ler accession) were provided by D. Preuss. Homozygote *fas1-1* (CS265 En background) *fas1-4* (SAIL_662_D10 Col background) and *fas2-4* (SALK_033228, Col background) seeds were obtained from the Arabidopsis Biological Research Center.

The KS22 enhancer-trap line (C24 accession) expressing the GFP reporter protein was generated in J. Haseloff's laboratory (www.plantsci.cam.ac.uk/Haseloff). Marker lines for cell identity in pollen refer to Table 1. pLAT52-GFP (Col) was a gift from Alice Cheung (Amherst, MA). AC26 was obtained by A. Chaboud (Unite Mixte de Recherche 9004, Lyon, France) from C24 plants transformed with pACTIN11-Histone-mRFP1; E1 GFP (Col) was a kind gift from G. Strompen (Strompen et al., 2005). ATGEX1 marker

line was a kind gift from Sheila McCormick (Engel et al., 2005). The marker HTR10-mRFP1 results from a genomic fusion of the male gametophyte specific histone 3 variant with mRFP1 (Ingouff et al., 2007).

2.1.2. Enzymes, primers and kits

Restriction enzymes were from New England Biolabs. Taq ploymerases used for genotyping were homemade Taq polymerase from Temasek Life Sciences Laboratory, Go-Taq from Promega and DNA polymerase from GE healthcare. KOD-plus DNA polymerase from TOYOBO was used for cloning. Kits were supplied from QIAGEN.

2.1.3. Cloning vectors and constructs

The following vectors and constructs were used in this work:

pGEM-T easy (Promega) for basic ligation and sequencing purposes

pAlligator 2 gateway vector (Bensmihen et al., 2004); (http://www.isv.cnrs-gif.fr/jg/alligator/vectors.html)

pTCP16-hp and pDONR207-RBRRNAi gateway vectors from David Twell's Lab

pGREENII (pGII)-based gateway vector: pGIInK-GW-mRFP1-35ter

2.1.4. Bacterial strains

For standard cloning the *Escherichia coli* strains XL-blue and DH5alpha were used. The DB3.1 strain, which is resistant to the ccdB gene, was used for the Gateway vectors. For plant transformation *Agrobacterium tumefaciens* strain C58 was used.

2.2. METHODS

2.2.1. Plant work

2.2.1.1. Plant growth conditions

After 3 days at 4°C in the dark, seeds were germinated and grown on soil or plates containing Murashige and Skoog medium. Plants were grown at 18°C in a growth room with an 8-hour day/16-hour night cycle until they formed rosettes. Flowering was then induced at 22°C in Conviron growth chambers with a 16-hour day/8-hour night cycle.

2.2.1.2. Seed surface sterilization

The seeds were sterilized by a 3 min incubation in 70% ethanol + 0.05% SDS followed by 1 min incubation in 95% ethanol. Afterwards the seeds were washed with absolute ethanol and then plated on MS-Agar plates within the plant hood.

Alternatively the seeds were sterilized in a small vacuum container. The seeds were put inside envelopes and placed in the middle of the container. 10 ml of bleach was placed at the bottom of the container. 3.5 ml of concentrated hydrogen chloride was added into the bleach and the lid of the vacuum container was closed immediately afterwards. The chlorine produced by this reaction was used to sterilize the surface of the seeds for overnight. The seeds were then plated as indicated above.

2.2.1.3. Crossing of plants

When the flowers were closed and the pollen of the anthers was not ripe, the anthers of the acceptor flower were removed completely using fine forceps. All remaining older and younger flowers from the same branch were also removed. In the morning of the following day, the stigma on top of the carpel was pollinated with mature pollen from the donor plant.

2.2.1.4. Plant transformation

Plants were transformed according to the "floral dip" method (Clough and Bent, 1998). Before transformation about 500 ml of Agrobacterium culture was raised. The bacterial culture was centrifuged and suspended in 5 % sucrose and 0.05 % Silwet L-77. The siliques of the plants were removed and the flower meristems were dipped in this solution for approximately 60 sec and then horizontally placed in a moist chamber in the dark. The plants were transferred to the greenhouse on the following day.

2.2.2. Molecular-biological methods

2.2.2.1. Genomic DNA preparation from plant tissue

1. Collect 2~3 rosette leaves in a 2 ml tube with a metal ball inside,
2. Freeze in liquid nitrogen and grind tissue using Tissuelyser machine for about 30 sec,
3. Add 400 µL of Edwards extraction buffer,
   (200 mM Tris-HCl pH7.5, 250 mM NaCl, 25 mM EDTA, 0.5% SDS)
4. Vortex 5 sec; leave at RT until all preps are ready,
5. Centrifuge at 13000 rpm for 5 min,
6. Transfer 300 µL of supernatant into a fresh tube,

7. Add 300 µL of isopropanol, mix, leave at RT 2 min,

8. Centrifuge 5 min at 13000 rpm, remove isopropanol,

9. Wash the pellet with 200 µL 70% EtOH and centrifuge 1 min at 13000rpm,

10. Remove EtOH; air dry pellet 15 min,

11. Resuspend in 100 µL of H2O and store at -20°C.

(Use 1 µL DNA sample for a 20 µL PCR reaction.)

2.2.2.2. Plasmid DNA preparation from bacteria

1. Centrifuge the bacterial culture in an eppendorf tube at 5000 rpm for 3 min,

2. Remove the LB medium,

3. Resuspend the pellet with 200 µL TE buffer, RNase 100 µg/mL,

4. Add 200 µL of NaOH, 0.2M; 1% SDS (fresh),

5. Add 200 µL CH_3COOK, 3M, pH=5 and mix by inverting the tube,

6. Centrifuge at 13000 rpm for 15 min RT,

7. Keep the supernatant and add to it 2 volumes of 100% EtOH,

8. Centrifuge at 13000 rpm for 5 min RT,

9. Wash the pellet with EtOH 70% at RT,

10. Centrifuge at 13000 rpm, 5 min,

11. Air dry the pellet 15 min at RT,

12. Resuspend in 20 µL of TE.

Alternatively, plasmid DNA was prepared with a Plasmid MiniPrep Kit from Qiagen.

2.2.2.3. Segregation and sequencing of *msi1-3, msi1-4*

The *msi1-3* allele initially was named MEE70 from an Ac/Ds screen (Pagnussat, 2005). *msi1-3* was sequenced using the Ds primer Ds5-3 (TACCTCGGGTTCGAAATCGAT, all primer sequences throughout the thesis abide the order from 5' to 3') and the *MSI1* specific primer 5g58220 (CTTCGCGAATTCGGAGCTTCC). The *msi1-3* mutant plants were linked to kanamycin resistance.

S184 (*msi1-4*) was transposon-mutagenized. The binary vector used to generate the lines contained a T-DNA that carried a non-autonomous Spm derivative containing the BAR gene selectable marker, a counter selectable genetic marker, and a Spm transposase. Germinated progeny of S184 in the presence of basta showed the ratio of resistant:sensitive = 1.3:1. The transposon insertion site identified by Inverse PCR was within the gene At5g55620, which is located at position 22547430-22548165. This position is 1025093 nucleotides from the *MSI1* gene (At5g58230). Two SALK lines with insertions in At5g55620 had no phenotype. Careful segregation analysis showed that the transposon insertion site was not responsible for the *msi1* phenotype.

DNA was extracted from *msi1-4/+* leaves and amplified by *MSI1* specific primers 1F (GGAATAACAAAGACATCGCCGA) and 6R (CCCACTTGCTACCATCCTCTCA). PCR products were ligated with pGEM-T easy vector (Promega) and transformed into DH5α competent cells. Plasmids were extracted by Miniprep Kit (Qiagen) and sequenced by SP6 and T7 promoter primers (Cat.# Q5011, Cat.# Q5021, Promega).

2.2.2.4. PCR and Genotyping

For *rbr-2*, use primers:

LBb1: GCGTGGACCGCTTGCTGCAACT

rbr1_F3429: GGCCATCGCTTGCATTGGAGA

RBR1_R4449: CTGTGGTTGCTTCCGGTAGT

Tm=65, Elongation for 60 seconds, 35 cycles

wt has 1 band, *rbr-2* heterozygote has 2 bands (one of the bands is the same as wt band).

For *rbr-3*, use primers:

RBR1_F2603: GGCGAACTTGATGAGAGGGT

RBR1_R4: CAGTACCAATTCAGCTGAGCA

o8409: ATATTGACCATCATACTCTCATTGCTGATC

Tm=62, Elongation for 40 seconds, 35 cycles

wt has 1 band, *rbr-3* heterozygote has 4 bands (one of the bands is the same as wt band).

For *cdka-1*, a fragment around 800 bp was amplified using the primers:

J504-Salk_LB: GCGTGGACCGCTTGCTGCAACTCTCTCAGG

N034-wtCDKA1: CCAGATTCTCCGTGGAATTGCG

Tm=65, Elongation for 60 seconds, 35 cycles

Only the mutant shows the band.

For *msi1-1* a fragment around 800 bp was amplified using the primers:

LB1: GCCTTTTCAGAAATGGATAAATAGCCT

3R: CCATCGAATGAGCAACCACAGA

Tm=62, Elongation for 45 seconds, 35 cycles

Only the mutant shows the band.

For *msi1-2*, a 122 bp fragment was amplified using the primers:

m2F: ATACCTCCGAGAGCGGGCC

m2R: CACAGCCAAAGCCACCAAAT

The fragment was digested for 3 h with AvaI to distinguish the wt fragment (103 bp) from the mutant fragment (122 bp).

For *msi1-3*, a fragment about 200 bp was amplified using the primers:

Ds5-3: TACCTCGGGTTCGAAATCGAT

MSI1 specific primer 5g58220: CTTCGCGAATTCGGAGCTTCC

Tm=60, Elongation for 30 seconds, 35 cycles

Only the mutant shows the band.

For *msi1-4*, a 505 bp fragment was amplified using the primers:

mF434: CTCGGTACCCAATTACTTGATGCT

R939: GAGCATCATCAGAGCCACT

Tm=62, Elongation for 30 seconds, 35 cycles

Only the mutant shows the band.

For *fas1-1*, a 276 bp fragment was amplified using the primers:

F345: GGTAGCTGTGAAGAGTGCTGT

R497: CCACGAACGGAACTCGGCATGA

The fragment was digested with *DdeI* to distinguish the wt pattern (155 bp + 121 bp) from the heterozygote pattern (155 bp + 121 bp + 109 bp) and homozygote pattern (155 bp + 109 bp).

2.2.2.5. RNA preparation from plant tissue

Sample tissues were collected and immediately frozen in liquid nitrogen. Tissues were ground, and total RNA was prepared using RNeasy mini kit (Qiagen). DNase treatment was done on 2 mg of total RNA using DNase free kit (Ambion).

2.2.2.6. RT-PCR

For reverse transcription, 500 ng of total RNA was incubated for 1 h at 42^{o}C with 200 units of murine leukemia virus reverse transcriptase (Fermentas) in a 20 ml reaction mixture containing 4 mM oligo(dT) primer (TTTTTTTTTTTT), reaction buffer, 1 mM deoxynucleotide triphosphate, and 40 units of recombinant RNasin ribonuclease inhibitor (Promega). The reaction was stopped by incubation at 90 ^{o}C for 10 min.

2.2.2.7. Cloning

RBR Hairpin Interference Plasmid Construction and Transformation

To express hairpin dsRNA targeted to RBR transcripts specifically in the vegetative cell, 500 bp of RBR coding sequence was cloned in sense and antisense orientations into a modified Gateway expression vector pK7LAT52RNAi harboring the vegetative cell-specific LAT52 promoter. A 495 bp LAT52 promoter fragment was amplified using

KOD HiFi DNA Polymerase (Novagen) with primers containing restriction sites for *HindIII* and *XhoI*. The LAT52 promoter fragment was cloned into a Gateway RNAi destination vector pK7gwiwgL using the *HindIII* and *XhoI* sites to generate the pK7LAT52hpRNAi vector. A 500 bp RBR fragment was amplified by PCR and cloned by recombination using the Gateway cloning system (Invitrogen) to generate the pLAT52hpRBR construct. Verified plasmid was transformed into *Agrobacterium tumefaciens* strain GV3101 and used to generate transgenic lines in *A. thaliana* ecotype Col-0. Transgenic progeny were selected for kanamycin resistance. Transgenic lines expressing the RBR RNAi construct under the control of the germ line-specific promoters of HTR10 and GEX2 were also generated similarly.

RBR:RBR-mRFP1 Plasmid Construction and Transformation

A 6968 bp fragment of *RBR* containing 2 kb upstream of the ATG until the last codon before the termination codon of the gene was amplified by PCR with the KOD-plus-PCR kit and cloned directionally between the Gateway attL recombination sites of the plasmid pENTR-D-TOPO (Invitrogen) to generate the pENTR-D-TOPO-P_{RBR}:RBR entry vector. The fragment containing the cassette Gateway attR, mRFP1, and the nopaline synthase (NOS) terminator (K7GW-mRFP1-NOS) was cloned into the binary plasmid pALLIGATOR2 to generate pAlli2-K7GWmRFP1-NOS. Recombination reactions were performed between the destination vector pAlli2-K7GW-mRFP1-NOS and the pENTR-D-TOPO-P_{RBR}:RBR entry vector to produce the vector pAlli2-P_{RBR}:RBR-mRFP1-NOS. *rbr-2*/+ mutant (kanamycin-selected) plants were transformed. The pALLIGATOR vectors contain the GFP gene driven by a seed storage protein promoter, At2S3, enabling

direct visual selection. Primary seed transformants were collected based on their fluorescence level in the seed and further selected on Murashige and Skoog plates supplemented with kanamycin (50 mg/L).

MSI1:MSI1-mRFP1 Plasmid Construction and Transformation

The full-length *MSI1* cDNA was amplified by PCR and inserted in frame between the gateway cassette (GW) and the monomeric Red fluorescent protein 1 (*mRFP1*) gene contained in the pGREENII (pGII)-based vector pGIInK-GW-mRFP1-35ter. A 3050bp DNA fragment consisting of the upstream region of *MSI1* corresponding to the putative promoter until the beginning of exon3 was amplified by PCR using the KOD-plus-PCR kit and cloned into pCR2-1 TOPO vector (Invitrogen). The final vector pGIInK-promMSI1::MSI1-mRFP1-35S consists of the upstream region of *MSI1*, its first two exons and introns and the remaining *MSI1* cDNA fused to the fluorescent reporter mRFP1. Heterozygous *msi1-1*/+ BASTA-selected plants were transformed.

2.2.3. Microscopy and cytological methods

2.2.3.1. Microscopy and image processing

Fluorescence associated with the KS22 GFP marker and AC26 RFP marker were examined with a stereomicroscope (DM6000, Leica), and images were recorded with a monochrome digital camera (Photometrics, Roper Scientific).

Seeds were cleared in Hoyer's medium (Boisnard-Lorig et al., 2001) and observed with differential interference contrast (DIC) optics with 20× or 40× planapo objective

(DM6000 B, Leica). Images were acquired with a DXM1200F digital camera (Nikon) and processed using Metamorph (version 6.2, Molecular Devices Corp).

For confocal microscopy, seeds were stained with Feulgen as described previously (Garcia et al., 2003) and examined with a Zeiss LSM 510 microscope using the 488-nm excitation line of an argon laser and an emission filter long pass of 510 nm, with a 63× Plan-Apochromat oil immersion objective (n. a. 1.4). Serial optical sections were recorded with 0.4 µm to 0.6µm depth and projections were realized using the Zeiss LSM 510 software. For the images of E1 GFP and DUO1 RFP, pollen grains from anthers were spread within a drop of water on microscope slides. GFP was examined by the 488-nm excitation line of an argon laser and an emission filter long pass of 510 nm. RFP was examined by the 543-nm excitation line of a HeNe laser and an emission filter of 585-615 nm. Figures were composed with Adobe Photoshop 5.5 and Illustrator 9 (Adobe Systems).

2.2.3.2. Sample preparation for Transmission Electron Microscopy

1. Fix overnight in 2.5 % glutaraldehyde in 0.1 M phosphate buffer, pH 7.2 at 4 ^{o}C,

2. Rinse in 0.1 M phosphate buffer, pH 7.2, three changes, 15 min each,

3. Post-fix in 1% osmium tetroxide in 0.1M phosphate buffer, pH 7.2, at RT for 1 hour,

4. Rinse in 0.1 M phosphate buffer, pH 7.2, three changes, and 15 min each,

5. Dehydrate 15 min each in increasing concentrations of ethanol 30%, 50%, 80%, 90%, and then 100% two changes, 15 min each,

6. Two changes in propylene oxide 15 minutes each,

7. Infiltrate with 1:1 propylene oxide-Spurr's resin for two hours,

8. Infiltrate overnight in 100% Spurr's resin,

9. Embed in Spurr's resin and polymerize overnight at 70 ^{o}C,

10. Prepare 85 nm thin sections on Leica Ultracut UCT ultramicrotome. Mount on 200 mesh grids,

11. Stain with 2% uranyl acetate and Reynolds' lead citrate,

12. Observe at 120 kV under a JEM-1230 electron microscope.

2.2.3.3. Whole-Mount preparation of seeds

Developing seeds or pistils were dissected and cleared with a derivative of Hoyer's medium (chloral hydrate:distilled water:glycerol 8:3:1) for 1 hour at RT or overnight at 4 °C before inspection with differential interference contrast optics.

2.2.3.4. LR-White embedding

1. Fix siliques in Acetic acid : Ethanol (1:1), 4^{o}C, 12 h,

2. Rinse with ethanol (100%) twice,

3. Hydration in ethanol: 90%, 70%, 50%, 30%, H_2O, 30 min/each,

4. Incubate in HCl : H_2O =1:1 mix (add H_2O first), 1 h, RT,

5. Incubate in Schiff reagent, 2 h, RT (5 ml),

6. Rinse with ice-cold water,

7. Dehydration in ethanol: 30%, 50%, 70%, 90%, 100%, 30 min/each,

8. Store at -20^{o}C,

9. Incubate in LR white Resin: Absolute ethanol (1:1) for 1 h in small glass dishes,

10. Replace with pure LR white, ~3 h,

11. Replace with pure LR white, overnight,

12. Wash slides by ethanol,

13. Put LR white drops on slide,

14. Dissect sample and put on slide, embedded in LR white,

15. Place number 0 coverslip,

16. In 60^{o}C incubator overnight,

17. In the morning take out slides from incubator,

18. Use razor blade to remove the coverslip,

19. Wash with ethanol to removed un-polymerzied resin.

2.2.3.5. Pollen preparation

Anthers were prepared from flowers of different developmental stages and put in a droplet (~15 µl) of DAPI working solution (0.1 M sodium phosphate, pH=7; 1 mM EDTA; 0.1% Triton X-100; 0.4 µg/mL 4',6-Diamidino-2-phenylindole) on a microscopy slide. The anther was then covered with a cover-slip and slightly squashed to free the pollen or microspores. The slides were then sealed with nail polish and placed in the dark. The preparations were checked for DAPI fluorescence under a fluorescence microscope with a UV-filter.

2.2.3.6. Pollen DNA measurements

Pollen DAPI slides were prepared as described previously. Relative DNA contents of sperm-cell nuclei were measured on the basis of DAPI fluorescence. Images were

analyzed for fluorescence with Metamorph. Relative fluorescence values for nuclei were recorded with a fixed area. A net value for each nucleus was obtained by subtracting a corresponding background reading from the cortical cytoplasm. In order to standardize the relative fluorescence per C value of DNA, we measured the DNA content of early interphase sperm, which by definition possess 1C DNA content. This data was used to calibrate the relative fluorescence per 1C unit.

2.2.3.7. Pollen viability assay

Pollen viability was assessed by Alexander staining.

Alexander staining solution:

95% Ethanol 10 ml,

Malachite green (1% in 95% Ethanol) 1 ml,

Fuchsin acid (1% in water) 5 ml,

Orange G (1% in water) 0.5 ml,

Phenol 5 g,

Chloral hydrate 5 g,

Glacial acetic acid 2 ml,

Glycerol 25 ml,

Distilled water 50 ml.

2.2.3.8. Pollen in vitro germination

For pollen in vitro germination assay, mature pollen at the stage of anther dehiscence was transferred to slides with solid germination medium (0.4 mM $CaCl_2$, 0.4 mM Boric Acid,

0.5 % Agarose, 10 % Sucrose in distilled water, pH adjusted to 7). Germination took place in a moist chamber at 25 °C in constant light overnight.

2.2.3.9. Flow cytometry using Propidium Iodide (PI)

0.5 g of healthy young seedlings, 10 Days after Germination (DAG), was chopped with a sharp razor blade in ice-cold buffer, to release single plant cells. The chopping buffer (15 ml) contained 14.5 ml $MgSO_4$ buffer (2.46 g $MgSO_4.7H_2O$, 3.7 g KCl, 1.2 g Hepes in 1 liter, pH 8.0), 15mg of Dithiothreitol (Sigma), 200 µl of PI Stock (10mg/ml -Sigma) and 375 µl Triton-X 100 Stock (10% w/v); as described by Arumuganathan and Earle (1991). The chopped seedlings were filtered through a 41 µm mesh nylon filter, and centrifuged at 13,000 rpm for 15-20 seconds at 4^oC. The pellet was resuspended in 400 µl Stain Solution (3 ml Chopping Buffer with 7.5 µl RNase; DNase free) and incubated at 37^oC for 15 min prior to flow cytometry analysis on FACSCalibur (Becton Dickson, San Jose).

CHAPTER III

RESULTS

3.1 CHROMATIN ASSEMBLY FACTOR 1 REGULATES THE CELL CYCLE BUT NOT CELL FATE DURING MALE GAMETOGENESIS IN *ARABIDOPSIS THALIANA*

3.1.1. Reduced paternal transmission of *msi1* loss-of-function alleles

MSI1, *FAS1* and *FAS2* are all expressed in mature pollen (Fig. 3-1A) in agreement with micro-array analyses, which also show a level of expression comparable to or lower than levels in leaves and roots (Fig. 3-2). In order to know precisely in which cell types *MSI1* expression takes place during pollen development we produced a translational reporter line for MSI1. We obtained plants that express MSI1 fused to the monomeric Red Fluorescent Protein 1 (mRFP1) under the control of *MSI1* 5' regulatory cis-elements (*pMSI1-MSI1-mRFP1*). The expression of this construct complements the loss of function allele *msi1-1* and thus its expression pattern likely reflects the pattern of MSI1 expression.

We compared our observations of MSI1-mRFP1 expression with the wild-type pattern of chromatin staining by DAPI. The microspore (Fig. 3-1B) undergoes an asymmetric division leading to production of bicellular pollen. This comprises the larger vegetative cell and the smaller generative cell initially positioned at the periphery and later engulfed by the vegetative cell (Fig. 3-1C). The generative cell further divides and produces the two sperm cells (Fig. 3-1D). In contrast to the sperm cells, the large spherical vegetative cell has a larger, less condensed nucleus positioned at the center of the tricellular pollen.

MSI1-mRFP1 is expressed at all stages of pollen development in both cell types (Fig. 3-1E,F,G) as reported in previous micro-array analyses (Honys and Twell, 2004). The level of MSI1-mRFP1 appears to increase in the vegetative cell throughout pollen development while the expression of MSI1 reported by micro-arrays decreases (Fig. 3-2). Our observations suggest that we do not detect only MSI1-mRFP1 inherited through meiosis but rather provide evidence for new synthesis of MSI1-mRFP1 during pollen development. The mRFP1 fluorescence in the generative cell is weaker than in the vegetative cell (Fig. 3-1F). Although the chromatin of the sperm cells is very compact, the MSI1-mRFP1 signal is rather low (Fig. 3-1G). *MSI1* thus appears to be differentially expressed between the vegetative and generative lineage during pollen development.

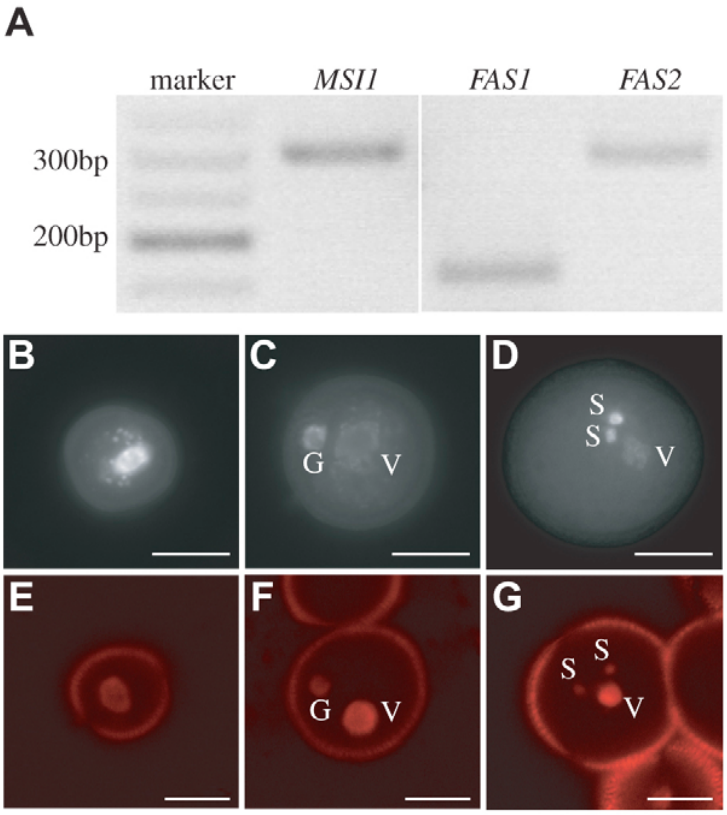

Fig. 3-1. Expression of CAF1 components in pollen.
(A) RT-PCR was performed from RNAs extracted from mature Arabidopsis thaliana pollen grains and shows expression of MSI1, FAS1 and FAS2. (B-D) Wild-type pollen development. Nuclei are stained with DAPI. The uni-nucleate microspore (B) undergoes an asymmetrical mitosis, leading to the bicellular stage (C). At that stage the pollen grain contains a large vegetative cell and a small generative cell with a nucleus showing relatively higher chromatin compaction. (D) The generative cell divides, giving rise to two sperm cells with highly condensed chromatin. (E-G) Expression pattern of promMSI1-MSI1-mRFP1 in pollen in microspore (E), and developing pollen at bicellular stage (F) and tricellular stage (G). Confocal sections. Scale bars: 10 µm. G, generative cell; S, sperm cell; V, vegetative cell.

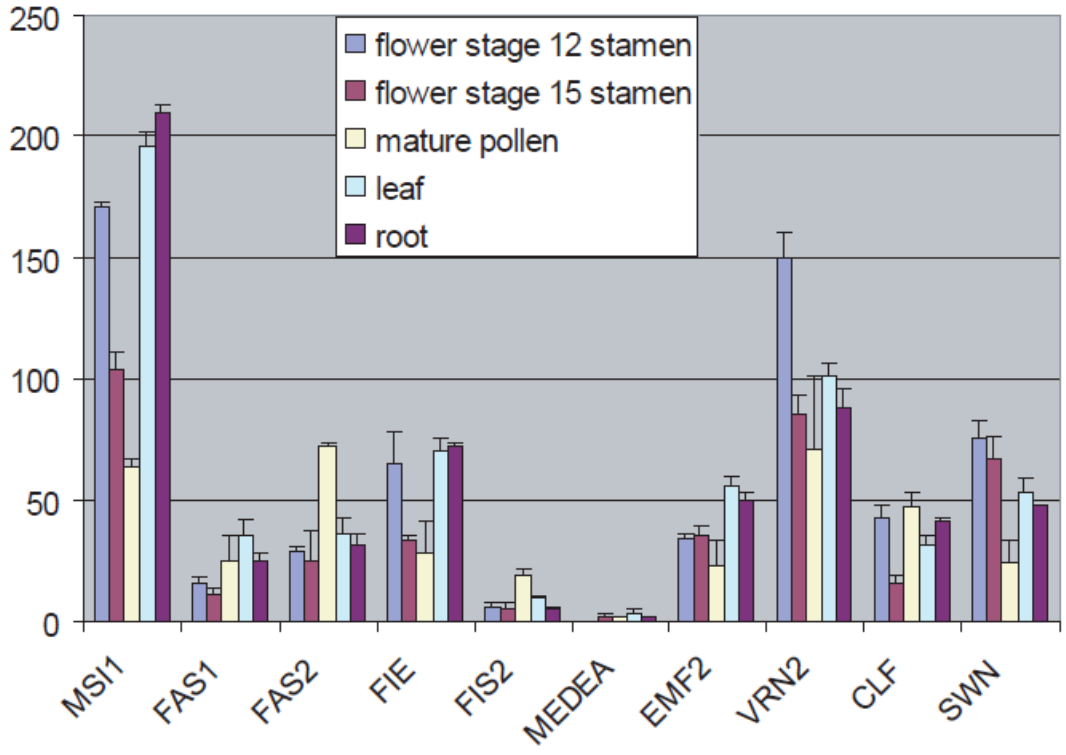

Fig. 3-2. Expression of genes encoding sub-units of the CAF1 and Pc-G complexes.
Data based on data available online from The A.thaliana Expression Database. (http://csbdb.mpimp-golm.mpg.de/csbdb/dbxp/ath/ath_xpmgq.html)

Reduced paternal transmission was reported for the allele *msi1-2* (Guitton et al., 2004) but not for the allele *msi1-1* (Kohler et al., 2003). The discrepancy may result from the distinct genetic background of each allele (C24 versus Col) or from distinct growth conditions. We isolated two new alleles of *msi1* in Ler (*msi1-3*) and Col (*msi1-4*) genetic backgrounds (Fig. 3-3). Imperfect insertions of a Ds transposon and of a T-DNA created a stop codon in the first exon of *MSI1* in the alleles *msi1-3* and *msi1-4*. Both alleles do not transmit *msi1* maternally and are presumably null alleles as concluded for the alleles *msi1-1* and *msi1-2* (Guitton et al., 2004) (Kohler et al., 2003).

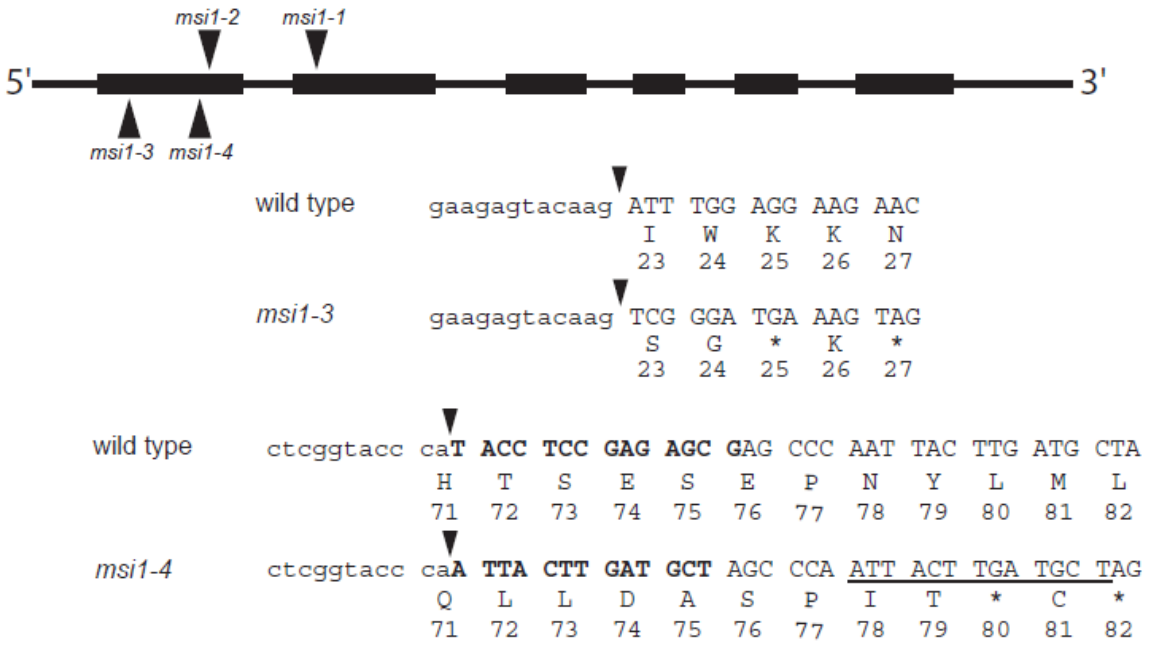

Fig. 3-3. Localization of mutations in the four *msi1* loss-of-function alleles.
The details of the mutations associated with the new alleles *msi1-3* and *msi1-4* are shown. Arrowheads indicate the precise location of base pair changes. Asterisks indicate stop codons. The sequence underlined was replicated and replaced the wild-type sequence as shown in bold in *msi1-4*.

Table 3-1. Paternal transmission of *msi1* alleles.

Female × male	% ± s.d. (mutant allele) in F1	*n*	T.E. %	Penetrance %
msi1-1/+ × *msi1-1*/+	35.7±5.0 (*msi1-1*)	206	56	44
Col × *msi1-1*/+	36.8±4.9 (*msi1-1*)	85	57	43
msi1-2/+ × *msi1-2*/+	33.7±5.1 (*msi1-2*)	132	50	50
C24 × *msi1-2*/+	35.9±6.6 (*msi1-2*)	206	56	44
msi1-3/+ × *msi1-3*/+	35.8±10.0 (*msi1-3*)	96	55	45
Ler × *msi1-3*/+	34.8±3.4 (*msi1-3*)	121	53	47
msi1-4/+ × *msi1-4*/+	37.0±6.1 (*msi1-4*)	143	59	41
Col × *msi1-4*/+	36.6±9.3 (*msi1-4*)	72	57	43
Col × *msi1-1*/+; *fas1-1*/+	28.8±4.9 (*msi1-1*)	255	40	60
Col × *msi1-3*/+; *fas1-4*/+	29.3±4.6 (*msi1-3*)	389	41	59
Col × *msi1-1*/+; *fas2-4*/+	28.5±2.2 (*msi1-1*)	84	40	60

The paternal transmission was calculated from the percentage of *msi1* plants in the progeny from crosses between pollen from *msi1*/+ plants and ovules of the relevant wild-type ecotype. This transmission is comparable to the transmission of *msi1* from self-pollinated *msi1*/+ plants. The effect of *fas1* and *fas2* on *msi1* transmission is indicated in the three last rows. n, The number of plants scored; T.E., Transmission efficiency.

We measured the paternal transmission in each *msi1* alleles grown in the same conditions (Table 3-1). Pollen development takes place after meiosis and crosses between wild-type ovules and pollen from *msi1*/+ plants are expected to transmit *msi1* in 50% of the offspring if there is full transmission. Paternal transmission was reduced to approximately 36% in every allele (Table 3-1). Reduced transmission could result from a paternal effect causing reduction of seed germination or seedling viability. The germination rate of wild-type seeds was 98.2%, (n = 277, s.d. = 0.53), hence comparable to the germination rate in seeds from crosses between wild-type ovules and pollen from *msi1-1*/+ plants (98.0%, n = 293, s.d. = 0.23). Similarly the survival rate of *msi1-1*/+ seedlings was not affected (99.6%, n = 273, s.d. = 0.07). Hence *msi1* effect on paternal transmission does not originate from an effect on seed development or on seedlings and must result from a reduction of male fertility. The reduction of paternal transmission of all four *msi1* alleles to 36% indicated a transmission efficiency of 56%. Hence a penetrance of 44% is associated with null mutations in *msi1* resulting in defective male gametogenesis in *msi1*/+ plants. We conclude that *msi1* causes defects during pollen development.

3.1.2. Reduced paternal transmission of *msi1* is enhanced by further loss of CAF1 function

MSI1 was shown to interact *in vitro* with the complex containing *FAS1* and *FAS2* (Kaya et al., 2001). We analyzed the paternal transmission associated with the loss-of-function alleles *fas1-4* and *fas2*-4 (Exner et al., 2006) (Ramirez-Parra and Gutierrez, 2007). Paternal transmission of the *fas1-4* allele analyzed from crosses between wild-type ovules and pollen from *fas1*-4/+ plants was 49.6% (n = 115, s.d. = 7.4). Similarly paternal

transmission of *fas2-4* was 48.6% (n = 140, s.d. = 5.2). According to these data, neither *fas1* nor *fas2* would appear to affect male gametogenesis. Nevertheless, if we assume that *fas1* and *fas2* affect paternal transmission, the associated transmission efficiency would be of the order of 98%. To test whether the CAF-1 pathway is responsible for the reduced transmission of *msi1* null alleles, we obtained double mutant lines between *msi1*/+ and loss-of-function alleles of *fas1*/+ and *fas2*/+. Paternal transmission of *msi1* mutant allele was similarly reduced by the introduction of *fas1* and *fas2* (Table 3-1). An additive interaction between *fas1* or *fas2* and *msi1* is predicted to lead to an increase of *msi1* transmission efficiency from 56 to 55 % in *fas1 or fas2* background. However In the *fas1* or the *fas2* background the transmission efficiency of *msi1* was reduced significantly from 56% to 40% (Table 3-1). In conclusion the interaction between *msi1* and *fas1* or *fas2* was not additive but synergistic. Additive interactions between null mutations indicate that each mutation affects a distinct pathway. However, a synergistic interaction is observed in combination of partially penetrant alleles of mutations affecting the same genetic pathway. The synergy observed between *msi1* and *fas1* or *fas2* on paternal transmission of *msi1* suggests that *MSI1*, *FAS1* and *FAS2* act in a common genetic pathway influencing male gametogenesis.

3.1.3. Loss of MSI1 arrests pollen development

We investigated the developmental origin of reduced male fertility in *msi1*/+ plants. In order to compare directly *msi1* and wild-type pollen development we used the mutant background *quartet* (*qrt*) where the four microspores produced by meiosis remain associated as a tetrad (Preuss et al., 1994). Hence *qrt/qrt*; *msi1-1*/+ plants produce tetrads

containing two wild-type and two *msi1* pollen grains. Alexander staining for pollen viability showed 7.3% lethality in *msi1* pollen at maturity (s.d. = 1.9; n = 800) in comparison to 1.0% in the wild type (s.d. = 0.7; n = 500) (Fig. 3-4). Tetrads of microspores produced by wild-type and *msi1-1*/+ plants in *qrt/qrt* background could not be distinguished (n = 120) (Fig. 3-5A). After PMI, in *qrt/qrt*, all tetrads consisted of four pollen grains with a vegetative cell and a generative cell (Fig. 3-5B). By contrast, a fraction of tetrads in pollen from *qrt/qrt; msi1-1*/+ plants contained an arrested microspore (Fig. 3-5C). At the mature stage, in contrast to wild-type pollen tetrads, a fraction of tetrads in *qrt/qrt; msi1-1*/+ plants contained an aborted microspore (Fig. 3-5D), or a pollen grain with one (Fig. 3-5E) or two nuclei (Fig. 3-5F). These results suggest that the absence of MSI1 causes pleiotropic arrest of pollen development before PMI, or PMII. The fraction of each class of arrest was measured in pollen produced by *msi1-1*/+ plants (Fig. 3-6). The percentage of arrested pollen cumulated with the percentage of aborted microspores amounted to 14.7%. This value is lower than the 22% abnormal pollen in a population of pollen from *msi1/*+ plants as predicted from the transmission efficiency of 56%. This suggested that 7.3% of pollen from *msi1/*+ plants contain two sperm cells and appear morphologically normal, albeit are not functional. These *msi1* tricellular pollen grains likely grow a pollen tube but the two sperm cells are incompetent for fertilization, causing ovule abortion. In agreement with this prediction, pollination of wild-type plants by *msi1*/+ plants caused 6% increase in ovule abortion (Fig. 3-7). In conclusion our observations show that *msi1* causes delays and arrests of pollen development leading to partial male sterility and reduced paternal transmission of *msi1*.

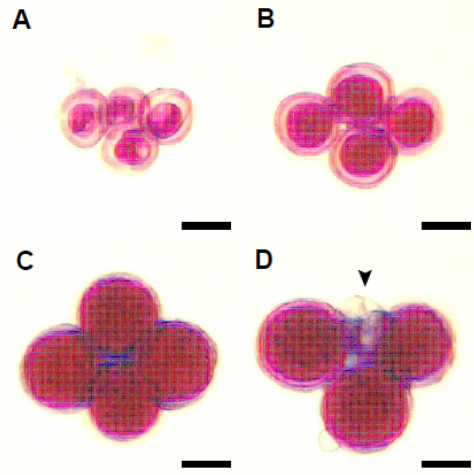

Fig. 3-4. Viability of pollen in *msi1*/+;*qrt*/*qrt* plants.
(A, C) Alexander staining of pollen from *qrt*/*qrt* (A-C) and from *msi1*/+;*qrt*/*qrt* (D) plants. Arrowhead indicates dead pollen grains. Scale bars: 10 µm.

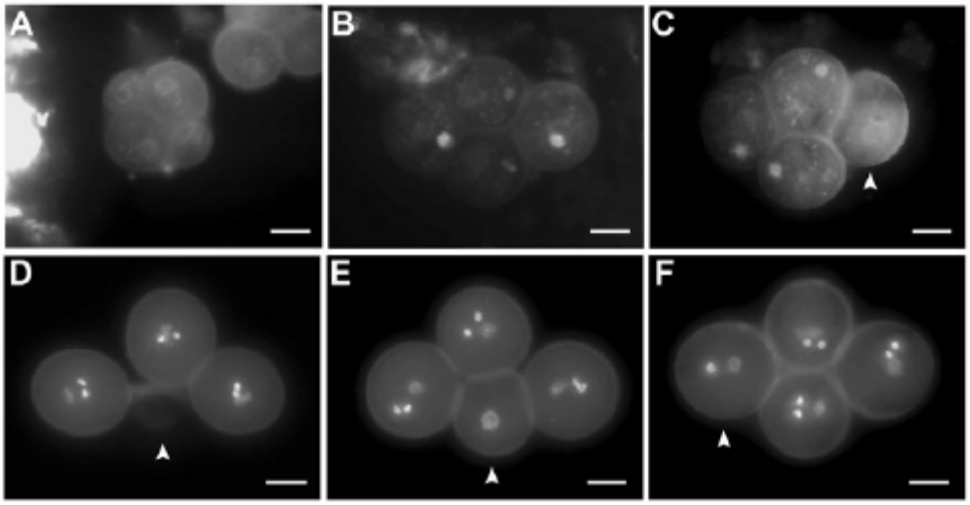

Fig. 3-5. Defects in pollen development in *msi1*/+ mutants.
Pollen development in meiotic tetrads from *qrt1*/*qrt1* and *qrt1*/*qrt1*; *msi1-1*/+ Arabidopsis plants. At uni-nucleate stage (A) microspore tetrads of wild-type and mutant plants are indistinguishable. In contrast to wild-type tetrads (B), *msi1*/+ tetrads at the bicellular stage contain one arrested microspore (C, arrowhead). (D-F) At the tricellular stage, *qrt1*/*qrt1*; *msi1-1*/+ plants produce tetrads containing three wild-type pollen grains and an abnormal pollen grain (arrowhead). The abnormal pollen is either a dead microspore (D), an arrested microspore (E) or a bicellular pollen grain (F). Epifluorescence micrographs of DAPI-stained pollen. Scale bars: 10 µm.

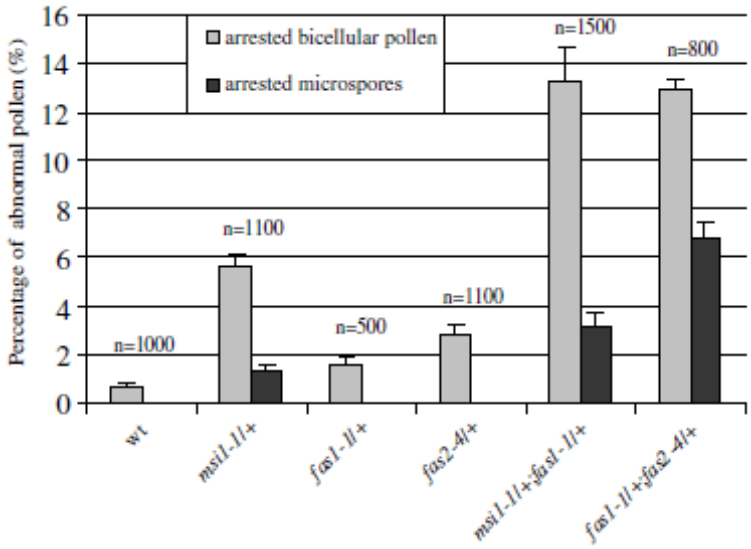

Fig. 3-6. Synergistic effects of combination between mutations in members of the CAF1 complex.
Bar chart showing percentage of the two types of abnormal pollen at the tricellular mature stage in *msi1-1/+*, *fas1-1/+*, *fas2-4/+*, *msi1-1/+;fas1-1/+* and *fas1-1/+;fas2-4/+*mutant *Arabidopsis* plants. Gray bars correspond to arrested bicellular pollen and black bars to arrested microspores. Error bars correspond to standard errors calculated on the basis of several samples of 100 pollen grains, and the size of the total population analyzed (*n*) is indicated above each column.

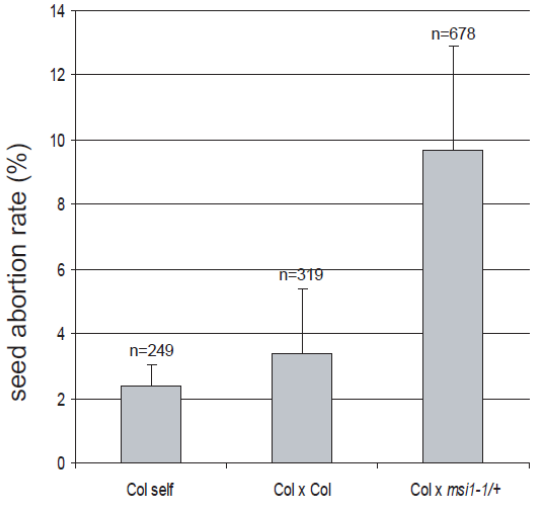

Fig. 3-7. Seed abortion caused by pollination with *msi1*/+.
The errors bars correspond to the standard deviation observed in the population (n).

3.1.4. Loss of CAF1 activity causes delay and arrest of the cell cycle in pollen

Since genetic interactions suggested that impairment of the CAF1 pathway affects male gametogenesis, we expected that loss-of-function of the other members of the CAF1 pathway would cause pollen arrests similar to *msi1*. A small proportion of pollen arrested at the bicellular stage was observed in *fas1*/+ and *fas2*/+ mutants (Fig. 3-6). This very limited penetrance of *fas* mutations was also supported by the very limited reduction of paternal transmission efficiency of *fas1* and *fas2*. By contrast, the combination of *fas1* and *fas2* in double heterozygous mutant plants caused a high proportion of arrest at the bicellular stage and an additional arrest as microspores, which was never observed in the single mutants. This observation demonstrates that the combination of *fas1* and *fas2* does not cause additional but synergistic effects, in agreement with the established participation of *fas1* and *fas2* to the CAF1 pathway. Similarly the combination of *fas1* to *msi1* caused a synergistic increase of the proportion of pollen developmental arrests (Fig. 3-6). A two-way analysis of variation confirmed that an additive phenotype could not explain the extra increase in single sperm pollen in the double mutants ($p = 0.0047$). The synergistic effects of the combinations between *fas1*, *fas2* and *msi1* on pollen development and paternal transmission indicate that *msi1* causes pollen developmental arrest through the CAF1 pathway.

To investigate the consequence of loss of activity of CAF-1 on cell cycle dynamics, we performed FACS analysis in young seedlings from wild-type and loss-of-function mutants for *MSI1*, *FAS1* and *FAS2* (Fig. 3-8). We used a plant line with reduced levels of MSI1 transcription as a result of RNA interference (*msi1 RNAi*) (Fig. 3-8B) and plants

homozygotes for the null alleles of *fas1* (Fig.3-8D) and *fas2* (Fig. 3-8F). In the wild type most cells are in G1 (2C DNA content) or G2 (4C) as they divide and only a small fraction of the cell population evidenced endoreduplication with an 8C DNA content (Fig. 3-8A,C,E). We noted a marked increased in the onset of endoreduplication with a larger proportion of cells with one endocycle (8C) and cells experiencing a second endocycle (16C) (Fig. 3-8B,D,F). These observations are in agreement with recent analyses done with seedlings and leaves in *fas1-1*, *fas1-4*, *fas2-1* and *msi1* antisense lines (Exner et al., 2006) (Kirik et al., 2006). We further observed that reduction of CAF-1 function in *msi1 RNAi*, *fas1* and *fas2* plants caused a marked increase of the proportion of cells in S phase and in G2 phase (Fig. 3-8G). We conclude that impairment of chromatin assembly causes stalling during S and G2 phases. The ensuing delays to proceed through the G2/M arrest may explain the bypass toward endoreduplication. To investigate the consequence of loss of activity of CAF-1 on cell cycle during pollen development, we measured DNA content at the early tricellular stage. We compared the DNA content in sperm cells of wild-type tri-cellular pollen with the single sperm-like cell in bicellular pollen from *msi1*/+; *fas1*/+ plants. Both measurements were compared to *duo1* pollen single sperm-like cells, which contain twice the amount of DNA contained in wild-type sperm cells at the early tricellular stage (Rotman et al., 2005). The single sperm-like cell in *msi1*/+; *fas1*/+ also contains approximately twice the amount of DNA in comparison to wild-type sperm cells (Fig. 3-9). These measurements suggest that the loss of CAF1 function delays the cell cycle pace in the generative cell, preventing the G2/M transition, which leads to PMII in the wild type.

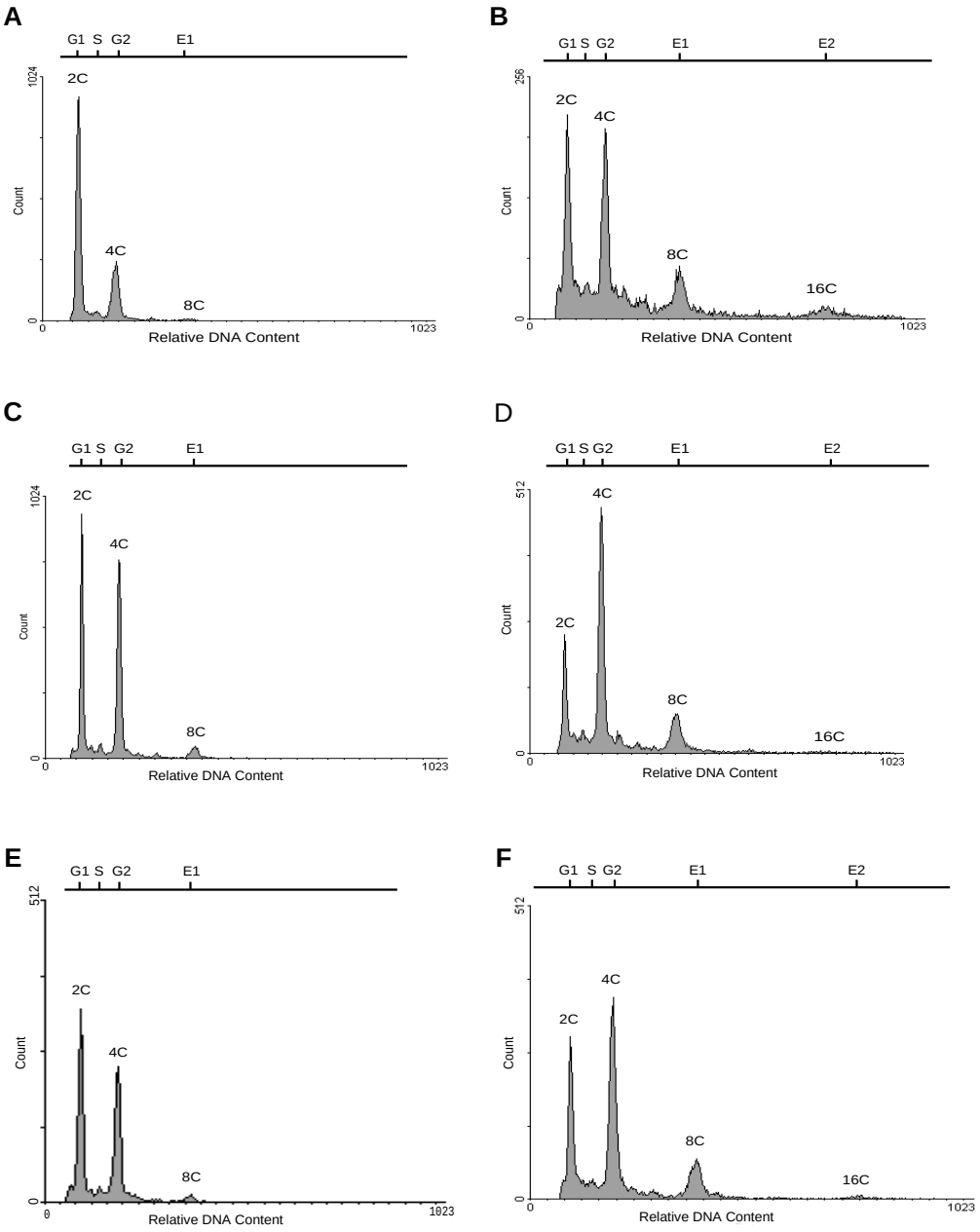

G

Sample:	2C (G1) %	S Phase %	4C (G2/M) %	8C %	16 C%
Ws (WT)	61.77	4.89	26.7	1.42	-
***msi*RNAi**	23.72	8.56	25.24	10.59	4.3
En (WT)	36.28	6.13	45.27	5.78	-
fas1/fas1	15.09	9.25	41.81	14.75	0.99
Col (WT)	46.52	6.73	38.47	2.29	-
fas2/fas2	25.69	6.9	41.64	13.99	1.31

Fig. 3-8. **Flow Cytometric analysis of DNA content of *Arabidopsis thaliana* 10 DAG seedlings, and stained using PI.**
(A) WS wild-type ecotype. (B) *msi1*RNAi in WS background. (C) En wild-type ecotype. (D) *fas1/fas1* in En background. (E) Col wild-type ecotype. (F) *fas2/fas2* in Col background. The three peaks of fluorescence correspond to nuclei having DNA contents of 2C, 4C and 8C, respectively. A fourth peak of 16C is distinctive in *msi1*RNAi. Above each graph, the corresponding position of the cell cycle phases G1, S and G2 and endoreduplication cycles 1 (E1) and 2 (E2) is indicated. (G) Percentage of cell population in each phase of cell cycle or stages of endoreduplication.

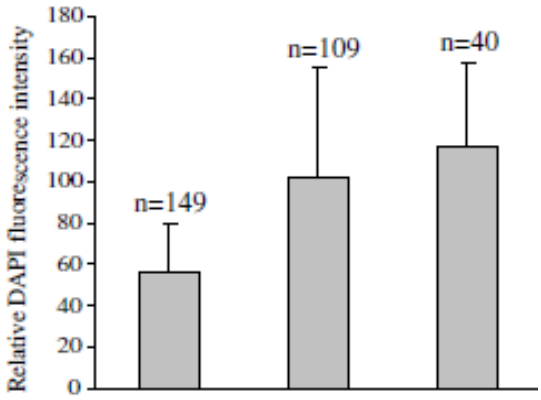

Fluorescence Intensity	wt	*msi1-1/fas1-1*	duo1-1
single sperm-like nucleus / sperm nucleus	N.A.	1.80	2.07

Fig. 3-9. Effect of *msi1* on DNA content in sperm cell nuclei.
The DNA content in *Arabidopsis* sperm cells was estimated relative to the fluorescence intensity after DAPI staining. The relative DAPI fluorescence intensity between control wild-type sperm cells and single sperm-like cells in *msi1-1*;*fas1-1* pollen and in *duo1-1* pollen is indicated under the graph. Error bars correspond to standard deviations, and the size of the sample (*n*) is indicated above each column.

3.1.5. Cell fate specification and differentiation is normal in CAF1 deficient pollen

Arabidopsis PM I is coupled to cell fate specification leading to specific expression of vegetative cell (Twell et al., 1991) and generative cell markers (Engel et al., 2005) (Rotman et al., 2005). The second mitosis is coupled to sperm cell differentiation, marked by the onset of DNA synthesis (Durbarry et al., 2005) and expression of specific genes (Engel et al., 2005). To further elucidate whether arrests of cell division in *msi1* pollen grain are associated with cell fate changes, we analyzed cell identities in pollen grains arrested at PMII produced by *msi1*/+ plants. These pollen grains contained a large vegetative-like cell nucleus and a sperm-like cell with condensed DNA (Fig. 3-10G). The marker AC26 is associated with expression of Histone2B-mRFP fusion protein under the control of the ACTIN11 promoter and is specifically expressed in wild-type vegetative cell nuclei (Rotman et al., 2005) (Fig. 3-10A,B). In *msi1* pollen arrested at PMII, AC26 was also expressed in the larger spherical cell in correlation with its vegetative identity (Fig. 3-10G,H). We never observed any pollen grain expressing AC26 in the condensed nucleus of the sperm-like cell nor in more than one nucleus indicating that loss of CAF1 function does not perturb the vegetative cell identity during pollen development. In addition, we performed a germination test to estimate whether the vegetative cell deficient in CAF1 is able to produce a pollen tube. We observed comparable germination rates between wild-type pollen and pollen from *msi1*/+, *fas1*/+, *fas2*/+ and the double mutant combinations, with a slight reduction corresponding to the proportion of dead pollen recorded for each genetic background (Fig. 3-11). Our results support the argument that the vegetative cell differentiation and function is not affected by the loss of CAF1 function.

In wild-type pollen the generative cell lineage is marked by pDUO1-DUO1-mRFP1, expressed in the generative cell and in the sperm cells (Rotman et al., 2005). The maturing sperm cells are further marked specifically by the accumulation of the vacuolar V-ATPase E1 GFP on the outer plasma membrane (Strompen et al., 2005) (Fig. 3-10D) and of the HISTONE3 variant HTR10 in the sperm nucleus (Ingouff et al., 2007) (Fig. 3-10E). Eventually the sperm cells specifically express AtGex1 (Engel et al., 2005) (Fig. 3-10F). We observed that all the markers of sperm cell maturation and identity were expressed only in the single sperm-like cell in *msi1* pollen arrested at PMII (Fig. 3-10J,K,L). The proportion of pollen with a single sperm cell expressing HTR10-mRFP1 (6%, n = 150; s.d. = 2) is similar to the proportion of pollen with a single sperm cell (Fig. 3-6). We conclude that all *msi1* single sperm cells express the cell fate marker HTR10-mRFP1. These findings indicate that cell fates are not affected in *msi1* pollen grains, which appear to comprise a vegetative cell and a single sperm cell.

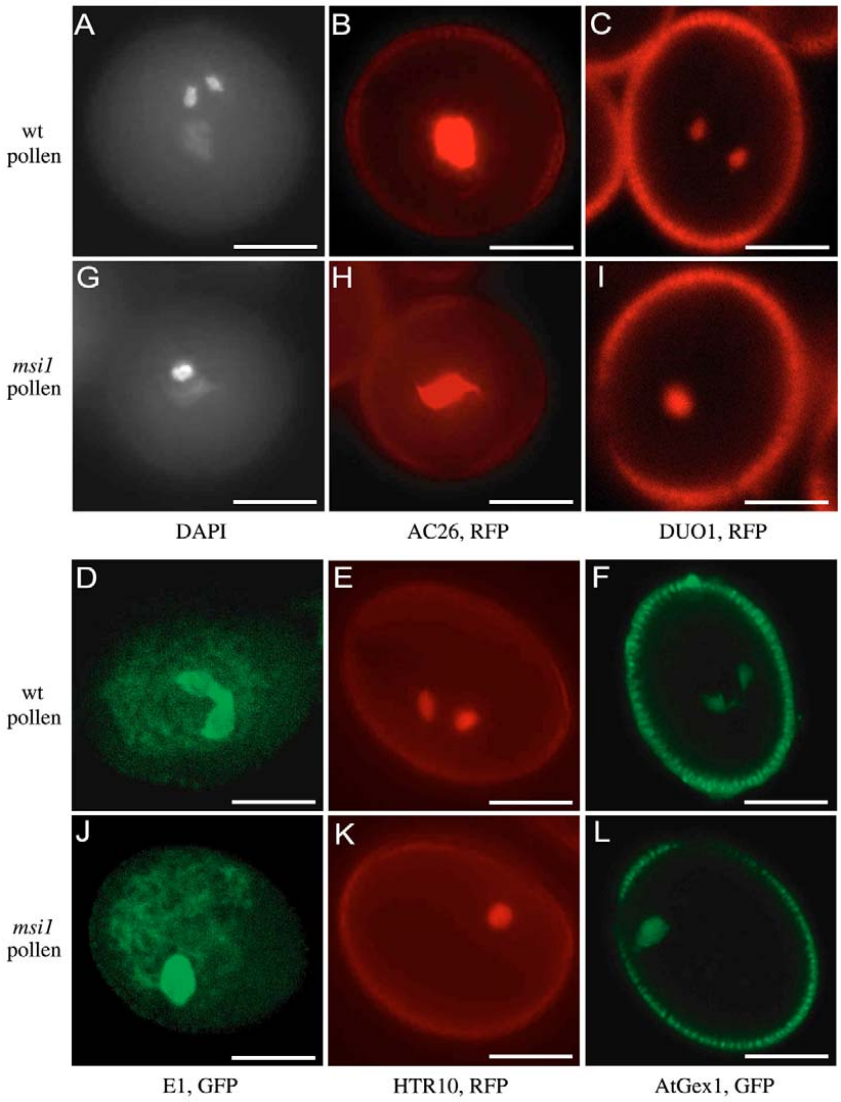

Fig. 3-10. Cell identities in bicellular *msi1* pollen.
(A-F) Wild-type *Arabidopsis* pollen at the tricellular stage. (G-L) Bicellular and tricellular pollen segregating from *msi1*/+ plants. (A,G) Fluorescence images of pollen grains stained with DAPI. (B,H) The same pollen grains as in A,G, respectively, expressing the vegetative cell marker AC26-Histone2B-mRFP1. (C,I) Pollen grains expressing the generative lineage marker pDUO1-DUO1-mRFP1. (D,J) Pollen grains expressing the generative lineage marker E1-GFP. (E,K) Pollen grains expressing the sperm cell marker HTR10-mRFP1. (F,L) Pollen grains expressing the sperm cell marker ATGEX1-GFP. GFP was examined using the 488 nm excitation line of an argon laser and an emission filter long pass of 510 nm. Fluorescence of mRFP1 was examined using the 543 nm excitation line of a HeNe laser and an emission filter of 585-615 nm. Scale bars: 10 μm.

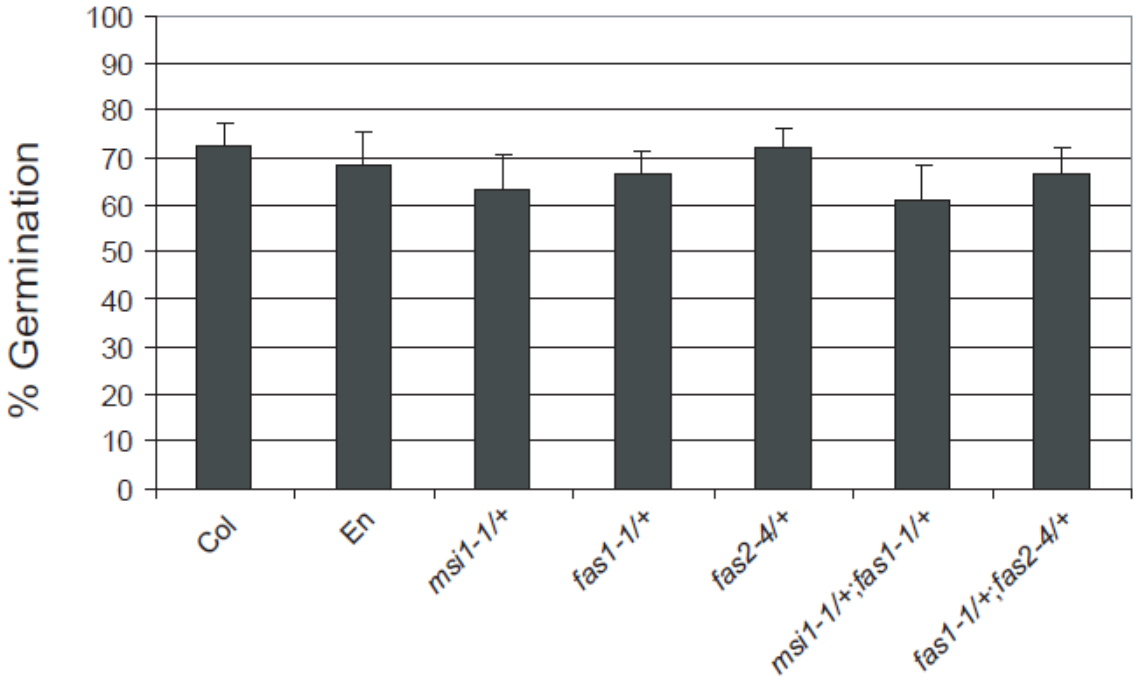

Fig. 3-11. In vitro pollen germination of combination between mutations in members of the CAF1 complex.
Three replicates were performed for each assay. In each replicate 300 pollen grains were scored for pollen germination rates. Error bars correspond to standard errors.

3.1.6. Pollination with *msi1* pollen causes single-fertilization events

In wild-type pollen the two sperm cells separately fertilize the female egg cell and the central cell producing the embryo and the endosperm respectively (Fig. 3-12A). The apparent correct establishment of cell fate in the single sperm-like cell present in *msi1* pollen suggested that it was able to perform fertilization as a wild-type sperm cell. We germinated pollen from *msi1-3*/+ plant lines expressing the sperm cell markers HTR12-GFP or HTR10-mRFP1 (Ingouff et al., 2007). We observed single *msi1* sperm cells transported by the pollen tubes (Fig. 3-13). We suspected that the single sperm cell in *msi1* pollen could fertilize either the egg cell or the central cell. Crossing wild-type ovules to pollen from *msi1*/+ plants produced a low proportion of seeds containing only endosperm (n = 20 out of 3600) (Fig. 3-12B) or an embryo (n = 18 out of 3600) (Fig. 3-12C). In both cases, these seeds contained residual material from the unfertilized egg cell or central cell (Fig. 3-12B,C) comparable to those observed in unfertilized ovules (Fig. 3-12D). We concluded that *msi1* pollen with a single sperm cell likely caused single fertilization events. Alternatively, single sperm cells may only fuse with one of the female gametes without the fusion of the parental genetic material (karyogamy) and autonomous development of embryo or endosperm would follow. If this were the case, the paternal genome would be excluded and the single embryo or the single endosperm should not express paternally derived alleles. We tested this hypothesis for the expression of endosperm marker KS22 (Ingouff et al., 2005) (Fig. 3-12E) provided by the pollen of *msi1*/+ plants crossed to wild-type ovules (Fig. 3-12F). Seeds with single endosperm showed expression of the paternally derived endosperm marker KS22 (Fig. 3-12F, n = 7). We conclude that the single endosperm likely develops from a central cell fertilized by

the single gamete in *msi1* pollen. To establish whether single sperm cells are able to fertilize the egg cell, we performed ploidy measurements on seeds containing a single embryo. We observed ten chromosomes at pre-prophase in single embryo cells (inset of Fig. 3-12G, n = 2). These embryos are thus diploid and have been produced by fertilization of the egg cell by the single sperm from *msi1* pollen. We conclude that a fraction of *msi1* pollen arrested at PMII contains a functional single sperm cell equally able to fertilize the egg cell or the central cell. Similarly pollination with pollen from *fas1*/+ and *fas2*/+ plants produced seeds containing either an endosperm or an embryo (0.3%, n = 400 and 0.4%, n=360). This result suggests that CAF1 deficient pollen produces functional single sperm cells.

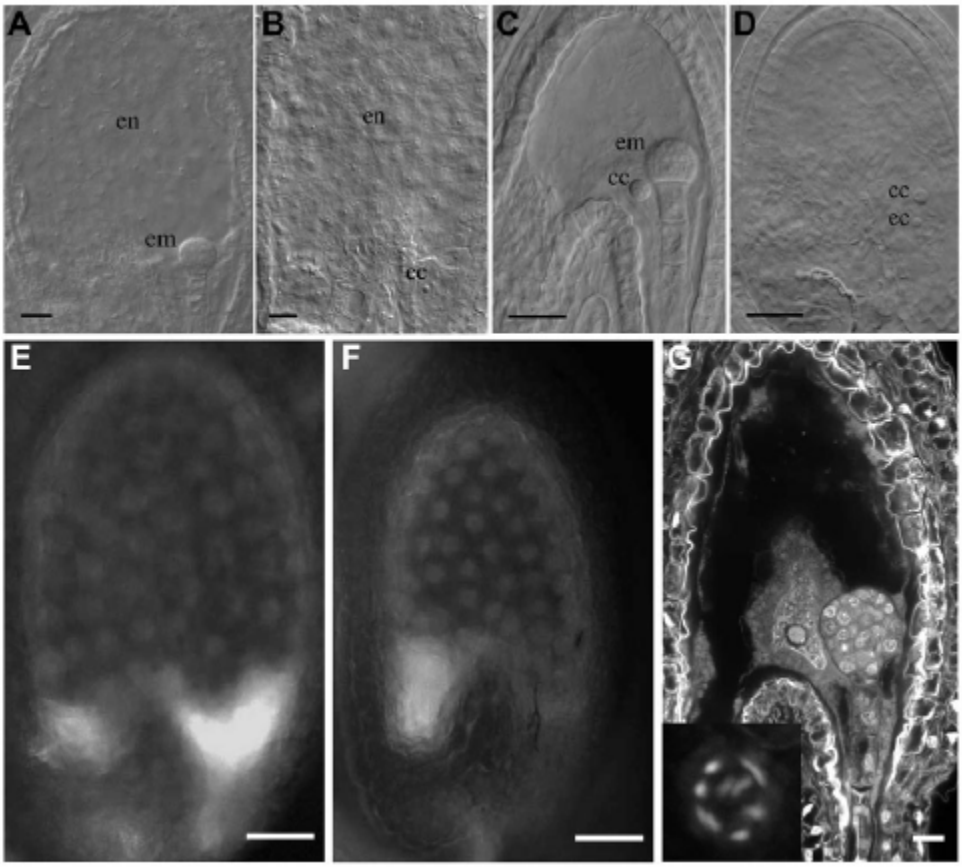

Fig. 3-12. Pollination of wild-type ovules with *msi1*pollen leads to single fertilization events.
(A) Wild-type *Arabidopsis* seed with an embryo and an endosperm, 2 days after pollination (2 DAP). (B) Seed with an endosperm but without an embryo, 3 DAP. At the embryo region, the egg cell remains unfertilized. (C) Seed with an embryo but without endosperm, 3 DAP. At the side of the embryo the nucleus of central cell that remains unfertilized is still observed. (D) Fully aborted ovule without embryo and endosperm, 3 DAP. The egg cell and the central cell remain unfertilized. (E) Expression of the fluorescent KS22 GFP endosperm marker in a wild-type seed at 3 DAP. (F) Expression of KS22 GFP in a seed containing only endosperm from a cross between wild-type ovules and *msi1-2*/+;KS22/KS22 pollen. (G) Confocal section of a seed containing only an embryo, produced by a cross between a wild-type ovule and *msi1-2* pollen. The nucleus of the unfertilized central cell remains associated with the surface of the embryo. Feulgen staining marks brightly the DNA in nuclei as described previously (Garcia et al., 2003). The inset shows ten chromocentres at pre-prophase in the nucleus from the single embryo. The single embryo is diploid and thus originates from a fertilized egg cell. Scale bars: 100 μm in A-D; 50 μm in E,F; 10 μm in G. cc, central cell; ec, egg cell; em, embryo; en, endosperm.

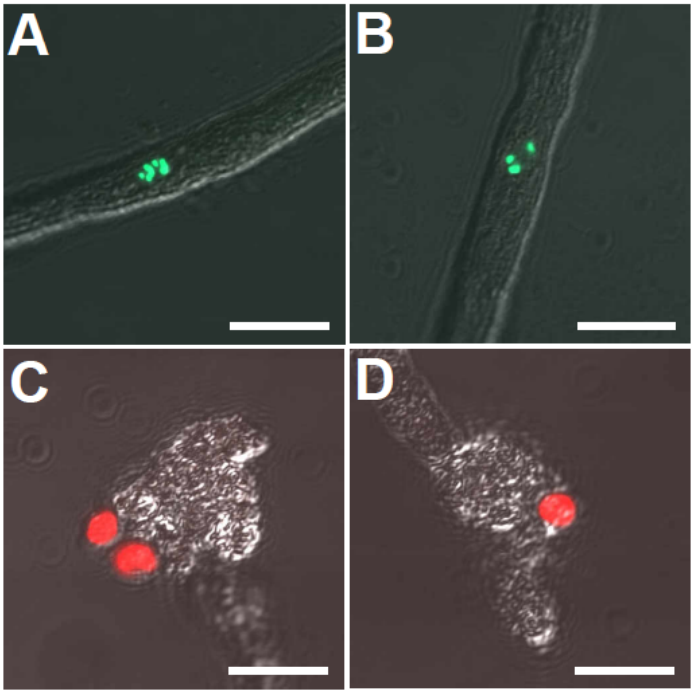

Fig. 3-13. Transport of sperm cells through the pollen tube.
Sperm cells marked by HTR12-GFP (A and B) and HTR10-mRFP1 (C and D) in wild-type (two sperm cells) (A, C) and *msi1-3* (one sperm-cell) (B, D) pollen.
HTR12 encodes Arabidopsis histone 3 variant localized at centromeres. HTR12-GFP allows differentiating the two sperm cells containing 10 chromosomes (showing 7-10 green dots) from a single sperm cell with only 5 chromosomes (showing 3-5 green dots). Scale bars: 4 μm.

However, the proportion of single fertilization events was of the order of 1%, whereas the proportion of *msi1* pollen with a single sperm cell was of the order of 6%. This suggested that either only a fraction of the single sperm cells was transported by the pollen tube or was able to perform single fertilization. Alternatively, a fraction of single sperm cells would divide during the transport by the pollen tube. We measured the proportion of single sperm cell at various times after pollen germination in vitro and observed a reduction of the percentage of pollen harboring a single sperm cell from 6 to 2% (Fig. 3-14A). Hence, *msi1* single sperm cells could be transported into the pollen tube as in wild-type pollen harboring two sperm cells (Fig. 3-14B,C). However, we could record the division of single sperm cells into two sperm cells during pollen tube growth (Fig. 3-14C,D; n=2). This observation and the decreased proportion of pollen tubes with single sperm cells following germination indicated that a fraction of sperm cells divide during their transport by the pollen tube, leading to a low proportion of pollen tubes delivering a single sperm cell. This low proportion is similar to the proportion of single fertilization events. We thus conclude that single fertilization of the egg cell or of the central cell is likely to result from the delivery of single sperm cells produced as a result of delayed cell cycle in CAF1-deficient pollen.

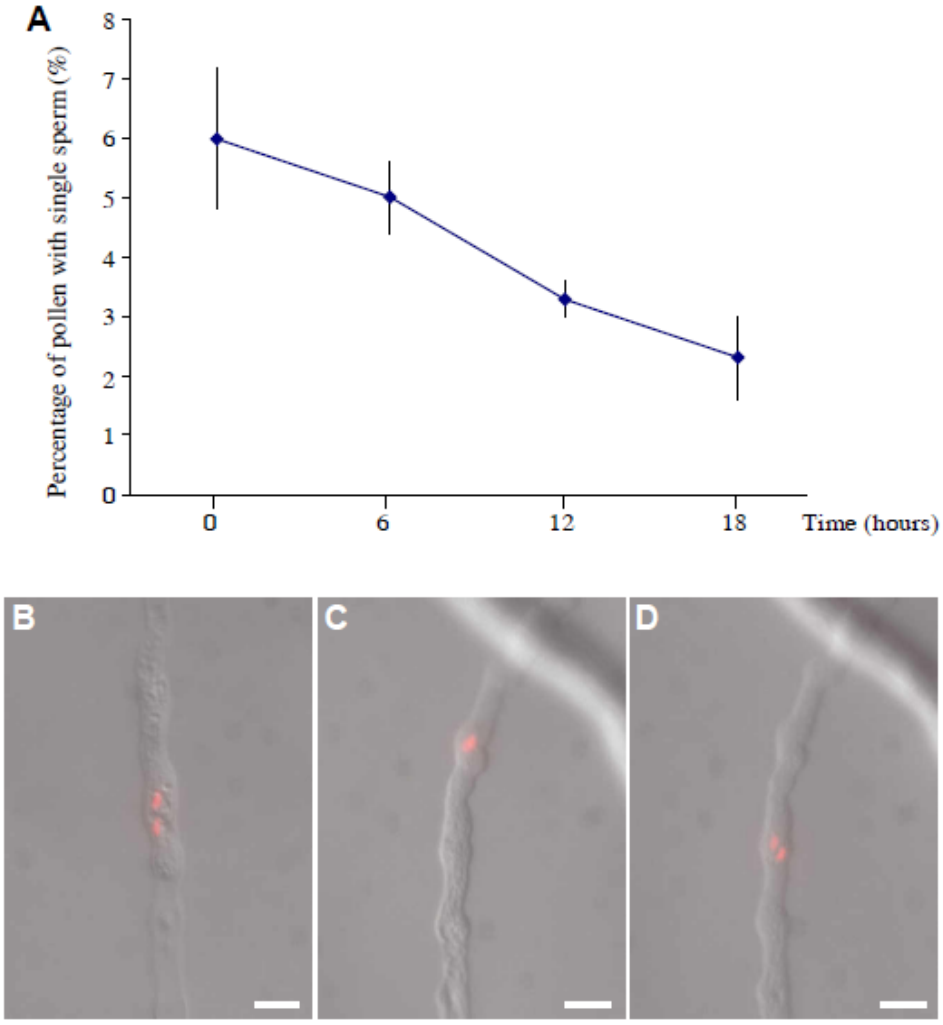

Fig. 3-14. Fate of the single sperm cell during *msi1* pollen tube growth.
(A) Percentage of pollen tubes transporting a single sperm cell from a *msi1-1*/+ *Arabidopsis* plant at different time points after pollen germination in vitro. Errors bars correspond to standard errors calculated on the basis of three replicates of 100 pollen grains. (B-D) Transport of sperm cells marked with HTR10-mRFP in pollen tube germinated in vitro from wild-type (B) and *msi1*/+ (C,D) plants. (B) At 6 hours after germination, wild-type pollen tubes transport two sperm cells (two fluorescent red dots). (C) By contrast, at 6 hours a *msi1* pollen tube transports a single sperm cell. (D) At 7 hours after germination the *msi1* single gamete had divided into two sperm cells. (B,C,D) Superimposed DIC images of the pollen tube with the mRFP1 fluorescence signal identifying the sperm cells. Scale bars: 20 μm.

3.2. PROLIFERATION AND CELL FATE ESTABLISHMENT DURING ARABIDOPSIS MALE GAMETOGENESIS DEPENDS ON THE RETINOBLASTOMA PROTEIN

3.2.1. Reduced paternal transmission of *rbr* alleles

We observed expression of Arabidopsis Retinoblastoma homologue *RBR* at all stages throughout pollen development in all cell types (Fig. 3-15). Two mutant allele *rbr-1* (Ebel et al., 2004) (Johnston et al., 2008) and *rbr-2* show reduced paternal transmission (Table 3-2). Reduced paternal transmission of *rbr* was linked to reduced pollen viability (Fig. 3-16). We further characterized at the cellular and molecular levels the defects caused by *rbr* mutations during pollen development.

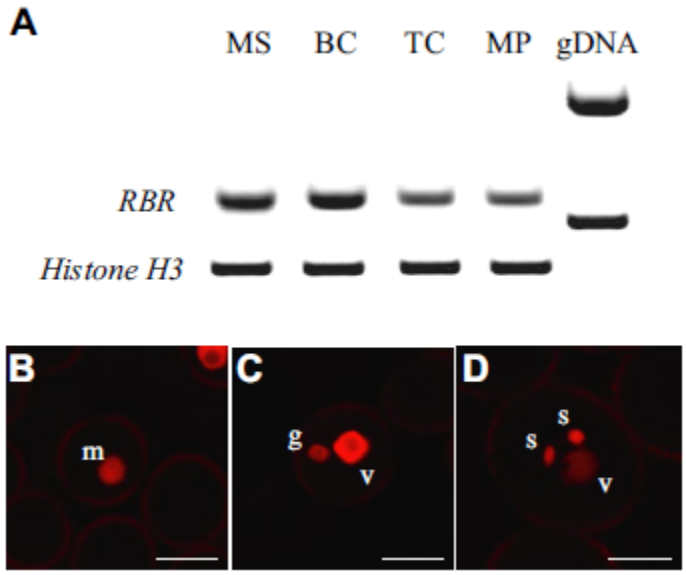

Fig. 3-15. Expression of *RBR* in pollen.
(A) RT-PCR analysis of *RBR* expression with RNA extracted from isolated spores at 4 stages of pollen development. High levels of transcript levels are present at the microspore stage (MS) and in bicellular pollen (BC), followed by small decline in tricellular (TC) and mature pollen (MP). Histone variant *H3.2* (At4g40040) was used as a control. (B-D) We studied the expression pattern of RBR at the cellular level using the expression of the translational reporter construct p*RBR-RBR*::*RFP*, which complements partially *rbr-2* (Table 3-2 and Fig. 3-16). We observed the expression of RBR-RFP in microspore (B), and developing pollen at bicellular stage (C) and tricellular stage (D). (Scale bars, 10 μm.) m, microspore nucleus; v, vegetative cell nucleus; g, generative cell nucleus; s, sperm cell nucleus.

Table 3-2. Paternal transmission of *rbr-2* and *cdka-1* alleles.

Female x Male	%± s.d. (mutant allele) in F1	T.E. %	n
Col x *rbr-2*/+	8.0±2.8 (*rbr-2*)	8.7	637
Col x *rbr-2*/+;RBR-RFP+/-	20.2± 5.1(*rbr-2*)	25.3	816
Col x *cdka-1*/+	8.2±2.1 (*cdka-1*)	8.9	477
Col x *rbr-2*/+;*cdka-1*/+	47.0±3.8 (*rbr-2*)	88.7	430

n = the number of plants scored; s.d. = the standard deviation;
T.E. (transmission efficiency) = number of mutant progeny / number of wild-type progeny

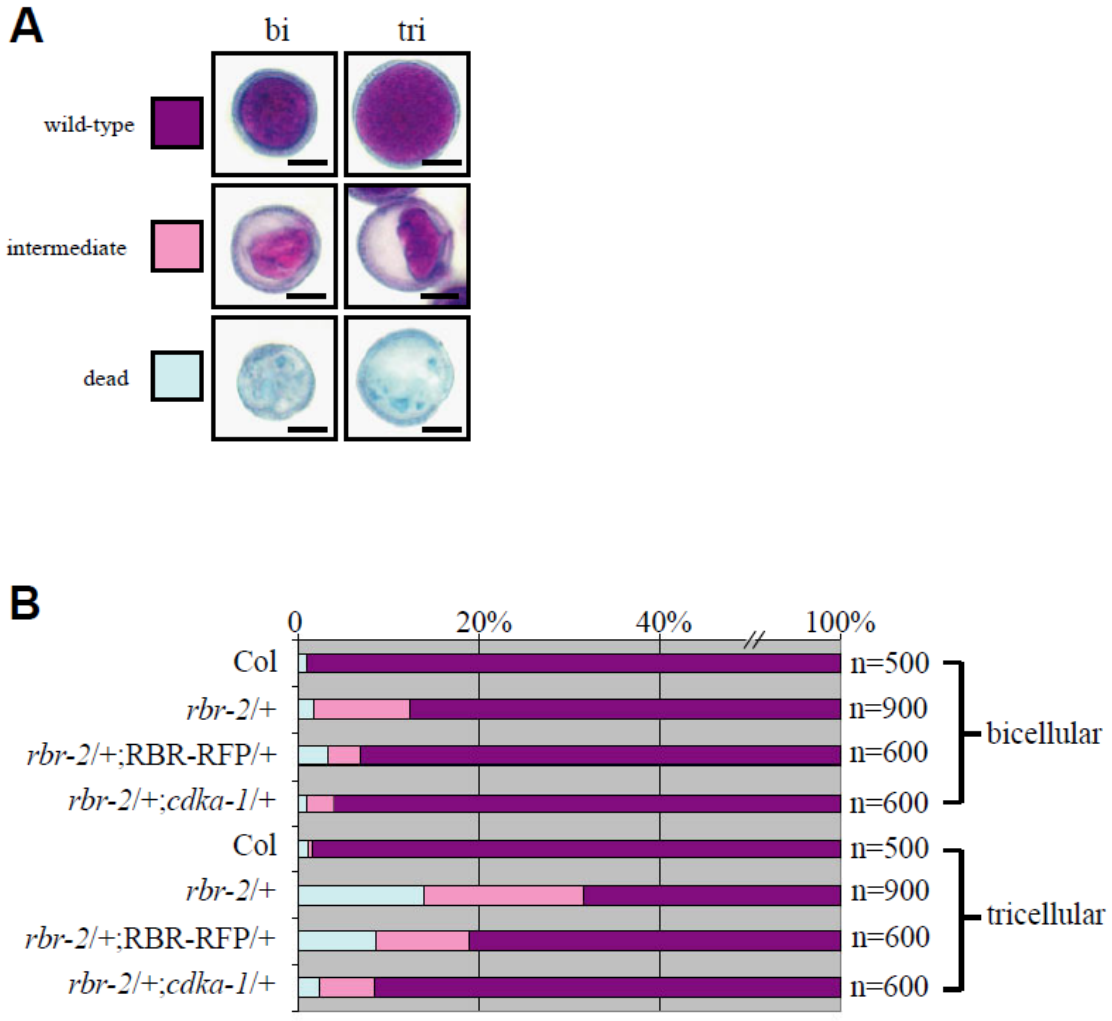

Fig. 3-16. Pollen death in *rbr* mutants.
(A) Alexander staining viability analysis showing WT pollen (purple), intermediate pollen (pink), and dead pollen (green) at bicellular and tricellular stages, respectively. (Scale bars, 10 μm.) (B) Bar chart showing percentage of 3 types of pollen from Col, *rbr-2*/+, *rbr-2*/+;RBR-RFP/+, and *rbr-2*/+;*cdka-1*/+, at bicellular and tricellular stages, respectively. The size of total population analyzed (n) is indicated (Right).

3.2.2. Limited cell over-proliferation in *rbr* pollen

A recent study reported hyperproliferation of the vegetative nucleus of *rbr* pollen (Johnston et al., 2008), but the origin of the supernumerary cells was not analyzed. We studied development of *rbr* pollen with nuclei stained by DAPI. WT microspores never divide equally (n = 1,000; Fig. 3-17A). In contrast, we observed in *rbr*/+ plants a very small fraction of microspores 0.67% (n = 600) that had divided equally into 2 cells (Fig. 3-17D). The very limited impact of *rbr* on microspore division might be explained by inheritance of residual RBR from the *rbr*/+ meiotic precursor.

The WT bicellular pollen comprises a vegetative cell with a large nucleus with de-condensed chromatin, and a smaller generative cell with a smaller nucleus (Fig. 3-17B). In contrast, *rbr*/+ plants produced 24.3% (n = 900) pollen containing 3 nuclei (Fig. 3-17E). One nucleus displayed the condensed chromatin typical of generative cells. The other 2 nuclei were larger with less condensed chromatin typical of vegetative cells (Fig. 3-17B,E). Wild-type bicellular pollen is marked by a transient eccentric cell wall (Fig. 3-17J,K). In contrast, the abnormal 3-celled *rbr* pollen observed at the bicellular WT stage showed an aberrant cell wall between the 2 vegetative cells (Fig. 3-17K,M). The proportion of pollen containing 2 vegetative cells rose sharply during late bicellular stage, affecting half of the *rbr* pollen (Fig. 3-17N). We never observed any 3-celled pollen at that stage, suggesting that *rbr* causes an ectopic division of the vegetative cell.

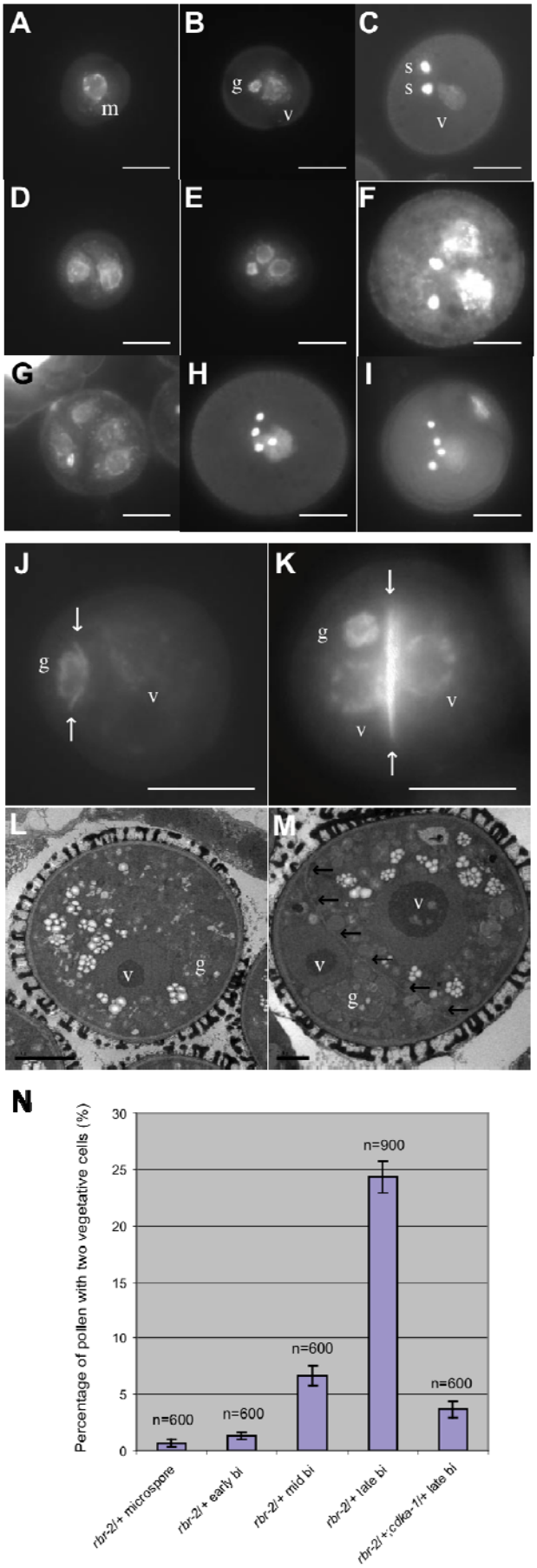
A
m
B
g
v
C
s
s
v
D
E
F
G
H
I
J
g
v
K
g
v
v
L
v
g
M
v
v
g
N
Percentage of pollen with two vegetative cells (%)
30
25
20
15
10
5
0
n=600
n=600
n=600
n=900
n=600
rbr-2/+ microspore
rbr-2/+ early bi
rbr-2/+ mid bi
rbr-2/+ late bi
rbr-2/+;cdka-1/+ late bi

Fig. 3-17. Cell over-proliferation during pollen development in *rbr*/+ mutants.
(A–C)WT pollen development. (A) The microspore with the undetermined cell fate undergoes an asymmetrical mitosis, leading to bicellular pollen (B). At that stage the pollen grain composes a large vegetative cell containing a small germ cell with a nucleus showing relatively higher chromatin compaction. The germ cell divides into 2 sperm cells with highly condensed chromatin, leading to the tricellular pollen grain (C). (D–I) *rbr* pollen development. Cell fates are determined on the basis of nuclear morphology. (D) At the microspore stage, *rbr* pollen grain with 2 undetermined cell nuclei. (E) Bicellular-stage *rbr* pollen grain with 2 vegetative cell nuclei and 1 germ cell nucleus. (F) Tricellular-stage *rbr* pollen with 2 vegetative cell nuclei and 2 sperm cell nuclei. (G) Tricellular-stage *rbr* pollen with 4 vegetative cell nuclei and 1 germ cell nucleus. (H) Tricellular-stage *rbr* pollen with 1 vegetative cell nucleus and 4 germ cell nuclei. (I) Tricellular-stage *rbr* pollen with 2 vegetative cell nuclei and 4 germ cell nuclei. Nuclei are stained with DAPI. (Scale bars, 10 μm.) (J) Bicellular-stage WT pollen. The cell wall (arrows) is asymmetrically placed between the vegetative nucleus and the generative nucleus. (K) Bicellular stage *rbr* pollen. The cell wall (arrows) is symmetrically placed between the 2 vegetative nuclei. Nuclei are stained with DAPI, and the cell walls are stained with aniline blue. (L and M) Transmission electron micrographs of bicellular-stage WT pollen (L) and *rbr* pollen (M). Note the internal wall indicated by arrows in *rbr* pollen. (Scale bars, 10 μm in J and K; 5 μm in L; 2 μm in M.) (N) Bar chart showing percentage of the pollen contains 2 vegetative cells in *rbr-2*/+ mutants at microspore, early bicellular, mid-bicellular, and late bicellular stages. At late bicellular stage, the over-proliferation in pollen from *rbr-2*/+;*cdka-1*/+ plants was reduced to one seventh of the over-proliferation in pollen from *rbr-2*/+ plants. Error bars correspond to SEs calculated on the basis of several samples of 100 pollen grains, and the size of total population analyzed (n) is indicated above each column. m, microspore nucleus; g, germ cell nucleus; v, vegetative cell nucleus; s, sperm cell nucleus.

Half of the pollen produced by *rbr*/+ plants inherits the *rbr* mutation. We estimated that 30% of the *rbr* pollen was dead at the bicellular stage (Fig. 3-16; percentages are expressed relative to the estimated *rbr* pollen population and are thus twice as shown on Fig. 3-16). Fifty percent of *rbr* pollen showed abnormal development and 20% showed WT morphology. At the tricellular stage, at least 60% of the *rbr* pollen was dead (Fig. 3-16). As *rbr-2* male transmission rate is of the order of 10% (Table 3-2), we could assume that 20% *rbr* pollen with normal morphology at bicellular stage underwent further development as WT. We thus estimated that, at the tricellular stage, less than 20% of the *rbr* pollen would derive from abnormal 3-celled pollen observed at bicellular stage. Corresponding to our estimate, we observed a total of 8% of abnormal pollen grains showing a complex array of phenotypes (n =1000 pollen from *rbr-2*/+ plants). A predominant class of abnormal pollen contained 2 vegetative nuclei and 2 small sperm-like cells (4.6%; Fig. 3-17F). This class of abnormal pollen likely originated from the class shown in Fig. 3-17E in which either the generative cell divided into 2 sperm-like cells or the additional vegetative cell divided again, producing a generative cell. Several other types of pollen were observed (Fig. 3-17G,H,I). Some pollen contained 4 vegetative nuclei and 1 sperm-like nucleus (1.6%; Fig. 3-17G). This pollen class likely results from an additional division of the 2 vegetative cells followed by 1 unequal division of 1 of the 4 vegetative cells producing a generative-like cell. We also observed pollen containing 4 sperm nuclei, either associated with 2 vegetative-like nuclei (1.2%; Fig. 3-17I) or inside 1 vegetative cell (3.4%; Fig. 3-17H). The latter class probably originates from a supernumerary division in the germ lineage. We did not observe any of the aforementioned phenotypes among WT pollen (n > 300 for each stage).

We targeted partial down-regulation of *RBR* in each pollen cell type by the expression of *RBR* hairpin RNAi constructs. Transgenic lines expressing the *RBR* RNAi construct under the control of the germ line-specific promoters of *HTR10* (Ingouff et al., 2007) (Okada et al., 2005) (47 lines observed) and *GEX2* (Engel et al., 2005) (34 lines observed) did not show any defect in pollen viability or phenotype. In contrast, *RBR* RNAi expression restricted to the vegetative cell using the *LAT52* promoter (Twell, 1992) caused a distinct increase in vegetative nuclear DNA fluorescence (Fig. 3-18) in 10%–25% of pollen, reflecting increased DNA synthesis. However we did not observe ectopic division of the vegetative cell. Hence, *RBR* RNAi expression under the *LAT52* promoter caused a limited reduction of RBR activity leading to defects milder than the complete loss of *RBR* in *rbr* mutant alleles.

We conclude that *rbr* loss of function mostly affects the vegetative lineage and prevents arrest of cell division typical of vegetative cell fate. The loss of *rbr* function does not cause more than 2 additional rounds of cell division in comparison to WT. Further hyperproliferation in *rbr* pollen may be prevented by the limited supply of nutrients during pollen development leading to developmental arrest or death.

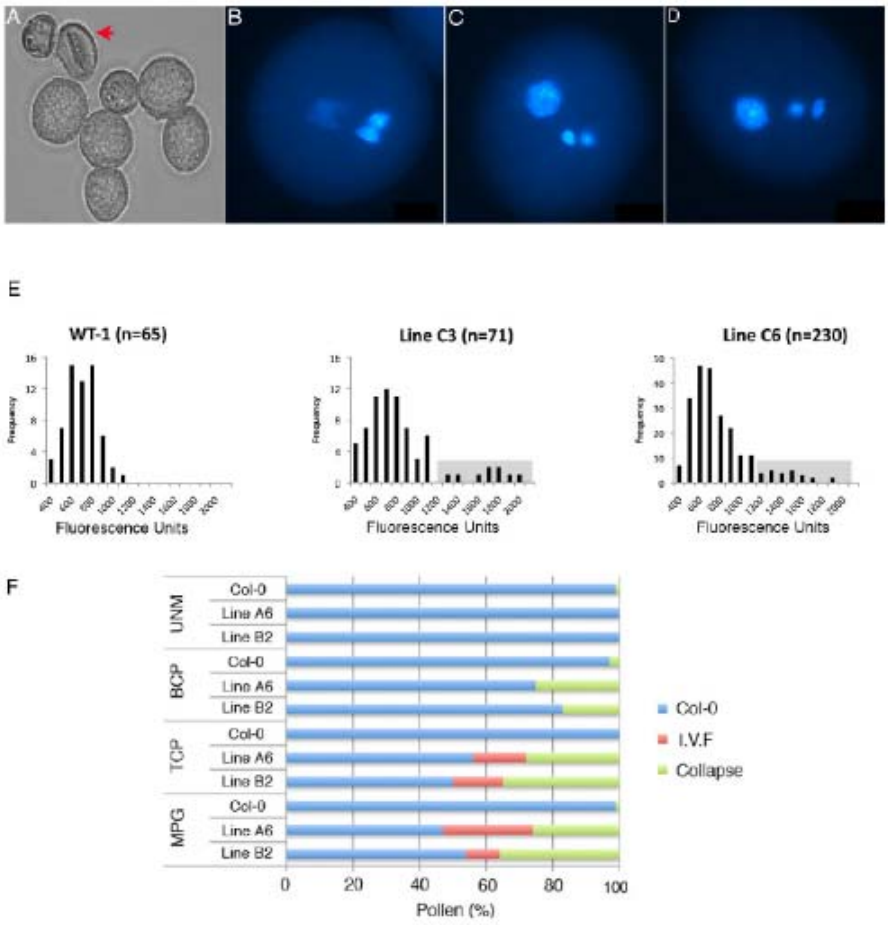

Fig. 3-18. Induced effect of *LAT52*-hp*RBR* construct during pollen development.
Cytological analysis of plants expressing hairpin dsRNA targeted to RBR mRNA specifically in the vegetative cell. (A) DIC image showing aborted pollen grains (red arrow) at the mature pollen stage. (B-D) DAPI stained mature pollen grains with a WT phenotype (B) and those with a novel phenotype showing increased vegetative nuclear intravascular fluorescent (I.V.F.) from 2 independent siblings (C and D). (E) Measurement of vegetative cell nucleus fluorescence following DAPI staining at the mature pollen stage emphasizing the new class of pollen grains (shaded box) with fluorescence units above that observed in the WT populations. Number of pollen grains analyzed is indicated in the parenthesis. Fluorescence intensity was measured using a Nikon TE2000 fluorescence microscope and OpenLab 5.0.2 software (Improvision). (F) Phenotypic analysis of 2 independent siblings at the uni-cellular microspore (UNM), bicellular pollen (BCP), tricellular pollen (TCP), and at mature pollen stage (MPG). Bar chart showing the origin of the aborted and I.V.F. phenotype as observed in 2 independent siblings. The aborted phenotype was traced to the bicellular stage, whereas the I.V.F. phenotype was initially detected at the tricellular stage and increased in mature pollen for line A6 but decreased in line B2.

3.2.3. Cell fate in *rbr* pollen

The nuclear morphology in *rbr* pollen suggested that cell over-proliferation in *rbr* pollen grains was associated with correct vegetative and germ cell fates. To address this question, we analyzed the expression of 6 cell fate markers in *rbr* pollen (Fig. 3-19 and Fig. 3-20). In the pollen displaying the rare phenotypic classes with duplication of the vegetative or germ cell lineages (Fig. 3-17), the *rbr* pollen expressed the vegetative cell markers *pLAT52-GFP* (Cheung et al., 2003) (Fig. 3-19F; n = 42) and *pAC26-H2BmRFP1* (Chen et al., 2008) (Fig. 3-19H; n =14) in the large vegetative-like cells and the germ line marker *pDUO1-DUO1-mRFP1* (Rotman et al., 2005) in the small germ-like cells (Fig. 3-19I; n = 9). These observations suggested that *rbr* does not affect cell fate in this class of pollen. Accordingly we observed that 0.3% (n = 1,327) of pollen grains from *rbr* mutant germinated 2 pollen tubes likely originating from 2 vegetative cells (Fig. 3-19J). We concluded that, despite cell over-proliferation in *rbr* pollen, the vegetative cell fate and sperm cell fate are not affected when pollen experiences a complete duplication.

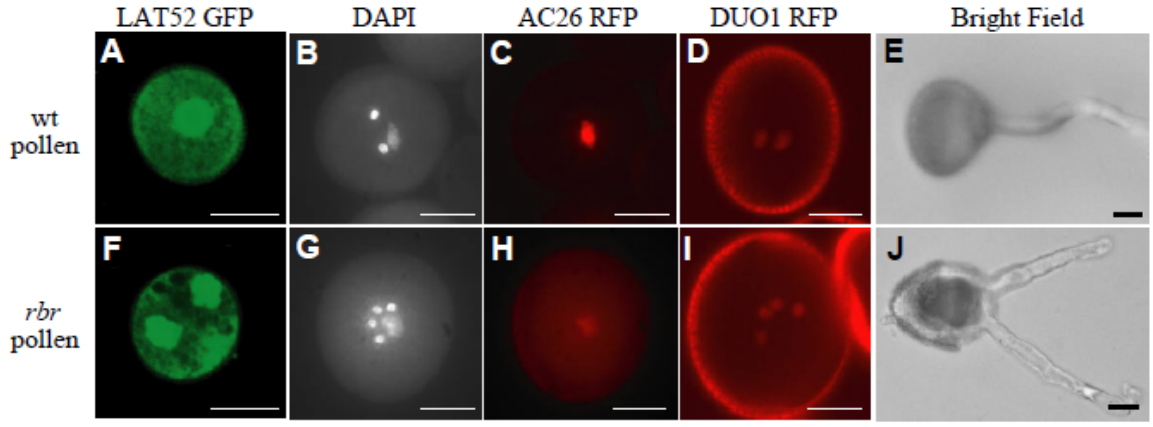

Fig. 3-19. Cell fate specification in *rbr* pollen.
(A–E)WT pollen grains. (F–J) *rbr* pollen grains. (A and F) Bicellular pollen grains expressing the vegetative cell marker *pLAT52-GFP*. (B and G) Fluorescence images of tricellular pollen grains stained with DAPI (C and H) The same pollen grains as B and G, respectively, expressing the vegetative cell marker *pAC26-H2B-mRFP*. WT pollen grain with 1 vegetative cell and 2 sperm cells (B) has only the vegetative cell nucleus expressing *pAC26-H2B-mRFP* (C). *rbr* pollen with 1 vegetative cells and 4 germ cells (G). Only the vegetative cell nucleus expresses *pAC26-H2B-mRFP* (*H*). (*D* and *I*) Tricellular pollen grains expressing the germ cell marker *pDUO1-DUO1-mRFP*. (E and J) In vitro pollen germination. WT pollen produces only 1 pollen tube germinated (E), whereas 2 pollen tubes germinated from the same *rbr* pollen grain (J). (Scale bars, 10 μm.)

We further studied the cell fates in the 3-celled *rbr* pollen, most representative of the *rbr* phenotype at WT bicellular stage (Fig. 3-20). In WT bicellular pollen, the germ cell expresses the markers *pHTR10-HTR10-mRFP* (Fig. 3-20A) and *pAC24-mRFP* (41) (Fig. 3-20D). In two thirds of *rbr* pollen with 1 germ cell nucleus and 2 vegetative cell nuclei, the markers were correctly expressed (Fig. 3-20B,E). However, in a third of 3-celled *rbr* pollen, both the germ cell nucleus and one of the vegetative-like nuclei expressed the germline markers (Fig. 3-20C,F). Such ectopic expression was never observed in WT pollen (n = 300 for each marker). In addition, when we observed the co-expression of the vegetative marker *pLAT52-GFP* and the germline marker *pDUO1-DUO1-mRFP* (Fig. 3-20G–J), a quarter of *rbr* pollen expressed the germline fate marker incorrectly. The additional vegetative-like cell expressed either the germline marker (n = 13 of 76; Fig. 3-20I) or both markers simultaneously (n = 7 of 76; Fig. 3-20J). We never observed mis-expression of the vegetative marker in the *rbr* germline (n = 76).

The *rbr* vegetative cell appears to behave like a microspore attempting imperfectly to reiterate an unequal division, producing an additional cell with vegetative fate, germ cell fate, or mixed fate identity. According to this hypothesis, genes expressed in the microspore but not later in the vegetative cell should be expressed in the vegetative cells of *rbr* pollen. Immunolocalization of the centromeric histone 3 variant HTR12 in WT tricellular pollen had shown that this protein marks only sperm cell nuclei (Talbert et al., 2002). Accordingly, the centromeric histone HTR12 fused to GFP (HTR12-GFP) placed under the control of its own promoter (Fang and Spector, 2005) was expressed in the WT microspore (Fig. 3-20K) but was no longer detected in the vegetative cell nucleus

after bicellular stage (Fig. 3-20L). *HTR12-GFP* expression was observed in all microspores from *rbr-2*/+ plants (n = 100; Fig. 3-20M), suggesting that RBR did not have a major impact on *HTR12-GFP* expression at that stage. In contrast to WT bicellular pollen, *rbr* 3-celled pollen showed ectopic expression of *HTR12-GFP* in vegetative cells (n = 24; Fig. 3-20N). This observation supported our hypothesis that the *rbr* vegetative cell retains the undetermined identity of the microspore. We thus concluded that *rbr* prevents cell fate establishment in the vegetative cell. A non-exclusive alternative explanation is that increased DNA methylation activity caused by increased *MET1* expression in *rbr* background (Jullien et al., 2008) impacts on heterochromatin organization, causing HTR12 recruitment. Our results thus led us to propose that loss of retinoblastoma function prevents cell fate establishment during male gametogenesis with an impact that depends on the cell type.

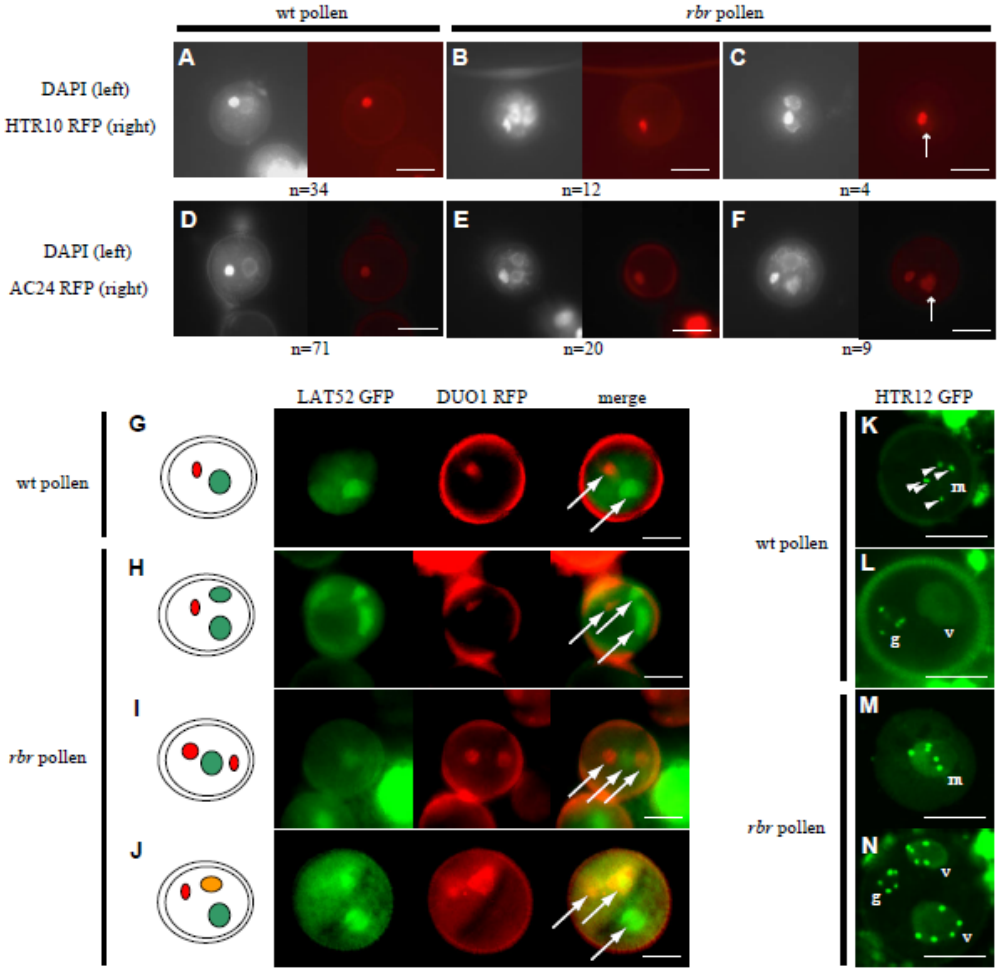

Fig. 3-20. Mis-specification of cell fate in *rbr* pollen.
(A–C) Fluorescence images of bicellular-stage pollen grains stained with DAPI (Left) and expressing *pHTR10-HTR10-mRFP* (Right). (D–F) Fluorescence images of bicellular-stage pollen grains stained with DAPI (Left) and expressing *pAC24-H2B-mRFP* (Right). Below each figure, n indicates the number of each case observed. (G–I) Fluorescence images of bicellular-stage pollen grains co-expressing the vegetative marker *pLAT52-GFP* and the germline marker *pHTR10-HTR10-mRFP*. Panels (Left to Right) are schematic representation of pollen co-expressing the 2 markers, GFP channel, RFP channel, and merged image. Arrows indicate the positions of cell nuclei. (K–N) Fluorescence images of microspores (K and M) and bicellular stage pollen grains (L and N) expressing the centromeric Histone 3 variant fused to GFP (HTR12-GFP). In WT (K and L), HTR12-GFP accumulates at the 5 chromocenters (arrowheads) of the microspore nucleus (m) (K) and the germ cell nucleus (g) (L), but it is not possible to distinguish chromocenters in the vegetative cell nucleus (v). In contrast, in *rbr* pollen, HTR12-GFP is detected at chromocenters in microspores (M) and in both cell types at bicellular stage (N). (Scale bars, 10 μm.)

3.2.4. *rbr* pollen defects are rescued by deregulation of the cell cycle

Perturbation of the RBR pathway by over-expression of cyclin D3 impacts on cell proliferation and the timing of endoreduplication in leaves and other vegetative tissues (Dewitte et al., 2003) (Dewitte et al., 2007). As endoreduplication usually marks differentiation in vegetative tissues, it was proposed that the cyclin D pathway controls cell differentiation (Dewitte et al., 2003). Although the impact on cell fate was not directly established in these studies, it is possible that the cyclin D pathway associated with cyclin-dependent kinase A (CDKA) regulates RBR function (Meijer and Murray, 2000) and mediates the transition toward differentiation via the promotion of endo-reduplication in plants.

We further hypothesized that, if *rbr* directly prevents cell commitment to differentiate, preventing hyperproliferation in an *rbr* background should not rescue the defective cell fate in *rbr* pollen. To prevent cell proliferation without affecting cell fate, we choose to manipulate the Cyclin Dependent Kinase A (CDKA), which controls RBR licensing of the entry to S phase but presumably not the involvement of RBR in chromatin remodeling complexes. In animals, a few reports have shown involvement of CDKA homologues in cell fate in Drosophila (Tio et al., 2001) and in *C. elegans* (Kostic et al., 2003). However, the mechanisms involving Cdks in cell polarity remain unclear. In *Arabidopsis* the function of the major Cdk CDKA has been solely linked to the control of the cell cycle in vegetative tissues (Beemster et al., 2002) and during male gametogenesis (Iwakawa et al., 2006) (Nowack et al., 2006) (Kim et al., 2008). We thus rationalized that antagonizing RBR regulation of the cell cycle by CDKA manipulation would allow us to

uncouple RBR functions in cell cycle regulation from other functions related to chromatin regulation. We tested in *rbr-2* pollen the effect of hypo-proliferation caused by the loss-of-function *cdka* mutant allele. In the *rbr-2*/+;*cdka-1*/+ double mutant, we studied the transmission of *rbr-2* and the phenotype of the pollen. The presence of *cdka-1* almost completely rescued the paternal transmission efficiency of *rbr-2* (Table 3-2), in agreement with the prediction of a complete viability of the *rbr-2*; *cdka-1* ($z = 32.52$, $P = 0.000001$, 2-tailed test if no complementation; $z = -1.24$, $P = 0.1075$, 2-tailed test if full complementation). Accordingly, pollen lethality (Fig. 3-21) and over-proliferation (Fig. 3-17N) were greatly decreased in *rbr-2*/+;*cdka-1*/+ plants. The percentage of defective pollen was decreased by more than half in *rbr-2*/+; *cdka-1*/+ plants in comparison to that from *rbr-2*/+ plants, both at bicellular and tricellular stages (Fig. 3-16B), leading to full rescue of pollen death in *rbr-2*/+; *cdka-1*/+ plants.

It thus appears that restoring proliferation to WT levels in an *rbr* background rescues the defects in cell fate establishment observed in the *rbr* mutant. We propose that the primary effect of the loss of function of RBR in male gametogenesis is mediated by its role in cell proliferation.

CHAPTER IV

DISCUSSION

4.1. CAF1 REGULATES CELL CYCLE BUT NOT CELL FATE DURING MALE GAMETOGENESIS

4.1.1. Loss of MSI1 function affects CAF1 function during pollen development

In *Arabidopsis*, MSI1 directly interacts with members of a conserved, endosperm-specific Polycomb group (Pc-G) complex (Guitton et al., 2004) (Kohler et al., 2003) and null *msi1* alleles cause production of autonomous endosperm and abnormal development of endosperm as the other mutants in genes encoding the subunits of the endosperm Pc-G complex (Guitton et al., 2004). MSI1 is also likely to be part of Pc-G complexes active during plant vegetative development (Berger et al., 2006) (Chanvivattana et al., 2004). Accordingly, partial reduction of MSI1 activity during vegetative development phenocopies the effect of mutations in vegetative Pc-G complexes (Hennig et al., 2005) (Hennig et al., 2003) (Katz et al., 2004) (Moon et al., 2003). However, *msi1*-null alleles also produce Pc-G independent phenotypes, including parthenogenesis and sporophytic embryo lethality, not observed in Pc-G mutants (Guitton and Berger, 2005b) (Guitton et al., 2004).

In my work I have shown that *msi1* affects pollen development and is associated with reduced paternal transmission. By contrast, loss-of-function mutations in all members of the Pc-G complex active in endosperm do not show male transmission or pollen defects (Chaudhury et al., 1997) (Grossniklaus et al., 1998). Other Pc-G genes are expressed during pollen development (Fig. 3-2), but their absence does not cause male sterility (Chanvivattana et al., 2004) (Gendall et al., 2001) (Goodrich et al., 1997) (Wang et al.,

2006). FIE is essential for Pc-G function (Guitton et al., 2004) (Ohad et al., 1996) and is expressed during pollen development (Honys and Twell, 2004). If defects in *msi1* pollen depended on Pc-G function, a similar reduction of paternal transmission should be expected for *msi1* and *fie*-null alleles. However, *fie* mutations are fully transmitted paternally (Guitton et al., 2004) (Ohad et al., 1996), and we could not observe any pollen defects in *fie*/+ mutant (transmission efficiency of the null *fie-11* allele from the male is 99.8%; *n*=800). We thus conclude that *fie* null mutations do not affect paternal transmission and that the effect of *msi1* on male transmission does not rely on Pc-G complexes.

Biochemical studies have demonstrated the potential association of MSI1 to the Rb-related protein RBR1 (Ach et al., 1997) but no direct evidence has been provided for a common function of RBR1 and MSI1 in *Arabidopsis*. Loss of RBR1 function alters pollen development. However the phenotypes associated with *rbr1* in pollen are dramatically distinct from *msi1* (Chen et al., 2009) and this difference does not support the association between RBR1 and MSI1 as the origin of pollen developmental defects in *msi1*.

Biochemical evidence has shown that MSI1 is also associated with the two core subunits of the CAF1 complex, FAS1 and FAS2 (Kaya et al., 2001). G2/M arrests have been reported in vegetative tissue of *fas1* and *fas2* homozygous mutants (Ramirez-Parra and Gutierrez, 2007). Our study shows the synergy between *fas1*, *fas2* and *msi1* mutations on

paternal transmission of *msi1* and on pollen development, strongly suggesting that the defects of *msi1* pollen development are caused by the loss of CAF1 function.

The limited penetrance of single mutations in *msi1*, *fas1* and *fas2* may originate from inheritance of wild-type proteins or transcripts from the microspore mother cell heterozygous for the mutation. In mammals and *Drosophila*, CAF1-independent histone chaperone activities include HISTONE REGULATORY A (HIRA) and ANTISILENCING FACTOR 1 (ASF1), which are associated directly with the deposition of histones H3 and H4 on newly synthesized chromatin (Polo and Almouzni, 2006). In *Arabidopsis*, the limited penetrance associated with the *fas1*, *fas2* and *msi1* mutations might also result from a redundant activity mediated by the putative HIRA homolog (Phelps-Durr et al., 2005) pathway or by a basic function of putative ASF1 homologs (www.chromdb.org).

4.1.2. Loss of CAF1 function in pollen arrests cell cycle but does not alter cell fate

Loss of CAF1 function causes activation of the DNA repair machinery (Endo et al., 2006) (Exner et al., 2006) (Kirik et al., 2006) (Ramirez-Parra and Gutierrez, 2007) and a decline in CDKA1 activity (Ramirez-Parra and Gutierrez, 2007). Moreover, the expression of FAS1 is activated at the G1-S transition by E2F (Ramirez-Parra and Gutierrez, 2007). Whether the cell cycle and cell fate deregulation observed in *fas1* and *fas2* vegetative tissues (Costa and Shaw, 2006) (Exner et al., 2006) originates directly from the deficit in CAF1 or results from more indirect epigenetic deregulations caused by the absence of CAF1 has remained unclear.

Within one to two cell divisions the pollen deficient for *MSI1* or *FAS1* and *FAS2* arrests before the first or the second pollen mitosis. DNA measurements suggested that the cell cycle arrest takes place at the G2-M transition, which is similar to that observed in vegetative tissues in plants and in other species. Hence we propose that loss of CAF1 function causes a cell cycle arrest before the first or the second mitosis during pollen development.

Cell cycle arrests at the G2-M transition would account for the most prominent phenotypes observed in *msi1* pollen. The wild-type sperm cells reach the mid-S phase, when pollen is shed from the anthers (Durbarry et al., 2005), and probably reach the G2-M transition, when they are released into the female gametes (Friedman, 1999). The transmission efficiency indicates that an additional fraction of *msi1* pollen is unable to transmit *msi1* (Fig. 4-1). It is thus possible that *msi1* pollen in this fraction contain two gametes that do not reach the G2-M transition when they are released into the female gametophyte and are unable to fertilize the female gamete, leading to ovule abortion.

It has become clear that some regulators of cell division take an active part in cell-fate decisions. In flowering plants, most cells in roots and in shoots are produced by the activity of meristems, which contain dividing stem cells (Benfey and Scheres, 2000) (Gegas and Doonan, 2006) (Scheres, 2001). In the root meristem, cell fate appears to be specified after the asymmetric division of the stem cell (Castellano and Sablowski, 2005) (Wildwater et al., 2005). However, the cell fate is established during the G1 phase (Caro

et al., 2007) (Costa and Shaw, 2006) and is not fixed until the last meristematic division, after which differentiation is initiated (Berger et al., 1998). Hence it is possible that cell division influences cell-fate commitment. The effects of mild alteration of cell cycle regulation during embryogenesis support the latter hypothesis (Jenik et al., 2005). Alteration of CAF1 causes aberrant morphogenesis of trichomes (Exner et al., 2006) and alters cell fate in root epidermal cells (Costa and Shaw, 2006). In contrast to cell-fate commitment in vegetative tissues, cell-fate establishment in pollen appears to be largely independent of cell-cycle deregulation in the *msi1* mutants, producing a fraction of bicellular pollen grains with a functional vegetative cell that delivers a functional single sperm-like cell. We have shown that *msi1* bicellular pollen correctly expresses cell-fate markers and produces a functional single sperm cell. Single sperm cells able to fertilize the egg cell are also produced by the mutant *cdka1* (Nowack et al., 2006). Hence cell fate and cell differentiation appear to be independent from cell-cycle regulation in pollen development.

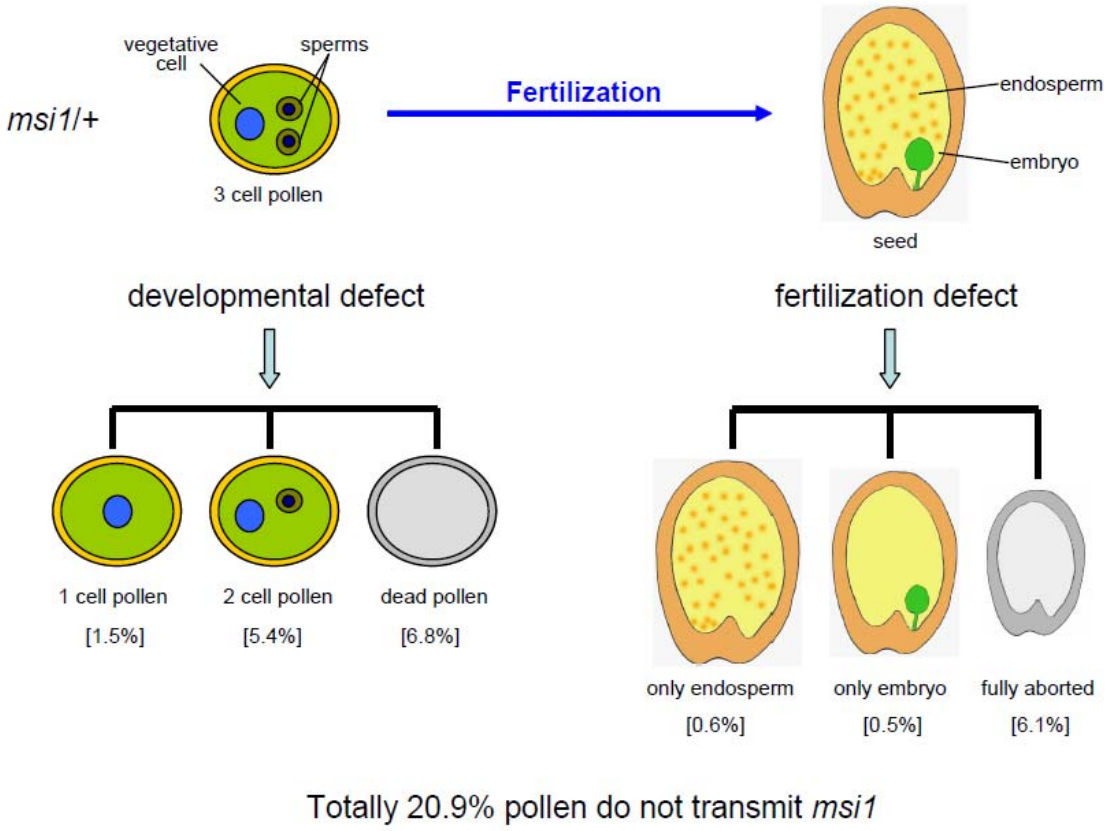

Fig. 4-1. Summary of the classes of abnormal pollen produced by *msi1* mutants and their impact on fertilization.

4.2. REGULATION OF SPERM FUSION DURING DOUBLE FERTILIZATION

4.2.1. Isomorphism or dimorphism of sperm cells

In *Plumbago zeylanica*, the two sperms are morphologically distinct and target a specific female gamete at fertilization. One sperm is larger, contains many mitochondria but few or no plastids, is directly associated with the vegetative nucleus, and is prone to fertilize the central cell. The smaller sperm containing many plastids but fewer mitochondria is likely to fuse with the egg cell (Russell, 1985). The morphologically distinct Plumbago sperms express different mRNAs (Gou et al., 2009). In maize, the egg cell is fertilized more frequently by sperm carrying B chromosomes than by sperm carrying only the A complement of chromosomes (Roman, 1948) (Faure et al., 2003). In Arabidopsis, the two sperm cells are morphologically identical (McCormick, 2004). All genes expressed in sperm studied thus far are expressed in both sperms (Engel et al., 2005) (Rotman et al., 2005) (Mori et al., 2006) (von Besser et al., 2006) (Ingouff et al., 2007), suggesting the two sperm cells do not differentiate from each other at the molecular level. Furthermore, when two wild-type sperm cells are delivered to *eostre* or *rbr* mutant female gametophytes that produces two egg cells rather than one, both egg cells can be fertilized, suggesting that both sperm cells have the capacity to fuse with an egg cell (Pagnussat et al., 2007) (Ingouff et al., 2009). These data suggest that Arabidopsis sperm cells are essentially interchangeable.

4.2.2. Preferential or random fertilization

Although sperm dimorphism was not reported in many species including Arabidopsis, it is nevertheless possible that isomorphic sperm cells differentiated to fertilize the egg cell or the central cell exclusively. This hypothesis was supported by the apparent preferential fertilization of the egg cell by single sperm cell produced in absence of either of two critical cell cycle regulators *CDKA* or *FBL17* (Iwakawa et al., 2006) (Nowack et al., 2006) (Kim et al., 2008) (Gusti et al., 2009). Three explanations for this egg-only fertilization were proposed. First, the relative position of the egg cell is closer than the central cell to the synergids where the pollen tube discharges the two sperms. Second, active signaling might be involved and the egg cell could attract the first sperm cell released by the pollen tube. Third, sperms could be predetermined for fertilization with the egg cell or the center cell (Nowack et al., 2006).

Our work showed that *msi1* pollen causes a low percentage of single fertilization events, leading either to embryo or endosperm development. The proportion of *msi1*/+ pollen that delivers single sperm cells is similar to the proportion of single fertilization events, suggesting that *msi1* single sperm cells are responsible for the single fertilization events. In addition we have shown that *msi1* single sperm cells express the terminal differentiation markers ATGEX1, accumulate HTR10 as wild-type sperms, and are transported by the pollen tube. We thus propose that *msi1*/+ plants produce a fraction of bicellular pollen with a single fully differentiated sperm cell able to fertilize either the egg or the central cell (Chen et al., 2008).

Recently, another type of pollen with a single sperm were generated by expression of the potent translation inhibitor, diphtheria toxin A subunit (DTA) (Frank and Johnson, 2009), driven from the *Arabidopsis thaliana HAP2 (GCS1)* promoter (von Besser et al., 2006). These pollen tubes targeted ovules and fertilized either the egg or the central cell, producing seeds with either only an embryo or only an endosperm. Endosperm-only seeds significantly outnumbered embryo-only seeds, suggesting that the single sperm preferentially fused with the central cell (Frank and Johnson, 2009).

As single sperm cells produced by *msi1* or by expression of *HAP2*:*DTA* are able to bypass the egg cell and fertilize the central cell, the relative position or active signaling by the egg cell to attract the first sperm cell could by ruled out as explanations for preferential fertilization of the egg cell by *cdka* or *fbl17* mutants. On the other hand, when two wild-type sperm cells are delivered to a mutant female gametophyte that produces two egg cells rather than one, both egg cells can be fertilized (Pagnussat et al., 2007) (Ingouff et al., 2009), ruling out that each of the two sperm cells has a predetermined target for fertilization.

4.2.3. Proposed mechanisms regulating the preference for fertilization

Although *cdka*, *fbl17*, *msi1* and expression of *HAP2*:*DTA* lead to similar pollen phenotypes in which pollen contains a single sperm cell, these mutants produce single sperm with different preferences for fertilization. One explanation is that each mutant has a different effect on male germline gene expression and this explanation assumes a factor that directs or enables the sperm cell to fuse with the egg cell or the central cell. *cdka* and

fbl17 specifically block cell cycle progression but are not expected to directly affect gene expression in the male germline, and the factor enables the sperm cell to fuse with the egg cell is properly expressed. Expression of *HAP2*:*DTA* blocks generative cell mitosis, and might also block translation of the factor expressed by *cdka* and *fbl17* single sperm cells that enables sperm to fuse with the egg cell. In agreement with this explanation, the single generative-like cell in *duo1* mutant is unable to fertilize because the expression of male germline-specific genes such as *HISTONE THREE RELATED 10* and *GEX1* is prevented (Brownfield et al., 2009), possibly including the factors that enable the sperm to fuse with the egg cell or the central cell. In *msi1* pollen, all germline fate markers analyzed are properly expressed, and the factor enabling the sperm to fuse with the female gametes is more likely expressed properly, so the single sperm fertilizes either the egg cell or the central cell.

The first explanation is based on the existence of factors that enable specific fusion between the male and female gametes. Another explanation would be the compatibility of the cell cycle between sperms and the female gametes. During double fertilization, the cellular components of the male and female gametes must synchronize their cell-cycle status to initiate harmoniously the developmental programs of the embryo and the endosperm. Several lines of evidence suggest that each female gamete is arrested at a distinct position in the cell cycle. First, RBR which controls the G1/S transition is expressed in the mature central cell but not in the egg cell (Ingouff et al., 2006); second, the initiation of the cell cycle is nearly immediate in the endosperm, whereas the first embryonic division takes place 16 hours after fertilization in the embryo (Faure et al.,

2002); third, the division of the zygote but not of the endosperm strictly requires the expression of the thymidylate kinase at the G1/S transition (Ronceret et al., 2008). On the male side, the single sperm cell produced in *cdka*, *fbl17*, *msi1*, *duo1* mutants and by expression of *HAP2*:*DTA* may arrest at different cell cycle stages. Loss of *CDKA* or *FBL17* blocks the generative cell cycle during S-phase and produces a single sperm cell with the DNA content at 1.5C (Nowack et al., 2006) (Kim et al., 2008). Loss of *MSI1* slows down the S-phase and the single sperm contains 1.8C DNA content (Chen et al., 2008). Expression of *HAP2*:*DTA* blocks generative cell mitosis and the single sperm DNA content is about 2C (Frank and Johnson, 2009). In *duo1*, the expression of cell cycle genes and male germline genes are disrupted (Brownfield et al., 2009), leading to a single generative-like cell with a DNA content of 2.5C (Durbarry et al., 2005). Considering the distinct fertilization behaviors and the different DNA contents of the single sperm cell from each mutant, we propose that the egg cell and the central cell may favor the sperm at a specific stage of cell cycle (Fig. 4-2). In wild-type pollen right after PMII, each sperm contains a DNA content of 1C. Sperm continues to synthesize DNA. When pollen tube reaches the ovary, the DNA content is about 1.75C DNA (Friedman, 1999). The single sperm in *msi1* has a similar DNA content of 1.8C, so it fertilizes randomly the two female gametes. The egg cell favors the sperm with a lower DNA content, so the single sperm from *cdka* or *fbl17* mutant preferentially fertilizes the egg cell. The central cell favors the sperm with a higher DNA content, so the single sperm resulting from expression of *HAP2*:*DTA* preferentially fertilizes the central cell. However, if the DNA content is too high, the sperm is no longer compatible for fertilization, as the case of *duo1* mutant.

Further experiments to compare the single sperm cell produced in these mutants may help to understand the mechanisms regulating the sperm fusion with its target. In vivo observation of double fertilization in Arabidopsis has been achieved (Ingouff et al., 2007). Live imaging of sperm release, sperm migration, and gamete fusion with increased time-resolution in the mutants producing single-sperm pollen will shed more light on whether the two sperms are identical and share an equal capacity to fertilize.

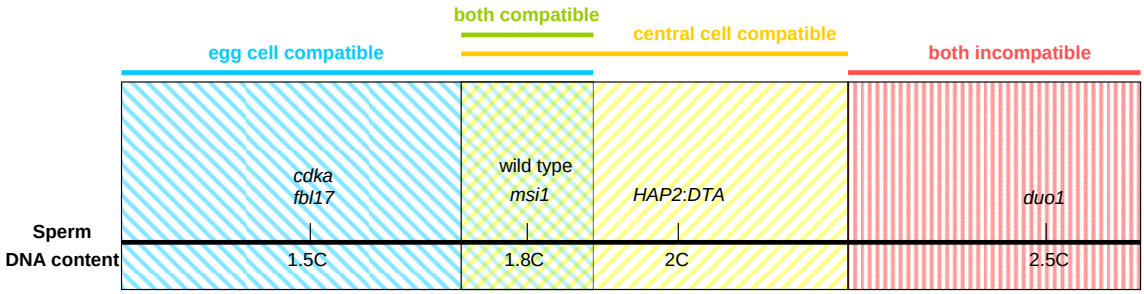

Fig. 4-2. The model of compatibility between sperm and female gametes during fertilization.
The egg cell favors the sperm cell with a lower DNA content (the range shown in blue). *cdka* or *fbl17* sperm has DNA content of 1.5C and preferentially fertilizes the egg cell. The central cell favors the sperm cell with a higher DNA content (the range show in yellow). Sperm produced by expression of *HAT*:*DTA* has a DNA content of 2C and preferentially fertilizes the central cell. Each wild-type sperm has a DNA content of 1.75C (the overlapping range of blue and yellow, shown in green) upon fertilization and two sperm fertilize the egg cell and the central cell. *msi1* sperm has a DNA content of 1.8C, similar as wild-type sperm, and fertilizes randomly the egg cell or the central cell. When the sperm DNA content goes too high (the range shown in red), as the case in *duo1*, it becomes incompatible with fertilization.

4.3. LOSS OF *RBR* CAUSES CELL OVER-PROLIFERATION WITH A SECONDARY IMPACT ON CELL FATE DURING MALE GAMETOGENESIS

4.3.1. Loss of *RBR* causes limited cell over-proliferation in pollen

The retinoblastoma tumor suppressor gene is functionally inactivated in most human carcinoma either by direct mutation or deletion (Weinberg, 1995), or indirectly through altered expression or activity of upstream regulators (Sherr and McCormick, 2002). In contrast to the situation in animals, disturbances in cell proliferation control are not associated with either cell death or oncogenic transformation. Plants are strikingly tolerant to altered levels of cell-cycle regulators. Arabidopsis genome contains the single retinoblastoma gene homologue *RBR* (Vandepoele et al., 2002). Genetic analysis suggests that RBR has essential functions in plant early development since the knock out *rbr* mutant is gametophytic lethal. Inactivation of *RBR* in Arabidopsis endosperm results in over-proliferation due to failure in blocking mitosis, indicating a negative regulatory role for RBR in the mitotic cell division cycle (Ebel et al., 2004). Decreasing the activity of RBR by inducible expression of a viral RBR-binding protein in Arabidopsis, causes abnormal leaf development, probably due to prolonged cell proliferation (Desvoyes et al., 2006). RBR could control differentiation as well. Ectopic expression in shoot and root apical meristems stimulates in early differentiation (Wyrzykowska et al., 2006) (Wildwater et al., 2005). Suppressing *RBR* expression in the root apical meristem by *RBR*-RNAi resulted in the production of several extra layers of undifferentiated cells in the columella root cap. Moreover, Arabidopsis RBR could work according to the

canonical CycD/RBR/E2F pathway model to regulate stem cell maintenance (Wildwater et al., 2005).

In order to dissect the role of RBR on cell proliferation and cell differentiation immediately after the loss of RBR function, we investigated the *rbr* pollen phenotypes. Our study shows that *rbr* loss of function leads to over-proliferation in all cell types at microspore, bicellular and tricellular stages. However, the vegetative lineage at bicellular stage over-proliferates the most (24.3%) in *rbr* mutants. At the microspore stage, only 0.67% microspores divide equally into 2 cells. The very limited impact of *rbr* on microspore division might be explained by inheritance of residual RBR from the *rbr*/+ meiotic precursor. At the tricellular stage, 4.6% pollen contains 4 sperm cells. The limited proliferation of sperm lineage might be explained by the endogenous RBR-independent mechanism to prevent sperm cell over-proliferation. In wild-type pollen right after PMII, each sperm contains a DNA content of 1C. Sperms reinitiate S phase and just prior to double fertilization sperm arrested at G2/M (Friedman, 1999). An unidentified mechanism acts to block the cell division until the zygote is formed.

The loss of RBR function does not cause more than 2 additional rounds of cell division in comparison to WT. The hyperproliferation in *rbr* pollen may be prevented by the limited supply of nutrients and limited cytoplasmic space constrained by the rigid pollen wall during pollen development. The over-proliferated cells compete for nutrients leading to developmental arrest or death (Fig.3-16).

4.3.2. Loss of *RBR* causes defects on cell fate establishment

Our study shows that the control of the degree of proliferation by RBR is essential for proper cell fate establishment during male gametogenesis. One scenario is that the loss of Retinoblastoma function primarily promotes hyperproliferation causing the production of additional cells. It is not clear how cell fate is established in the bicellular pollen but gradients of fate determinants have been hypothesized (McCormick, 2004) (Eady et al., 1995). The additional cells produced by the *rbr* pollen might be positioned improperly relative to developmental cues, causing anomalous or mixed cell fate. An alternative scenario proposes that RBR controls simultaneously cell division and cell fate commitment. This could be mediated directly by the cell cycle machinery as suggested by a role of CDKA homologues in cell fate reported in a few cell types (Tio et al., 2001) (Kostic et al., 2003) (Cowan and Hyman, 2006). A third non-exclusive hypothesis relates to the role of the Rb protein in chromatin modifications. In mammals amongst the several chromatin remodeling complexes interacting with Rb (Harbour and Dean, 2000c) (Dahiya et al., 2001) (Nielsen et al., 2001) (Vandel et al., 2001) (Macaluso et al., 2006), Rb appears to recruit during S phase a multiprotein complex containing the DNA methyltransferase Dnmt1 and the histone 3 methyltransferase G9a (Sharif et al., 2007). It is tempting to speculate that this complex is conserved in plants and that cell fate establishment of the two pollen cell types requires chromatin modifications dependent on the synthesis of new DNA and histone incorporation (Fig. 4-3). Our data showing the perturbed heterochomatin structure in *rbr* vegetative cells rather supports this hypothesis. In the absence of RBR function, hyperproliferation coupled to the absence of recruitment of chromatin modifying complexes prevents cell fate establishment. Such defects are

rescued directly by antagonizing hyperproliferation by mutation of *CDKA*. Our results suggest that RBR coordinates cell fate determination with cell proliferation during development. Such a role would explain why it has not been possible to separate the developmental and proliferative effects linked to deregulation of Retinoblastoma.

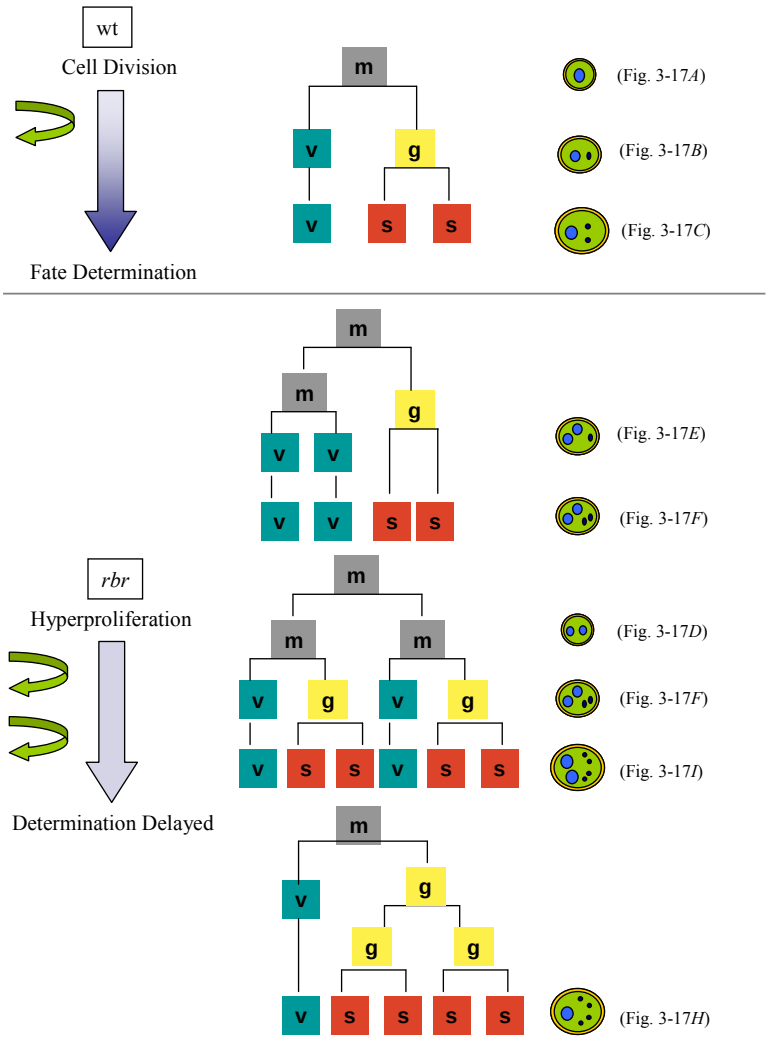

Fig. 4-3. **Model of RBR in the control of cell proliferation and fate determination.** In absence of RBR, the different cell types observed during pollen development, experience one or exceptionally two rounds of additional proliferation. In most cases this affects the vegetative cell (v) that maintains a microspore fate (m), dividing into two v cells or one v cell and one germ cell (g). In less common cases, the m cell or the g cell duplicates. In all cases fate determination appears delayed, which is likely the direct consequence of the loss of RBR function. However fate determination delay is prevented by proliferation arrest. This leads the hypothesis that in wild-type pollen, RBR promotes the progressive accumulation of cell fate determinants (blue gradient in the temporal arrow) according to mechanisms that necessitate cell DNA replication (green curved arrows). These mechanisms may involve RBR containing complexes causing chromatin modification. In *rbr* pollen, hyper-proliferation coupled to the loss of recruitment of RBR containing complexes prevents accumulation of cell fate determinants (no gradient in the arrow) and fate determination.

REFERENCES

Ach, R.A., Taranto, P., and Gruissem, W. (1997). A conserved family of WD-40 proteins binds to the retinoblastoma protein in both plants and animals. The Plant cell **9,** 1595-1606.

Beemster, G.T., De Vusser, K., De Tavernier, E., De Bock, K., and Inze, D. (2002). Variation in growth rate between Arabidopsis ecotypes is correlated with cell division and A-type cyclin-dependent kinase activity. Plant physiology **129,** 854-864.

Benfey, P.N., and Scheres, B. (2000). Root development. Curr Biol **10,** R813-815.

Bensmihen, S., To, A., Lambert, G., Kroj, T., Giraudat, J., and Parcy, F. (2004). Analysis of an activated ABI5 allele using a new selection method for transgenic Arabidopsis seeds. FEBS Lett **561,** 127-131.

Berger, F., Grini, P.E., and Schnittger, A. (2006). Endosperm: an integrator of seed growth and development. Curr Opin Plant Biol **9,** 664-670.

Berger, F., Haseloff, J., Schiefelbein, J., and Dolan, L. (1998). Positional information in root epidermis is defined during embryogenesis and acts in domains with strict boundaries. Curr Biol **8,** 421-430.

Berger, F., Hamamura, Y., Ingouff, M., and Higashiyama, T. (2008). Double fertilization - caught in the act. Trends in plant science **13,** 437-443.

Berleth, T., and Chatfield, S. (2002). Embryogenesis: Pattern Formation from a Single Cell. The Arabidopsis Book.

Blanc, G., Barakat, A., Guyot, R., Cooke, R., and Delseny, M. (2000). Extensive duplication and reshuffling in the Arabidopsis genome. The Plant cell **12,** 1093-1101.

Boisnard-Lorig, C., Colon-Carmona, A., Bauch, M., Hodge, S., Doerner, P., Bancharel, E., Dumas, C., Haseloff, J., and Berger, F. (2001). Dynamic analyses of the expression of the HISTONE::YFP fusion protein in arabidopsis show that syncytial endosperm is divided in mitotic domains. The Plant cell **13,** 495-509.

Brehm, A., and Kouzarides, T. (1999). Retinoblastoma protein meets chromatin. Trends in biochemical sciences **24,** 142-145.

Brownfield, L., Hafidh, S., Borg, M., Sidorova, A., Mori, T., and Twell, D. (2009). A plant germline-specific integrator of sperm specification and cell cycle progression. PLoS Genet **5,** e1000430.

Caro, E., Castellano, M.M., and Gutierrez, C. (2007). A chromatin link that couples cell division to root epidermis patterning in Arabidopsis. Nature **447,** 213-217.

Castellano, M.M., and Sablowski, R. (2005). Intercellular signalling in the transition from stem cells to organogenesis in meristems. Curr Opin Plant Biol **8,** 26-31.

Chan, S.W., Henderson, I.R., and Jacobsen, S.E. (2005). Gardening the genome: DNA methylation in Arabidopsis thaliana. Nat Rev Genet **6,** 351-360.

Chanvivattana, Y., Bishopp, A., Schubert, D., Stock, C., Moon, Y.H., Sung, Z.R., and Goodrich, J. (2004). Interaction of Polycomb-group proteins controlling flowering in Arabidopsis. Development **131,** 5263-5276.

Chaudhury, A.M., Ming, L., Miller, C., Craig, S., Dennis, E.S., and Peacock, W.J. (1997). Fertilization-independent seed development in Arabidopsis thaliana. Proc Natl Acad Sci U S A **94,** 4223-4228.

Chen, Y.C., and McCormick, S. (1996). sidecar pollen, an Arabidopsis thaliana male gametophytic mutant with aberrant cell divisions during pollen development. Development **122,** 3243-3253.

Chen, Z., Tan, J.L., Ingouff, M., Sundaresan, V., and Berger, F. (2008). Chromatin assembly factor 1 regulates the cell cycle but not cell fate during male gametogenesis in Arabidopsis thaliana. Development **135,** 65-73.

Chen, Z., Hafidh, S., Poh, S.H., Twell, D., and Berger, F. (2009). Proliferation and cell fate establishment during Arabidopsis male gametogenesis depends on the Retinoblastoma protein. Proc Natl Acad Sci U S A **106,** 7257-7262.

Cheung, A.Y., Chen, C.Y., Tao, L.Z., Andreyeva, T., Twell, D., and Wu, H.M. (2003). Regulation of pollen tube growth by Rac-like GTPases. J Exp Bot **54,** 73-81.

Chia, W., Somers, W.G., and Wang, H. (2008). Drosophila neuroblast asymmetric divisions: cell cycle regulators, asymmetric protein localization, and tumorigenesis. The Journal of cell biology **180,** 267-272.

Clough, S.J., and Bent, A.F. (1998). Floral dip: a simplified method for Agrobacterium-mediated transformation of Arabidopsis thaliana. Plant J **16,** 735-743.

Costa, S., and Shaw, P. (2006). Chromatin organization and cell fate switch respond to positional information in Arabidopsis. Nature **439,** 493-496.

Cowan, C.R., and Hyman, A.A. (2006). Cyclin E-Cdk2 temporally regulates centrosome assembly and establishment of polarity in Caenorhabditis elegans embryos. Nature cell biology **8,** 1441-1447.

Dahiya, A., Wong, S., Gonzalo, S., Gavin, M., and Dean, D.C. (2001). Linking the Rb and polycomb pathways. Molecular cell **8,** 557-569.

Desvoyes, B., Ramirez-Parra, E., Xie, Q., Chua, N.H., and Gutierrez, C. (2006). Cell type-specific role of the retinoblastoma/E2F pathway during Arabidopsis leaf development. Plant physiology **140,** 67-80.

Dewitte, W., Riou-Khamlichi, C., Scofield, S., Healy, J.M., Jacqmard, A., Kilby, N.J., and Murray, J.A. (2003). Altered cell cycle distribution, hyperplasia, and inhibited differentiation in Arabidopsis caused by the D-type cyclin CYCD3. The Plant cell **15,** 79-92.

Dewitte, W., Scofield, S., Alcasabas, A.A., Maughan, S.C., Menges, M., Braun, N., Collins, C., Nieuwland, J., Prinsen, E., Sundaresan, V., and Murray, J.A. (2007). Arabidopsis CYCD3 D-type cyclins link cell proliferation and endocycles and are rate-limiting for cytokinin responses. Proc Natl Acad Sci U S A **104,** 14537-14542.

Dimova, D.K., and Dyson, N.J. (2005). The E2F transcriptional network: old acquaintances with new faces. Oncogene **24,** 2810-2826.

Durbarry, A., Vizir, I., and Twell, D. (2005). Male germ line development in Arabidopsis. duo pollen mutants reveal gametophytic regulators of generative cell cycle progression. Plant physiology **137,** 297-307.

Eady, C., Lindsey, K., and Twell, D. (1995). The Significance of Microspore Division and Division Symmetry for Vegetative Cell-Specific Transcription and Generative Cell Differentiation. The Plant cell **7,** 65-74.

Ebel, C., Mariconti, L., and Gruissem, W. (2004). Plant retinoblastoma homologues control nuclear proliferation in the female gametophyte. Nature **429,** 776-780.

Endo, M., Ishikawa, Y., Osakabe, K., Nakayama, S., Kaya, H., Araki, T., Shibahara, K., Abe, K., Ichikawa, H., Valentine, L., Hohn, B., and Toki, S. (2006). Increased frequency of homologous recombination and T-DNA integration in Arabidopsis CAF-1 mutants. EMBO J **25,** 5579-5590.

Engel, M.L., Holmes-Davis, R., and McCormick, S. (2005). Green sperm. Identification of male gamete promoters in Arabidopsis. Plant physiology **138,** 2124-2133.

Exner, V., Taranto, P., Schonrock, N., Gruissem, W., and Hennig, L. (2006). Chromatin assembly factor CAF-1 is required for cellular differentiation during plant development. Development **133,** 4163-4172.

Fang, Y., and Spector, D.L. (2005). Centromere positioning and dynamics in living Arabidopsis plants. Mol Biol Cell **16,** 5710-5718.

Faure, J.E., Rotman, N., Fortune, P., and Dumas, C. (2002). Fertilization in Arabidopsis thaliana wild type: developmental stages and time course. Plant J **30,** 481-488.

Faure, J.E., Rusche, M.L., Thomas, A., Keim, P., Dumas, C., Mogensen, H.L., Rougier, M., and Chaboud, A. (2003). Double fertilization in maize: the two male gametes from a pollen grain have the ability to fuse with egg cells. Plant J **33,** 1051-1062.

Francis, D. (2007). The plant cell cycle--15 years on. New Phytol **174,** 261-278.

Frank, A.C., and Johnson, M.A. (2009). Expressing the diphtheria toxin A subunit from the HAP2(GCS1) promoter blocks sperm maturation and produces single sperm-like cells capable of fertilization. Plant physiology.

Friedman, W.E. (1999). Expression of the cell cycle in sperm of Arabidopsis: implications for understanding patterns of gametogenesis and fertilization in plants and other eukaryotes. Development **126,** 1065-1075.

Friend, S.H., Bernards, R., Rogelj, S., Weinberg, R.A., Rapaport, J.M., Albert, D.M., and Dryja, T.P. (1986). A human DNA segment with properties of the gene that predisposes to retinoblastoma and osteosarcoma. Nature **323,** 643-646.

Funayama, R., and Ishikawa, F. (2007). Cellular senescence and chromatin structure. Chromosoma **116,** 431-440.

Garcia, D., Saingery, V., Chambrier, P., Mayer, U., Jurgens, G., and Berger, F. (2003). Arabidopsis haiku mutants reveal new controls of seed size by endosperm. Plant physiology **131,** 1661-1670.

Gegas, V.C., and Doonan, J.H. (2006). Expression of cell cycle genes in shoot apical meristems. Plant Mol Biol **60,** 947-961.

Gendall, A.R., Levy, Y.Y., Wilson, A., and Dean, C. (2001). The VERNALIZATION 2 gene mediates the epigenetic regulation of vernalization in Arabidopsis. Cell **107,** 525-535.

Goodrich, J., Puangsomlee, P., Martin, M., Long, D., Meyerowitz, E.M., and Coupland, G. (1997). A Polycomb-group gene regulates homeotic gene expression in Arabidopsis. Nature **386,** 44-51.

Gou, X., Yuan, T., Wei, X., and Russell, S.D. (2009). Gene expression in the dimorphic sperm cells of Plumbago zeylanica: transcript profiling, diversity, and relationship to cell type. Plant J.

Grossniklaus, U., Vielle-Calzada, J.P., Hoeppner, M.A., and Gagliano, W.B. (1998). Maternal control of embryogenesis by MEDEA, a polycomb group gene in Arabidopsis. Science (New York, N.Y **280,** 446-450.

Guitton, A.E., and Berger, F. (2005a). Control of reproduction by Polycomb Group complexes in animals and plants. Int J Dev Biol **49,** 707-716.

Guitton, A.E., and Berger, F. (2005b). Loss of function of MULTICOPY SUPPRESSOR OF IRA 1 produces nonviable parthenogenetic embryos in Arabidopsis. Curr Biol **15,** 750-754.

Guitton, A.E., Page, D.R., Chambrier, P., Lionnet, C., Faure, J.E., Grossniklaus, U., and Berger, F. (2004). Identification of new members of Fertilisation Independent Seed Polycomb Group pathway involved in the control of seed development in Arabidopsis thaliana. Development **131,** 2971-2981.

Gusti, A., Baumberger, N., Nowack, M., Pusch, S., Eisler, H., Potuschak, T., De Veylder, L., Schnittger, A., and Genschik, P. (2009). The Arabidopsis thaliana F-box protein FBL17 is essential for progression through the second mitosis during pollen development. PLoS ONE **4,** e4780.

Haerizadeh, F., Singh, M.B., and Bhalla, P.L. (2006). Transcriptional repression distinguishes somatic from germ cell lineages in a plant. Science (New York, N.Y **313,** 496-499.

Harbour, J.W., and Dean, D.C. (2000a). The Rb/E2F pathway: expanding roles and emerging paradigms. Genes & development **14,** 2393-2409.

Harbour, J.W., and Dean, D.C. (2000b). Rb function in cell-cycle regulation and apoptosis. Nature cell biology **2,** E65-67.

Harbour, J.W., and Dean, D.C. (2000c). Chromatin remodeling and Rb activity. Current opinion in cell biology **12,** 685-689.

Haushalter, K.A., and Kadonaga, J.T. (2003). Chromatin assembly by DNA-translocating motors. Nat Rev Mol Cell Biol **4,** 613-620.

Helin, K., Lees, J.A., Vidal, M., Dyson, N., Harlow, E., and Fattaey, A. (1992). A cDNA encoding a pRB-binding protein with properties of the transcription factor E2F. Cell **70,** 337-350.

Helin, K., Wu, C.L., Fattaey, A.R., Lees, J.A., Dynlacht, B.D., Ngwu, C., and Harlow, E. (1993). Heterodimerization of the transcription factors E2F-1 and DP-1 leads to cooperative trans-activation. Genes & development **7,** 1850-1861.

Hennig, L., Bouveret, R., and Gruissem, W. (2005). MSI1-like proteins: an escort service for chromatin assembly and remodeling complexes. Trends Cell Biol **15,** 295-302.

Hennig, L., Taranto, P., Walser, M., Schonrock, N., and Gruissem, W. (2003). Arabidopsis MSI1 is required for epigenetic maintenance of reproductive development. Development **130,** 2555-2565.

Higashiyama, T., Yabe, S., Sasaki, N., Nishimura, Y., Miyagishima, S., Kuroiwa, H., and Kuroiwa, T. (2001). Pollen tube attraction by the synergid cell. Science (New York, N.Y **293,** 1480-1483.

Honys, D., and Twell, D. (2004). Transcriptome analysis of haploid male gametophyte development in Arabidopsis. Genome Biol **5,** R85.

Ingouff, M., Haseloff, J., and Berger, F. (2005). Polycomb group genes control developmental timing of endosperm. Plant J **42,** 663-674.

Ingouff, M., Jullien, P.E., and Berger, F. (2006). The female gametophyte and the endosperm control cell proliferation and differentiation of the seed coat in Arabidopsis. The Plant cell **18,** 3491-3501.

Ingouff, M., Hamamura, Y., Gourgues, M., Higashiyama, T., and Berger, F. (2007). Distinct dynamics of HISTONE3 variants between the two fertilization products in plants. Curr Biol **17,** 1032-1037.

Ingouff, M., Sakata, T., Li, J., Sprunck, S., Dresselhaus, T., and Berger, F. (2009). The two male gametes share equal ability to fertilize the egg cell in Arabidopsis thaliana. Curr Biol **19,** R19-20.

Iwakawa, H., Shinmyo, A., and Sekine, M. (2006). Arabidopsis CDKA;1, a cdc2 homologue, controls proliferation of generative cells in male gametogenesis. Plant J **45,** 819-831.

Jacks, T., Fazeli, A., Schmitt, E.M., Bronson, R.T., Goodell, M.A., and Weinberg, R.A. (1992). Effects of an Rb mutation in the mouse. Nature **359,** 295-300.

Jenik, P.D., Jurkuta, R.E., and Barton, M.K. (2005). Interactions between the cell cycle and embryonic patterning in Arabidopsis uncovered by a mutation in DNA polymerase epsilon. The Plant cell **17,** 3362-3377.

Johnston, A.J., Matveeva, E., Kirioukhova, O., Grossniklaus, U., and Gruissem, W. (2008). A dynamic reciprocal RBR-PRC2 regulatory circuit controls Arabidopsis gametophyte development. Curr Biol **18,** 1680-1686.

Joubes, J., Chevalier, C., Dudits, D., Heberle-Bors, E., Inze, D., Umeda, M., and Renaudin, J.P. (2000). CDK-related protein kinases in plants. Plant Mol Biol **43,** 607-620.

Jullien, P.E., Mosquna, A., Ingouff, M., Sakata, T., Ohad, N., and Berger, F. (2008). Retinoblastoma and Its Binding Partner MSI1 Control Imprinting in Arabidopsis. PLoS biology **6,** e194.

Katz, A., Oliva, M., Mosquna, A., Hakim, O., and Ohad, N. (2004). FIE and CURLY LEAF polycomb proteins interact in the regulation of homeobox gene expression during sporophyte development. Plant J **37,** 707-719.

Kaya, H., Shibahara, K.I., Taoka, K.I., Iwabuchi, M., Stillman, B., and Araki, T. (2001). FASCIATA genes for chromatin assembly factor-1 in arabidopsis maintain the cellular organization of apical meristems. Cell **104,** 131-142.

Kim, H.J., Oh, S.A., Brownfield, L., Hong, S.H., Ryu, H., Hwang, I., Twell, D., and Nam, H.G. (2008). Control of plant germline proliferation by SCF(FBL17) degradation of cell cycle inhibitors. Nature **455,** 1134-1137.

Kirik, A., Pecinka, A., Wendeler, E., and Reiss, B. (2006). The chromatin assembly factor subunit FASCIATA1 is involved in homologous recombination in plants. The Plant cell **18,** 2431-2442.

Kohler, C., Hennig, L., Bouveret, R., Gheyselinck, J., Grossniklaus, U., and Gruissem, W. (2003). Arabidopsis MSI1 is a component of the MEA/FIE Polycomb group complex and required for seed development. EMBO J **22,** 4804-4814.

Korenjak, M., and Brehm, A. (2005). E2F-Rb complexes regulating transcription of genes important for differentiation and development. Current opinion in genetics & development **15,** 520-527.

Kostic, I., Li, S., and Roy, R. (2003). cki-1 links cell division and cell fate acquisition in the C. elegans somatic gonad. Dev Biol **263,** 242-252.

Lee, Y.R., Li, Y., and Liu, B. (2007). Two Arabidopsis phragmoplast-associated kinesins play a critical role in cytokinesis during male gametogenesis. The Plant cell **19,** 2595-2605.

Linger, J., and Tyler, J.K. (2005). The yeast histone chaperone chromatin assembly factor 1 protects against double-strand DNA-damaging agents. Genetics **171,** 1513-1522.

Liu, J., and Qu, L.J. (2008). Meiotic and Mitotic Cell Cycle Mutants Involved in Gametophyte Development in Arabidopsis. Molecular Plant **1,** 564-574.

Macaluso, M., Montanari, M., and Giordano, A. (2006). Rb family proteins as modulators of gene expression and new aspects regarding the interaction with chromatin remodeling enzymes. Oncogene **25,** 5263-5267.

Mathieu, O., Reinders, J., Caikovski, M., Smathajitt, C., and Paszkowski, J. (2007). Transgenerational stability of the Arabidopsis epigenome is coordinated by CG methylation. Cell **130,** 851-862.

McCormick, S. (2004). Control of male gametophyte development. The Plant cell **16 Suppl,** S142-153.

Meijer, M., and Murray, J.A.H. (2000). The role and regulation of D-type cyclins in the plant cell cycle. Plant Mol Biol **43,** 621-633.

Moon, Y.H., Chen, L., Pan, R.L., Chang, H.S., Zhu, T., Maffeo, D.M., and Sung, Z.R. (2003). EMF genes maintain vegetative development by repressing the flower program in Arabidopsis. The Plant cell **15,** 681-693.

Morgan, D.O. (1997). Cyclin-dependent kinases: engines, clocks, and microprocessors. Annual review of cell and developmental biology **13,** 261-291.

Mori, T., Kuroiwa, H., Higashiyama, T., and Kuroiwa, T. (2006). GENERATIVE CELL SPECIFIC 1 is essential for angiosperm fertilization. Nature cell biology **8,** 64-71.

Nielsen, S.J., Schneider, R., Bauer, U.M., Bannister, A.J., Morrison, A., O'Carroll, D., Firestein, R., Cleary, M., Jenuwein, T., Herrera, R.E., and Kouzarides, T. (2001). Rb targets histone H3 methylation and HP1 to promoters. Nature **412,** 561-565.

Nowack, M.K., Grini, P.E., Jakoby, M.J., Lafos, M., Koncz, C., and Schnittger, A. (2006). A positive signal from the fertilization of the egg cell sets off endosperm proliferation in angiosperm embryogenesis. Nat Genet **38,** 63-67.

Oh, S.A., Bourdon, V., Das, M., Dickinson, H., and Twell, D. (2008). Arabidopsis Kinesins HINKEL and TETRASPORE Act Redundantly to Control Cell Plate Expansion during Cytokinesis in the Male Gametophyte. Molecular Plant **1,** 794-799.

Oh, S.A., Johnson, A., Smertenko, A., Rahman, D., Park, S.K., Hussey, P.J., and Twell, D. (2005). A divergent cellular role for the FUSED kinase family in the plant-specific cytokinetic phragmoplast. Curr Biol **15,** 2107-2111.

Ohad, N., Margossian, L., Hsu, Y.C., Williams, C., Repetti, P., and Fischer, R.L. (1996). A mutation that allows endosperm development without fertilization. Proc Natl Acad Sci U S A **93,** 5319-5324.

Okada, T., Endo, M., Singh, M.B., and Bhalla, P.L. (2005). Analysis of the histone H3 gene family in Arabidopsis and identification of the male-gamete-specific variant AtMGH3. Plant J **44,** 557-568.

Okuda, S., Tsutsui, H., Shiina, K., Sprunck, S., Takeuchi, H., Yui, R., Kasahara, R.D., Hamamura, Y., Mizukami, A., Susaki, D., Kawano, N., Sakakibara, T., Namiki, S., Itoh, K., Otsuka, K., Matsuzaki, M., Nozaki, H., Kuroiwa, T., Nakano, A., Kanaoka, M.M., Dresselhaus, T., Sasaki, N., and Higashiyama, T. (2009). Defensin-like polypeptide LUREs are pollen tube attractants secreted from synergid cells. Nature **458,** 357-361.

Ono, T., Kaya, H., Takeda, S., Abe, M., Ogawa, Y., Kato, M., Kakutani, T., Mittelsten Scheid, O., Araki, T., and Shibahara, K. (2006). Chromatin assembly factor 1 ensures the stable maintenance of silent chromatin states in Arabidopsis. Genes Cells **11,** 153-162.

Pagnussat, G.C., Yu, H.J., and Sundaresan, V. (2007). Cell-fate switch of synergid to egg cell in Arabidopsis eostre mutant embryo sacs arises from misexpression of the BEL1-like homeodomain gene BLH1. The Plant cell **19,** 3578-3592.

Park, J.A., Ahn, J.W., Kim, Y.K., Kim, S.J., Kim, J.K., Kim, W.T., and Pai, H.S. (2005). Retinoblastoma protein regulates cell proliferation, differentiation, and endoreduplication in plants. Plant J **42,** 153-163.

Park, S.K., and Twell, D. (2001). Novel patterns of ectopic cell plate growth and lipid body distribution in the Arabidopsis gemini pollen1 mutant. Plant physiology **126,** 899-909.

Park, S.K., Howden, R., and Twell, D. (1998). The Arabidopsis thaliana gametophytic mutation gemini pollen1 disrupts microspore polarity, division asymmetry and pollen cell fate. Development **125,** 3789-3799.

Park, S.K., Rahman, D., Oh, S.A., and Twell, D. (2004). gemini pollen 2, a male and female gametophytic cytokinesis defective mutation. Sex Plant Reprod **17,** 63-70.

Phelps-Durr, T.L., Thomas, J., Vahab, P., and Timmermans, M.C. (2005). Maize rough sheath2 and its Arabidopsis orthologue ASYMMETRIC LEAVES1 interact with HIRA, a predicted histone chaperone, to maintain knox gene silencing and determinacy during organogenesis. The Plant cell **17,** 2886-2898.

Polo, S.E., and Almouzni, G. (2006). Chromatin assembly: a basic recipe with various flavours. Current opinion in genetics & development **16,** 104-111.

Preuss, D., Rhee, S.Y., and Davis, R.W. (1994). Tetrad analysis possible in Arabidopsis with mutation of the QUARTET (QRT) genes. Science (New York, N.Y **264,** 1458-1460.

Ramirez-Parra, E., and Gutierrez, C. (2007). E2F regulates FASCIATA1, a chromatin assembly gene whose loss switches on the endocycle and activates gene expression by changing the epigenetic status. Plant physiology **144,** 105-120.

Ridgway, P., and Almouzni, G. (2001). Chromatin assembly and organization. J Cell Sci **114,** 2711-2712.

Riou-Khamlichi, C., Huntley, R., Jacqmard, A., and Murray, J.A. (1999). Cytokinin activation of Arabidopsis cell division through a D-type cyclin. Science (New York, N.Y **283,** 1541-1544.

Riou-Khamlichi, C., Menges, M., Healy, J.M., and Murray, J.A. (2000). Sugar control of the plant cell cycle: differential regulation of Arabidopsis D-type cyclin gene expression. Molecular and cellular biology **20,** 4513-4521.

Roman, H. (1948). Directed fertilization in maize. Proc Natl Acad Sci U S A **34,** 36-42.

Ronceret, A., Gadea-Vacas, J., Guilleminot, J., Lincker, F., Delorme, V., Lahmy, S., Pelletier, G., Chaboute, M.E., and Devic, M. (2008). The first zygotic division in Arabidopsis requires de novo transcription of thymidylate kinase. Plant J **53,** 776-789.

Rotman, N., Durbarry, A., Wardle, A., Yang, W.C., Chaboud, A., Faure, J.E., Berger, F., and Twell, D. (2005). A novel class of MYB factors controls sperm-cell formation in plants. Curr Biol **15,** 244-248.

Rusche, M.L., Mogensen, H.L., Shi, L., Keim, P., Rougier, M., Chaboud, A., and Dumas, C. (1997). B chromosome behavior in maize pollen as determined by a molecular probe. Genetics **147,** 1915-1921.

Russell, S.D. (1985). Preferential fertilization in Plumbago: Ultrastructural evidence for gamete-level recognition in an angiosperm. Proc Natl Acad Sci U S A **82,** 6129-6132.

Scheres, B. (2001). Plant cell identity. The role of position and lineage. Plant physiology **125,** 112-114.

Schonrock, N., Exner, V., Probst, A., Gruissem, W., and Hennig, L. (2006). Functional genomic analysis of CAF-1 mutants in Arabidopsis thaliana. J Biol Chem **281,** 9560-9568.

Sharif, J., Muto, M., Takebayashi, S., Suetake, I., Iwamatsu, A., Endo, T.A., Shinga, J., Mizutani-Koseki, Y., Toyoda, T., Okamura, K., Tajima, S., Mitsuya, K., Okano, M., and Koseki, H. (2007). The SRA protein Np95 mediates epigenetic inheritance by recruiting Dnmt1 to methylated DNA. Nature **450,** 908-912.

Shen, W.H. (2002). The plant E2F-Rb pathway and epigenetic control. Trends in plant science **7,** 505-511.

Sherr, C.J., and Roberts, J.M. (1999). CDK inhibitors: positive and negative regulators of G1-phase progression. Genes & development **13,** 1501-1512.

Sherr, C.J., and McCormick, F. (2002). The RB and p53 pathways in cancer. Cancer Cell **2,** 103-112.

Sorensen, M.B., Mayer, U., Lukowitz, W., Robert, H., Chambrier, P., Jurgens, G., Somerville, C., Lepiniec, L., and Berger, F. (2002). Cellularisation in the endosperm of Arabidopsis thaliana is coupled to mitosis and shares multiple components with cytokinesis. Development **129,** 5567-5576.

Stals, H., and Inze, D. (2001). When plant cells decide to divide. Trends in plant science **6,** 359-364.

Strompen, G., Dettmer, J., Stierhof, Y.D., Schumacher, K., Jurgens, G., and Mayer, U. (2005). Arabidopsis vacuolar H-ATPase subunit E isoform 1 is required for Golgi organization and vacuole function in embryogenesis. Plant J **41,** 125-132.

Talbert, P.B., Masuelli, R., Tyagi, A.P., Comai, L., and Henikoff, S. (2002). Centromeric localization and adaptive evolution of an Arabidopsis histone H3 variant. The Plant cell **14,** 1053-1066.

Taylor-Harding, B., Binne, U.K., Korenjak, M., Brehm, A., and Dyson, N.J. (2004). p55, the Drosophila ortholog of RbAp46/RbAp48, is required for the repression of dE2F2/RBF-regulated genes. Molecular and cellular biology **24,** 9124-9136.

Tio, M., Udolph, G., Yang, X., and Chia, W. (2001). cdc2 links the Drosophila cell cycle and asymmetric division machineries. Nature **409,** 1063-1067.

Twell, D. (1992). Use of a nuclear-targeted β-glucuronidase fusion protein to demonstrate vegetative cell-specific gene expression in developing pollen. The Plant Journal **2,** 887-892.

Twell, D., Yamaguchi, J., Wing, R.A., Ushiba, J., and McCormick, S. (1991). Promoter analysis of genes that are coordinately expressed during pollen development reveals pollen-specific enhancer sequences and shared regulatory elements. Genes & development **5,** 496-507.

Twell, D., Park, S.K., Hawkins, T.J., Schubert, D., Schmidt, R., Smertenko, A., and Hussey, P.J. (2002). MOR1/GEM1 has an essential role in the plant-specific cytokinetic phragmoplast. Nature cell biology **4,** 711-714.

Vandel, L., Nicolas, E., Vaute, O., Ferreira, R., Ait-Si-Ali, S., and Trouche, D. (2001). Transcriptional repression by the retinoblastoma protein through the recruitment of a histone methyltransferase. Molecular and cellular biology **21,** 6484-6494.

Vandepoele, K., Raes, J., De Veylder, L., Rouze, P., Rombauts, S., and Inze, D. (2002). Genome-wide analysis of core cell cycle genes in Arabidopsis. The Plant cell **14,** 903-916.

Vision, T.J., Brown, D.G., and Tanksley, S.D. (2000). The origins of genomic duplications in Arabidopsis. Science (New York, N.Y **290,** 2114-2117.

von Besser, K., Frank, A.C., Johnson, M.A., and Preuss, D. (2006). Arabidopsis HAP2 (GCS1) is a sperm-specific gene required for pollen tube guidance and fertilization. Development **133,** 4761-4769.

Wang, D., Tyson, M.D., Jackson, S.S., and Yadegari, R. (2006). Partially redundant functions of two SET-domain polycomb-group proteins in controlling initiation of seed development in Arabidopsis. Proc Natl Acad Sci U S A **103,** 13244-13249.

Weinberg, R.A. (1995). The retinoblastoma protein and cell cycle control. Cell **81,** 323-330.

Wildwater, M., Campilho, A., Perez-Perez, J.M., Heidstra, R., Blilou, I., Korthout, H., Chatterjee, J., Mariconti, L., Gruissem, W., and Scheres, B. (2005). The RETINOBLASTOMA-RELATED gene regulates stem cell maintenance in Arabidopsis roots. Cell **123,** 1337-1349.

Wyrzykowska, J., Schorderet, M., Pien, S., Gruissem, W., and Fleming, A.J. (2006). Induction of differentiation in the shoot apical meristem by transient overexpression of a retinoblastoma-related protein. Plant physiology **141,** 1338-1348.

Yadegari, R., and Drews, G.N. (2004). Female gametophyte development. The Plant cell **16 Suppl,** S133-141.

APPENDIX I

A SUPPRESSOR SCREEN FOR NOVEL RBR INTERACTING PATHWAYS

INTRODUCTION

Suppressor screens are powerful strategies to uncover more information about a known gene or mutation, leading to the identification of other interacting components in a pathway. A suppressor screen starts with a known mutation and then identifies second-site mutations that suppress the mutant phenotype. One of the greatest strength of a suppressor screen is that many of the isolated alleles possess silent or weak phenotypes on their own and hence will only be isolated by such a screen.

A suppressor screen of the mutation *lin-35 in the Rb ortholog of C. elegans* successfully identified four classes of *lin-35* synthetic mutations (Bender et al., 2004). Interestingly, only one of those mutations, defined by *fzr-1*, affected a gene connected to cell cycle regulation. Other mutations were associated to novel functions for the Rb pathway. For instance, *xnp-1* encodes the *C. elegans* homolog of ATR-X, a human disease gene associated with severe forms of mental retardation and urogenital developmental defects. *xnp-1*/ATR-X is a member of the Swi2/Snf2 family of ATP-dependent helicases, which function in nucleosome remodeling and transcriptional regulation. The success from the suppressor screen performed in *C. elegans* implicates that a Rb suppressor screen is feasible and the genetic amenability of *Arabidopsis* makes it a good system to conduct this kind of screen.

Based on the observation that *cdka-1* rescues *rbr-2* (Chen et al., 2009), we started a suppressor screen in the *rbr-2* line, which carries a T-DNA insert in *RBR* associated with kanamycin resistance (Fig. 1). EMS (ethane methyl sulfonate) which alkylates primarily

guanine leading to mispairing (alkylated G pairs to T instead of C) was used as a mutagen. The *rbr-2* mutation associated with kanamycin resistance has no maternal transmission and the paternal transmission is around 10% (Ebel et al., 2004). We reasoned that mutations in an *RBR* suppressor would partially rescue the *rbr-2* transmission rate. This could be easily reflected by the increased number of surviving seedlings on kanamycin selection plates.

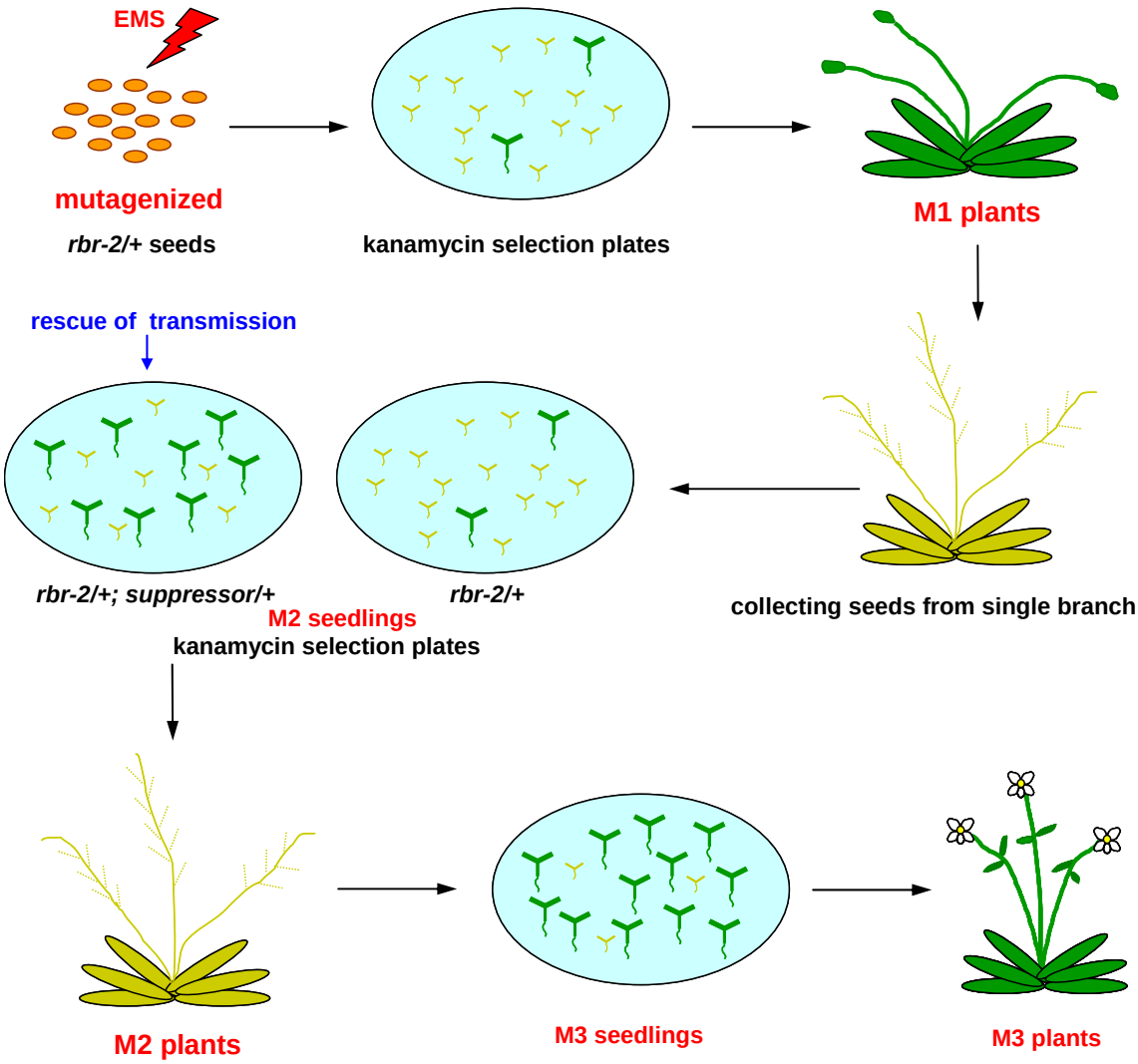

Fig. 1. Steps for the suppressor screen based on *rbr-2* transmission rate. 100,000 seeds were mutagenized by EMS. Around 5000 geminated seedlings on kanamycin selection plates were planted on soil. The primary shoot of each plant (M1) was cut off. When the plants became old, seeds from each plant were collected from a single branch. Then the seeds were put on kanamycin selection plates. The lines (M2) that showed an increased number of viable seedlings due to the rescue by a second mutation (suppressor mutation) associated with *rbr-2* were found. Seeds from M2 plants were collected and the *rbr-2* transmission rate of potential suppressor lines was confirmed in a successive generation (M3).

MATERIALS AND METHODS

EMS mutagenesis

Pretreatment of the seeds: Weigh 2 g of seeds (1 seed = 0.02 mg). Imbibe the seeds in a humid chamber on a fine plastic mesh and leave at 4^{o}C for 4 days. Blot the mesh with the wet seeds on dry filter paper and leave in growth chamber at 25^{o}C for 24 h. Keep the seeds in an envelope and perform seed surface sterilization by chlorine in vacuum container.

Mutagenesis: In chemical hood, inject 0.1 ml EMS (SIGMA) to 50 ml ddH_2O in a 100 ml Pyrex bottle. Use magnetic stirrer carefully to disperse the EMS for 5 min. Add the seeds to the EMS solution. Swing the Pyrex bottle carefully to disperse the seeds. Close the bottle cap and incubate for 8h. Put anything that had contact with the EMS solution into the decontaminating solution in a 5 L beaker (160 g NaOH in 4 L H_2O and add 50 ml thioglysolic acid).

Plant the mutagenized seeds: Decant EMS solution. Wash with distilled water for 3 times. Transfer the seeds in a 250 ml beaker and wash with distilled water for 10 times. Transfer seeds with 60 ml ddH_2O in a 100 ml beaker and add 40 ml hot MS medium. Swing to mix and then use plastic pipette to suck seeds and disperse on Kanamycin selection plates.

One day after mutagenesis: Aliquot the decontaminating solution and neutralize with HCl. Pour the solution down the drain and dilute with tap water. Fish out decontaminated

materials. Enclose waste in triple layered plastic bag and seal properly. Rinse glassware thoroughly and clean the working area.

RESULTS

Suppressor screen based on *rbr-2* transmission rate

After EMS treatment, around 5000 geminated seedlings showing kanamycin resistance on selection plates were planted on soil. We used an EMS concentration sufficiently low such that the estimated number of mutations per plant would not exceed 10. This was evaluated by earlier screens during which the proportion of mutations leading to albino seedlings was measured. We then estimated that saturation should be reached for 1000 M1 plants. Since the mutagen could mutate a single cell in the embryonic cell pool from which the entire plant derives, the existence of a mosaic in the primary shoot could obscure the effect of suppressor. By cutting off the primary shoot, each secondary shoot is derived from a single embryonic cell, so the mosaic effect could be eliminated in the M1 generation. Seeds from each M1 plant were collected from a single branch. Due to the lethality caused by EMS, we collected around 3000 lines from fertile M1 plants.

Seeds collected from the M1 were selected for kanamycin resistance. We screened 2076 lines and found 68 lines had a significant increase of surviving seedlings (surviving seedlings > 30%) (Table 1). 20 individuals from each of the 68 lines were grown on soil. Seeds from each individual were collected separately and grouped according to the 68 lines.

Table 1. M2 lines show the increase of *rbr-2* transmission.

Line ID	R	S	R/Total (%)	Line ID	R	S	R/Total (%)
1	74	107	40.884	**35**	72	39	64.865
2	56	32	63.636	**36**	71	54	56.800
3	69	158	30.396	**37**	90	6	93.750
4	41	95	30.147	**38**	98	7	93.333
5	72	24	75.000	**39**	92	16	85.185
6	83	37	69.167	**40**	88	13	87.129
7	74	37	66.667	**41**	77	30	71.963
8	54	114	32.143	**42**	119	11	91.538
9	50	104	32.468	**43**	31	58	34.831
10	63	147	30.000	**44**	75	62	54.745
11	56	48	53.846	**45**	37	59	38.542
12	56	114	32.941	**46**	77	32	70.642
13	80	160	33.333	**47**	85	6	93.407
14	51	102	33.333	**48**	64	45	58.716
15	50	66	43.103	**49**	84	42	66.667
16	40	86	31.746	**50**	83	65	56.081
17	57	27	67.857	**51**	45	38	54.217
18	45	107	29.605	**52**	120	24	83.333
19	26	51	33.766	**53**	67	34	66.337
20	68	76	47.222	**54**	25	16	60.976
21	81	37	68.644	**55**	24	27	47.059
22	49	40	55.056	**56**	33	19	63.462
23	44	64	40.741	**57**	62	96	39.241
24	95	103	47.980	**58**	31	44	41.333
25	69	77	47.260	**59**	80	17	82.474
26	27	23	54.000	**60**	43	35	55.128
27	66	46	58.929	**61**	61	22	73.494
28	102	28	78.462	**62**	37	65	36.275
29	80	171	31.873	**63**	34	43	44.156
30	49	29	62.821	**64**	21	21	50.000
31	91	45	66.912	**65**	50	117	29.940
32	40	32	55.556	**66**	9	13	40.909
33	52	42	55.319	**67**	25	25	50.000
34	76	84	47.500	**68**	54	57	48.649

After EMS treatment, the M1 plants should contain the suppressor mutations. And the suppressor should be heterozygous. In M2 seedlings, if the suppressor could rescue *rbr-2* transmission during both male and female gametogenesis, according to genetic combination, by theory, we should see the highest *rbr-2* transmission at 55.6% (Table 2). Among the 68 M2 lines which showed the *rbr-2* transmission rates more than 30%, 25 lines had a *rbr-2* transmission rate more than 60% (Fig. 2).

Table 2. Genetic combination of the genotypes of M2 if the suppressor rescues the *rbr-2* during both male and female gametogenesis.

parents	r	s	r;s	+
r	rr	r/s	rr/s	r
s	r/s	ss	r/ss	s
r;s	rr/s	r/ss	rr/ss	r/s
+	r	s	r/s	+

As *rbr-2* paternal transmission is estimated at 10%, to simplify the calculation, it is considered as no transmission. 9 combinations of genotypes in green survive, and among them 5 combinations contain *rbr-2*. So the theoretical transmission rate of *rbr-2* rescued by a suppressor acting on both parental germlines could be 5/9=55.6%.
s, suppressor; r, *rbr-2*; +, wild type. Red color indicates the dead genotype, and green color indicates the surviving genotype.

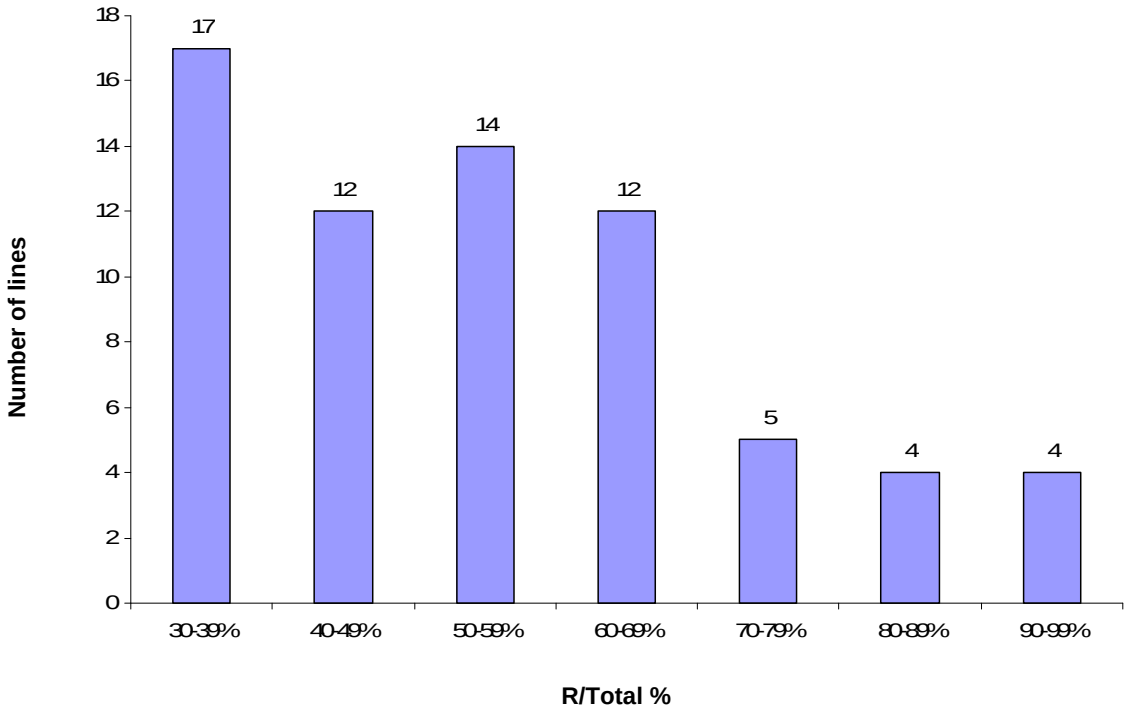

Fig. 2. The distribution of the *rbr-2* transmission rate among the M2 lines.

For each of the 68 M2 suppressor lines, we collected seeds from 20 individuals. In the M3 seedlings, we observed the variation of *rbr-2* transmission rates of the individuals from the same M2 lines. This variation may reflect a segregation of the heterozygote and homozygote of the potential suppressor. We only replicated 43 lines that had the highest *rbr-2* transmission rates (surviving seedlings > 50%) on selection plates (Table 3). Thus we predicted that the seeds collected from the M3 were more likely the suppressor homozygotes associated with *rbr-2* background.

Table 3. M3 lines show the highest *rbr-2* transmission rate.

Line ID	R/(R+S)	Line ID	R/(R+S)
C1	~100%	**M37**	~75%
C2	~100%	**M38**	~80%
C3	~100%	**M40**	~90%
C4	~100%	**M42**	~80%
M2	~80%	**M44**	~80%
M5	~100%	**M47**	~80%
M6	~100%	**M49**	~60%
M7	~90%	**M50**	~50%
M11	~80%	**M51**	~60%
M17	~80%	**M52**	~70%
M20	~70%	**M53**	~70%
M21	~80%	**M55**	~70%
M24	~50%	**M56**	~80%
M25	~70%	**M57**	~80%
M26	~70%	**M58**	~70%
M30	~60%	**M59**	~80%
M31	~60%	**M63**	~50%
M32	~50%	**M64**	~60%
M33	~70%	**M66**	~80%
M34	~85%	**M67**	~60%
M35	~80%	**M68**	~50%
M36	~80%		

The EMS mutagen creates random point mutations in the whole genome. From our estimation, each seed may contain about 5 to10 mutations. Some of the mutations will affect essential processes in development and reproduction. We observed a large number of sterile lines and a portion of the seeds we collected could not germinate. From M1 to M3, the mutant plants were selfed twice, in order to eliminate the sporophytic lethal mutations. To further eliminate remaining unwanted mutations, we performed additional backcrosses.

Suppressor screen based on pollen phenotype

In wild type background suppressors may not show a cytological phenotype. Therefore, to backcross or map these "silent" suppressors the original suppressed *rbr-2* must be included in all backcrossing and mapping strains. This can prove very difficult, so we focused primarily on the mutants that showed a phenotype in pollen development. We chose the "single sperm pollen" phenotype as one of the visible phenotypes of the suppressors to narrow down the number of candidate suppressors (Fig. 3).

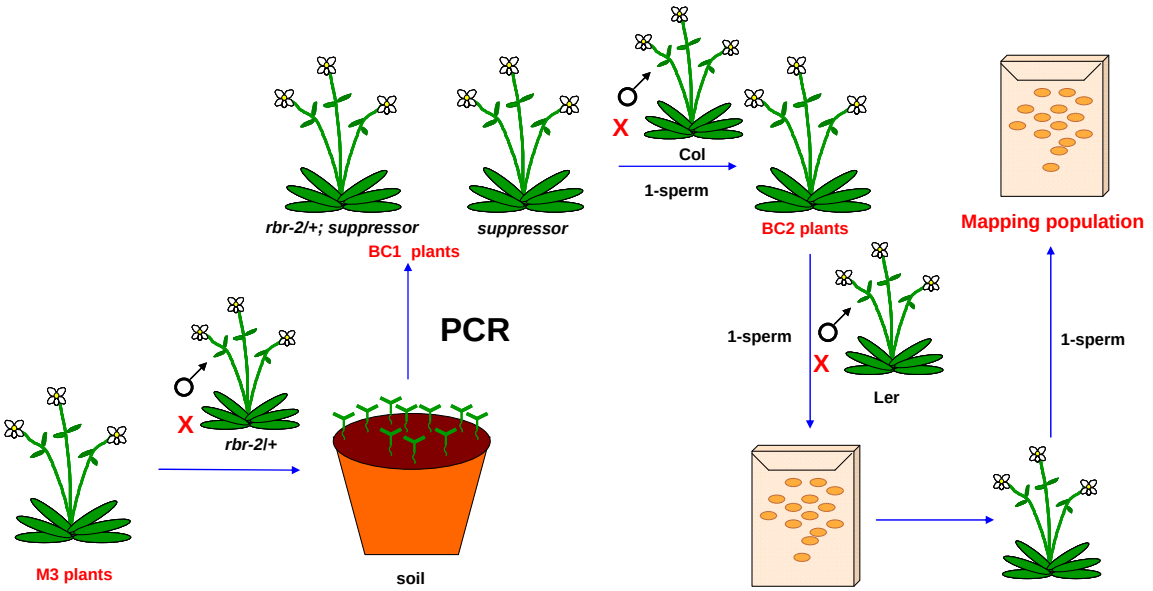

Fig. 3. Steps for the suppressor screen based on pollen phenotype. 43 M3 lines were backcrossed with *rbr-2*/+ father. The progeny were genotyped by PCR. The BC1 suppressors without *rbr-2* background were screened for single sperm pollen phenotype and the 12 lines showed the phenotype were backcrossed to Col father. The single sperm pollen phenotype was later confirmed in only four BC2 lines. They were backcrossed to Ler father. The progeny was propagated for the mapping population.

The 43 Backcross 1 (BC1) lines were backcrossed to *rbr-2* father (Fig. 3). The plants of the BC1 were genotyped by PCR (Table 4). The suppressor lines without *rbr-2* background were examined for pollen phenotype. Twelve BC1 lines were found to have more than 10% pollen containing a single sperm cell (Table 4).

Table 4. BC1 lines show 1-sperm pollen phenotype.

Line ID	*rbr-2*	total	%*rbr-2*	1-sperm pollen phenotype
C1-2	4	8	50.00	~15% (3 out of 6 plants checked)
M6-1	12	24	50.00	~10% (3 out of 3 plants checked)
M31-2	2	12	16.67	~15% (2 out of 2 plants checked)
M34-0	20	30	66.67	~10% (3 out of 3 plants checked)
M35-0	22	48	45.83	~30% (5 out of 7 plants checked)
M36-0	7	16	43.75	~20% (4 out of 4 plants checked)
M37-2	18	31	58.06	~30% (1 out of 4 plants checked)
M38-0	22	46	47.83	~10% (5 out of 6 plants checked)
M40-0	22	42	52.38	~30% (6 out of 6 plants checked)
M42-2	21	30	70.00	~20% (2 out of 4 plants checked)
M44-2	11	15	73.33	~10% (2 out of 4 plants checked)
M47-0	13	15	86.67	~15% (1 out of 3 plants checked)

The twelve BC1 lines were backcrossed to a Col as male (Fig. 3). Then the Backcross 2 (BC2) lines were examined for pollen phenotypes once more in order to see whether the pollen phenotype was heritable. Only four BC2 lines were found to produce pollen with single sperm (Table 5). Interestingly, line M40-0-51 had approximately 30% pollen that was unicellular.

Table 5. BC2 lines show 1-sperm pollen phenotype.

Line ID	total	1 sperm	pollen phenotype
M36-0-53	4	3	~40% pollen with 1-sperm
M37-2-84	12	1	~30% pollen with 1-sperm
M38-0-21	8	2	~30% pollen with 1-sperm
M42-2-7	16	2	~20% pollen with 1-sperm

The DNA of the four lines were extracted and will be used for sequencing in order to see whether any of them is the known mutant that gives the phenotype of a single sperm pollen, such as *cdka* (Nowack et al., 2006) (Iwakawa et al., 2006) or *fbl17* (Kim et al., 2008) (Gusti et al., 2009). The four lines M36-0-53, M37-2-84, M38-0-21 and M42-2-7 were crossed to Ler as males. The seeds were collected and grown for propagation. The mapping population was harvested. If the lines are not mutants of *cdka-1*or *fbl17*, they will be mapped by positional cloning.

In total, the suppressor lines were backcrossed for three times. In theory the number of mutations should be diluted 8 times. According to our estimation each line may contain about 5-10 mutations. After the two selfed generations and three backcrosses, each suppressor line should contain only one suppressor mutation.

Suppressor screen based on root phenotypes

In addition to the single-sperm phenotype during gametophytic phase, some suppressor lines were also expected to display sporophytic phenotypes. We chose to examine the root phenotypes because the root phenotypes present much earlier in the vegetative growth of Arabidopsis life cycle. We used the progeny from 44 BC1 suppressor lines without *rbr-2* background to screen for root phenotypes (Fig. 4).

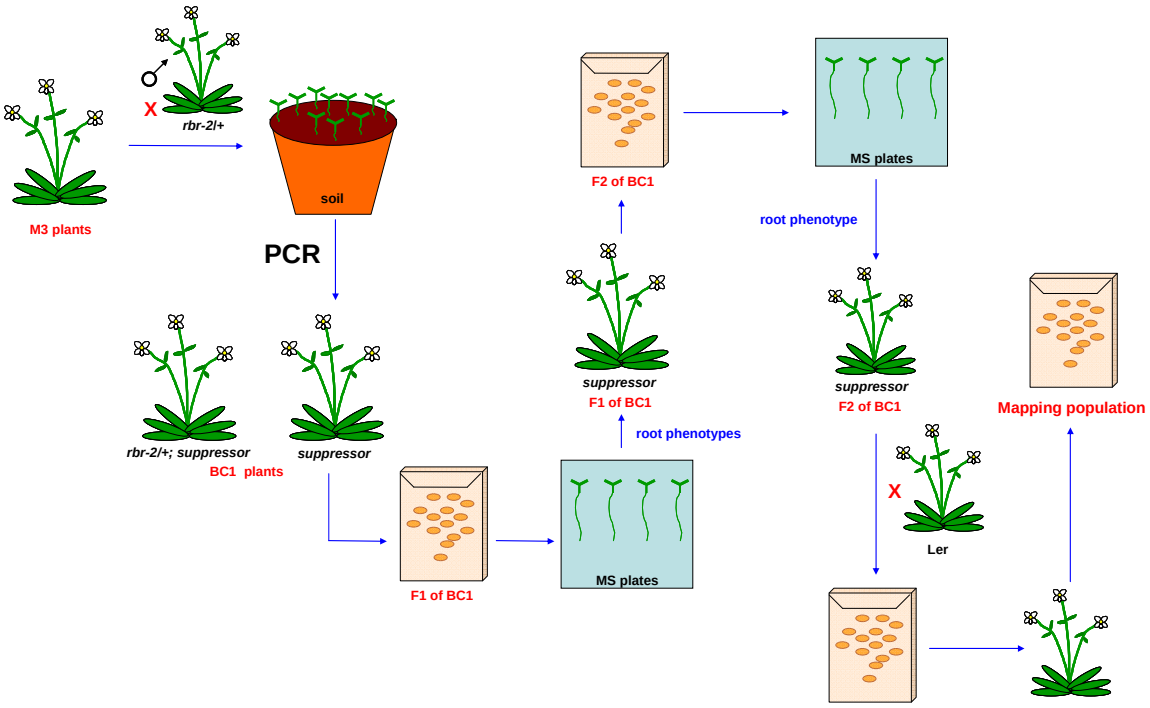

Fig. 4. Steps for the suppressor screen based on root phenotypes. The progeny from 44 BC1 suppressor lines without *rbr-2*/+ background were grown on MS plates with Col control. The lines with long roots, short roots and hairy roots were replicated and the seeds were collected. Then the seeds were grown and the root phenotypes were verified for another generation. 20 F2 of BC1 lines showed the inheritable root phenotypes. They were backcrossed to Ler and the progeny was propagated for the mapping population.

In each square Petri dish with MS medium, we put 4 wild-type Col seeds as control and 20 seeds from individual line (Fig 5). The Petri dishes were placed upright.

The root length and root hair were considered as main phenotypic factors. The F1 of BC1 suppressor lines with long roots, short roots or hairy roots were replicated and the seeds were collected (Table 6). Then the seeds were grown and the root phenotypes were verified for another generation. Notably, one quarter of the suppressor lines examined showed heritable hairy root phenotype (Fig. 6).

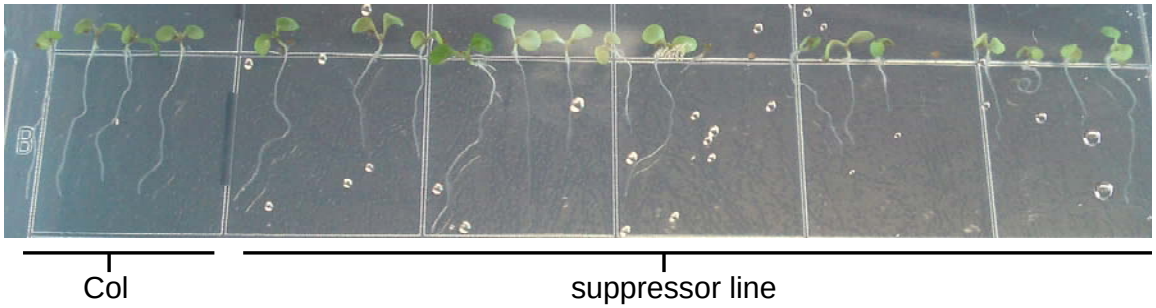

Fig. 5. The seeds of suppressor line and Col were geminated on Petri dish.

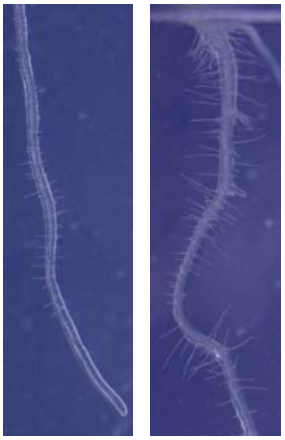

Fig. 6. Roots of Col and the suppressor line. The root from the suppressor line is highly hairy.

Table 6. Suppressor lines display root phenotypes.

Line of M3	Line of BC1	geminated	long	short	hairy (Y/N)	Line of F1 of BC1 with phenotype*	Line of F2 of BC1 with phenotype *
C1-2	7L	20	3	10	Y	L1	
C1-2	7R	20	2	10	N	L1,L2	
C1-2	8L	20	3	7	Y	L1,H1,H2	L1, H1
C1-2	8R	18	5	10	Y	L1,L2.H1,S1	
M6-1	1	15	1	7	N	L1	
M6-1	2	18	2	5	N	L1	
M6-1	3	17	1	9	N		
M31-2	1	20	0	10	N	H1	
M31-2	2	20	0	5	N	H1,H2	
M34-0	1	20	2	15	Y	L1,L2,H1	
M34-0	2	20	1	7	Y	L1,L2,H1,H2	L1, H2
M34-0	16	8	0	7	N	L1	
M35-0	10	16	5	6	Y	L1,L2,L3	L1, L2
M35-0	21	17	0	11	N		
M35-0	23	16	1	10	Y		
M35-0	45	17	2	8	Y		
M35-0	47	18	2	12	Y		
M36-0	51	20	0	8	Y	L1,L2,L3,H1,H2	H1, H2
M36-0	53	19	2	8	N	S1,S2	
M36-0	57	19	3	7	N	L1,L2	L2
M36-0	58	19	6	5	Y	L1,L2,L3,S1,H1	L3, H1
M37-2	84	20	1	11	Y		
M37-2	86	20	2	9	Y	L1	
M37-2	90	19	2	9	N		
M38-0	18	20	1	10	N	L1,L2	
M38-0	21	20	3	12	N		
M38-0	24	19	1	15	Y		
M38-0	30	17	0	12	N		
M38-0	36	20	1	15	N	L1,L2,H1,H2	H1, H2
M38-0	46	20	2	7	Y		
M40-0	51	19	3	7	Y	L1,L2,H1,H2,H3,H4	H1
M40-0	53	18	8	7	Y	L1	
M40-0	55	19	2	9	Y		
M40-0	57	19	5	5	Y	H1	
M40-0	68	16	3	4	Y	H1,H2	
M40-0	70	16	1	11	Y	H1,H2,H3,H4	H4
M42-2	3	20	2	9	Y	H1,H2	H1
M42-2	7	16	3	10	Y	H1,H2	H1
M42-2	18	18	2	6	Y	H1,H2	H2
M42-2	27	15	3	5	Y	H1,H2	H1
M44-2	35	16	2	9	N		
M44-2	42	13	2	6	Y		
M44-2	47	17	2	12	N	L1,L2,L3.L4	L1
M47-0	63	15	3	6	Y	H1,H2,H3	

*Note: L, long root. S, short root. H, hairy root.

In F2 of BC1, 20 lines showed the heritable root phenotypes were crossed to Ler. The seeds were collected and grown for propagation. The mapping population was harvested and they will be mapped by positional cloning.

Other categories of mutants found in the screen

During the screen we could see other phenotypes. In M2 plants, line 6 and line 54 were apparently tetraploid. In M3 plants, line M30 showed phenotypes characteristic of *ap1*mutant. In BC1 plants, line M57-6 grew much faster and stronger. In BC2 plants, line M40-0-51 produced unicellular pollen (arrested at microspore stage). As these phenotypes are beyond our current research scope; we focused only the 4 BC2 lines that show a single-sperm pollen phenotype.

DISCUSSION

The *rbr-2* screen identifies mutants of genes controlling pollen division

Among the 43 M3 suppressor lines isolated on the basis of *rbr-2* transmission, 4 lines eventually showed the single sperm pollen phenotype when they were isolated from *rbr-2* background. Lines M37-2-84, M38-0-21 and M42-2-7 produced similar percentages (20% to 30%) of single sperm pollen, and they showed similar *rbr-2* transmission rates. Thus, these mutants may belong to the same allelic group. The *cdka* mutant produced around 40% pollen with single sperm (Nowack et al., 2006) (Iwakawa et al., 2006), and the percentage of single sperm pollen in *fbl17* mutant was around 50% (Kim et al., 2008) (Gusti et al., 2009). Thus the lines M37-2-84, M38-0-21 and M42-2-7 might not be *cdka*

and *fbl17* alleles, but we cannot exclude that they are weak *cdka* or *fbl17* alleles containing a lower percentage of single sperm pollen. We will sequence the *CDKA* and *FBL17* gene loci in these suppressor lines.

The single sperm of *cdka* or *fbl17* mutant preferentially fertilizes the egg cell (Nowack et al., 2006) (Iwakawa et al., 2006) (Kim et al., 2008) (Gusti et al., 2009). However, the single sperm of *msi1* mutant fertilizes randomly one of the two female gametes (Chen et al., 2008). We will investigate the fertilization capacity of the single sperm from these suppressor lines. Finally, we will introduce cell fate markers in these suppressor lines to determine whether the single sperm phenotype is due to the cell cycle arrest or other developmental defects.

The rescue of *rbr-2* transmission hints at a role for RBR in meiosis

When we screened the M2 seedlings, if the suppressor could rescue *rbr-2* transmission during both male and female gametogenesis, we should see the highest *rbr-2* transmission at 55.6% (Table 2). However, among the 68 M2 lines which showed a *rbr-2* transmission rate greater than 30%, 25 lines had *rbr-2* transmission rate greater than 60% (Fig. 2). This high *rbr-2* transmission could not be explained by the gametophytic rescue. Among the M2 lines, 5 lines showed the percentage around 70% to 79%, and we observed 8 lines that had extremely high percentage of transmission (>80%) This high degree of *rbr-2* rescue may result from several causes, (1) the bigger deviation associated with relative small number of M2 seedlings (around 50-250) scored per line. (2) if the seeds were not evenly scattered on the selection plate, the local high density of the

seedlings may affect the Kanamycin selection. (3) We cannot exclude that in M2, the suppressor per se may not be able to survive, which will distort the theoretical highest *rbr-2* transmission to 90% (Table 7). (4) Alternatively, the high transmission may hint that the rescue occurs before the stage of gametogenesis, that is, in meiosis. Then the *rbr-2* could be transmitted both maternally and paternally and in theory we will obtain 50% *rbr-2* heterzygotes and 25% *rbr-2* homozyogtes. We should see 75% Kanamycin resistant seedlings.

Table 7. Genetic combination of the genotypes of M2 if the suppressor rescues the *rbr-2* both maternally and paternally, and the suppressor per se cannot survive.

parents	**r**	**s**	**r;s**	**+**
r	rr	r/s	rr/s	r
s	r/s	ss	r/ss	s
r;s	rr/s	r/ss	rr/ss	r/s
+	r	s	r/s	+

10 combinations of genotypes in green survive, and among them 9 combinations contain *rbr-2*. So *rbr-2* transmission rate could be up to 9/10=90%.
s, suppressor; r, *rbr-2*; +, wild type. Red color indicates the dead genotype, and green color indicates the surviving genotype.

Although a large number of genes essential for meiosis have been identified in Arabidopsis, little is known about the cell cycle machinery that controls the meiotic program. This is explained by the high overlap between the components for mitotic and meiotic cell cycles, causing mutations in key cell cycle regulators to affect plant growth in the sporophyte prior to meiosis (as plant development is post-embryonic). Still a study of an unusual "mimicry" allele of *cdka* in Arabidopsis suggested that the control of meiosis and mitosis by general cell cycle regulators might be distinct between meiosis and mitosis (Dissmeyer et al., 2007). From our genetic screen, we found that RBR may have a role in meiosis, and the potential suppressor may rescue the *rbr-2* defects during meiotic stage. Further investigations need to be done to examine the role of RBR during meiosis in detail.

RBR may interact with pathways regulating chromatin organization and histone modification to switch cell fate in roots

In addition to looking for the suppressors by gametophytic phenotype, we examined the sporophytic phenotype as well. We found a large number of the suppressor lines produced hairy roots. In Arabidopsis, root epidermal cells differentiate into hair and non-hair cells in a position-dependent manner (Dolan et al., 1993). Previous studies have shown that the position-dependent root epidermal patterning is determined by interactions of several patterning genes. TTG, GL3, EGL3 and WER are required to specify the non-hair fate. CPC, TRY and ETC1 are required to specify the root-hair fate (Schiefelbein et al., 2009). The expression level of these patterning genes may influence the cell fate switch in root epidermis. For example, the *wer* mutant produces excessive root hair cells

(Lee and Schiefelbein, 1999); whereas the *cpc* mutant produces a reduced number of root hair cells (Wada et al., 1997). It is still unclear whether the *rbr-2* suppressors that cause the hairy root phenotype produce ectopic hair cells. This remains to be investigated using hair cell fate markers and cytological markers.

Chromatin regulation influences root epidermal cell-type specification. In the *fas2* mutant, the activity of one of the three subunits of CAF1 is defective, which leads to the loss of the patterned chromatin organization at the GL2 locus (Costa and Shaw, 2006). The other CAF1 subunit MSI1 is physically bound to RBR (Jullien et al., 2008), thus the RBR suppressor may affect the chromatin assembly pathway to switch root epidermal cell fate.

Histone acetylation affects the expression of root epidermal patterning genes. Treatment of Trichostatin A (TSA), a specific inhibitor of histone deacelylase (HDAC) (Yoshida et al., 1990), produces roots with excessive hairs (Xu et al., 2005). The Rb protein was reported to be able to recruit a range of chromatin remodeling enzymes including HDAC (Nicolas et al., 2000). The recruitment of HDAC by Rb can reverse histone acetylation at promoters and lead to active repression of transcription. Thus the RBR suppressor may affect the histone modification pathway to switch root epidermal cell fate.

PERSPECTIVES

The suppressors that we screened based on pollen phenotype will likely lead us to identify new RBR interacting pathways involved in cell cycle and cell fate regulation. The suppressors that we screened based on root phenotype are more likely lead us to identify novel RBR interacting pathways involved in chromatin remodeling, including chromatin assembly and histone modification. In this respect the suppressor screen might be comparable to the screen performed in *C. elegans* (Bender et al., 2004). In addition, the unexpected high degree of rescue observed in some *rbr1-2* suppressors indicates that RBR may play a specific role in meiosis during Arabidopsis.

REFERENCES

Bender, A.M., Wells, O., and Fay, D.S. (2004). lin-35/Rb and xnp-1/ATR-X function redundantly to control somatic gonad development in C. elegans. Dev Biol **273,** 335-349.

Chen, Z., Tan, J.L., Ingouff, M., Sundaresan, V., and Berger, F. (2008). Chromatin assembly factor 1 regulates the cell cycle but not cell fate during male gametogenesis in Arabidopsis thaliana. Development **135,** 65-73.

Chen, Z., Hafidh, S., Poh, S.H., Twell, D., and Berger, F. (2009). Proliferation and cell fate establishment during Arabidopsis male gametogenesis depends on the Retinoblastoma protein. Proc Natl Acad Sci U S A **106,** 7257-7262.

Costa, S., and Shaw, P. (2006). Chromatin organization and cell fate switch respond to positional information in Arabidopsis. Nature **439,** 493-496.

Dissmeyer, N., Nowack, M.K., Pusch, S., Stals, H., Inze, D., Grini, P.E., and Schnittger, A. (2007). T-loop phosphorylation of Arabidopsis CDKA;1 is required for its function and can be partially substituted by an aspartate residue. Plant Cell **19,** 972-985.

Dolan, L., Janmaat, K., Willemsen, V., Linstead, P., Poethig, S., Roberts, K., and Scheres, B. (1993). Cellular organisation of the Arabidopsis thaliana root. Development **119,** 71-84.

Ebel, C., Mariconti, L., and Gruissem, W. (2004). Plant retinoblastoma homologues control nuclear proliferation in the female gametophyte. Nature **429,** 776-780.

Gusti, A., Baumberger, N., Nowack, M., Pusch, S., Eisler, H., Potuschak, T., De Veylder, L., Schnittger, A., and Genschik, P. (2009). The Arabidopsis thaliana F-box protein FBL17 is essential for progression through the second mitosis during pollen development. PLoS ONE **4,** e4780.

Iwakawa, H., Shinmyo, A., and Sekine, M. (2006). Arabidopsis CDKA;1, a cdc2 homologue, controls proliferation of generative cells in male gametogenesis. Plant J **45,** 819-831.

Jullien, P.E., Mosquna, A., Ingouff, M., Sakata, T., Ohad, N., and Berger, F. (2008). Retinoblastoma and its binding partner MSI1 control imprinting in Arabidopsis. PLoS Biol **6,** e194.

Kim, H.J., Oh, S.A., Brownfield, L., Hong, S.H., Ryu, H., Hwang, I., Twell, D., and Nam, H.G. (2008). Control of plant germline proliferation by SCF(FBL17) degradation of cell cycle inhibitors. Nature **455,** 1134-1137.

Lee, M.M., and Schiefelbein, J. (1999). WEREWOLF, a MYB-related protein in Arabidopsis, is a position-dependent regulator of epidermal cell patterning. Cell **99,** 473-483.

Nicolas, E., Morales, V., Magnaghi-Jaulin, L., Harel-Bellan, A., Richard-Foy, H., and Trouche, D. (2000). RbAp48 belongs to the histone deacetylase complex that associates with the retinoblastoma protein. J Biol Chem **275,** 9797-9804.

Nowack, M.K., Grini, P.E., Jakoby, M.J., Lafos, M., Koncz, C., and Schnittger, A. (2006). A positive signal from the fertilization of the egg cell sets off endosperm proliferation in angiosperm embryogenesis. Nat Genet **38,** 63-67.

Schiefelbein, J., Kwak, S.H., Wieckowski, Y., Barron, C., and Bruex, A. (2009). The gene regulatory network for root epidermal cell-type pattern formation in Arabidopsis. J Exp Bot **60,** 1515-1521.

Wada, T., Tachibana, T., Shimura, Y., and Okada, K. (1997). Epidermal cell differentiation in Arabidopsis determined by a Myb homolog, CPC. Science **277,** 1113-1116.

Xu, C.R., Liu, C., Wang, Y.L., Li, L.C., Chen, W.Q., Xu, Z.H., and Bai, S.N. (2005). Histone acetylation affects expression of cellular patterning genes in the Arabidopsis root epidermis. Proc Natl Acad Sci U S A **102,** 14469-14474.

Yoshida, M., Hoshikawa, Y., Koseki, K., Mori, K., and Beppu, T. (1990). Structural specificity for biological activity of trichostatin A, a specific inhibitor of mammalian cell cycle with potent differentiation-inducing activity in Friend leukemia cells. J Antibiot (Tokyo) **43,** 1101-1106.

APPENDIX II

PUBLICATIONS

Chen, Z., Tan, J.L., Ingouff, M., Sundaresan, V., and Berger, F. (2008). Chromatin assembly factor 1 regulates the cell cycle but not cell fate during male gametogenesis in Arabidopsis thaliana. *Development* **135,** 65-73.

Chen, Z., Hafidh, S., Poh, S.H., Twell, D., and Berger, F. (2009). Proliferation and cell fate establishment during Arabidopsis male gametogenesis depends on the Retinoblastoma protein. *Proc Natl Acad Sci USA* **106,** 7257-7262.

Andreuzza, S., Li, J., Guitton, A.E., Faure, J.E., Casanova, S., Park, J.S., Choi, Y., Chen, Z., and Berger, F. (2010). DNA LIGASE I exerts a maternal effect on seed development in Arabidopsis thaliana. *Development* **137,** 71-81.

Development 135, 65-73 (2008) doi:10.1242/dev.010108

Chromatin assembly factor 1 regulates the cell cycle but not cell fate during male gametogenesis in *Arabidopsis thaliana*

Zhong Chen[1], Jeanie Tan Li Hui[1], Mathieu Ingouff[1], Venkatesan Sundaresan[2] and Frederic Berger[1,*]

The interdependence of cell cycle control, chromatin remodeling and cell fate determination remains unclear in flowering plants. Pollen development provides an interesting model, as it comprises only two cell types produced by two sequential cell divisions. The first division separates the vegetative cell from the generative cell. The generative cell divides and produces the two sperm cells, transported to the female gametes by the pollen tube produced by the vegetative cell. We show in *Arabidopsis thaliana* that loss of activity of the Chromatin assembly factor 1 (CAF1) pathway causes delay and arrest of the cell cycle during pollen development. Prevention of the second pollen mitosis generates a fraction of CAF1-deficient pollen grains comprising a vegetative cell and a single sperm cell, which both express correctly cell fate markers. The single sperm is functional and fertilizes indiscriminately either female gamete. Our results thus suggest that pollen cell fate is independent from cell cycle regulation.

KEY WORDS: Pollen, CAF1, Cell cycle, *Arabidopsis thaliana*

INTRODUCTION

The Chromatin assembly factor 1 (CAF1) (Hennig et al., 2005; Kaya et al., 2001) has a conserved chaperone activity for chromatin assembly at the DNA replication fork during S phase. CAF1 targets acetylated histone H3-H4 dimers to newly synthesized DNA, thus allowing nucleosome assembly (Polo and Almouzni, 2006). In mammals, CAF1 is essential for cell viability and consists of the three proteins p150, p60 and p48. Loss of function of CAF1 activity in mammalian cells leads to activation of a DNA-damage signaling pathway that slows down the S phase and arrests the cell cycle (Haushalter and Kadonaga, 2003). In yeast, the CAF1 assembly complex subunits Cac1, Cac2 and Cac3 are dispensable for cell viability (Haushalter and Kadonaga, 2003; Ridgway and Almouzni, 2001), but loss of function of CAF1 causes increased sensitivity to DNA-damaging stresses (Linger and Tyler, 2005). *Arabidopsis* CAF1 contains a core of three proteins encoded respectively by the p150 homolog *FASCIATA1* (*FAS1*), the p60 homolog *FASCIATA2* (*FAS2*) and the pRbAp48 homolog *MULTICOPY SUPPRESSOR OF IRA1* (*MSI1*) (Kaya et al., 2001). The WD40 domain proteins MSI1 and pRbAp46/48 also bind to Retinoblastoma-related proteins (Ach et al., 1997; Qian and Lee, 1995; Rossi et al., 2003). This presumably regulates activity of the downstream E2F transcription factor, thereby influencing the gene activation required for entrance into S phase (Hennig et al., 2005). In *Arabidopsis*, reduction of *FAS1* and *FAS2* activities upregulates the expression of genes in the DNA-damage response pathway (Schonrock et al., 2006). In the absence of CAF1 activity, cells endoreduplicate to higher levels, suggesting that loss of function of *FAS1* or *FAS2* affects the S-G2 and the G2-M transitions in *Arabidopsis* (Endo et al., 2006; Exner et al., 2006; Kirik et al., 2006; Ramirez-Parra and Gutierrez, 2007). In parallel to the deregulation of the cell cycle, the loss of CAF1 function causes a reduction of the heterochromatic fraction (Kirik et al., 2006), releases transcriptional gene silencing from endogenous transposons (Ono et al., 2006) and alters the pattern of histone acetylation and methylation at promoters of genes encoding components and regulators of the cell cycle (Ramirez-Parra and Gutierrez, 2007). It remains unclear whether the vegetative developmental defects in *fas1* and *fas2* mutants (Costa and Shaw, 2006; Exner et al., 2006) are direct consequences of the loss of CAF1 on the cell cycle or result indirectly from the gradual accumulation of epigenetic defects.

In pollen produced from *msi1*/+ plants, the loss of MSI1 affects only half of the haploid pollen produced after meiosis. It is thus possible to investigate the immediate developmental consequence of the loss of CAF1 function using male gametogenesis as a model. Reduced paternal transmission of *msi1* was recorded from the null allele *msi1-2* (Guitton et al., 2004), suggesting the alteration of pollen development by removal of CAF1 function. Pollen development is characterized by a relatively simple series of events involving simultaneously cell fate and cell cycle regulation (McCormick, 2004). We report that loss of function of CAF1 complex members affects pollen development. Null alleles of *msi1* prevent division in a fraction of pollen. The effect of *msi1* on pollen arrest is synergistically enhanced when CAF1 activity is further compromised in *fas1* and *fas2* mutants. We further investigate the fate and differentiation of the pollen in the absence of CAF1.

MATERIALS AND METHODS

Plant material

The wild-type ecotypes Columbia (Col-0), Landsberg *erecta* (Ler), Enkheim (En) and C24 were provided by the Nottingham *Arabidopsis* Stock Centre. The mutant allele *msi1-1* (Col background) was previously characterized and kindly provided by Lars Hennig (Köhler et al., 2003). The mutant allele *msi1-2* (C24 background) was previously described in the laboratory in F.B. group (Guitton et al., 2004). The mutant allele *msi1-3* (Ler background) was obtained by V.S. The mutant allele *msi1-4* (Col background) was obtained and kindly provided by Gary Drews and Jayson Punwani (University of Utah). Seeds from *qrt1/qrt1* (Ler accession) were provided by D. Preuss. Homozygote *fas1-1* (CS265 En background) *fas1-4* (SAIL_662_D10 Col background) and *fas2-4* (SALK_033228, Col background) seeds were obtained from the *Arabidopsis* Biological Research Center. The KS22 enhancer-trap line (C24 accession) expressing the GFP reporter protein was generated in J. Haseloff's laboratory (www.plantsci.cam.ac.uk/Haseloff). Marker lines for cell identity in pollen pDUO1-DUO1-mRFP1 (C24) was obtained by N. Rotman (Rotman et al., 2005), AC26 mRFP (C24)

[1]Temasek Life Sciences Laboratory, 1 Research Link, National University of Singapore, Department of Biological Sciences, 117604, Singapore. [2]Section of Plant Biology, University of California, Davis, 1 Shields Avenue, Davis, CA 95616, USA.

*Author for correspondence (e-mail: fred@tll.org.sg)

Accepted 26 September 2007

was obtained by A. Chaboud (Unite Mixte de Recherche 9004, Lyon, France) from C24 plants transformed with pACTIN11-Histone-mRFP1; E1 GFP (Col) was a kind gift from G. Strompen (Strompen et al., 2005). ATGEX1 marker line was the kind gift from Sheila McCormick (Engel et al., 2005). The marker HTR10-mRFP1 results from a genomic fusion described in Ingouff et al. (Ingouff et al., 2007).

MSI1:MSI1-mRFP1 plasmid construction and transformation

The full-length *MSI1* cDNA was amplified by PCR and inserted in frame between the gateway cassette (GW) and the monomeric Red fluorescent protein 1 (*mRFP1*) gene contained in the pGREENII (pGII)-based vector pGIInK-GW-mRFP1-35ter.

A 3050 bp DNA fragment consisting of the upstream region of *MSI1* corresponding to the putative promoter until the beginning of exon3 was amplified by PCR using the KOD-plus-PCR kit (TOYOBO, Japan) and cloned into pCR2-1 TOPO vector (Invitrogen, Carlsbad, CA). The final vector pGIInK-promMSI1::MSI1-mRFP1-35S consists of the upstream region of *MSI1*, its first two exons and introns and the remaining *MSI1* cDNA fused to the fluorescent reporter mRFP1. Heterozygous *msi1-1*/+ mutant BASTA-selected plants were transformed using the *Agrobacterium*-mediated floral dip method.

Fifteen transgenic lines were obtained, all showing a similar pattern of expression. Maternal transmission of *msi1-1* mutation, which is null in the mutant background was completely restored by expression of *promMSI1:MSI1-mRFP1* (46.6% transmission of *msi1* from seeds produced by *msi1*/+; *promMSI1:MSI1-mRFP1*/*promMSI1:MSI1-mRFP1* ovules crossed to wild-type pollen, *n*=250). Plants homozygous for *msi1-1* and homozygous for *promMSI1:MSI1-mRFP1* were obtained.

RESULTS

Reduced paternal transmission of *msi1* loss-of-function alleles

MSI1, *FAS1* and *FAS2* were all expressed in mature pollen (Fig. 1A), in agreement with microarray analyses, which also showed a level of expression comparable to or lower than levels in leaves and roots (see Fig. S1 in the supplementary material). In order to know precisely in which cell types *MSI1* expression takes place during pollen development, we produced a translational reporter line for MSI1. We obtained plants that express MSI1 fused to the monomeric Red fluorescent protein 1 (mRFP1) under the control of *MSI1* 5′ regulatory cis-elements (*pMSI1-MSI1-mRFP1*). The expression of this construct complemented the loss-of-function allele *msi1-1*, and thus its expression pattern was likely to reflect the pattern of MSI1 expression.

We compared our observations of MSI1-mRFP1 expression with the wild-type pattern of chromatin staining by DAPI. The microspore (Fig. 1B) underwent an asymmetric division (PMI), leading to production of bicellular pollen. This comprises the larger vegetative cell and the smaller generative cell initially positioned at the periphery and later engulfed by the vegetative cell (Fig. 1C). The generative cell further divided (PMII) and produced the two sperm cells (Fig. 1D). In contrast to the sperm cells, the large spherical vegetative cell had a larger, less condensed nucleus positioned at the center of the tricellular pollen.

MSI1-mRFP1 was expressed at all stages of pollen development in both cell types (Fig. 1E-G), as reported in previous microarray analyses (Honys and Twell, 2004). The level of MSI1-mRFP1 appeared to increase in the vegetative cell throughout pollen development, whereas the expression of MSI1 reported by microarrays decreased (see Fig. S1 in the supplementary material). We favor the idea that the increase of MSI1-mRFP1 signals provides evidence for new synthesis and accumulation of MSI1-mRFP1 during pollen development. It is thus unlikely that detected MSI1-mRFP1 was inherited through meiosis. The mRFP1 fluorescence in the generative cell was weaker than in the vegetative cell (Fig. 1F). Although the chromatin of the sperm cells was very compact, the MSI1-mRFP1 signal was rather low (Fig. 1G). *MSI1* thus appears to be differentially expressed between the vegetative and generative lineage during pollen development.

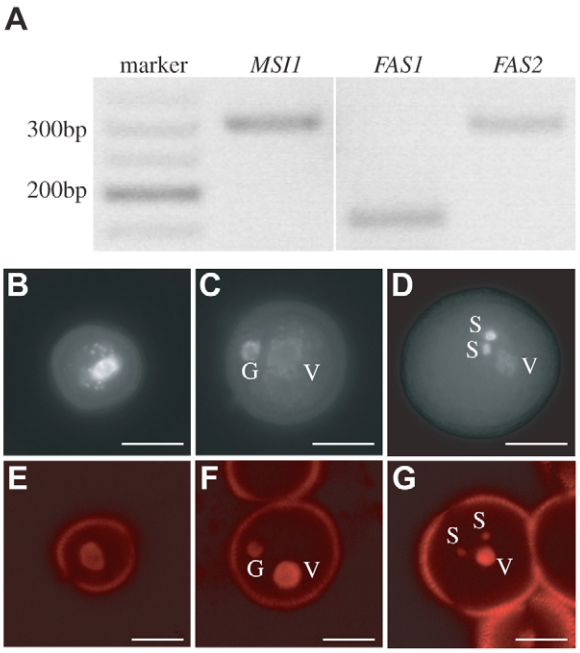

Fig. 1. Expression of CAF1 components in pollen. (**A**) RT-PCR was performed from RNAs extracted from mature *Arabidopsis thaliana* pollen grains and shows expression of *MSI1*, *FAS1* and *FAS2*. (**B-D**) Wild-type pollen development. Nuclei are stained with DAPI. The uni-nucleate microspore (B) undergoes an asymmetrical mitosis, leading to the bicellular stage (C). At that stage the pollen grain contains a large vegetative cell and a small generative cell with a nucleus showing relatively higher chromatin compaction. (D) The generative cell divides, giving rise to two sperm cells with highly condensed chromatin. (**E-G**) Expression pattern of *promMSI1-MSI1-mRFP1* in pollen in microspore (E), and developing pollen at bicellular stage (F) and tricellular stage (G). Confocal sections. Scale bars: 10 μm. G, generative cell; S, sperm cell; V, vegetative cell.

Reduced paternal transmission is reported for the allele *msi1-2* (Guitton et al., 2004) but not for the allele *msi1-1* (Köhler et al., 2003). This discrepancy may result from the distinct genetic background of each allele (C24 versus Col) or from distinct growth conditions. We isolated two new alleles of *msi1* in Ler (*msi1-3*) and Col (*msi1-4*) genetic backgrounds (see Fig. S2 in the supplementary material). Imperfect insertions of a Ds transposon and of a T-DNA created a stop codon in the first exon of *MSI1* in the alleles *msi1-3* and *msi1-4*. Both alleles do not transmit *msi1* maternally and are presumably null alleles as concluded for the alleles *msi1-1* and *msi1-2* (Guitton et al., 2004; Köhler et al., 2003).

We measured the paternal transmission in each *msi1* allele grown in the same conditions (Table 1). Pollen development takes place after meiosis, and crosses between wild-type ovules and pollen from *msi1*/+ plants are expected to transmit *msi1* in 50% of the offspring if there is full transmission. Paternal transmission was reduced to approximately 36% in every allele (Table 1). Reduced transmission could result from a paternal effect causing reduction of seed germination or seedling viability. The germination rate of wild-type

Table 1. Paternal transmission of *msi1* alleles

Female × male	% ± s.d. (mutant allele) in F1	*n*	T.E. %	Penetrance %
msi1-1/+ × *msi1-1*/+	35.7±5.0 (*msi1-1*)	206	56	44
Col × *msi1-1*/+	36.8±4.9 (*msi1-1*)	85	57	43
msi1-2/+ × *msi1-2*/+	33.7±5.1 (*msi1-2*)	132	50	50
C24 × *msi1-2*/+	35.9±6.6 (*msi1-2*)	206	56	44
msi1-3/+ × *msi1-3*/+	35.8±10.0 (*msi1-3*)	96	55	45
Ler × *msi1-3*/+	34.8±3.4 (*msi1-3*)	121	53	47
msi1-4/+ × *msi1-4*/+	37.0±6.1 (*msi1-4*)	143	59	41
Col × *msi1-4*/+	36.6±9.3 (*msi1-4*)	72	57	43
Col × *msi1-1*/+; *fas1-1*/+	28.8±4.9 (*msi1-1*)	255	40	60
Col × *msi1-3*/+; *fas1-4*/+	29.3±4.6 (*msi1-3*)	389	41	59
Col × *msi1-1*/+; *fas2-4*/+	28.5±2.2 (*msi1-1*)	84	40	60

The paternal transmission was calculated from the percentage of *msi1* plants in the progeny from crosses between pollen from *msi1*/+ plants and ovules of the relevant wild-type ecotype. This transmission is comparable to the transmission of *msi1* from self-pollinated *msi1*/+ plants. The effect of *fas1* and *fas2* on *msi1* transmission is indicated in the three last rows.
n, The number of plants scored.
T.E., Transmission efficiency.

seeds was 98.2% (*n*=277, s.d.=0.53), hence comparable to the germination rate in seeds from crosses between wild-type ovules and pollen from *msi1-1*/+ plants (98.0%, *n*=293, s.d.=0.23). Similarly the survival rate of *msi1-1*/+ seedlings was not affected (99.6%, *n*=273, s.d.=0.07). Hence *msi1* effect on paternal transmission does not originate from an effect on seed development or on seedlings, and must result from a reduction of male fertility. The reduction of paternal transmission of all four *msi1* alleles to 36% indicated a transmission efficiency of 56%. Hence a penetrance of 44% is associated with null mutations in *msi1*, resulting in defective male gametogenesis in *msi1*/+ plants. We conclude that *msi1* causes defects during pollen development.

Reduced paternal transmission of *msi1* is enhanced by further loss of CAF1 function

MSI1 was shown to interact in vitro with the complex containing *FAS1* and *FAS2* (Kaya et al., 2001). We analyzed the paternal transmission associated with the loss-of-function alleles *fas1-4* and *fas2-4* (Exner et al., 2006; Ramirez-Parra and Gutierrez, 2007). Paternal transmission of the *fas1-4* allele analyzed from crosses between wild-type ovules and pollen from *fas1*-4/+ plants was 49.6% (*n*=115, s.d.=7.4). Similarly paternal transmission of *fas2-4* was 48.6% (*n*=140, s.d.=5.2). According to these data, neither *fas1* nor *fas2* appear to affect male gametogenesis. Nevertheless, if we assume that *fas1* and *fas2* affect paternal transmission, the associated transmission efficiency would be of the order of 98%. To test whether the CAF1 pathway is responsible for the reduced transmission of *msi1* null alleles, we obtained double mutant lines between *msi1*/+ and loss-of-function alleles of *fas1*/+ and *fas2*/+. Paternal transmission of *msi1* mutant allele was similarly reduced by the introduction of *fas1* and *fas2* (Table 1). An additive interaction between *fas1* or *fas2* and *msi1* is predicted to lead to a decrease of *msi1* transmission efficiency from 56 to 55% in *fas1 or fas2* background. However, in the *fas1* or the *fas2* background the transmission efficiency of *msi1* was reduced significantly from 56% to 40% (Table 1). In conclusion, the interaction between *msi1* and *fas1* or *fas2* was not additive but synergistic. Additive interactions between null mutations indicate that each mutation affects a distinct pathway. However, a synergistic interaction is observed in combination of partially penetrant alleles of mutations affecting the same genetic pathway. The synergy observed between *msi1* and *fas1* or *fas2* on paternal transmission of *msi1* suggests that *MSI1*, *FAS1* and *FAS2* act in a common genetic pathway influencing male gametogenesis.

Loss of MSI1 arrests pollen development

We investigated the developmental origin of the reduced male fertility in *msi1*/+ plants. In order to compare directly *msi1* and wild-type pollen development, we used the mutant *quartet* (*qrt*), which produces four microspores remaining associated as a tetrad (Preuss et al., 1994). Hence *qrt*/*qrt*; *msi1-1*/+ plants produce tetrads containing two wild-type and two *msi1* pollen grains. Alexander staining for pollen viability showed 7.3% lethality in *msi1* pollen at maturity (s.d.=1.9; *n*=800) in comparison with 1.0% in the wild type (s.d.=0.7; *n*=500) (see Fig. S3 in the supplementary material). Tetrads of microspores produced by wild-type and *msi1-1*/+ plants

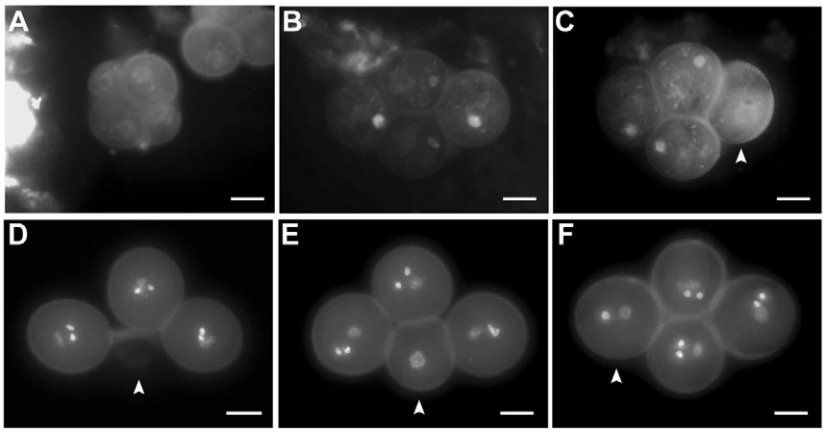

Fig. 2. Defects in pollen development in *msi1*/+ mutants. Pollen development in meiotic tetrads from *qrt1/qrt1* and *qrt1/qrt1*; *msi1-1*/+ *Arabidopsis* plants. At uni-nucleate stage (**A**) microspore tetrads of wild-type and mutant plants are indistinguishable. In contrast to wild-type tetrads (**B**), *msi1*/+ tetrads at the bicellular stage contain one arrested microspore (**C**, arrowhead). (**D-F**) At the tricellular stage, *qrt1/qrt1*; *msi1-1*/+ plants produce tetrads containing three wild-type pollen grains and an abnormal pollen grain (arrowhead). The abnormal pollen is either a dead microspore (D), an arrested microspore (E) or a bicellular pollen grain (F). Epifluorescence micrographs of DAPI-stained pollen. Scale bars: 10 μm.

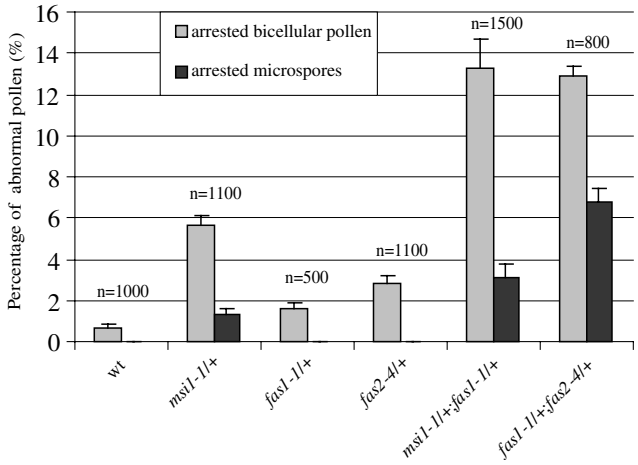

Fig. 3. Synergistic effects of combination between mutations in members of the CAF1 complex. Bar chart showing percentage of the two types of abnormal pollen at the tricellular mature stage in *msi1-1*/+, *fas1-1*/+, *fas2-4*/+, *msi1-1*/+;*fas1-1*/+ and *fas1-1*/+;*fas2-4*/+ mutant *Arabidopsis* plants. Gray bars correspond to arrested bicellular pollen and black bars to arrested microspores. Error bars correspond to standard errors calculated on the basis of several samples of 100 pollen grains, and the size of the total population analyzed (*n*) is indicated above each column.

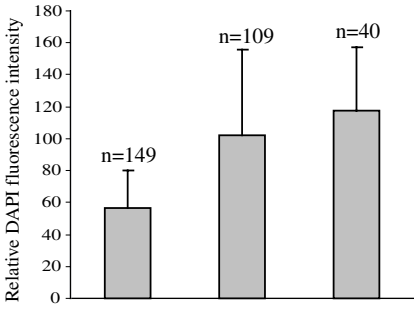

Fluorescence Intensity	wt	*msi1-1/fas1-1*	duo1-1
single sperm-like nucleus / sperm nucleus	N.A.	1.80	2.07

Fig. 4. Effect of *msi1* on DNA content in sperm cell nuclei. The DNA content in *Arabidopsis* sperm cells was estimated relative to the fluorescence intensity after DAPI staining. The relative DAPI fluorescence intensity between control wild-type sperm cells and single sperm-like cells in *msi1-1*;*fas1-1* pollen and in *duo1-1* pollen is indicated under the graph. Error bars correspond to standard deviations, and the size of the sample (*n*) is indicated above each column.

in *qrt*/*qrt* background could not be distinguished (*n*=120) (Fig. 2A). After PMI, in *qrt*/*qrt*, all tetrads consisted of four pollen grains with a vegetative cell and a generative cell (Fig. 2B). By contrast, a fraction of tetrads in pollen from *qrt*/*qrt*; *msi1-1*/+ plants contained an arrested microspore (Fig. 2C). At the mature stage, in contrast to wild-type pollen tetrads, a fraction of tetrads in *qrt*/*qrt*; *msi1-1*/+ plants contained an aborted microspore (Fig. 2D), or a pollen grain with one (Fig. 2E) or two (Fig. 2F) nuclei. These results suggest that the absence of MSI1 causes pleiotropic arrest of pollen development before PMI, or PMII. The fraction of each class of arrest was measured in pollen produced by *msi1-1*/+ plants (Fig. 3). The percentage of arrested pollen cumulated with the percentage of aborted microspores amounted to 14.7%. This value is lower than the 22% abnormal pollen in a population of pollen from *msi1*/+ plants, as predicted from the transmission efficiency of 56%. This suggested that 7.3% of pollen from *msi1*/+ plants contain two sperm cells and appear morphologically normal, albeit not functional. These *msi1* tricellular pollen grains probably grow a pollen tube, but the two sperm cells are incompetent for fertilization, causing ovule abortion. In agreement with this prediction, pollination of wild-type plants by *msi1*/+ plants caused a 6% increase in ovule abortion (see Fig. S4 in the supplementary material). In conclusion, our observations show that *msi1* causes delays and arrests of pollen development, leading to partial male sterility and reduced paternal transmission of *msi1*.

Loss of CAF1 activity causes delay and arrest of the cell cycle in pollen

As genetic interactions suggested that impairment of the CAF1 pathway affects male gametogenesis, we expected that loss of function of the other members of the CAF1 pathway would cause pollen arrests similar to *msi1*. A small proportion of pollen arrested at the bicellular stage was observed in *fas1*/+ and *fas2*/+ mutants (Fig. 3). This very limited penetrance of *fas* mutations was also supported by the very limited reduction of paternal transmission efficiency of *fas1* and *fas2*. By contrast, the combination of *fas1* and *fas2* in double heterozygous mutant plants caused a high proportion of arrest at the bicellular stage and an additional arrest as microspores, which was never observed in the single mutants. This observation demonstrates that the combination of *fas1* and *fas2* does not cause additional, but synergistic, effects, in agreement with the established participation of *fas1* and *fas2* to the CAF1 pathway. Similarly the combination of *fas1* to *msi1* caused a synergistic increase in the proportion of pollen developmental arrests (Fig. 3). A two-way analysis of variation confirmed that an additive phenotype could not explain the extra increase in single sperm pollen in the double mutants (P=0.0047). The synergistic effects of the combinations between *fas1*, *fas2* and *msi1* on pollen development and paternal transmission indicate that *msi1* causes pollen developmental arrest through the CAF1 pathway.

FACS analyses in young seedlings have shown that loss-of-function mutants for *MSI1*, *FAS1* and *FAS2* lead to a G2/M arrest, presumably as a result of the activation of the DNA repair pathway following stalling of the DNA replication fork (Endo et al., 2006; Exner et al., 2006; Honys and Twell, 2004; Kirik et al., 2006; Ramirez-Parra and Gutierrez, 2007). To investigate the consequence of loss of activity of CAF1 on cell cycle during pollen development, we measured DNA content at the early tricellular stage. We compared the DNA content in sperm cells of wild-type tricellular pollen with the single sperm-like cell in bicellular pollen from *msi1*/+;*fas1*/+ plants. Both measurements were compared to *duo1* pollen single sperm-like cells, which contain twice the amount of DNA contained in wild-type sperm cells at the early tricellular stage (Rotman et al., 2005). The single sperm-like cell in *msi1*/+;*fas1*/+ also contained approximately twice the amount of DNA in comparison to wild-type sperm cells (Fig. 4). These measurements suggest that the loss of CAF1 function delays the cell cycle pace in the generative cell, preventing the G2-M transition, which leads to PMII in the wild type.

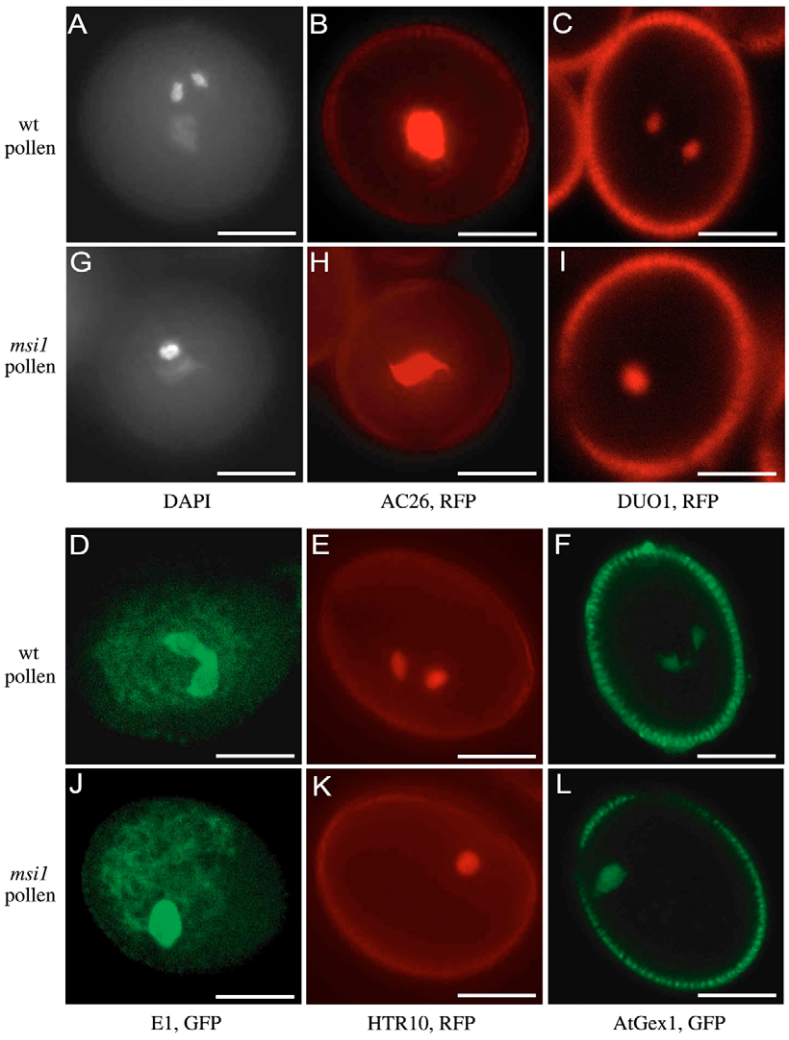

Fig. 5. Cell identities in bicellular *msi1* pollen. (**A-F**) Wild-type *Arabidopsis* pollen at the tricellular stage. (**G-L**) Bicellular and tricellular pollen segregating from *msi1*/+ plants. (A,G) Fluorescence images of pollen grains stained with DAPI. (B,H) The same pollen grains as in A,G, respectively, expressing the vegetative cell marker AC26-Histone2B-mRFP1. (C,I) Pollen grains expressing the generative lineage marker pDUO1-DUO1-mRFP1. (D,J) Pollen grains expressing the generative lineage marker E1-GFP. (E,K) Pollen grains expressing the sperm cell marker HTR10-mRFP1. (F,L) Pollen grains expressing the sperm cell marker ATGEX1-GFP. GFP was examined using the 488 nm excitation line of an argon laser and an emission filter long pass of 510 nm. Fluorescence of mRFP1 was examined using the 543 nm excitation line of a HeNe laser and an emission filter of 585-615 nm. Scale bars: 10 μm.

Cell-fate specification and differentiation is normal in CAF1-deficient pollen

Arabidopsis PMI is coupled to cell-fate specification, leading to specific expression of vegetative cell (Twell et al., 1991) and generative cell (Engel et al., 2005; Rotman et al., 2005) markers. The second mitosis is coupled with sperm cell differentiation, marked by the onset of DNA synthesis (Durbarry et al., 2005) and expression of specific genes (Engel et al., 2005). To further elucidate whether arrests of cell division in *msi1* pollen grain are associated with cell fate changes, we analyzed cell identities in pollen grains arrested at PMII produced by *msi1*/+ plants. These pollen grains contained a large vegetative-like cell nucleus and a sperm-like cell with condensed DNA (Fig. 5G). The marker AC26 is associated with expression of HISTONE 2B-mRFP fusion protein under the control of the *ACTIN-11* promoter and is specifically expressed in wild-type vegetative cell nuclei (Rotman et al., 2005) (Fig. 5A,B). In *msi1* pollen arrested at PMII, AC26 was also expressed in the larger spherical cell in correlation with its vegetative identity (Fig. 5G,H). We never observed any pollen grain expressing AC26 in the condensed nucleus of the sperm-like cell, nor in more than one nucleus, indicating that loss of CAF1 function does not perturb the vegetative cell identity during pollen development. In addition, we performed a germination test to estimate whether the vegetative cell deficient in CAF1 is able to produce a pollen tube. We observed comparable germination rates between wild-type pollen and pollen from *msi1*/+, *fas1*/+, *fas2*/+ and the double mutant combinations, with a slight reduction corresponding to the proportion of dead pollen recorded for each genetic background (see Fig. S5 in the supplementary material). Our results support the argument that the vegetative cell differentiation and function is not affected by the loss of CAF1 function.

In wild-type pollen, the generative cell lineage is marked by pDUO1-DUO1-mRFP1, expressed in the generative cell and in the sperm cells (Rotman et al., 2005) (Fig. 5C). The maturing sperm cells are further marked specifically by the accumulation of the vacuolar V-ATPase E1 GFP on the outer plasma membrane (Strompen et al., 2005) (Fig. 5D) and of the HISTONE3 variant HTR10 in the sperm nucleus (Ingouff et al., 2007) (Fig. 5E). Eventually, the sperm cells specifically express ATGEX1 (Engel et al., 2005) (Fig. 5F). We observed that all the markers of sperm cell maturation and identity were expressed only in the single sperm-like cell in *msi1* pollen arrested at PMII (Fig. 5I-L). The proportion of pollen with a single sperm cell expressing HTR10-mRFP1 (6%, n=150; s.d.=2) is similar to the proportion of pollen with a single sperm cell (Fig. 3). We conclude that all *msi1* single sperm cells express sperm cell fate markers. These findings indicate that cell fates are not affected in *msi1* pollen grains arrested at PMII, which appear to comprise a vegetative cell and a single sperm cell.

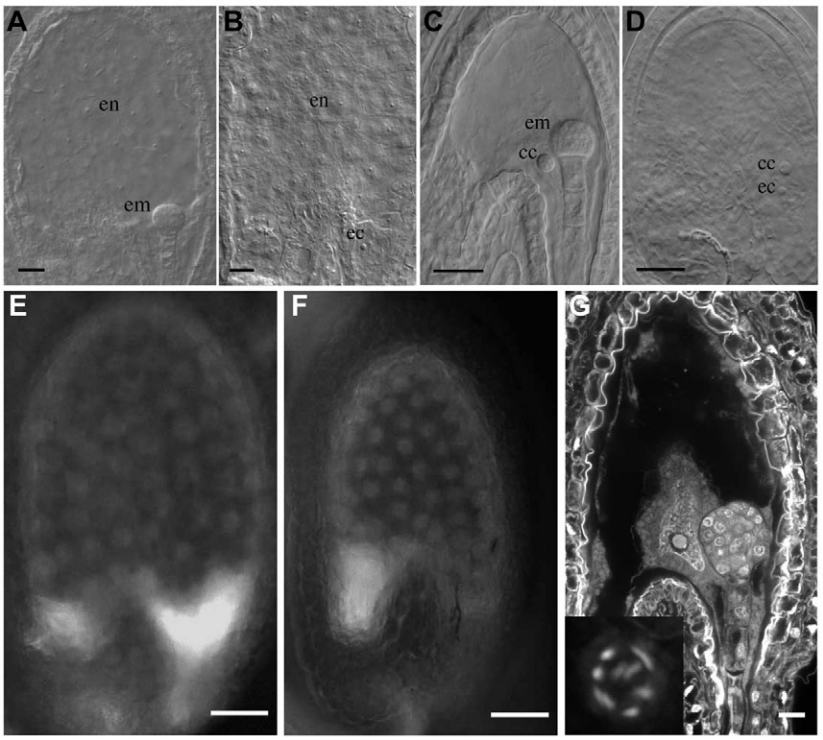

Fig. 6. Pollination of wild-type ovules with *msi1* pollen leads to single fertilization events. (**A**) Wild-type *Arabidopsis* seed with an embryo and an endosperm, 2 days after pollination (2 DAP). (**B**) Seed with an endosperm but without an embryo, 3 DAP. At the embryo region, the egg cell remains unfertilized. (**C**) Seed with an embryo but without endosperm, 3 DAP. At the side of the embryo the nucleus of central cell that remains unfertilized is still observed. (**D**) Fully aborted ovule without embryo and endosperm, 3 DAP. The egg cell and the central cell remain unfertilized. (**E**) Expression of the fluorescent KS22 GFP endosperm marker in a wild-type seed at 3 DAP. (**F**) Expression of KS22 GFP in a seed containing only endosperm from a cross between wild-type ovules and *msi1-2*/+; KS22/KS22 pollen. (**G**) Confocal section of a seed containing only an embryo, produced by a cross between a wild-type ovule and *msi1-2* pollen. The nucleus of the unfertilized central cell remains associated with the surface of the embryo. Feulgen staining marks brightly the DNA in nuclei as described previously (Garcia et al., 2003). The inset shows ten chromocentres at pre-prophase in the nucleus from the single embryo. The single embryo is diploid and thus originates from a fertilized egg cell. Scale bars: 100 μm in A-D; 50 μm in E,F; 10 μm in G. cc, central cell; ec, egg cell; em, embryo; en, endosperm.

Pollination with *msi1* pollen causes single-fertilization events

In wild-type pollen, the two sperm cells separately fertilize the female egg cell and the central cell producing the embryo and the endosperm, respectively (Fig. 6A). The apparent correct establishment of cell fate in the single sperm-like cell present in *msi1* pollen suggested that it was able to perform fertilization as a wild-type sperm cell. We suspected that the single sperm cell in *msi1* pollen could fertilize either the egg cell or the central cell. Crossing wild-type ovules to pollen from *msi1*/+ plants produced a low proportion of seeds containing only endosperm (n=20 out of 3600) (Fig. 6B) or an embryo (n=18 out of 3600) (Fig. 6C). In both cases, these seeds contained residual material from the unfertilized egg cell or central cell (Fig. 6B,C), comparable to those observed in unfertilized ovules (Fig. 6D). We concluded that *msi1* pollen with a single sperm cell probably caused single fertilization events. Alternatively, single sperm cells may only fuse with one of the female gametes without the fusion of the parental genetic material (karyogamy), and autonomous development of embryo or endosperm would follow. If this were the case, the paternal genome would be excluded and the single embryo or the single endosperm should not express paternally derived alleles. We tested this hypothesis for the expression of the endosperm marker KS22 (Ingouff et al., 2005) (Fig. 6E), provided by the pollen of *msi1*/+ plants crossed to wild-type ovules (Fig. 6F). Seeds with single endosperm showed expression of the paternally derived endosperm marker KS22 (Fig. 6F, n=7). We conclude that the single endosperm develops from a central cell fertilized by the single gamete in *msi1* pollen. To establish whether single sperm cells are able to fertilize the egg cell, we performed ploidy measurements on seeds containing a single embryo. We observed ten chromosomes at pre-prophase in single embryo cells (inset in Fig. 6G, n=2). These embryos are thus diploid and have been produced by fertilization of the egg cell by the single sperm from *msi1* pollen. We conclude that a fraction of *msi1* pollen arrested at PMII delivers a functional single sperm cell equally able to fertilize the egg cell or the central cell. Similarly, pollination with pollen from *fas1*/+ and *fas2*/+ plants produced seeds containing either an endosperm or an embryo (0.3%, n=400; and 0.4%, n=360). This result suggests that CAF1-deficient pollen produces functional single sperm cells.

However, the proportion of single fertilization events was of the order of 1%, whereas the proportion of *msi1* pollen with a single sperm cell was of the order of 6%. This suggested that either only a fraction of the single sperm cells was transported by the pollen tube or was able to perform single fertilization. Alternatively, a fraction of single sperm cells would divide during the transport by the pollen tube. We measured the proportion of single sperm cell at various times after pollen germination in vitro and observed a reduction of the percentage of pollen harboring a single sperm cell from 6 to 2% (Fig. 7A). Hence, *msi1* single sperm cells could be transported into the pollen tube as in wild-type pollen harboring two sperm cells (Fig. 7B,C). However, we could record the division of single sperm cells into two sperm cells during pollen tube growth (Fig. 7C,D; n=2). This observation and the decreased proportion of pollen tubes with single sperm cells following germination indicated that a fraction of sperm cells divide during their transport by the pollen tube, leading to a low proportion of pollen tubes delivering a single sperm cell. This low proportion is similar to the proportion of single fertilization events. We thus conclude that single fertilization of the egg cell or of the central cell is likely to result from the delivery of single sperm cells produced as a result of delayed cell cycle in CAF1-deficient pollen.

DISCUSSION

Loss of *MSI1* function affects CAF1 function during pollen development

In *Arabidopsis*, MSI1 directly interacts with members of a conserved, endosperm-specific Polycomb group (Pc-G) complex (Guitton et al., 2004; Köhler et al., 2003) and null *msi1* alleles cause

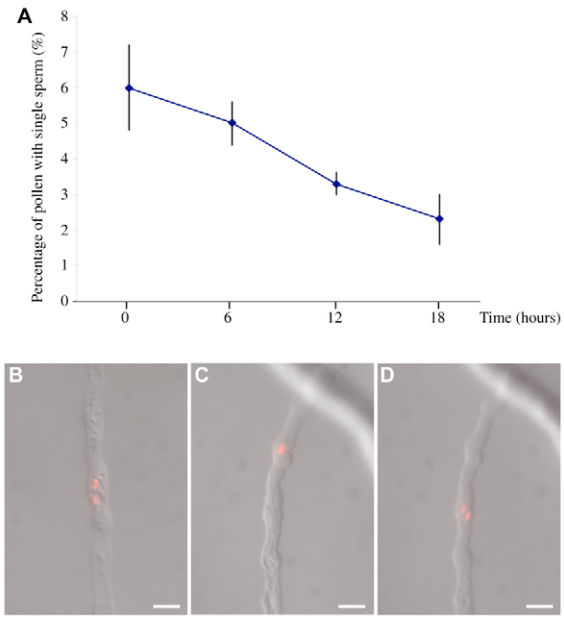

Fig. 7. Fate of the single sperm cell during *msi1* pollen tube growth. (**A**) Percentage of pollen tubes transporting a single sperm cell from a *msi1-1*/+ *Arabidopsis* plant at different time points after pollen germination in vitro. Errors bars correspond to standard errors calculated on the basis of three replicates of 100 pollen grains. (**B-D**) Transport of sperm cells marked with HTR10-mRFP in pollen tube germinated in vitro from wild-type (B) and *msi1*/+ (C,D) plants. (B) At 6 hours after germination, wild-type pollen tubes transport two sperm cells (two fluorescent red dots). (C) By contrast, at 6 hours a *msi1* pollen tube transports a single sperm cell. (D) At 7 hours after germination the *msi1* single gamete had divided into two sperm cells. (B,C,D) Superimposed DIC images of the pollen tube with the mRFP1 fluorescence signal identifying the sperm cells. Scale bars: 20 μm.

production of autonomous endosperm and abnormal development of endosperm as the other mutants in genes encoding the subunits of the endosperm Pc-G complex (Guitton et al., 2004). MSI1 is also likely to be part of Pc-G complexes active during plant vegetative development (Berger et al., 2006; Chanvivattana et al., 2004). Accordingly, partial reduction of MSI1 activity during vegetative development phenocopies the effect of mutations in vegetative Pc-G complexes (Hennig et al., 2005; Hennig et al., 2003; Katz et al., 2004; Moon et al., 2003). However, *msi1*-null alleles also produce Pc-G independent phenotypes, including parthenogenesis and sporophytic embryo lethality, not observed in Pc-G mutants (Guitton and Berger, 2005; Guitton et al., 2004).

In this study, we report that *msi1* affects pollen development and is associated with reduced paternal transmission. By contrast, loss-of-function mutations in all members of the Pc-G complex active in endosperm do not show male transmission or pollen defects (Chaudhury et al., 1997; Grossniklaus et al., 1998). Other Pc-G genes are expressed during pollen development (see Fig. S1 in the supplementary material), but their absence does not cause male sterility (Chanvivattana et al., 2004; Gendall et al., 2001; Goodrich et al., 1997; Wang et al., 2006). FIE is essential for Pc-G function (Guitton et al., 2004; Ohad et al., 1996) and is expressed during pollen development (Honys and Twell, 2004). If defects in *msi1* pollen depended on Pc-G function, a similar reduction of paternal transmission should be expected for *msi1* and *fie*-null alleles. However, *fie* mutations are fully transmitted paternally (Guitton et al., 2004; Ohad et al., 1996), and we could not observe any pollen defects in *fie*/+ mutant (transmission efficiency of the null *fie-11* allele from the male is 99.8%; *n*=800). We thus conclude that *fie* null mutations do not affect paternal transmission and that the effect of *msi1* on male transmission does not rely on Pc-G complexes.

Biochemical studies have demonstrated the potential association of MSI1 to the Rb-related protein RBR1 (Ach et al., 1997) but no direct evidence has been provided for a common function of RBR1 and MSI1 in *Arabidopsis*. Loss of RBR1 function alters pollen development. However the phenotypes associated with *rbr1* in pollen are dramatically distinct from *msi1* (C.Z. and F.B., unpublished data) and this difference does not support the association between RBR1 and MSI1 as the origin of pollen developmental defects in *msi1*.

Biochemical evidence has shown that MSI1 is also associated with the two core subunits of the CAF1 complex, FAS1 and FAS2 (Kaya et al., 2001). G2/M arrests have been reported in vegetative tissue of *fas1* and *fas2* homozygous mutants (Ramirez-Parra and Gutierrez, 2007). Our study shows the synergy between *fas1*, *fas2* and *msi1* mutations on paternal transmission of *msi1* and on pollen development, strongly suggesting that the defects of *msi1* pollen development are caused by the loss of CAF1 function.

The limited penetrance of single mutations in *msi1*, *fas1* and *fas2* may originate from inheritance of wild-type proteins or transcripts from the microspore mother cell heterozygous for the mutation. In mammals and *Drosophila*, CAF1-independent histone chaperone activities include HISTONE REGULATORY A (HIRA) and ANTISILENCING FACTOR 1 (ASF1), which are associated directly with the deposition of histones H3 and H4 on newly synthesized chromatin (Polo and Almouzni, 2006). In *Arabidopsis*, the limited penetrance associated with the *fas1*, *fas2* and *msi1* mutations might also result from a redundant activity mediated by the putative HIRA homolog (Phelps-Durr et al., 2005) pathway or by a basic function of putative ASF1 homologs (www.chromdb.org).

Loss of CAF1 function during pollen development arrests the cell cycle but does not alter cell fate

Loss of CAF1 function causes activation of the DNA repair machinery (Endo et al., 2006; Exner et al., 2006; Kirik et al., 2006; Ramirez-Parra and Gutierrez, 2007) and a decline in CDKA1 activity (Ramirez-Parra and Gutierrez, 2007). Moreover, the expression of FAS1 is activated at the G1-S transition by E2F (Ramirez-Parra and Gutierrez, 2007). Whether the cell cycle and cell fate deregulation observed in *fas1* and *fas2* vegetative tissues (Costa and Shaw, 2006; Exner et al., 2006) originates directly from the deficit in CAF1 or results from more indirect epigenetic deregulations caused by the absence of CAF1 has remained unclear.

Within one to two cell divisions the pollen deficient for *MSI1* or *FAS1* and *FAS2* arrests before the first or the second pollen mitosis. DNA measurements suggested that the cell cycle arrest takes place at the G2-M transition, which is similar to that observed in vegetative tissues in plants and in other species. Hence we propose that loss of CAF1 function causes a cell cycle arrest before the first or the second mitosis during pollen development.

Cell cycle arrests at the G2-M transition would account for the most prominent phenotypes observed in *msi1* pollen. The wild-type sperm cells reach the mid-S phase, when pollen is shed from the anthers (Durbarry et al., 2005), and probably reach the G2-M transition, when they are released into the female gametes (Friedman, 1999). The transmission efficiency indicates that an additional fraction of *msi1* pollen is unable to transmit *msi1* (see Fig. S6 in the supplementary material). It is thus possible that *msi1* pollen

in this fraction contain two gametes that do not reach the G2-M transition when they are released into the female gametophyte and are unable to fertilize the female gamete, leading to ovule abortion.

Cell cycle impairment does not prevent differentiation during male gametogenesis

It has become clear that some regulators of cell division take an active part in cell-fate decisions. In flowering plants, most cells in roots and in shoots are produced by the activity of meristems, which contain dividing stem cells (Benfey and Scheres, 2000; Gegas and Doonan, 2006; Scheres, 2001). In the root meristem, cell fate appears to be specified after the asymmetric division of the stem cell (Castellano and Sablowski, 2005; Wildwater et al., 2005). However, the cell fate is established during the G1 phase (Caro et al., 2007; Costa and Shaw, 2006) and is not fixed until the last meristematic division, after which differentiation is initiated (Berger et al., 1998). Hence it is possible that cell division influences cell-fate commitment. The effects of mild alteration of cell cycle regulation during embryogenesis support the latter hypothesis (Jenik et al., 2005). Alteration of CAF1 causes aberrant morphogenesis of trichomes (Exner et al., 2006) and alters cell fate in root epidermal cells (Costa and Shaw, 2006). In contrast to cell-fate commitment in vegetative tissues, cell-fate establishment in pollen appears to be largely independent of cell-cycle deregulation in the *msi1* mutants, producing a fraction of bicellular pollen grains with a functional vegetative cell that delivers a functional single sperm-like cell. We have shown that *msi1* bicellular pollen correctly expresses cell-fate markers and produces a functional single sperm cell. Single sperm cells able to fertilize the egg cell are also produced by the mutant *cdka1* (Nowack et al., 2006). Hence cell fate and cell differentiation appear to be independent from cell-cycle regulation in pollen development.

Are male gametes specialized for specific fusion with each type of female gamete?

Plumbago zeylanica produces dimorphic sperm cells with specialized organelle content that specifies the target female gamete (Russell, 1983; Russell, 1985). Several degrees of polymorphism have been reported in other species and in maize lines harboring supernumerary B chromosomes (Faure et al., 2003). Interestingly, B chromosomes are transmitted at higher frequency to the egg cell (Roman, 1948). Although such dimorphism was not reported in many species, including *Arabidopsis* (Faure et al., 2003; McCormick, 2004), it is nevertheless possible that isomorphic sperm cells differentiate to fertilize the egg cell or the central cell exclusively. This hypothesis was supported by the apparent preferential fertilization of the egg cell by single sperm cell produced in absence of the cyclin kinase *cdka1* (Iwakawa et al., 2006; Nowack et al., 2006). However, the *cdka1* single sperm cell may be able to fertilize the central cell, but this fertilization product may not be viable and was not detected as such. According to this hypothesis, sperm cell differentiation would rely on cell-cycle regulation by *cdka1*. However, such an event would cause a type of seed abortion, which was not detected in two independent studies (Iwakawa et al., 2006; Nowack et al., 2006). In contrast to *cdka1* pollen, *msi1* pollen causes a low percentage of single fertilization events, leading either to embryo or endosperm development. The proportion of *msi1*/+ pollen that delivers single sperm cells is similar to the proportion of single fertilization events, suggesting that *msi1* single sperm cells are responsible for the single fertilization events. In addition we have shown that *msi1* single sperm cells express the terminal differentiation markers ATGEX1, accumulate HTR10 as wild-type sperms, and are transported by the pollen tube. We thus propose that *msi1*/+ plants produce a fraction of bicellular pollen with a single fully differentiated sperm cell able to fertilize either the egg or the central cell.

Thus, the origin of the absence of fertilization of the central cell by *cdka1* pollen remains unclear. The differentiation status of the *cdka1* single sperm cell has not been established and it could be incompletely functional and able to fertilize only the egg cell. Similarly, it is still possible that the two sperm cells produced in some *msi1* pollen may not reach full competence for fertilization, and one fertilization may fail and block further development. This could explain why when a single embryo is produced by *msi1* pollen, no autonomous endosperm development occurs, as reported in cases of single fertilization events by *cdka1* pollen (Nowack et al., 2006).

Whether in the wild type each of the two sperm cells has an equal capacity to fertilize either the egg or the central cell for each sperm cell remains unresolved. Our results rather support the argument that the two sperm cells are identical, in agreement with the identical morphology of the two sperm cells, the identical expression of any molecular marker studied to date in *Arabidopsis*, and the apparent capacity to fertilize either female gamete. The results obtained from the study of *cdka1* pollen rather support the opposite idea, which has been so far clearly shown only in the species *Plumbago zeylanica* (Russell, 1983; Russell, 1985). In vivo observation of double fertilization in *Arabidopsis* has been achieved recently (Ingouff et al., 2007) and might provide an answer to this long-standing problem.

C.Z. is supported by the Junior Research fellow program of Temasek Life Sciences Laboratory and Singapore Millennium Foundation and contributed most of the experimental work reported. J.T. contributed the FACS analysis. M.I. contributed the MSI-mRFP1 reporter line. F.B. contributed to the conceptual supervision of the project and writing the manuscript. V.S. is supported by the University of California, Davis, USA and the NSF program Arabidopsis 2010 and contributed the *msi1*-3 allele. V.S. and Jonathan Fitz Gerald contributed to critical revisions of the manuscript.

Supplementary material

Supplementary material for this article is available at http://dev.biologists.org/cgi/content/full/135/1/65/DC1

References

Ach, R. A., Taranto, P. and Gruissem, W. (1997). A conserved family of WD-40 proteins binds to the retinoblastoma protein in both plants and animals. *Plant Cell* **9**, 1595-1606.

Benfey, P. N. and Scheres, B. (2000). Root development. *Curr. Biol.* **10**, R813-R815.

Berger, F., Haseloff, J., Schiefelbein, J. and Dolan, L. (1998). Positional information in root epidermis is defined during embryogenesis and acts in domains with strict boundaries. *Curr. Biol.* **8**, 421-430.

Berger, F., Grini, P. and Schnittger, A. (2006). Endosperm: an integrator of seed growth and development. *Curr. Opin. Plant Sci.* **9**, 664-670.

Caro, E., Castellano, M. M. and Gutierrez, C. (2007). A chromatin link that couples cell division to root epidermis patterning in *Arabidopsis*. *Nature* **447**, 213-217.

Castellano, M. M. and Sablowski, R. (2005). Intercellular signalling in the transition from stem cells to organogenesis in meristems. *Curr. Opin. Plant Biol.* **8**, 26-31.

Chanvivattana, Y., Bishopp, A., Schubert, D., Stock, C., Moon, Y. H., Sung, Z. R. and Goodrich, J. (2004). Interaction of Polycomb-group proteins controlling flowering in *Arabidopsis*. *Development* **131**, 5263-5276.

Chaudhury, A. M., Ming, L., Miller, C., Craig, S., Dennis, E. S. and Peacock, W. J. (1997). Fertilization-independent seed development in *Arabidopsis thaliana*. *Proc. Natl. Acad. Sci. USA* **94**, 4223-4228.

Costa, S. and Shaw, P. (2006). Chromatin organization and cell fate switch respond to positional information in *Arabidopsis*. *Nature* **439**, 493-496.

Durbarry, A., Vizir, I. and Twell, D. (2005). Male germ line development in *Arabidopsis*. duo pollen mutants reveal gametophytic regulators of generative cell cycle progression. *Plant Physiol.* **137**, 297-307.

Endo, M., Ishikawa, Y., Osakabe, K., Nakayama, S., Kaya, H., Araki, T.,

Shibahara, K., Abe, K., Ichikawa, H., Valentine, L. et al. (2006). Increased frequency of homologous recombination and T-DNA integration in *Arabidopsis CAF-1* mutants. *EMBO J*. **25**, 5579-5790.
Engel, M. L., Holmes-Davis, R. and McCormick, S. (2005). Green sperm. Identification of male gamete promoters in *Arabidopsis*. *Plant Physiol*. **138**, 2124-2133.
Exner, V., Taranto, P., Schonrock, N., Gruissem, W. and Hennig, L. (2006). Chromatin assembly factor CAF-1 is required for cellular differentiation during plant development. *Development* **133**, 4163-4172.
Faure, J. E., Rusche, M. L., Thomas, A., Keim, P., Dumas, C., Mogensen, H. L., Rougier, M. and Chaboud, A. (2003). Double fertilization in maize: the two male gametes from a pollen grain have the ability to fuse with egg cells. *Plant J*. **33**, 1051-1062.
Friedman, W. E. (1999). Expression of the cell cycle in sperm of *Arabidopsis*: implications for understanding patterns of gametogenesis and fertilization in plants and other eukaryotes. *Development* **126**, 1065-1075.
Garcia, D., Saingery, V., Chambrier, P., Mayer, U., Jurgens, G. and Berger, F. (2003). *Arabidopsis haiku* mutants reveal new controls of seed size by endosperm. *Plant Physiol*. **131**, 1661-1670.
Gegas, V. C. and Doonan, J. H. (2006). Expression of cell cycle genes in shoot apical meristems. *Plant Mol. Biol*. **60**, 947-961.
Gendall, A. R., Levy, Y. Y., Wilson, A. and Dean, C. (2001). The VERNALIZATION 2 gene mediates the epigenetic regulation of vernalization in *Arabidopsis*. *Cell* **107**, 525-535.
Goodrich, J., Puangsomlee, P., Martin, M., Long, D., Meyerowitz, E. M. and Coupland, G. (1997). A Polycomb-group gene regulates homeotic gene expression in *Arabidopsis*. *Nature* **386**, 44-51.
Grossniklaus, U., Vielle-Calzada, J. P., Hoeppner, M. A. and Gagliano, W. B. (1998). Maternal control of embryogenesis by *MEDEA*, a polycomb group gene in *Arabidopsis*. *Science* **280**, 446-450.
Guitton, A. E. and Berger, F. (2005). Loss of function of MULTICOPY SUPPRESSOR OF IRA 1 produces nonviable parthenogenetic embryos in *Arabidopsis*. *Curr. Biol*. **15**, 750-754.
Guitton, A. E., Page, D. R., Chambrier, P., Lionnet, C., Faure, J. E., Grossniklaus, U. and Berger, F. (2004). Identification of new members of Fertilisation Independent Seed Polycomb Group pathway involved in the control of seed development in *Arabidopsis thaliana*. *Development* **131**, 2971-2981.
Haushalter, K. A. and Kadonaga, J. T. (2003). Chromatin assembly by DNA-translocating motors. *Nat. Rev. Mol. Cell Biol*. **4**, 613-620.
Hennig, L., Taranto, P., Walser, M., Schonrock, N. and Gruissem, W. (2003). *Arabidopsis* MSI1 is required for epigenetic maintenance of reproductive development. *Development* **130**, 2555-2565.
Hennig, L., Bouveret, R. and Gruissem, W. (2005). MSI1-like proteins: an escort service for chromatin assembly and remodeling complexes. *Trends Cell Biol*. **15**, 295-302.
Honys, D. and Twell, D. (2004). Transcriptome analysis of haploid male gametophyte development in *Arabidopsis*. *Genome Biol*. **5**, R85.
Ingouff, M., Haseloff, J. and Berger, F. (2005). Polycomb group genes control developmental timing of endosperm. *Plant J*. **42**, 663-674.
Ingouff, M., Hamamura, Y., Gourgues, M., Higashiyama, T. and Berger, F. (2007). Distinct dynamics of HISTONE3 variants between the two fertilization products in plants. *Curr. Biol*. **17**, 1032-1037.
Iwakawa, H., Shinmyo, A. and Sekine, M. (2006). *Arabidopsis* CDKA;1, a cdc2 homologue, controls proliferation of generative cells in male gametogenesis. *Plant J*. **45**, 819-831.
Jenik, P. D., Jurkuta, R. E. and Barton, M. K. (2005). Interactions between the cell cycle and embryonic patterning in *Arabidopsis* uncovered by a mutation in DNA polymerase epsilon. *Plant Cell* **17**, 3362-3377.
Katz, A., Oliva, M., Mosquna, A., Hakim, O. and Ohad, N. (2004). FIE and CURLY LEAF polycomb proteins interact in the regulation of homeobox gene expression during sporophyte development. *Plant J*. **37**, 707-719.
Kaya, H., Shibahara, K. I., Taoka, K. I., Iwabuchi, M., Stillman, B. and Araki, T. (2001). FASCIATA genes for chromatin assembly factor-1 in *Arabidopsis* maintain the cellular organization of apical meristems. *Cell* **104**, 131-142.
Kirik, A., Pecinka, A., Wendeler, E. and Reiss, B. (2006). The Chromatin Assembly Factor subunit FASCIATA1 is involved in homologous recombination in plants. *Plant Cell* **18**, 2431-2442.
Köhler, C., Hennig, L., Bouveret, R., Gheyselinck, J., Grossniklaus, U. and Gruissem, W. (2003). *Arabidopsis* MSI1 is a component of the MEA/FIE Polycomb group complex and required for seed development. *EMBO J*. **22**, 4804-4814.
Linger, J. and Tyler, J. K. (2005). The yeast histone chaperone chromatin assembly factor 1 protects against double-strand DNA-damaging agents. *Genetics* **171**, 1513-1522.
McCormick, S. (2004). Control of male gametophyte development. *Plant Cell* **16**, S142-S153.
Moon, Y. H., Chen, L., Pan, R. L., Chang, H. S., Zhu, T., Maffeo, D. M. and Sung, Z. R. (2003). *EMF* genes maintain vegetative development by repressing the flower program in *Arabidopsis*. *Plant Cell* **15**, 681-693.
Nowack, M. K., Grini, P. E., Jakoby, M. J., Lafos, M., Koncz, C. and Schnittger, A. (2006). A positive signal from the fertilization of the egg cell sets off endosperm proliferation in angiosperm embryogenesis. *Nat. Genet*. **38**, 63-67.
Ohad, N., Margossian, L., Hsu, Y. C., Williams, C., Repetti, P. and Fischer, R. L. (1996). A mutation that allows endosperm development without fertilization. *Proc. Natl. Acad. Sci. USA* **93**, 5319-5324.
Ono, T., Kaya, H., Takeda, S., Abe, M., Ogawa, Y., Kato, M., Kakutani, T., Scheid, O. M., Araki, T. and Shibahara, K. (2006). Chromatin assembly factor 1 ensures the stable maintenance of silent chromatin states in *Arabidopsis*. *Genes Cells* **11**, 153-162.
Phelps-Durr, T. L., Thomas, J., Vahab, P. and Timmermans, M. C. (2005). Maize *rough sheath2* and its *Arabidopsis* orthologue *ASYMMETRIC LEAVES1* interact with *HIRA*, a predicted histone chaperone, to maintain *knox* gene silencing and determinacy during organogenesis. *Plant Cell* **17**, 2886-2898.
Polo, S. E. and Almouzni, G. (2006). Chromatin assembly: a basic recipe with various flavours. *Curr. Opin. Genet. Dev*. **16**, 104-111.
Preuss, D., Rhee, S. Y. and Davis, R. W. (1994). Tetrad analysis possible in *Arabidopsis* with mutation of the *QUARTET* (*QRT*) genes. *Science* **264**, 1458-1460.
Qian, Y. W. and Lee, E. Y. (1995). Dual retinoblastoma-binding proteins with properties related to a negative regulator of ras in yeast. *J. Biol. Chem*. **270**, 25507-25513.
Ramirez-Parra, E. and Gutierrez, C. (2007). E2F regulates *FASCIATA1*, a Chromatin Assembly gene whose loss switches on the endocycle and activates gene expression by changing the epigenetic status. *Plant Physiol*. **144**, 105-120.
Ridgway, P. and Almouzni, G. (2001). Chromatin assembly and organization. *J. Cell Sci*. **114**, 2711-2712.
Roman, H. (1948). Directed fertilization in maize. *Proc. Natl. Acad. Sci. USA* **34**, 36-42.
Rossi, V., Locatelli, S., Lanzanova, C., Boniotti, M. B., Varotto, S., Pipal, A., Goralik-Schramel, M., Lusser, A., Gatz, C., Gutierrez, C. et al. (2003). A maize histone deacetylase and retinoblastoma-related protein physically interact and cooperate in repressing gene transcription. *Plant Mol. Biol*. **51**, 401-413.
Rotman, N., Durbarry, A., Wardle, A., Yang, W. C., Chaboud, A., Faure, J. E., Berger, F. and Twell, D. (2005). A novel class of MYB factors controls sperm-cell formation in plants. *Curr. Biol*. **15**, 244-248.
Russell, S. D. (1983). Fertilization in *Plumbago zeylanica*: gametic fusion and fate of the male cytoplasm. *Am. J. Bot*. **70**, 416-434.
Russell, S. D. (1985). Preferential fertilization in *Plumbago*: ultrastructural evidence for gamete-level recognition in an angiosperm. *Proc. Natl. Acad. Sci. USA* **82**, 6129-6132.
Scheres, B. (2001). Plant cell identity. The role of position and lineage. *Plant Physiol*. **125**, 112-114.
Schonrock, N., Exner, V., Probst, A., Gruissem, W. and Hennig, L. (2006). Functional genomic analysis of *CAF-1* mutants in *Arabidopsis thaliana*. *J. Biol. Chem*. **281**, 9560-9568.
Strompen, G., Dettmer, J., Stierhof, Y. D., Schumacher, K., Jurgens, G. and Mayer, U. (2005). *Arabidopsis* vacuolar H-ATPase subunit E isoform 1 is required for Golgi organization and vacuole function in embryogenesis. *Plant J*. **41**, 125-132.
Twell, D., Yamaguchi, J., Wing, R. A., Ushiba, J. and McCormick, S. (1991). Promoter analysis of genes that are coordinately expressed during pollen development reveals pollen-specific enhancer sequences and shared regulatory elements. *Genes Dev*. **5**, 496-507.
Wang, D., Tyson, M. D., Jackson, S. S. and Yadegari, R. (2006). Partially redundant functions of two SET-domain polycomb-group proteins in controlling initiation of seed development in *Arabidopsis*. *Proc. Natl. Acad. Sci. USA* **103**, 13244-13249.
Wildwater, M., Campilho, A., Perez-Perez, J. M., Heidstra, R., Blilou, I., Korthout, H., Chatterjee, J., Mariconti, L., Gruissem, W. and Scheres, B. (2005). The *RETINOBLASTOMA-RELATED* gene regulates stem cell maintenance in *Arabidopsis* roots. *Cell* **123**, 1337-1349.

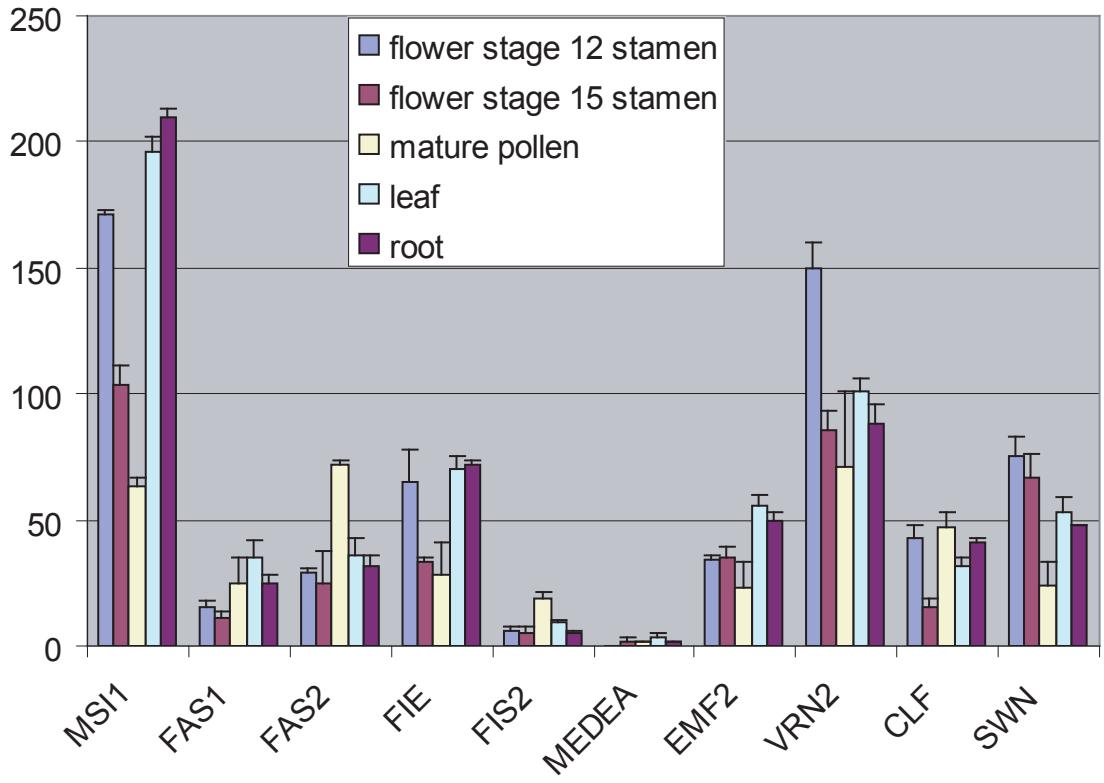

Supplementary Figure S1. Expression of genes encoding sub-units of the CAF1 and Pc-G complexes based on data available online from The A.thaliana Expression Database (http://csbdb.mpimp-golm.mpg.de/csbdb/dbxp/ath/ath_xpmgq.html).

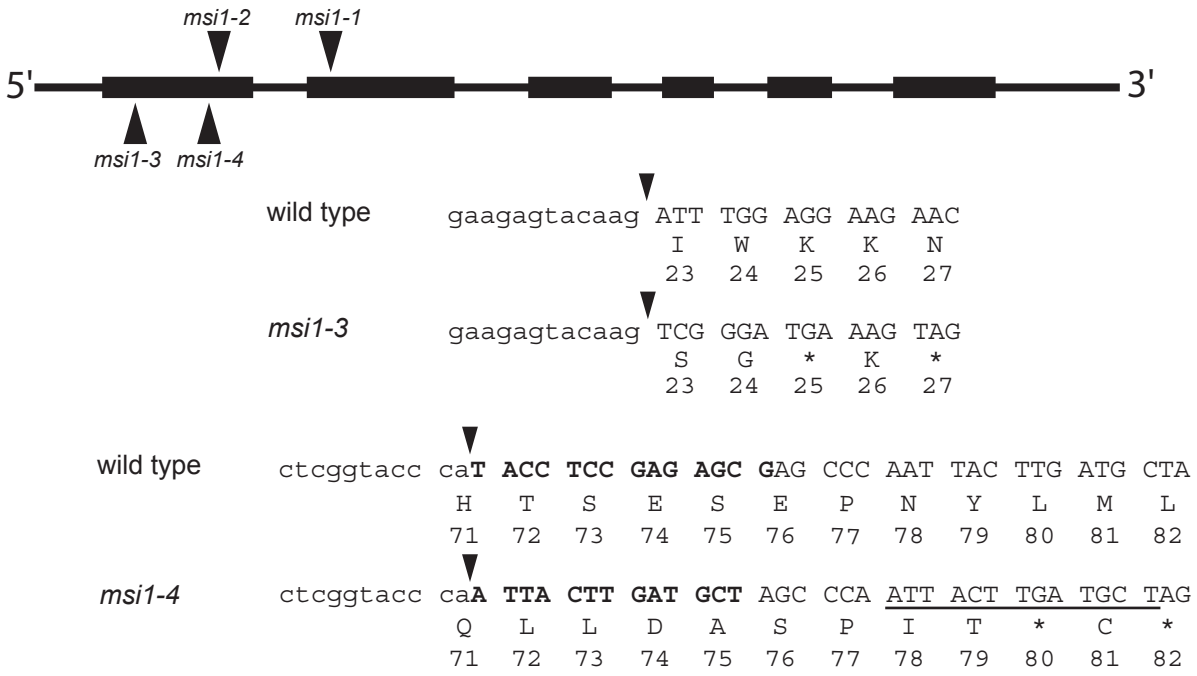

Supplementary Figure S2.
Localization of mutations in the four *msi1* loss-of-function alleles used in our study.
The details of the mutations associated with the new alleles *msi1-3* and *msi1-4* are shown.
Arrowheads indicate the precise location of base pair changes. Asterisks indicate stop codons.
The sequence underlined was replicated and replaced the wild-type sequence as shown
in bold in *msi1-4*.

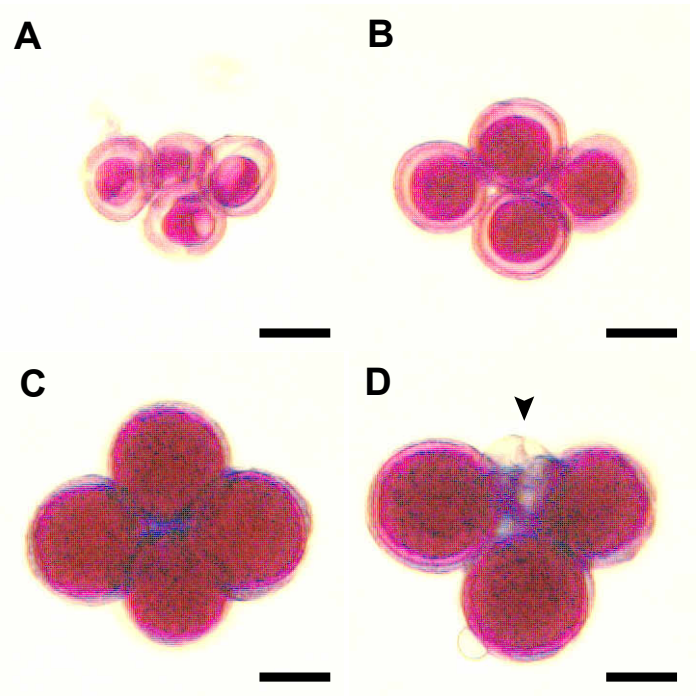

Supplementary Figure S3. Viability of pollen in *msi1*/+;*qrt*/*qrt* plants.
(A, C) Alexander staining of pollen from *qrt*/*qrt* (A-C) and from *msi1*/+;*qrt*/*qrt* (D) plants. Arrowhead indicates dead pollen grains. Scale bars: 10 μm.

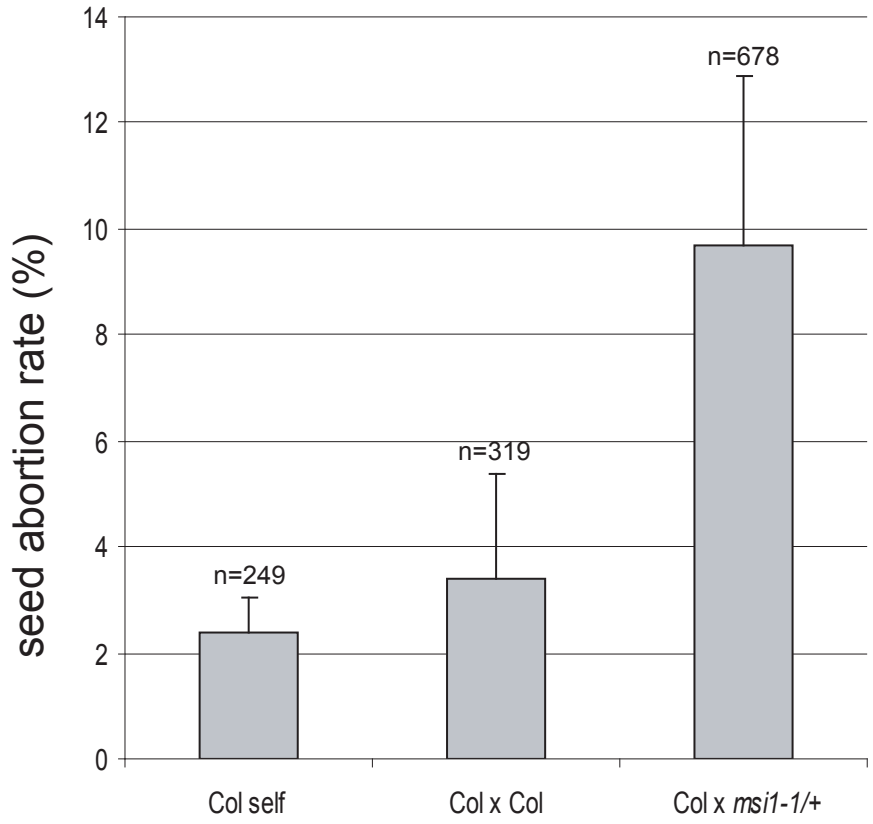

Supplementary Figure S4. Seed abortion caused by pollination with *msi1*/+.
The errors bars correspond to the standard deviation observed in the population (n).

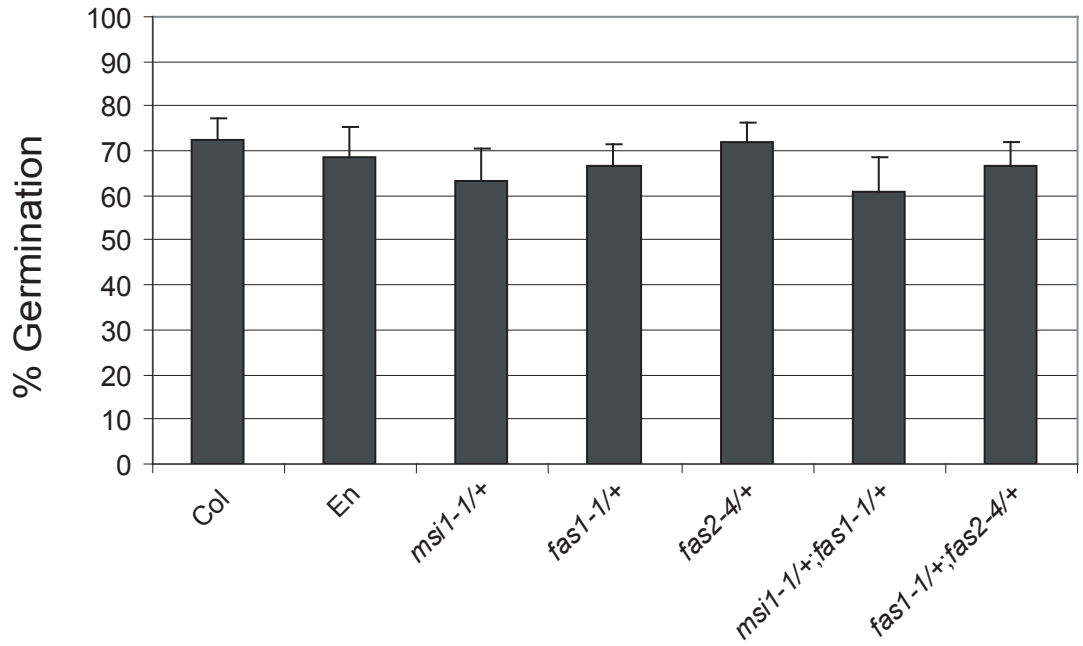

Supplementary Figure S5. In vitro pollen germination of combination between mutations in members of the CAF1 complex. Three replicates were performed for each assay. In each replicate 300 pollen grains were scored for pollen germination rates. Error bars corresponse to standard errors. Germination condition is referred to:
Boavida LC, McCormick S. (2007). Temperature as a determinant factor for increased and reproducible in vitro pollen germination in Arabidopsis thaliana. *Plant J.*
doi: 10.1111/j.1365-313X.2007.03248.x.

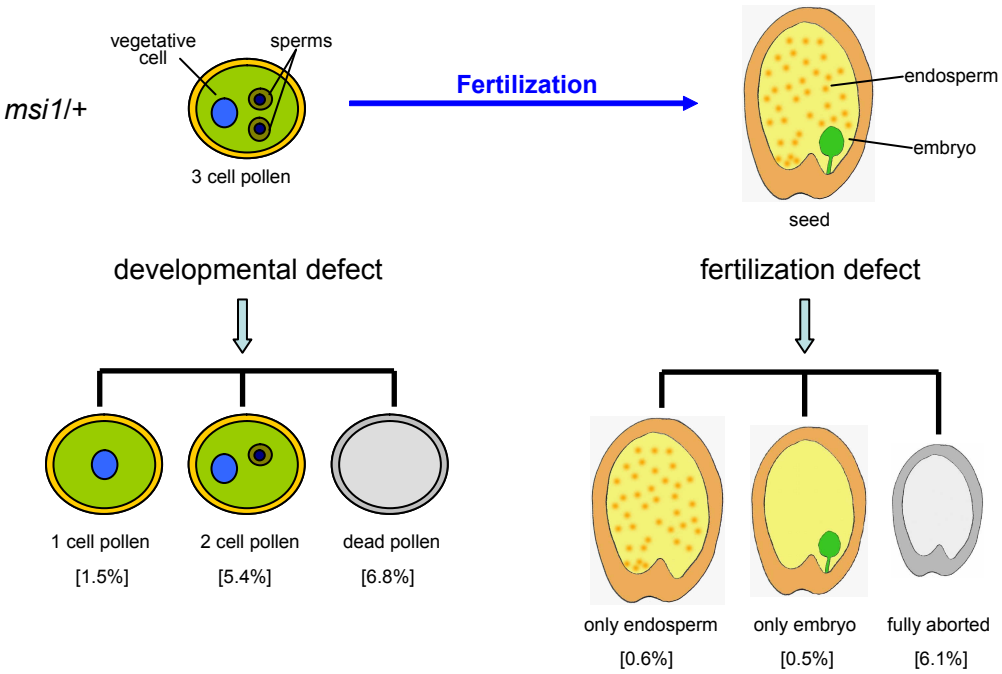

Totally 20.9% pollen do not transmit *msi1*

Supplementary Figure S6. Summary of the classes of abnormal pollen produced by *msi1* mutants and their impact on fertilization.

Proliferation and cell fate establishment during *Arabidopsis* male gametogenesis depends on the Retinoblastoma protein

Zhong Chen[a], Said Hafidh[b], Shi Hui Poh[a], David Twell[b], and Frederic Berger[a,1]

[a]Temasek LifeSciences Laboratory, 1 Research Link, National University of Singapore, 117604 Singapore; and [b]Department of Biology, University of Leicester, Leicester LE1 7RH, United Kingdom

Edited by Caroline Dean, John Innes Centre, Norwich, United Kingdom, and approved March 12, 2009 (received for review October 30, 2008)

The Retinoblastoma (Rb) protein is a conserved repressor of cell proliferation. In animals and plants, deregulation of Rb protein causes hyperproliferation and perturbs cell differentiation to various degrees. However, the primary developmental impact of the loss of Rb protein has remained unclear. In this study we investigated the direct consequences of Rb protein knockout in the *Arabidopsis* male germline using cytological and molecular markers. The *Arabidopsis* germ line derives from the unequal division of the microspore, producing a small germ cell and a large terminally differentiated vegetative cell. A single division of the germ cell produces the 2 sperm cells. We observed that the loss of Rb protein does not have a major impact on microspore division but causes limited hyperproliferation of the vegetative cell and, to a lesser degree, of the sperm cells. In addition, cell fate is perturbed in a fraction of Rb-defective vegetative cells. These defects are rescued by preventing cell proliferation arising from down-regulation of cyclin-dependent kinase A1. Our results indicate that hyperproliferation caused by the loss of Rb protein prevents or delays cell determination during plant male gametogenesis, providing further evidence for a direct link between fate determination and cell proliferation.

male germline | pollen | cell cycle

In multicellular organisms, cell proliferation and cell differentiation are tightly coordinated both spatially and temporally. One key coordinator is the Rb-E2F pathway (1, 2). As the first identified tumor suppressor gene (3), Rb encodes the retinoblastoma (Rb) protein, which controls cell cycle progression from G1 into S phase (4). Upon phosphorylation by cyclin-dependent kinases (Cdks) at late G1 stage, the Rb protein loses its binding affinity for E2F family transcription factors. The released E2F transcription factors activate downstream cell cycle genes and commit cells to S phase. The Rb protein not only binds to E2F to repress transcription, but also recruits chromatin remodeling factors (5–10). Thus, the Rb protein exerts a broad range of cellular functions beyond cell cycle control, including differentiation (11), senescence (12), and apoptosis (13). $Rb^{-/-}$ knockout mice die from abnormal placenta development (14, 15). Mammalian genomes encode 2 other proteins related to the Rb protein: p107 and p130 (16–18), which further complicates the dissection of Rb function in mammals. It still remains unclear how the Rb protein coordinates cell proliferation and differentiation in animals (16).

In plants, the Rb-E2F pathway is conserved (19). The maize (*Zea mays*) genome contains 3 Rb genes, as in mammals (20–22). *Arabidopsis thaliana* contains a single Rb gene (*RBR*) (23). Loss of function of *RBR* completely impairs female gametogenesis, which precludes direct assessment of the role of the Rb protein in post-embryonic development (24, 25). Loss of RBR during female gametogenesis causes over-proliferation but does not appear to have a major effect on cell fate (25–28). To understand the role of RBR in development, different inducible systems disrupting *RBR* expression or over-expressing *RBR* were developed. Virus-induced gene silencing of NbRBR in Tobacco (*Nicotiana benthamiana*) caused deregulation of cell proliferation, differentiation, and endo-reduplication (29). RNA interference and inducible over-expression of *Arabidopsis RBR* impaired stem cell maintenance in roots (30). Inducible expression of a geminivirus RBR-binding protein in *Arabidopsis* leaves suggested that RBR prevents cell division and endoreduplication in a cell type-dependent manner (31).

As RBR represses *MET1* expression (27) and likely recruits members of chromatin modifying complexes, the loss of *RBR* is expected to causes epigenetic modifications inherited through cell divisions (32, 33). Such modifications could impact on cell fate with secondary effects on proliferation. Alternatively deregulation of cell proliferation could impact directly on differentiation and cell fate as shown recently in Drosophila neuroblasts (34). It is thus difficult to analyze the direct effect of RBR on differentiation in experimental strategies perturbing RBR function during a large number of cell divisions before differentiation takes place.

In contrast to organogenesis of vegetative tissues, male gametogenesis comprises only 2 cell divisions. The first asymmetrical division of the meiotic microspore produces the larger vegetative cell and the smaller generative cell, which functions as a germ cell. The germ cell divides equally only once, producing 2 identical sperm cells. The differentiated vegetative cell produces the pollen tube, which delivers the 2 sperm cells to the 2 female gametes (35). In half of the haploid *rbr* microspores from heterozygous *rbr*/+ plants, the sudden deprivation of a functional *RBR* allele allows monitoring of the direct effect of the loss of RBR on cell proliferation and cell fate in the developing pollen.

We report that loss of *RBR* causes limited over-proliferation of the 2 pollen cell types. We further study the effect on cell fate using several markers and observe only a limited impact of *rbr*. The *rbr* phenotype is completely reversed in the absence of the cyclin dependent kinase A, leading to the hypothesis that *rbr* primarily targets cell cycle regulation with a secondary impact on cell fate.

Results and Discussion

We observed expression of *RBR* throughout pollen development in all cell types [supporting information (SI) Fig. S1]. Two mutant alleles *rbr-1* (24, 26) and *rbr-2*, show reduced paternal transmission (Table S1) linked with reduced pollen viability (Fig. S2). We further characterized at the cellular and

Author contributions: Z.C., D.T., and F.B. designed research; Z.C., S.H., and S.H.P. performed research; Z.C., S.H., D.T., and F.B. analyzed data; and Z.C., D.T., and F.B. wrote the paper.

The authors declare no conflict of interest.

This article is a PNAS Direct Submission.

[1]To whom correspondence should be addressed. E-mail: fred@tll.org.sg.

This article contains supporting information online at www.pnas.org/cgi/content/full/0810992106/DCSupplemental.

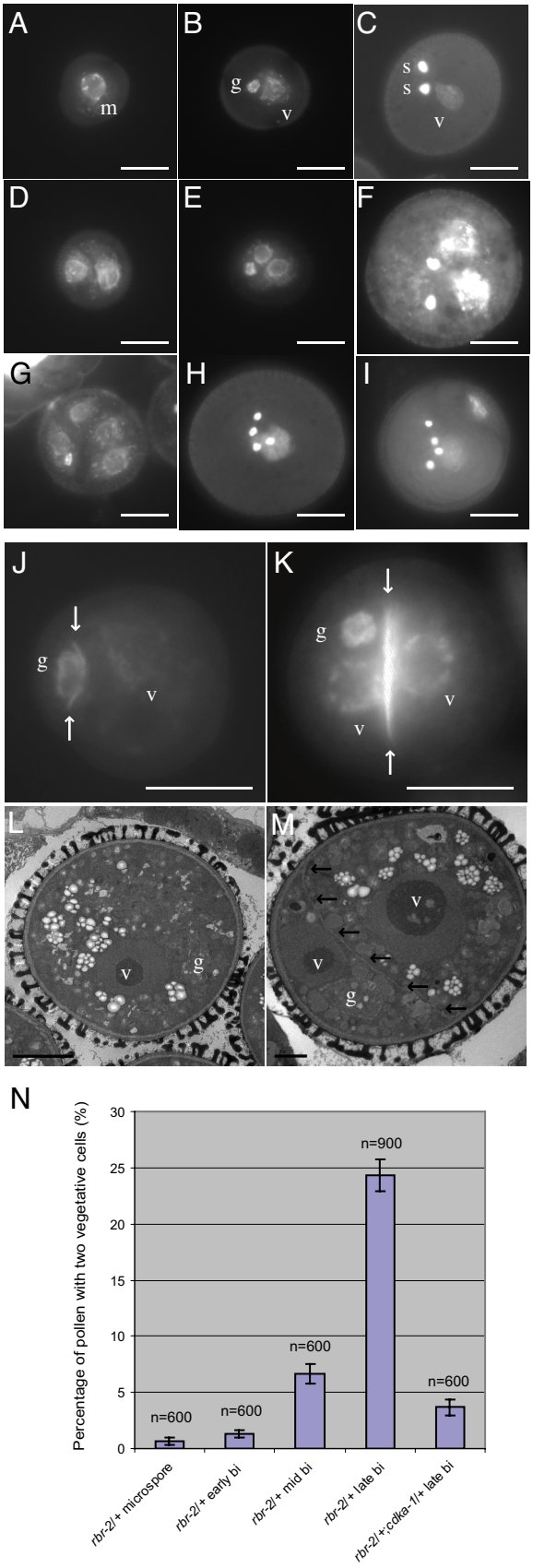

Fig. 1. Cell over-proliferation during pollen development in *rbr*/+ mutants. (*A–C*) WT pollen development. (*A*) The microspore with the undetermined cell fate undergoes an asymmetrical mitosis, leading to bicellular pollen (*B*). At that stage the pollen grain composes a large vegetative cell containing a small germ cell with a nucleus showing relatively higher chromatin compaction. The germ cell divides into 2 sperm cells with highly condensed chromatin, leading to the tricellular pollen grain (*C*). (*D–I*) *rbr* pollen development. Cell fates are determined on the basis of nuclear morphology. (*D*) At the microspore stage, *rbr* pollen grain with 2 undetermined cell nuclei. (*E*) Bi-cellular-stage *rbr* pollen grain with 2 vegetative cell nuclei and 1 germ cell nucleus. (*F*) Tri-cellular-stage *rbr* pollen with 2 vegetative cell nuclei and 2 sperm cell nuclei. (*G*) Tri-cellular-stage *rbr* pollen with 4 vegetative cell nuclei and 1 germ cell nucleus. (*H*) Tri cellular-stage *rbr* pollen with 1 vegetative cell nucleus and 4 germ cell nuclei. (*I*) Tri-cellular-stage *rbr* pollen with 2 vegetative cell nuclei and 4 germ cell nuclei. Nuclei are stained with DAPI. (Scale bars, 10 μm.) (*J*) Bi-cellular-stage WT pollen. The cell wall (arrows) is asymmetrically placed between the vegetative nucleus and the generative nucleus. (*K*) Bi-cellular-stage *rbr* pollen. The cell wall (arrows) is symmetrically placed between the 2 vegetative nuclei. Nuclei are stained with DAPI, and the cell walls are stained with aniline blue. (*L* and *M*) Transmission electron micrographs of bi-cellular-stage WT pollen (*L*) and *rbr* pollen (*M*). Note the internal wall indicated by arrows in *rbr* pollen. (Scale bars, 10 μm in *J* and *K*; 5 μm in *L*; 2 μm in *M*.) (*N*) Bar chart showing percentage of the pollen contains 2 vegetative cells in *rbr-2*/+ mutants at microspore, early bi-cellular, mid-bi-cellular, and late bi-cellular stages. At late bi-cellular stage, the over-proliferation in pollen from *rbr-2*/+;*cdka-1*/+ plants was reduced to one seventh of the over-proliferation in pollen from *rbr-2*/+ plants. Error bars correspond to SEs calculated on the basis of several samples of 100 pollen grains, and the size of total population analyzed (*n*) is indicated above each column. *m*, microspore nucleus; *g*, germ cell nucleus; *v*, vegetative cell nucleus; *s*, sperm cell nucleus.

molecular levels the defects caused by *rbr* mutations during pollen development.

Limited Cell Over-Proliferation in *rbr* Pollen. A recent study reported hyperproliferation of the vegetative nucleus of *rbr* pollen (26), but the origin of the supernumerary cells was not analyzed. We studied development of *rbr* pollen with nuclei stained by DAPI. WT microspores never divide equally (n = 1,000; Fig. 1*A*). In contrast, we observed in *rbr*/+ plants a very small fraction of microspores 0.67% (n = 600) that had divided equally into 2 cells (Fig. 1*D*). The very limited impact of *rbr* on microspore division might be explained by inheritance of residual RBR from the *rbr*/+ meiotic precursor.

The WT bicellular pollen comprises a vegetative cell with a large nucleus with de-condensed chromatin, and a smaller generative cell with a smaller nucleus (Fig. 1*B*). In contrast, *rbr*/+ plants produced 24.3% (n = 900) pollen containing 3 nuclei (Fig. 1*E*). One nucleus displayed the condensed chromatin typical of generative cells. The other 2 nuclei were larger with less condensed chromatin typical of vegetative cells (Fig. 1 *B* and *E*). Wild-type bicellular pollen is marked by a transient eccentric cell wall (Fig. 1 *J* and *K*). In contrast, the abnormal 3-celled *rbr* pollen observed at the bicellular WT stage showed an aberrant cell wall between the 2 vegetative cells (Fig. 1 *K* and *M*). The proportion of pollen containing 2 vegetative cells rose sharply during late bicellular stage, affecting half of the *rbr* pollen (Fig. 1*N*). We never observed any 3-celled pollen at that stage, suggesting that *rbr* causes an ectopic division of the vegetative cell.

Half of the pollen produced by *rbr*/+ plants inherits the *rbr* mutation. We estimated that 30% of the *rbr* pollen was dead at the bicellular stage (Fig. S2*B*; percentages are expressed relative to the estimated *rbr* pollen population and are thus twice as shown on Fig. S2*B*). Fifty percent of *rbr* pollen showed abnormal development and 20% showed WT morphology. At the tricellular stage, at least 60% of the *rbr* pollen was dead (Fig. S2*B*). As *rbr-2* male transmission rate is of the order of 10% (Table S1), we could assume that 20% *rbr* pollen with normal morphology at bicellular stage underwent further development as WT. We thus estimated that, at the tricellular stage, less than 20% of the *rbr* pollen would derive from abnormal 3-celled pollen observed at bicellular stage. Corresponding to our estimate, we observed

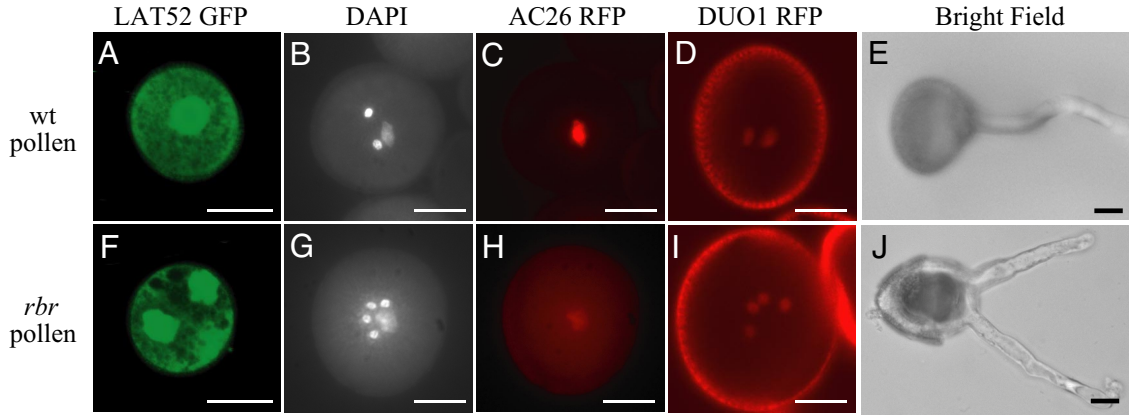

Fig. 2. Cell fate specification in *rbr* pollen. (*A–E*) WT pollen grains. (*F–J*) *rbr* pollen grains. (*A* and *F*) Bi-cellular pollen grains expressing the vegetative cell marker *pLAT52-GFP*. (*B* and *G*) Fluorescence images of tri-cellular pollen grains stained with DAPI (*C* and *H*) The same pollen grains as *B* and *G*, respectively, expressing the vegetative cell marker *pAC26-H2B-mRFP*. WT pollen grain with 1 vegetative cell and 2 sperm cells (*B*) has only the vegetative cell nucleus expressing *pAC26-H2B-mRFP* (*C*). *rbr* pollen with 1 vegetative cells and 4 germ cells (*G*). Only the vegetative cell nucleus expresses *pAC26-H2B-mRFP* (*H*). (*D* and *I*) Tri-cellular pollen grains expressing the germ cell marker *pDUO1-DUO1-mRFP*. (*E* and *J*) In vitro pollen germination. WT pollen produces only 1 pollen tube germinated (*E*), whereas 2 pollen tubes germinated from the same *rbr* pollen grain (*J*). (Scale bars, 10 μm.)

a total of 8% of abnormal pollen grains showing a complex array of phenotypes (n = 1000 pollen from *rbr-2*/+ plants). A predominant class of abnormal pollen contained 2 vegetative nuclei and 2 small sperm-like cells (4.6%; Fig. 1*F*). This class of abnormal pollen likely originated from the class shown in Fig. 1*E* in which either the generative cell divided into 2 sperm-like cells or the additional vegetative cell divided again, producing a generative cell. Several other types of pollen were observed (Fig. 1 *G–I*). Some pollen contained 4 vegetative nuclei and 1 sperm-like nucleus (1.6%; Fig. 1*G*). This pollen class likely results from an additional division of the 2 vegetative cells followed by 1 unequal division of 1 of the 4 vegetative cells producing a generative-like cell. We also observed pollen containing 4 sperm nuclei, either associated with 2 vegetative-like nuclei (1.2%; Fig. 1*I*) or inside 1 vegetative cell (3.4%; Fig. 1*H*). The latter class probably originates from a supernumerary division in the germ lineage. We did not observe any of the aforementioned phenotypes among WT pollen ($n > 300$ for each stage).

We targeted partial down-regulation of *RBR* in each pollen cell type by the expression of *RBR* hairpin RNAi constructs. Transgenic lines expressing the *RBR* RNAi construct under the control of the germ line-specific promoters of *HTR10* (33,36,37) (47 lines observed) and *GEX2* (38) (34 lines observed) did not show any defect in pollen viability or phenotype. In contrast, *RBR* RNAi expression restricted to the vegetative cell using the *LAT52* promoter (39) caused a distinct increase in vegetative nuclear DNA fluorescence (Fig. S3) in 10%–25% of pollen, reflecting increased DNA synthesis. However we did not observe ectopic division of the vegetative cell. Hence, *RBR* RNAi expression under the *LAT52* promoter caused a limited reduction of RBR activity leading to defects milder than the complete loss of *RBR* in *rbr* mutant alleles.

We conclude that *rbr* loss of function mostly affects the vegetative lineage and prevents arrest of cell division typical of vegetative cell fate. The loss of *rbr* function does not cause more than 2 additional rounds of cell division in comparison to WT. Further hyperproliferation in *rbr* pollen may be prevented by the limited supply of nutrients during pollen development leading to developmental arrest or death.

Cell Fate in *rbr* Pollen. The nuclear morphology in *rbr* pollen suggested that cell over-proliferation in *rbr* pollen grains was associated with correct vegetative and germ cell fates. To address this question, we analyzed the expression of 6 cell fate markers in *rbr* pollen (Figs. 2 and 3). In the pollen displaying the rare phenotypic classes with duplication of the vegetative or germ cell lineages (Fig. 1*I*), the *rbr* pollen expressed the vegetative cell markers *pLAT52-GFP* (40) (Fig. 2*F*; n = 42) and *pAC26-H2B-mRFP1* (41) (Fig. 2*H*; n = 14) in the large vegetative-like cells and the germ line marker *pDUO1-DUO1-mRFP1* (42) in the small germ-like cells (Fig. 2*I*; n = 9). These observations suggested that *rbr* does not affect cell fate in this class of pollen. Accordingly we observed that 0.3% (n = 1,327) of pollen grains from *rbr* mutant germinated 2 pollen tubes likely originating from 2 vegetative cells (Fig. 2*J*). We concluded that, despite cell over-proliferation in *rbr* pollen, the vegetative cell fate and sperm cell fate are not affected when pollen experiences a complete duplication.

We further studied the cell fates in the 3-celled *rbr* pollen, most representative of the *rbr* phenotype at WT bicellular stage (Fig. 3). In WT bi-cellular pollen, the germ cell expresses the markers *pHTR10-HTR10-mRFP* (Fig. 3*A*) and *pAC24-mRFP* (41) (Fig. 3*D*). In two thirds of *rbr* pollen with 1 germ cell nucleus and 2 vegetative cell nuclei, the markers were correctly expressed (Fig. 3 *B* and *E*). However, in a third of 3-celled *rbr* pollen, both the germ cell nucleus and one of the vegetative-like nuclei expressed the germline markers (Fig. 3 *C* and *F*). Such ectopic expression was never observed in WT pollen ($n > 300$ for each marker). In addition, when we observed the co-expression of the vegetative marker *pLAT52-GFP* and the germline marker *pDUO1-DUO1-mRFP* (Fig. 3 *G–J*), a quarter of *rbr* pollen expressed the germline fate marker incorrectly. The additional vegetative-like cell expressed either the germline marker (n = 13 of 76; Fig. 3*I*) or both markers simultaneously (n = 7 of 76; Fig. 3*J*). We never observed mis-expression of the vegetative marker in the *rbr* germline (n = 76).

The *rbr* vegetative cell appears to behave like a microspore attempting imperfectly to reiterate an unequal division, producing an additional cell with vegetative fate, germ cell fate, or mixed fate identity. According to this hypothesis, genes expressed in the microspore but not later in the vegetative cell should be expressed in the vegetative cells of *rbr* pollen. Immunolocalization of the centromeric histone 3 variant HTR12 in WT tri-cellular pollen had shown that this protein marks only sperm cell nuclei (43). Accordingly, the centromeric histone HTR12 fused to GFP (HTR12-GFP) placed under the control

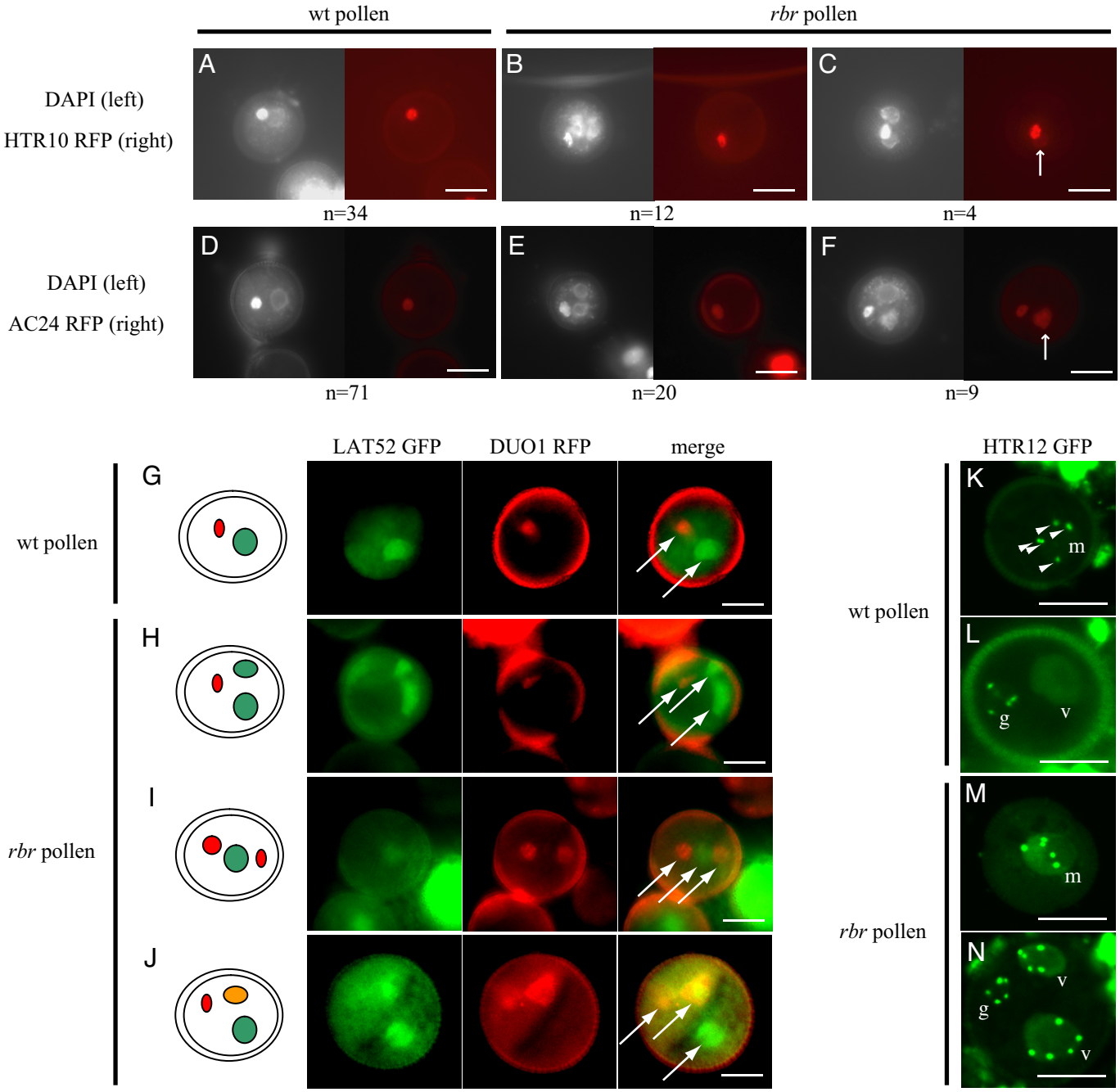

Fig. 3. Mis-specification of cell fate in *rbr* pollen. (*A–C*) Fluorescence images of bi-cellular-stage pollen grains stained with DAPI (*Left*) and expressing *pHTR10-HTR10-mRFP* (*Right*). (*D–F*) Fluorescence images of bi-cellular-stage pollen grains stained with DAPI (*Left*) and expressing *pAC24-H2B-mRFP* (*Right*). Below each figure, *n* indicates the number of each case observed. (*G–I*) Fluorescence images of bi-cellular-stage pollen grains co-expressing the vegetative marker *pLAT52-GFP* and the germline marker *pHTR10-HTR10-mRFP*. Panels (*Left* to *Right*) are schematic representation of pollen co-expressing the 2 markers, GFP channel, RFP channel, and merged image. Arrows indicate the positions of cell nuclei. (*K–N*) Fluorescence images of microspores (*K* and*M*) and bi-cellular-stage pollen grains (*L* and *N*) expressing the centromeric Histone 3 variant fused to GFP (HTR12-GFP). In WT (*K* and *L*), HTR12-GFP accumulates at the 5 chromocenters (arrowheads) of the microspore nucleus (*m*) (*K*) and the germ cell nucleus (*g*) (*L*), but it is not possible to distinguish chromocenters in the vegetative cell nucleus (*v*). In contrast, in *rbr* pollen, HTR12-GFP is detected at chromocenters in microspores (*M*) and in both cell types at bi-cellular stage (*N*). (Scale bars, 10 μm.)

of its own promoter (44) was expressed in the WT microspore (Fig. 3*K*) but was no longer detected in the vegetative cell nucleus after bi-cellular stage (Fig. 3*L*). *HTR12-GFP* expression was observed in all microspores from *rbr-2*/+ plants (n = 100; Fig. 3*M*), suggesting that RBR did not have a major impact on *HTR12-GFP* expression at that stage. In contrast to WT bicellular pollen, *rbr* 3-celled pollen showed ectopic expression of *HTR12-GFP* in vegetative cells (n = 24; Fig. 3*N*). This observation supported our hypothesis that the *rbr* vegetative cell retains the undetermined identity of the microspore. We thus concluded that *rbr* prevents cell fate establishment in the vegetative cell. A non-exclusive alternative explanation is that increased DNA methylation activity caused by increased *MET1* expression in *rbr* background (27) impacts on heterochromatin organization, causing HTR12 recruitment. Our results thus led us to propose that loss of retinoblastoma function prevents cell

fate establishment during male gametogenesis with an impact that depends on the cell type.

***rbr* Pollen Defects Are Rescued by Deregulation of the Cell Cycle.** Perturbation of the RBR pathway by over-expression of cyclin D3 impacts on cell proliferation and the timing of endo-reduplication in leaves and other vegetative tissues (45, 46). As endoreduplication usually marks differentiation in vegetative tissues, it was proposed that the cyclin D pathway controls cell differentiation (45). Although the impact on cell fate was not directly established in these studies, it is possible that the cyclin D pathway associated with cyclin-dependent kinase A (CDKA) regulates RBR function (47) and mediates the transition toward differentiation via the promotion of endo-reduplication in plants.

We further hypothesized that, if *rbr* directly prevents cell commitment to differentiate, preventing hyperproliferation in an *rbr* background should not rescue the defective cell fate in *rbr* pollen. To prevent cell proliferation without affecting cell fate, we choose to manipulate the Cyclin Dependent Kinase A (CDKA), which controls RBR licensing of the entry to S phase but presumably not the involvement of RBR in chromatin remodeling complexes. In animals, a few reports have shown involvement of CDKA homologues in cell fate in Drosophila (48) and in *C. elegans* (49). However, the mechanisms involving Cdks in cell polarity remain unclear. In *Arabidopsis* the function of the major Cdk CDKA has been solely linked to the control of the cell cycle in vegetative tissues (50) and during male gametogenesis (51–53). We thus rationalized that antagonizing RBR regulation of the cell cycle by CDKA manipulation would allow us to uncouple RBR functions in cell cycle regulation from other functions related to chromatin regulation. We tested in *rbr-2* pollen the effect of hypo-proliferation caused by the loss-of-function *cdka* mutant allele. In the *rbr-2*/+;*cdka-1*/+ double mutant, we studied the transmission of *rbr-2* and the phenotype of the pollen. The presence of *cdka-1* almost completely rescued the paternal transmission efficiency of *rbr-2* (Table S1), in agreement with the prediction of a complete viability of the *rbr-2*; *cdka-1* ($z = 32.52$, $P < 0.000001$, 2-tailed test if no complementation; $z = -1.24$, $P = 0.1075$, 2-tailed test if full complementation). Accordingly, pollen lethality (Fig. S4) and over-proliferation (Fig. 1*N*) were greatly decreased in *rbr-2*/+; *cdka-1*/+ plants. The percentage of defective pollen was decreased by more than half in *rbr-2*/+; *cdka-1*/+ plants in comparison to that from *rbr-2*/+ plants, both at bicellular and tricellular stages (Fig. S2*B*), leading to full rescue of pollen death in *rbr-2*/+; *cdka-1*/+ plants.

It thus appears that restoring proliferation to WT levels in an *rbr* background rescues the defects in cell fate establishment observed in the *rbr* mutant. We propose that the primary effect of the loss of function of RBR in male gametogenesis is mediated by its role in cell proliferation.

Conclusions

Our study suggests that the control of the degree of proliferation by RBR is essential for proper cell fate establishment during male gametogenesis. One scenario is that the loss of retinoblastoma function primarily promotes hyperproliferation with secondary effects on commitment to cell fate during early development. It is not clear how cell fate is established in the bicellular pollen, but gradients of fate determinants have been hypothesized (35, 55). The additional cells produced by the *rbr* pollen might be positioned improperly relative to developmental cues, causing anomalous or mixed-cell fate. An alternative scenario proposes that RBR directly coordinates cell division and cell fate commitment. This could be mediated directly by the cell cycle machinery as suggested by a role of CDKA homologues in cell fate reported in a few cell types (48,49,56). A third non-exclusive hypothesis relates to the role of the Rb protein in chromatin modifications. In mammals it was shown that the Rb protein interacts with several chromatin remodeling complexes (6–9,11). These complexes might be conserved in plants. Cell fate establishment would then require chromatin modifications dependent on DNA duplication. We propose that, in the absence of *RBR* function, hyperproliferation coupled to the absence of recruitment of chromatin modifying complexes prevents this cell fate establishment.

Experimental Procedures

Plant Strains and Growth Conditions. The WT ecotype Columbia (Col-0) was provided by the Nottingham *Arabidopsis* Stock Centre. The *A. thaliana rbr* mutant alleles (Columbia accession) used in this study were *rbr-2* (SALK_002946; SALK collection), and *rbr-3* (GABI_170G02; GABI-Kat collection) (23). Marker lines for cell identity were *pDUO1-DUO1-mRFP* (C24) (42), *pAC24-H2B-mRFP*, *pAC26-H2B-mRFP* (C24), and *pHTR10-HTR10m-RFP* (Col) (36). *pLAT52-GFP* (Col) was a gift from Alice Cheung (Amherst, MA).

RT-PCR. Pollen at different stages of development were isolated and RNA extracted as described previously (41). Total RNA was prepared using the RNeasy mini kit (Qiagen) followed by DNase treatment (Ambion). Reverse transcription was performed by M-MuLV reverse transcriptase (New England Biolabs) with RNA ribonuclease inhibitor (Promega).

***RBR* Hairpin Interference Plasmid Construction and Transformation.** To express hairpin dsRNA targeted to *RBR* transcripts specifically in the vegetative cell, 500 bp of *RBR* coding sequence was cloned in sense and antisense orientations into a modified Gateway expression vector *pK7LAT52RNAi* harboring the vegetative cell-specific *LAT52* promoter. A 495-bp *LAT52* promoter fragment was amplified using KOD HiFi DNA Polymerase (Novagen) with primers containing restriction sites for HindIII and XhoI. The *LAT52* promoter fragment was cloned into a Gateway RNAi destination vector pK7gwiwgL using the HindIII and XhoI sites to generate the *pK7LAT52hpRNAi* vector. A 500-bp *RBR* fragment was amplified by PCR and cloned by recombination using the Gateway cloning system according to manufacturer's instructions (Invitrogen) to generate the *pLAT52hpRBR* construct. Verified plasmid was transformed into *Agrobacterium tumefaciens* strain GV3101 and used to generate transgenic lines in *A. thaliana* ecotype Col-0 using the floral dip method. Transgenic progeny were selected for kanamycin resistance.

Microscopy and Image Processing. Alexander staining and DAPI fluorescence in pollen grains were visualized as described previously (41). Light microscopy was performed on a stereomicroscope (DM6000; Leica). Images were recorded with a monochrome digital camera (Photometrics; Roper Scientific). Fluorescence was imaged using laser scanning confocal microscopy (LSM 510 META upright; Zeiss). Figures were composed with Adobe Photoshop 7.0.1 and Illustrator 10.0.3 (Adobe Systems). Transmission electron microscopy was performed with 85-nm thin sections were prepared on a Leica Ultracut UCT ultramicrotome. Samples were observed at 120 kV under a JEM-1230 transmission electron microscope (JEOL).

ACKNOWLEDGMENTS. This work was funded by Temasek LifeSciences Laboratory and the Singapore Millenium Foundation (F.B., Z.C., S.H.P.); and by the University of Leicester and the United Kingdom Biotechnology and Biological Sciences Research Council (D.T., S.H.). Additional support was received from the Department of Biological Sciences at National University of Singapore.

1. Harbour JW, Dean DC (2000) The Rb/E2F pathway: expanding roles and emerging paradigms. *Genes Dev* 14:2393–2409.
2. Korenjak M, Brehm A (2005) E2F-Rb complexes regulating transcription of genes important for differentiation and development. *Curr Opin Genet Dev* 15:520–527.
3. Friend SH, et al. (1986) A human DNA segment with properties of the gene that predisposes to retinoblastoma and osteosarcoma. *Nature* 323:643–646.
4. Weinberg RA (1995) The retinoblastoma protein and cell cycle control. *Cell* 81:323–330.
5. Brehm A, Kouzarides T (1999) Retinoblastoma protein meets chromatin. *Trends Biochem Sci* 24:142–145.
6. Harbour JW, Dean DC (2000) Chromatin remodeling and Rb activity. *Curr Opin Cell Biol* 12:685–689.
7. Dahiya A, Wong S, Gonzalo S, Gavin M, Dean DC (2001) Linking the Rb and polycomb pathways. *Mol Cell* 8:557–569.
8. Nielsen SJ, et al. (2001) Rb targets histone H3 methylation and HP1 to promoters. *Nature* 412:561–565.

9. Vandel L, et al. (2001) Transcriptional repression by the retinoblastoma protein through the recruitment of a histone methyltransferase. *Mol Cell Biol* 21:6484–6494.
10. Sharif J, et al. (2007) The SRA protein Np95 mediates epigenetic inheritance by recruiting Dnmt1 to methylated DNA. *Nature* 450:908–912.
11. Macaluso M, Montanari M, Giordano A (2006) Rb family proteins as modulators of gene expression and new aspects regarding the interaction with chromatin remodeling enzymes. *Oncogene* 25:5263–5267.
12. Funayama R, Ishikawa F (2007) Cellular senescence and chromatin structure. *Chromosoma* 116:431–440.
13. Harbour JW, Dean DC (2000) Rb function in cell-cycle regulation and apoptosis. *Nat Cell Biol* 2:E65–67.
14. de Bruin A, et al. (2003) Identification and characterization of E2F7, a novel mammalian E2F family member capable of blocking cellular proliferation. *J Biol Chem* 278:42041–42049.
15. Wu L, et al. (2003) Extra-embryonic function of Rb is essential for embryonic development and viability. *Nature* 421:942–947.
16. Wikenheiser-Brokamp KA (2006) Retinoblastoma family proteins: insights gained through genetic manipulation of mice. *Cell Mol Life Sci* 63:767–780.
17. Giordano A, Rossi A, Romano G, Bagella L (2007) Tumor suppressor pRb2/p130 gene and its derived product Spa310 spacer domain as perspective candidates for cancer therapy. *J Cell Physiol* 213:403–406.
18. Stevaux O, Dyson NJ (2002) A revised picture of the E2F transcriptional network and RB function. *Curr Opin Cell Biol* 14:684–691.
19. Shen WH (2002) The plant E2F-Rb pathway and epigenetic control. *Trends Plants Sci* 7:505–511.
20. Gordon-Kamm W, et al. (2002) Stimulation of the cell cycle and maize transformation by disruption of the plant retinoblastoma pathway. *Proc Natl Acad Sci USA* 99:11975–11980.
21. Grafi G, et al. (1996) A maize cDNA encoding a member of the retinoblastoma protein family: involvement in endoreduplication. *Proc Natl Acad Sci USA* 93:8962–8967.
22. Sabelli PA, et al. (2005) RBR3, a member of the retinoblastoma-related family from maize, is regulated by the RBR1/E2F pathway. *Proc Natl Acad Sci USA* 102:13005–13012.
23. Vandepoele K, et al. (2002) Genome-wide analysis of core cell cycle genes in Arabidopsis. *Plant Cell* 14:903–916.
24. Ebel C, Mariconti L, Gruissem W (2004) Plant retinoblastoma homologues control nuclear proliferation in the female gametophyte. *Nature* 429:776–780.
25. Ingouff M, Jullien PE, Berger F (2006) The female gametophyte and the endosperm control cell proliferation and differentiation of the seed coat in Arabidopsis. *Plant Cell* 18:3491–3501.
26. Johnston AJ, Matveeva E, Kirioukhova O, Grossniklaus U, Gruissem W (2008) A dynamic reciprocal RBR-PRC2 regulatory circuit controls Arabidopsis gametophyte development. *Curr Biol* 18:1680–1686.
27. Jullien PE, et al. (2008) Retinoblastoma and Its binding partner MSI1 control imprinting in Arabidopsis. *PLoS Biol* 6:e194.
28. Ingouff M, et al. (2009) The two male gametes share equal ability to fertilize the egg cell in Arabidopsis thaliana. *Curr Biol* 19:R19–R20.
29. Park JA, et al. (2005) Retinoblastoma protein regulates cell proliferation, differentiation, and endoreduplication in plants. *Plant J* 42:153–163.
30. Wildwater M, et al. (2005) The RETINOBLASTOMA-RELATED gene regulates stem cell maintenance in Arabidopsis roots. *Cell* 123:1337–1349.
31. Desvoyes B, Ramirez-Parra E, Xie Q, Chua NH, Gutierrez C (2006) Cell type-specific role of the retinoblastoma/E2F pathway during Arabidopsis leaf development. *Plant Physiol* 140:67–80.
32. Chan SW, Henderson IR, Jacobsen SE (2005) Gardening the genome: DNA methylation in Arabidopsis thaliana. *Nat Rev Genet* 6:351–360.
33. Mathieu O, Reinders J, Caikovski M, Smathajitt C, Paszkowski J (2007) Transgenerational stability of the Arabidopsis epigenome is coordinated by CG methylation. *Cell* 130:851–862.
34. Chia W, Somers WG, Wang H (2008) Drosophila neuroblast asymmetric divisions: cell cycle regulators, asymmetric protein localization, and tumorigenesis. *J Cell Biol* 180:267–272.
35. McCormick S (2004) Control of male gametophyte development. *Plant Cell* 16(suppl):S142–S153.
36. Ingouff M, Hamamura Y, Gourgues M, Higashiyama T, Berger F (2007) Distinct dynamics of HISTONE3 variants between the two fertilization products in plants. *Curr Biol* 17:1032–1037.
37. Okada T, Endo M, Singh MB, Bhalla PL (2005) Analysis of the histone H3 gene family in Arabidopsis and identification of the male-gamete-specific variant AtMGH3. *Plant J* 44:557–568.
38. Engel ML, Holmes-Davis R, McCormick S (2005) Green sperm. Identification of male gamete promoters in Arabidopsis. *Plant Physiol* 138:2124–2133.
39. Twell D (1992) Use of a nuclear-targeted ß-glucuronidase fusion protein to demonstrate vegetative cell-specific gene expression in developing pollen. *Plant J* 2:887–892.
40. Cheung AY, et al. (2003) Regulation of pollen tube growth by Rac-like GTPases. *J Exp Bot* 54:73–81.
41. Chen Z, Tan JL, Ingouff M, Sundaresan V, Berger F (2008) Chromatin assembly factor 1 regulates the cell cycle but not cell fate during male gametogenesis in Arabidopsis thaliana. *Development* 135:65–73.
42. Rotman N, et al. (2005) A novel class of MYB factors controls sperm-cell formation in plants. *Curr Biol* 15:244–248.
43. Talbert PB, Masuelli R, Tyagi AP, Comai L, Henikoff S (2002) Centromeric localization and adaptive evolution of an Arabidopsis histone H3 variant. *Plant Cell* 14:1053–1066.
44. Fang Y, Spector DL (2005) Centromere positioning and dynamics in living Arabidopsis plants. *Mol Biol Cell* 16:5710–5718.
45. Dewitte W, et al. (2003) Altered cell cycle distribution, hyperplasia, and inhibited differentiation in Arabidopsis caused by the D-type cyclin CYCD3. *Plant Cell* 15:79–92.
46. Dewitte W, et al. (2007) Arabidopsis CYCD3 D-type cyclins link cell proliferation and endocycles and are rate-limiting for cytokinin responses. *Proc Natl Acad Sci USA* 104:14537–14542.
47. Meijer M, Murray JAH (2000) The role and regulation of D-type cyclins in the plant cell cycle. *Plant Mol Biol* 43:621–633.
48. Tio M, Udolph G, Yang X, Chia W (2001) cdc2 links the Drosophila cell cycle and asymmetric division machineries. *Nature* 409:1063–1067.
49. Kostic I, Li S, Roy R (2003) cki-1 links cell division and cell fate acquisition in the C. elegans somatic gonad. *Dev Biol* 263:242–252.
50. Beemster GT, De Vusser K, De Tavernier E, De Bock K, Inze D (2002) Variation in growth rate between Arabidopsis ecotypes is correlated with cell division and A-type cyclin-dependent kinase activity. *Plant Physiol* 129:854–864.
51. Iwakawa H, Shinmyo A, Sekine M (2006) Arabidopsis CDKA;1, a cdc2 homologue, controls proliferation of generative cells in male gametogenesis. *Plant J* 45:819–831.
52. Nowack MK, et al. (2006) A positive signal from the fertilization of the egg cell sets off endosperm proliferation in angiosperm embryogenesis. *Nat Genet* 38:63–67.
53. Kim HJ, et al. (2008) Control of plant germline proliferation by SCF(FBL17) degradation of cell cycle inhibitors. *Nature* 455:1134–1137.
54. Boxem M, van den Heuvel S (2001) lin-35 Rb and cki-1 Cip/Kip cooperate in developmental regulation of G1 progression in C. elegans. *Development* 128:4349–4359.
55. Eady C, Lindsey K, Twell D (1995) The Significance of Microspore Division and Division Symmetry for Vegetative Cell-Specific Transcription and Generative Cell Differentiation. *Plant Cell* 7:65–74.
56. Cowan CR, Hyman AA (2006) Cyclin E-Cdk2 temporally regulates centrosome assembly and establishment of polarity in Caenorhabditis elegans embryos. *Nat Cell Biol* 8:1441–1447.

Supporting Information

Chen et al. 10.1073/pnas.0810992106

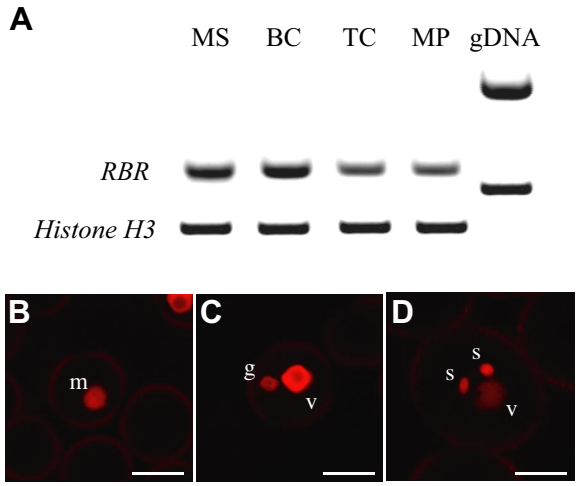

Fig. S1. Expression of *RBR* in pollen. (*A*) RT-PCR analysis of *RBR* expression with RNA extracted from isolated spores at 4 stages of pollen development. High levels of transcript levels are present at the microspore stage (*MS*) and in bi-cellular pollen (*BC*), followed by small decline in tri-cellular (*TC*) and mature pollen (*MP*). Histone variant *H3.2* (At4g40040) was used as a control. (*B-D*) We studied the expression pattern of RBR at the cellular level using the expression of the translational reporter construct p*RBR-RBR::RFP*, which complements partially *rbr-2* (Table S1 and Fig. S2*B*). We observed the expression of RBR-RFP in microspore (*B*), and developing pollen at bi-cellular stage (*C*) and tri-cellular stage (*D*). (Scale bars, 10 μm.) *m*, microspore nucleus; *v*, vegetative cell nucleus; *g*, generative cell nucleus; *s*, sperm cell nucleus.

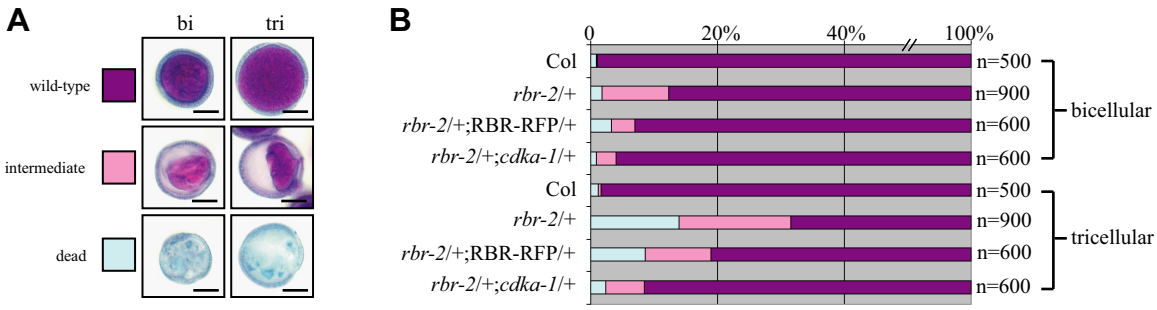

Fig. S2. Pollen death in *rbr* mutants. (*A*) Alexander staining viability analysis showing WT pollen (purple), intermediate pollen (pink), and dead pollen (green) at bi-cellular and tri-cellular stages, respectively. (Scale bars, 10 μm.) (*B*) Bar chart showing percentage of 3 types of pollen from Col, *rbr-2*/+, *rbr-2*/+;RBR-RFP/+, and *rbr-2*/+;*cdka-1*/+, at bi-cellular and tri-cellular stages, respectively. The size of total population analyzed (*n*) is indicated (*Right*).

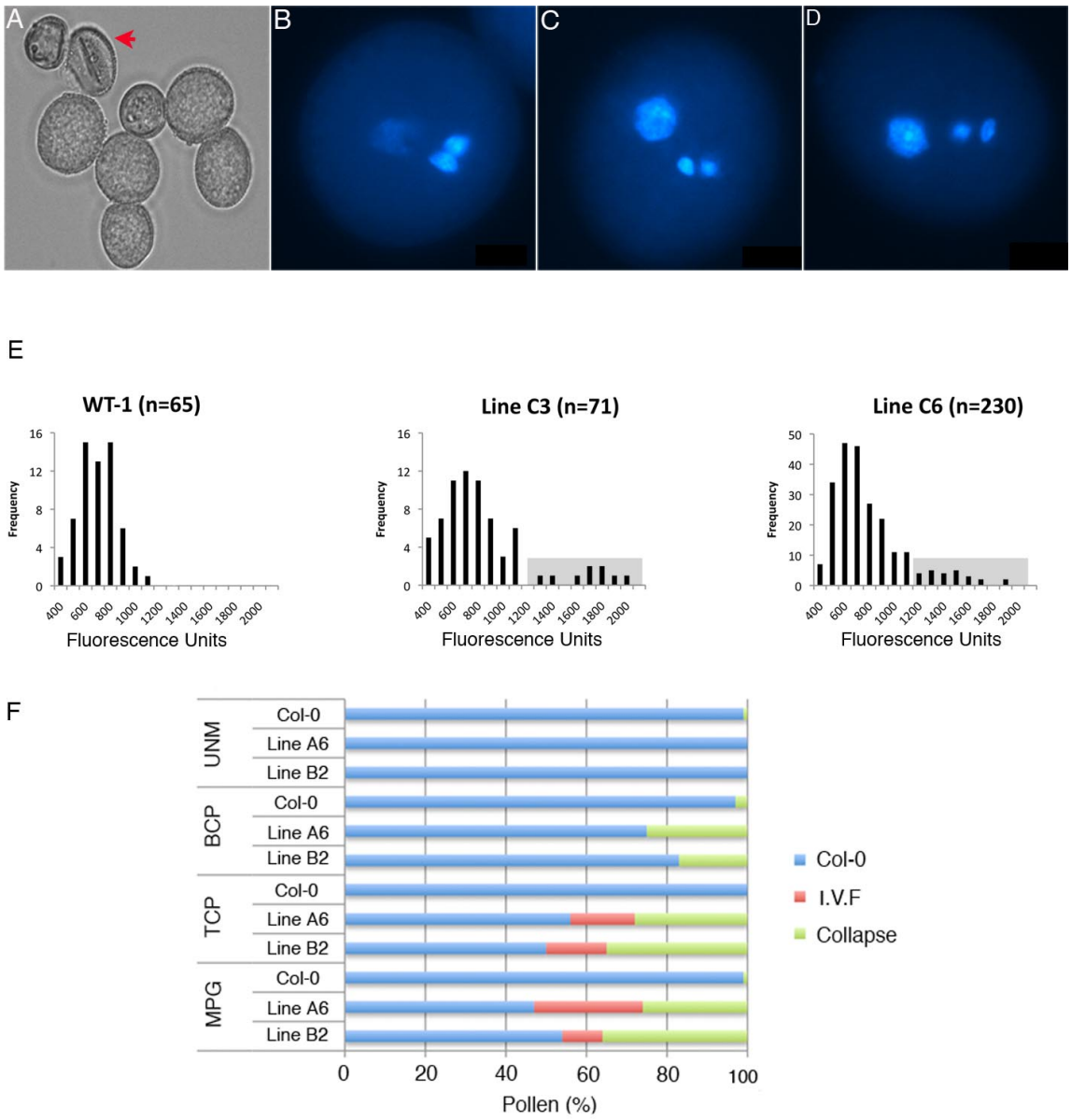

Fig. S3. Induced effect of *LAT52*-hp*RBR* construct during pollen development. Cytological analysis of plants expressing hairpin dsRNA targeted to *RBR* mRNA specifically in the vegetative cell. (*A*) DIC image showing aborted pollen grains (red arrow) at the mature pollen stage. (*B-D*) DAPI stained mature pollen grains with a WT phenotype (*B*) and those with a novel phenotype showing increased vegetative nuclear intravascular fluorescent (*I.V.F.*) from 2 independent siblings (*C* and *D*). (*E*) Measurement of vegetative cell nucleus fluorescence following DAPI staining at the mature pollen stage emphasizing the new class of pollen grains (shaded box) with fluorescence units above that observed in the WT populations. Number of pollen grains analyzed are indicated in the parenthesis. Fluorescence intensity was measured using a Nikon TE2000 fluorescence microscope and OpenLab 5.0.2 software (Improvision). (*F*) Phenotypic analysis of 2 independent siblings at the uni-cellular microspore (*UNM*), bi-cellular pollen (*BCP*), tri-cellular pollen (*TCP*), and at mature pollen stage (*MPG*). Bar chart showing the origin of the aborted and I.V.F. phenotype as observed in 2 independent siblings. The aborted phenotype was traced to the bi-cellular stage, whereas the I.V.F. phenotype was initially detected at the tri-cellular stage and increased in mature pollen for line A6 but decreased in line B2.

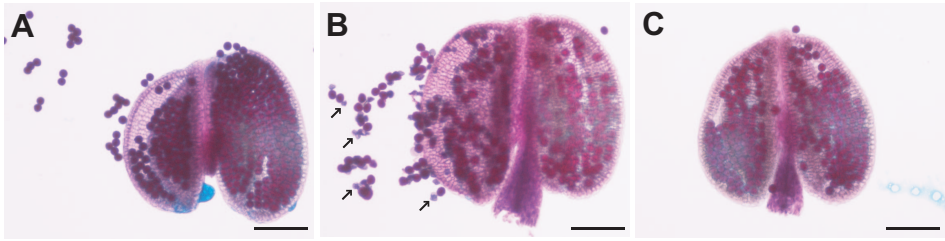

Fig. S4. Pollen death in *rbr* mutants and the rescue of pollen death by *cdka-1*. Alexander staining of Col (*A*), *rbr-2*/+ (*B*), and *rbr-2*/+;*cdka-1*/+ (*C*) anthers. Arrows indicate dead pollen. (Scale bars, 100 μm.)

Table S1. Paternal transmission of *rbr-2* and *cdka-1* alleles

Female × Male	Mean transmission ± SD (mutant allele) in F1, %	Transmission efficiency, %	n
Col × *rbr-2*/+	8.0 ± 2.8 (*rbr-2*)	8.7	637
Col × *rbr-2*/+;RBR-RFP+/−	20.2 ± 5.1(*rbr-2*)	25.3	816
Col × *cdka-1*/+	8.2 ± 2.1(*cdka-1*)	8.9	477
Col × *rbr-2*/+;*cdka-1*/+	47.0 ± 3.8 (*rbr-2*)	88.7	430

[a]Transmission efficiency is the number of mutant progeny divided by the number of WT progeny.

BIBLIOGRAPHY

Civil Status:

Family Name	CHEN
Given Name	ZHONG
Date of Birth	April 24, 1980
Place of Birth	Beijing, CHINA
Marital Status	Married
Nationality	CHINA
Address	BLK60, TEBAN GARDENS ROAD, #16-456, S600060
Official Email	chenz@tll.org.sg
Private Email	cheerzone@gmail.com

Education:

Sep. 1986-Jul. 1990	Primary School Affiliated to China Institute of Atomic Energy, Beijing, CHINA
Sep. 1990-Jul. 1992	ZhongGuanCun 3rd Primary School, Beijing, CHINA
Sep. 1992-Jul. 1998	ZhongGuanCun High School, Beijing, CHINA
Sep. 1998-Jul. 2003	Peking University, Beijing, CHINA (Bachelor of Basic Medical Sciences)
From Jan. 2005	PhD student, Department of Biological Sciences, National University of Singapore, SINGAPORE (Junior Research Fellow, Chromatin and Reproduction Group, Temasek Life Sciences Laboratory, SINGAPORE) Supervisor: Prof. Frederic BERGER